

NOVEL TECHNIQUES FOR IDENTIFICATION AND LOCATING FAULTS IN POWER SYSTEM COMPENSATED WITH FACTs DEVICES

Submitted in partial fulfilment of the requirements
for the award of the degree of

DOCTOR OF PHILOSOPHY

By
Saptarshi Roy
(Roll No. 714121)

Supervisor:

Dr. P.Suresh Babu
Assistant Professor



**DEPARTMENT OF ELECTRICAL ENGINEERING
NATIONAL INSTITUTE OF TECHNOLOGY
WARANGAL – 506004, TELANGANA STATE, INDIA
APRIL-2018**

APPROVAL SHEET

This Thesis entitled "**Novel Techniques for Identification and Locating Faults in Power System Compensated with FACTs Devices**" by **Saptarshi Roy** is approved for the degree of Doctor of Philosophy

Examiners

Supervisor

Dr. P.Suresh Babu
Assistant Professor
EED, NIT Warangal

Chairman

Dr. Somasekhar V. T
Professor & Head,
EED, NIT Warangal

Date: _____

**DEPARTMENT OF ELECTRICAL ENGINEERING
NATIONAL INSTITUTE OF TECHNOLOGY
WARANGAL – 506 004**

**DEPARTMENT OF ELECTRICAL ENGINEERING
NATIONAL INSTITUTE OF TECHNOLOGY WARANGAL**



CERTIFICATE

This is to certify that the thesis entitled "**“Novel Techniques for Identification and Locating Faults in Power System Compensated with FACTs Devices”**", which is being submitted by **Mr. Saptarshi Roy** (Roll No. 714121), is a bonafide work submitted to National Institute of Technology, Warangal in partial fulfilment of the requirement for the award of the degree of **Doctor of Philosophy** in Department of Electrical Engineering. To the best of my knowledge, the work incorporated in this thesis has not been submitted elsewhere for the award of any degree.

Date:

Place: Warangal

Dr. P.Suresh Babu

(Supervisor)

Assistant Professor

Department of Electrical Engineering

National Institute of Technology

Warangal – 506004

DECLARATION

This is to certify that the work presented in the thesis entitled "**Novel Techniques for Identification and Locating Faults in Power System Compensated with FACTs Devices**" is a bonafide work done by me under the supervision of **Dr. P.Suresh Babu**, Department of Electrical Engineering, National Institute of Technology, Warangal, India and was not submitted elsewhere for the award of any degree.

I declare that this written submission represents my ideas in my own words and where others ideas or words have been included; I have adequately cited and referenced the original sources. I also declare that I have adhered to all principles of academic honesty and integrity and have not misrepresented or fabricated or falsified any idea/date/fact/source in my submission. I understand that any violation of the above will be a cause for disciplinary action by the institute and can also evoke penal action from the sources which have thus not been properly cited or from whom proper permission has not been taken when needed.

Saptarshi Roy
(Roll.No: 714121)

Date:

Place: Warangal

ACKNOWLEDGEMENTS

It gives me immense pleasure to express my deep sense of gratitude and thanks to my supervisor **Dr. P.Suresh Babu**, Assistant Professor, Department of Electrical Engineering, National Institute of Technology Warangal, for his invaluable guidance, support, and suggestions. His knowledge, suggestions, and discussions helped me to become a capable researcher. He has shown me the interesting side of this wonderful and potential research area. His encouragement helped me to overcome the difficulties encountered in my research as well in my life.

I am very much thankful to **Prof. Somasekhar V. T**, Head, Department of Electrical Engineering for his constant encouragement, support and cooperation.

I take this privilege to thank all my Doctoral Scrutiny Committee members, **Dr. D.M Vinod Kumar**, Professor, Department of Electrical Engineering, **Dr. A.V.Giridhar** Assistant Professor, Department of Electrical Engineering and **Dr. K.V.Sai Srinadh**, Professor, Department of Mechanical Engineering for their detailed review, constructive suggestions and excellent advice during the progress of this research work.

I also appreciate the encouragement from teaching, non-teaching members, and fraternity of Department of Electrical Engineering of NIT Warangal. They have always been encouraging and supportive.

I wish to express my sincere thanks to **Prof. N.V.Ramana Rao**, Director, NIT Warangal for his official support and encouragement.

I convey my special thanks to contemporary Research Scholars Mr. Vijaybabu Koreboina, Mr. OVSR Varaprasad, Mr. M Vishnu Prasad, Mr. B Anil Kumar, Mr. Durga Harikiran B, Mr. T Kiran, Mr. Phanendra Babu N V, Mr. Venu Sonti, Mr. Ratna Rahul T, Mr. Hareesh M, Mr. Pranay Kumar A, Mr. Sachidananda Prasad, Mr. Suman Dhara, Mr. Rohit Chandan (SRF) and Dr. Siva Prasad Nandyala (ECE) and also power systems M.Tech students M.Lohith (2015), C Purushotham Reddy(2016) and Abhishek Kumar (2017).

I acknowledge my gratitude to all my teachers and colleagues at various places for supporting and co-operating me to complete the work.

My special, sincere acknowledge, heartfelt gratitude and indebtedness are due to my parents Shri. Jayanta Kumar Roy & Smt. Krishna Roy and my elder brother Shri. Rajarshi Roy for their sincere prayers, blessings, constant encouragement, shouldering the responsibilities and moral support rendered to me throughout my life, without which my research work would not have been possible. I heartily acknowledge all my relatives for their love and affection towards me.

Above all, I express my deepest regards and gratitude to "**ALMIGHTY**" whose divine light and warmth showered upon me the perseverance, inspiration, faith and enough strength to keep the momentum of work high even at tough moments of research work.

Saptarshi Roy

Ж

ABSTRACT

Protection of power system is an important issue for reliable and smooth operation of power network. If proper protection arrangements are not provided, the whole power network can even suffer complete black out. Black out will cause inconvenience and huge financial losses. So, the several techniques and issues related to fault identification and location calculations of power system under various operating conditions should be studied thoroughly to ensure security of the power network.

Modern power systems are large in size and complex. Hence they are provided with wide area measurement systems(WAMS). WAMS collects time synchronized sampled values from wave forms(voltage, current etc) or signals. Those are required for analysis. The use of WAMS prevents cascaded tripping and blackout of whole network due to failure in a single area. Thus it is increasing reliability and efficiency of whole power network.

To ensure a smooth, hazardless and reliable operation of power system several issues should be taken care of. The salient issues are as follows:

- i)Proper compensation should be provided in the network to maintain smooth voltage profile via FACTs devices (by keeping P and Q in limits, system voltage also maintained as constant).
- ii)Designing efficient backup protection scheme capable to support even in case of simultaneous faults in power system.
- iii) Proper relay coordination should be arranged to ensure a smooth and uninterrupted power supply during faults.
- iv)Fault location algorithms should be studied thoroughly for identification, confirmation and location of power system faults under various operating conditions with or without the knowledge of transmission line parameters in order to keep healthy and smooth operation of power supply in the network.

This thesis work has made an effort to develop an improved protection system which fulfils all the aspects for smooth power system operation with appropriate fault identification and location techniques in the presence of FACTs devices. Appropriate relay coordination is

important in order to keep the smooth flow of power during faulted conditions. So, proposed work has taken care of relay coordination aspect also during faulted conditions.

At first, the introductory chapter describes an introduction and state of art on different fault identification and location techniques of power system. Brief introduction of Wide Area Monitoring systems (WAMs) and Phasor measurement unit(PMU) have been presented. The scope of the work has been highlighted and author's contribution in the research area has been summarized.

The Second Chapter presents an optimal placement approach of two FACTs devices, Thyristor controlled series capacitor (TCSC) and Thyristor controlled phase angle regulator (TCPAR) based on sensitivity analysis. In this method, reduction of line losses and overloading are taken care of. Sensitivity indexes are used to find proper place of FACTs devices in the network. After placing FACTs devices the performance of the network is also analyzed. Which FACTs device is more suitable for the network is also analyzed with the impact of change of generation. Effectiveness of the method is tested on a WSCC-3-Machine-9 bus system and an IEEE 57 bus test system with various single and multiple contingency combinations. The results obtained are accurate and satisfactory. The whole simulation work is done by using Power World 12.0 commercial version.

The Third Chapter presents an work related to distance relay and directional relaying aspect of series compensated transmission line. In this work the behaviour of series compensated EHV transmission lines during faults is simulated. The use of series capacitors for compensating part of the inductive reactance of long transmission lines increases the power transmission capacity. Emphasis is given on the impact of modern capacitor protection techniques (MOV protection). A novel methodology is proposed to identify faulty phases based on correlation factor computation. Under various fault conditions the proposed method is tested for its validation. The proposed method is tested on series capacitor compensated transmission lines (SCCTLs) with their different configurations and contingency combinations. Distance characteristics are also drawn for various zones of protection. Simulation results show that proposed method has identified correct fault location.

Relay coordination is an important aspect to maintain proper power system operation and control. Relays should be organized in such a way that every relay should have a backup

and Coordination Time Interval (CTI) between primary and back up and different zones of the relay should be maintained to achieve proper fault identification and fault clearance sequence. The relays should operate in minimum desirable time satisfying all the co-ordination constraints. So, relay coordination is nothing but highly constraint problem. Heuristic techniques are often used to get optimal solution of this kind of problem.

In the **Fourth chapter** this constraint problem is solved by Teaching learning based optimization(TLBO) on several test systems from IEEE 5 bus to IEEE 30 bus test system. Proper desirable Time Setting Multiplier (TSM) with minimum operating time of relays is calculated, intelligent over current relay characteristics selection is also incorporated to get the desired results in this work. The results seem to be satisfactory as the results obtained from TLBO are comparatively better than so called conventional methods like Genetic Algorithm(GA) and Particle Swarm Optimization (PSO).

The **Fifth chapter** presents a synchronized phasor measurement-based wide-area backup protection scheme which uses the magnitude of sequence voltages of buses at a system protection centre to identify the faulted bus closest to the fault and faulted line. The technique is tested for various faults including simultaneous faults in various systems. The scheme is found to be accurate and fast with today's synchronized measurement technology. Analysis using simultaneous faults is a novel contribution in this work. It is expected that this scheme will reduce the number of disastrous blackouts and improve the reliability and security of the power system. The required information is able to distinguish between balanced and unbalanced fault in the system. The study of new back up protection scheme is done on a WSCC-3 machine-9 bus system and an IEEE 14 bus test system. The data is simulated through EMTDC/PSCAD and MATLAB /SIMULINK packages.

Exact fault location detection is vital for power system restoration and security purposes. The line parameters plays a key role for accurately detecting fault location in a transmission line of a power network. In other fault location algorithms, line parameters used are approximately constant and they varies with weather and loading conditions also. So, an algorithm which is independent of the line parameters, is more accurate, flexible and robust.

The **Sixth Chapter** presents a work, which proposes a numerical algorithm for locating fault in a transmission line with improved accuracy. This algorithm is independent of the line parameters for locating fault and accuracy of the algorithm is improved by using filtering

algorithm. The performance of the algorithm is tested on several power networks by Simulation carried out by PSCAD/EMTDC. A fault classification approach by use of zero sequence components of power and a faulty phase detection approach by the study of change of phase currents are also presented in the work.

The Seventh Chapter presents the conclusions and future scope of research of this whole work.

The appendix and the references are mentioned at the end of the thesis.

PSCAD, MATLAB-SIMULINK, POWER WORLD softwares are used to do the different sub works of the thesis. MATLAB codings are used for doing large and complex calculations where ever necessary.

Table of Contents

Acknowledgement.....	i
Abstract	iii
Table of contents.....	vii
List of Figure.....	viii
List of Tables.....	xii
Abbreviations.....	xiii
List of Symbols.....	xv
Chapter 1 Introduction.....	2
1.1 General Overview.....	3
1.2 State of Art on Several Issues in Power System Protection.....	4
1.3 Motivation and Objectives of the Thesis.....	8
1.4 Contributions.....	9
1.5 Organization of the Thesis.....	10
Chapter 2 Strength of Standard IEEE Power Systems.....	15
2.1 Introduction	155
2.1.1 Load Flow Study	Error! Bookmark not defined. 6
2.1.2 Well conditioned and ill-conditioned system	Error! Bookmark not defined. 7
2.1.3 Gauss Method.....	Error! Bookmark not defined.
2.1.4 Gauss-Seidel Method (GS).....	18
2.1.5 Significance of acceleration factor.....	18
2.1.6 PV- Bus treatment.....	18
2.1.7 Merits of the GS Method.....	20
2.1.8 Demerits of the GS Method.....	20
2.2 NR load flow (NRLF)	Error! Bookmark not defined. 1
2.2.1 Merits of NRLF	Error! Bookmark not defined. 1
2.2.2 Demerits of NRLF	Error! Bookmark not defined. 2
2.3 Advanced Newton's Decoupled (NDC)/ Fast Decoupled (FDC) Load Flow Method.....	Error! Bookmark not defined. 2

2.3.1	Merits of FDC.....	Error! Bookmark not defined.	3
2.3.2	Demerits of FDC	Error! Bookmark not defined.	3
2.4	Best Suitable Method for Our Work.....	Error! Bookmark not defined.	3
2.5	General View About Power World Simulator	Error! Bookmark not defined.	4
2.6	Different Voltages Levels and Permissible Voltage Fluctuations.....	24	
2.7	Simulated Test System	Error! Bookmark not defined.	25
2.8	Results		27
2.9	Summary.....		29
Chapter 3	High Step-Down Coupled Inductor Buck PFC Based LED Driver.....		30
3.1	Introduction	Error! Bookmark not defined.	
3.2	High Step-Down CIB Converter	Error! Bookmark not defined.	
3.2.1	Modes of Operation	Error! Bookmark not defined.	
3.2.2	Voltage Gain of CIB PFC Converter.....	Error! Bookmark not defined.	
3.2.3	Design Considerations and Device Stress Calculations	Error! Bookmark not defined.	
3.3	Control Scheme	Error! Bookmark not defined.	
3.4	Implementation and Result Analysis	Error! Bookmark not defined.	
3.4.1	Simulation Results and Discussions.....	Error! Bookmark not defined.	
3.4.2	Experimental Results and Discussions..	Error! Bookmark not defined.	
3.5	Summary.....	Error! Bookmark not defined.	
Chapter 4	Electrolytic Capacitor less Ripple Free LED Driver.....		46
4.1	Introduction		47
4.2	Operation and Design of NIBB PFC Converter	Error! Bookmark not defined.	
4.2.1	Principle of operation of NIBB converter	Error! Bookmark not defined.	
4.2.2	Design and analysis of NIBB PFC converter	Error! Bookmark not defined.	
4.3	Operation and Design of E-Cap Less LED Driver	Error! Bookmark not defined.	
4.3.1	Operation of E-cap less LED driver	Error! Bookmark not defined.	
4.3.2	Design of BDC topology	Error! Bookmark not defined.	
4.4	Implementation and Results Analysis of Proposed LED Driver	Error! Bookmark not defined.	
4.4.1	Simulation results and discussions	Error! Bookmark not defined.	
4.4.2	Experimental results and discussions	Error! Bookmark not defined.	
4.5	Summary.....	Error! Bookmark not defined.	

Chapter 5 A Dual Output ZVS-Coupled Inductor Buck Converter Based LED Driver	65
5.1 Introduction	66
5.2 Proposed converter and Design Analysis	Error! Bookmark not defined.
5.2.1 Modes of Operation	Error! Bookmark not defined.
5.2.2 Design Considerations	Error! Bookmark not defined.
5.2.3 Switching device selection	Error! Bookmark not defined.
5.2.4 Energy recycling capacitor	Error! Bookmark not defined.
5.2.5 Output capacitors design	Error! Bookmark not defined.
5.3 Dimming Control.....	Error! Bookmark not defined.
5.4 Implementation and Result Discussion	Error! Bookmark not defined.
5.4.1 Simulation Results and Analysis	Error! Bookmark not defined.
5.4.2 Experimental Results and Analysis	Error! Bookmark not defined.
5.5 Summary.....	Error! Bookmark not defined.
Chapter 6 Conclusions and Scope for Future work	100
6.1 Conclusions	175
6.2 Scope for Future Work	176
References.....	114
Publications	121
Appendix-A	122

List of Figures

Figure 1.1 Distribution of power consumed by appliances in India**Error! Bookmark not defined.**

Figure 1.2 Operating principle of a LED**Error! Bookmark not defined.**

Figure 1.3 Symbol and its equivalent electrical model of a LED**Error! Bookmark not defined.**

Figure 1.4 Schematic view of LED driver**Error! Bookmark not defined.**

Figure 2.1 A simple offline passive LED driver [15]**Error! Bookmark not defined.**

Figure 2.2 Passive type-1 (P_1) LED driver [16].....**Error! Bookmark not defined.**

Figure 2.3 Valley fill Passive type-2 (P_2) LED driver [17] ...**Error! Bookmark not defined.**

Figure 2.4 Modified passive type-II (P_2) LED driver [18]**Error! Bookmark not defined.**

Figure 2.5 Ballast based P_2 LED driver [19]**Error! Bookmark not defined.**

Figure 2.6 Switched mode single-stage Type-A (S_{IA}) LED driver**Error! Bookmark not defined.**

Figure 2.7 Buck converter based S_{IA} LED driver [21].....**Error! Bookmark not defined.**

Figure 2.8 Flyback converter based S_{IA} LED driver [22]**Error! Bookmark not defined.**

Figure 2.9 Switched mode single-stage S_{IB} driver.....**Error! Bookmark not defined.**

Figure 2.10 CCM buck converter fed PFC LED driver [25] ...**Error! Bookmark not defined.**

Figure 2.11 Modified Zeta converter fed LED driver [26]**Error! Bookmark not defined.**

Figure 2.12 Switched mode two-stage Type-A (S_{2A}) driver**Error! Bookmark not defined.**

Figure 2.13 Switched mode two-stage Type-B (S_{2B}) driver**Error! Bookmark not defined.**

Figure 2.14 Three-stage switched mode (S_3) LED driver.....**Error! Bookmark not defined.**

Figure 2.15 Schematic of VMC PWM technique**Error! Bookmark not defined.**

Figure 2.16 Peak current mode control.....**Error! Bookmark not defined.**

Figure 2.17 Average current mode control technique.....**Error! Bookmark not defined.**

Figure 2.18 Hysteresis current mode (HCM) control**Error! Bookmark not defined.**

Figure 3.1 Proposed CIB PFC LED driver**Error! Bookmark not defined.**

Figure 3.2 Idealized waveforms of proposed CIB PFC LED driver**Error! Bookmark not defined.**

Figure 3.3 Equivalent modes of proposed CIB PFC converter;**Error! Bookmark not defined.**

Figure 3.4 Gain versus duty cycle of different converters**Error! Bookmark not defined.**

Figure 3.5 Control scheme diagram of single-loop VMC**Error! Bookmark not defined.**

Figure 3.6 Closed loop VMC coupled-inductor buck PFC converter.**Error! Bookmark not defined.**

Figure 3.7 Simulation results of the source voltage and source current.**Error! Bookmark not defined.**

Figure 3.8 Simulation results of switch voltage (v_{ds}) and switch current (i_{ds})**Error! Bookmark not defined.**

Figure 3.9 Simulation results of diode voltage (v_d) and diode current (i_d)**Error! Bookmark not defined.**

Figure 3.10 Simulation results of output voltage and output current.**Error! Bookmark not defined.**

Figure 3.11 THD spectrum of source current.**Error! Bookmark not defined.**

Figure 3.12 Experimental results of source voltage and source current**Error! Bookmark not defined.**

Figure 3.13 Experimental results of switch and diode at $v_s=110 V_{rms}$.**Error! Bookmark not defined.**

Figure 3.14 Experimental results of coupled inductor at $v_s=110 V_{rms}$.**Error! Bookmark not defined.**

Figure 3.15 Experimental results of output voltage and output current**Error! Bookmark not defined.**

Figure 3.16 Experimental results under source voltage variations under full load condition**Error! Bookmark not defined.**

Figure 3.17 Experimental results of source current and harmonic spectrum**Error! Bookmark not defined.**

Figure 3.18 THD (%) versus source voltage under different load condition**Error! Bookmark not defined.**

Figure 3.19 Harmonic comparison of proposed converter with IEC standards**Error! Bookmark not defined.**

Figure 3.20 Experimental comparisons of THD (%) versus source voltage**Error! Bookmark not defined.**

Figure 3.21 Experimental comparisons of efficiency (%) versus source voltage**Error! Bookmark not defined.**

Figure 4.1 (a) Non-inverting buck-boost PFC converter; (b) Theoretical waveforms of NIBB PFC converter**Error! Bookmark not defined.**

Figure 4.2 (a) E-cap less ripple free LED driver; (b) Ideal waveforms of E-cap less ripple free LED driver**Error! Bookmark not defined.**

Figure 4.3 Key waveforms of proposed E-cap less ripple free LED driver**Error! Bookmark not defined.**

Figure 4.4 Equivalent circuits of proposed E-cap less ripple free LED driver**Error! Bookmark not defined.**

Figure 4.5 Equivalent circuit of BDC topology**Error! Bookmark not defined.**

Figure 4.6 (a) Altium designer schematic view, (b) Control logic using XILINK block sets in MATLAB**Error! Bookmark not defined.**

Figure 4.7 Simulation results of source voltage and source current of proposed LED driver.....**Error! Bookmark not defined.**

Figure 4.8 Simulation waveforms of NIBB PFC converter at $50 V_{rms}$ **Error! Bookmark not defined.**

Figure 4.9 Simulation waveforms of NIBB PFC converter at $70 V_{rms}$ **Error! Bookmark not defined.**

Figure 4.10 Simulation waveforms of BDC current (i_2) and inductor current (i_{Lbc}); (a) $v_s=50 V_{rms}$; (b) $v_s=70 V_{rms}$;.....**Error! Bookmark not defined.**

Figure 4.11 Simulation waveforms of BDC switch voltages (v_{Qbc} & $v_{Q'bc}$) & capacitor voltage (v_{cbc}) **Error! Bookmark not defined.**

Figure 4.12 Simulation waveforms V_o and i_o (i) NIBB PFC without BDC (ii) NIBB PFC with BDC **Error! Bookmark not defined.**

Figure 4.13 Simulation THD plot of source current **Error! Bookmark not defined.**

Figure 4.14 Experimental set of proposed E-cap less LED driver **Error! Bookmark not defined.**

Figure 4.15 Experimental results of source voltage and source current; (a) $v_s=50 V_{rms}$; (b) $v_s=70 V_{rms}$; **Error! Bookmark not defined.**

Figure 4.16 Experimental waveforms of NIBB PFC converter at $50 V_{rms}$ **Error! Bookmark not defined.**

Figure 4.17 Experimental waveforms of BDC input current & inductor current; (a) $v_s=50 V_{rms}$; (b) $v_s=70 V_{rms}$; **Error! Bookmark not defined.**

Figure 4.18 Experimental waveforms of bi-directional converter at $50 V_{rms}$ **Error! Bookmark not defined.**

Figure 4.19 Experimental waveforms V_o and i_o (i) NIBB PFC without BDC (ii) NIBB PFC with BDC **Error! Bookmark not defined.**

Figure 4.20 Experimental THD plot of source current **Error! Bookmark not defined.**

Figure 4.21 Measured source current harmonics **Error! Bookmark not defined.**

Figure 4.22 Efficiency versus source voltage **Error! Bookmark not defined.**

Figure 5.1 Proposed high step-down ZVS-DOCIB converter **Error! Bookmark not defined.**

Figure 5.2. Equivalent circuit of proposed high step-down ZVS-DOCIB converter **Error! Bookmark not defined.**

Figure 5.3 Idealized waveforms of proposed ZVS-DOCIB converter **Error! Bookmark not defined.**

Figure 5.4 Equivalent modes of ZVS-DOCIB converter **Error! Bookmark not defined.**

Figure 5.5 Characteristic curves of ZVS-DOCIB converter .. **Error! Bookmark not defined.**

Figure 5.6 Double pulse width modulation control scheme .. **Error! Bookmark not defined.**

Figure 5.7 Simulation waveforms of switching devices **Error! Bookmark not defined.**

Figure 5.8 Simulation waveforms of CI , L_x & C_I **Error! Bookmark not defined.**

Figure 5.9 Simulation waveforms of output voltages/currents at 100% dimming; (a) V_{o1} & i_{o1} , (b) V_{o2} & i_{o2} **Error! Bookmark not defined.**

Figure 5.10 Simulation waveforms of output voltages/currents at 50% dimming; (a) V_{o1} & i_{o1} , (b) V_{o2} & i_{o2} **Error! Bookmark not defined.**

Figure 5.11 Simulation waveforms of output voltages/currents at 80% dimming; (a) V_{o1} & i_{o1} , (b) V_{o2} & i_{o2} **Error! Bookmark not defined.**

Figure 5.12 Experimental set-up of proposed ZVS-DOCIB LED driver**Error! Bookmark not defined.**

Figure 5.13 Experimental waveforms of switching devices; (a) v_{gs1} , v_{ds1} & i_{S1} ; (b) v_{gs2} , v_{ds2} & i_{S2} ; (c) v_{d1} & i_{d1} ; (d) v_{d2} & i_{d2} **Error! Bookmark not defined.**

Figure 5.14 Experimental waveforms of CI , L_x & C_I : (a) i_{Lkp} & i_{Ls} ; (b) v_{Lx} & i_{Lx} ; (c) v_{Lp} & v_{Ls} ; (d) v_{CI} & i_{CI} ;**Error! Bookmark not defined.**

Figure 5.15 Experimental waveforms of output voltages/currents at 100% dimming: (a) V_{o1} & i_{o1} ; (b) V_{o2} & i_{o2} ;**Error! Bookmark not defined.**

Figure 5.16 Experimental enlarged waveforms of switch S_1 , S_2 ; (a) V_{gs1} & V_{ds1} ; (b) V_{gs2} & V_{ds2} **Error! Bookmark not defined.**

Figure 5.17 Experimental switching pulses; (a) 50% dimming, (b) 80% dimming**Error! Bookmark not defined.**

Figure 5.18 Experimental waveforms of output voltages/currents at 50% dimming: (a) V_{o1} & i_{o1} ; (b) V_{o2} & i_{o2} ;**Error! Bookmark not defined.**

Figure 5.19 Experimental waveforms of output voltages/currents at 80% dimming: (a) V_{o1} & i_{o1} ; (b) V_{o2} & i_{o2} ;**Error! Bookmark not defined.**

Figure 5.20 Measured efficiency versus load power**Error! Bookmark not defined.**

Figure 5.21 Extended configuration of the proposed converter for multiple loads.**Error! Bookmark not defined.**

Figure A.1 Simulink model of closed loop conventional buck PFC LED driver**Error! Bookmark not defined.**

Figure A.2 Simulink model of voltage mode controller for buck PFC LED driver**Error! Bookmark not defined.**

Figure A.3 Simulink model of conventional buck PFC LED driver**Error! Bookmark not defined.**

Figure A.4 Simulink model of closed loop coupled inductor buck PFC LED driver**Error! Bookmark not defined.**

Figure A.5 Simulink model of voltage mode controller for coupled inductor buck PFC LED driver**Error! Bookmark not defined.**

Figure A.6 Simulink model of coupled inductor buck PFC LED driver**Error! Bookmark not defined.**

Figure A.7 Simulink model of NIBB PFC LED driver without BDC**Error! Bookmark not defined.**

Figure A.8 Simulink model of complete E-cap less LED driver**Error! Bookmark not defined.**

Figure A.9 Control pulses for E-cap less LED driver**Error! Bookmark not defined.**

Figure A.10 Simulink model of E-cap less LED driver**Error! Bookmark not defined.**

Figure A.11 complete Simulink model of dual output ZVS-CIB LED driver**Error! Bookmark not defined.**

Figure A.12 Simulink model of dual output ZVS-CIB LED driver**Error! Bookmark not defined.**

Figure A.13 Simulink model for pulse generation of dual output ZVS-CIB LED driver**Error! Bookmark not defined.**

List of Tables

Table 2.1	Harmonic limits of IEC 61000 3-2 standards	Error! Bookmark not defined.
Table 2.2	Comparisons of various passive LED drivers	Error! Bookmark not defined.
Table 3.1	Parameters used in simulation of proposed CIB PFC LED driver	Error! Bookmark not defined.
Table 3.2	Parameters used in experimentation of proposed CIB PFC LED driver	Error! Bookmark not defined.
Table 4.1	Parameters used in simulation of proposed E-cap less LED driver	Error! Bookmark not defined.
Table 4.2	Specifications & design values of proposed E-Ca-less LED driver	Error! Bookmark not defined.
Table 5. 1	Parameters used in simulation of ZVS-DOCIB converter	Error! Bookmark not defined.
Table 5. 2	Comparative studies of ZVS-DOCIB converter with other works in literature	Error! Bookmark not defined.

Abbreviations

AC	Alternating current
ANN	Artificial Neural Network
CPU	Central Processing Unit
CTI	Coordination Time Interval
DCLF	Direct Current Load Flow
EHV	Extra High Voltage
EMTDC	Electromagnetic Transient Direct Current
FACTs	Flexible AC Transmission System
FFT	Fast Fourier Transform
FLA	Fault Location Algorithm
FLI	Faulted Line Identification
GA	Genetic Algorithm
IDMT	Inverse Definite Minimum Time
IEEE	Institute of Electrical and Electronics Engineers
LFB	Line Flow Based
LG	Line to Ground
LL	Line to Line
LLG	Line to Line to Ground
LLL	Line to Line to Line
LLLG	Line to Line to Line to Ground
MOV	Metal Oxide Varistor
NRLF	Newton Raphson Load Flow
NRPG	Northern Regional Power Grid
PCR	Protection Correlation Region
PF	Power factor
PDC	Phasor Data Concentrator
PMU	Phasor Measurement Unit
PSO	Particle Swarm Optimization
PSCAD	Power System Computer Aided Design

PSM	Plug Setting Multiplier
SCCTL	Series Capacitor Compensated Transmission Line
SCPU	Series Capacitor Protection Unit
SLDC	State Load Dispatch Centre
SPDC	Super Phasor Data Concentrator
SRPG	Southern Regional Power Grid
STFLA	Single Terminal Fault Location Algorithm
TCSC	Thyristor Controlled Series Capacitor
TCPAR	Thyristor Controlled Phase Angle Reactor
TCPST	Thyristor Controlled Phase Shifting Transformer
TLBO	Teaching Learning based Optimization
TSM	Time Setting Multiplier
WABP	Wide Area Back up Protection
WAMS	Wide Area Measurement System
WAPS	Wide Area Protection System
WSCC	Western Standard Coordinating Council
ZCD	Zero Crossing Detector

List of symbols

\emptyset	Phase Shift
\emptyset_k	Phase shift produced by TCPAR
a_1	Sensitivity index for TCSC
a_2	Sensitivity index for TCPAR
δ_{mn}	Sending end torque angle of bus m
ω	Angular frequency
ω_c	Cut off frequency
Ω	Ohm
B_{mn}	Suceptance of line mn
B_{sh}	Shunt Suceptance of line
C	Capacitance
f	Frequency
G_{mn}	Conductance of line mn
I	Current
ΔI	Change of current
I_f	Fault current
I_p	Pick up current
I_R^n	Negative sequence receiving end current
I_R^P	Positive sequence receiving end current
I_S^n	Negative sequence sending end current
I_S^P	Positive sequence sending end current
L	Inductance
P	Active Power
P_{base}	Base case real power
$P_{contingency}$	Real power at contingency
P_{lk}	Power loss in line k
P_{mn}	Active power flow from bus m to bus n
P_{nm}	Active power flow from bus n to bus m

Q	Reactive Power
Q_{mn}	rective power flow from bus m to bus n
Q_{nm}	rective power flow from bus n to bus m
R	Resistance
R_F	Fault resistance
r_{mn}	Resistance of line mn
T_F	Teaching Factor
t_{op}	Time of operation of relay
V	Voltage
ΔV	Change of voltage
V_a	Voltage of Phase A
V_b	Voltage of Phase B
V_c	Voltage of Phase C
V_F	Fault voltage
V_F^P	Positive sequence fault voltage
V_m	Voltage at Bus m
V_{m0}	Zero sequence voltage
V_{m1}	Positive sequence voltage
V_{m2}	Negative sequence voltage
V_n	Voltage at Bus n
V_R^n	Negative sequence Receiving end voltage
V_R^P	Positive sequence Receiving end voltage
V_S^n	Negative sequence sending end voltage
V_s^P	Positive sequence sending end voltage
x	Reactance
x_c	Static Reactance
x_{ck}	TCSC reactance
x_{mn}	Line mn reactance
$X_{j,k\text{best},i}$	Best learner

Chapter1

Introduction

Chapter 1

Introduction

Protection of power system is an important issue for reliable and smooth operation of power network. If proper protection arrangements are not provided, the whole power network can even suffer complete black out. Black out will cause inconvenience and huge financial losses. So, the several issues related to power system protection should be studied thoroughly to ensure security of the power network.

Modern power systems are big and complex. Hence they are provided with wide area measurement systems(WAMS). WAMS collects time synchronized sampled values from wave forms(voltage, current etc) or signals. Those are required for analysis. The use of WAMS prevents cascaded tripping and blackout of whole network due to failure in a single area. Thus it is increasing reliability and efficiency of whole power network.

To ensure a smooth, hazardless and reliable operation of power system several issues should be taken care of. The salient issues important for the power system protection aspects are as follows:

- i)Various fault detection, identification, location and classification techniques.
- ii)Designing efficient backup protection scheme capable to support even in case of simultaneous faults in power system.
- iii)Proper compensation should be provided in the network to increase power transfer capability, scarcity of reactive power in the network if any and smooth voltage profile etc via fixed capacitor or by using FACTs devices. Now a days , trend is to use FACTs devices more instead of using any fixed capacitor.
- iv) Proper relay coordination should be arranged to ensure a smooth and uninterrupted power supply.

This thesis work has made an effort to develop an improved and reliable wide area protection system which fulfils all the aspects discussed above. The thesis proposes different aspects like fault location, detection, identification techniques; backup protection even in case of simultaneous faults; optimum FACTs placement and improvement of voltage profiles by

Introduction

using series compensation and intelligent relay co-ordination with a novel technique, which converges in fastest CPU elapsed time with respect to other contemporary techniques.

1.1 General Overview

A wide area system having several components. e.g- Phasor measurement unit (PMU), phasor data concentrator (PDC), GPS satellite system, super PDC (SPDC) as shown in Fig1(a) & 1(b). The real time data from the various remote areas are collected by PMUs and sent to local data concentrator called phasor data concentrator through communication system. This system is same as the backup protection system for Wide Area Protection System (WAPS) and it is capable of acting as the substitution of conventional backup protection in power system. The relay decision is taken based on collected data via communication network. The suggested technique increases the accuracy ,reliability and stability of the system. Usually the data collection activity follows the below hierarchy. Level 1 being the lowest and level 4 is the highest position as indicated in Fig 1(a).In case of a power network level 1 can be compared as feeder level data , level 2 can be compared as substation level data, level 3 can be compared with a State board or grid data and level 4 can be compared with a load dispatch centre data (e.g – Northern Regional Load dispatch centre or Southern Region Load dispatch centre in context to India).

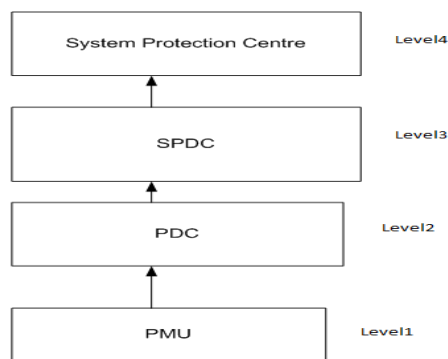


Fig 1(a): Collection of Data Hierarchy

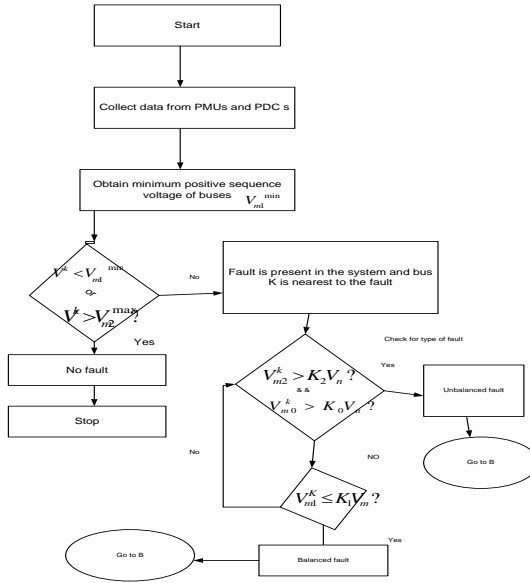


Fig: 1(b): Wide Area Measurement Back Up Protection

1.2 State of Art on Several Issues in Power System Protection

Altuve H.J, Joseph B.M and Alexander G.E (2009) told in their paper “Advances in series -compensated line protection “ , Whenever there is a change in load, the system voltage level changes. The demand of reactive power in power system increases With the drop in voltage level. If the reactive power demand is not met, then it leads to further decline in bus voltage resulting in the cascading effect on adjacent power networks. Hence determination of the strength of buses and maintaining the voltage profile within permissible limits becomes essential.

Tajudeen H. Sikiru, Adisa A. Jimoh, Yskandar Hamam, John T. Agee and Roger Ceschi (2012) told in the paper “Voltage profile improvement based on network structural characteristics “ , voltage profile is to be maintained. So, it is necessary to have knowledge about strong and weak buses with respect to voltage profile.

Vahedipour Z and Daneshian B (2013) told in the paper “On the solution of ill-conditioned systems of linear equations“, about Poor convergence characteristics on ill-conditioned system .

Introduction

Vanishree J and Ramesh V(2014) told in the paper “Voltage profile improvement in power system – a review “, if the reactive power demand in power system is not satisfied , then it leads to further decline in bus voltage resulting in the cascading effect on adjacent power systems.

Vyas B ,Maheswari R.P and Das B (2014) told in the paper “Protection of series compensated transmission line: Issues an state of art “,Weak voltage profile of buses is a serious problem in power network which can harm the security and reliability of power system.

J. Izykowski, E. Rosolowski, P.balcerek, M.Fulczyk and M. M. Saha (2011) described in their literature “Accurate non iterative fault location algorithm utilizing two-end unsynchronized measurements “, a phasor based technique for fault location. But they did not discussed the impact of series capacitor protection unit in fault location and phase of the fault.

J. Izykowski, E. Rosolowski, P. Balcerek, M. Fulczyk, M.M. Saha (2011) described in their literature “Fault location on double-circuit series-compensated lines using two-end unsynchronized measurements“, a fault location technique on double-circuit series-compensated lines using two-end unsynchronized measurements. Here MOV is considered in its natural environment avoiding any modeling inaccuracies. But series capacitor protection unit operation has not been considered.

R. Rubeena, M.R. D. Zadeh, T.P.S. Bains (2013) in their literature ,” Challenges and Recommendations for Fault Location in Series Compensated Transmission Lines “,described a brief introduction to phasor-based fault location algorithm. Then the impacts of SCPU operation and series capacitor location on fault location are investigated along with the analysis. But fault phase detection part is not done, application of the proposed algorithm in case of any communication link failure is not discussed and fault direction estimation part is also not discussed.

C. W. Liu, K. P. Lien, C. S. Chen, and J. A. Jiang (2008) told in the literature ,“ A universal fault location technique for –terminal transmission lines “ about a method which can identify the faulted sections by multi-end measurements first and then locate the fault along the identified section by the double-end methods. But it needs proper knowledge about line parameters (R,L,C) and line length which can vary depending on weather conditions.

Y. Liao and S. Elangovan (2006) in their literature ,” Unsynchronized two-terminal transmission line fault-location without using line parameters“, described a fault location

Introduction

algorithm which does not require any prior knowledge about any line parameter to locate fault. But this method is having limitations in locating symmetrical fault.

Y. Liao (2008) in his literature ,” Transmission line fault location algorithms without requiring line parameters “, proposed another method which is capable of locating fault without having prior knowledge about transmission line parameters. But similar to previous method, it also have limitations to locate symmetrical fault.

Y. Liao and N. Kang (2009) proposed a fault location technique in their literature ,” Fault-location algorithms without utilizing line parameters based on the distributed parameter line model “, which uses iterative techniques to determine the fault location. But the process is time consuming and requires large memory requirements .

V Terzija , Z M.Radojevic and G Preston (2015) proposed a fault location technique in the paper,” Flexible Synchronized Measurement Technology-Based Fault Locator “, based on short line approximation of a short transmission line which does not require the knowledge about line parameters to locate fault. But problem regarding this algorithm is it does not use appropriate filtering technique and further , fault classification and phase detection are not done .

J. Ma, J. Li, J. S. Thorp, A. J. Arana, Q. Yang, and A. G. Phadke (2011) in their literature ,” A fault steady state component-based wide area backup protection algorithm “, describes a technique where The steady-state component of differential currents in each protection correlation region(PCR) is used to identify the PCR with the fault. But Simultaneous faults effects is not addressed here.

Z.He, Z. Zhang, W.Chen, O. P.Malik, andX. Yin (2011) in their literature ,” Wide-area backup protection algorithm based on fault component voltage distribution “, described a back up protection scheme based on fault component of voltage and current. In this scheme, the fault component of voltage at one terminal of the line is estimated by utilizing the measured values of fault component voltage and current at other terminals, and the faulted line is identified based on the ratio of estimated values to measured values. But lacuna in this work are the accuracy of the scheme depends on the estimated value and Composite fault cases are not addressed.

P.K. Nayak, A.K.Pradhan, and P. Bajpai (2014) describes a back up protection scheme in their literature ,” Wide-Area Measurement-Based Backup Protection for Power Network

Introduction

with Series Compensation “,which compares the magnitude of sequence voltages of buses at a system protection center to identify the bus closest to the fault. But they also not discussed the effect of simultaneous fault cases.

Singh S.N (2001) described a technique in his paper titled ,” Location of FACTS devices for enhancing power systems security“, which uses Sensitivity analysis for placing FACTS devices and reduction in real power flow performance index to enhance security of power system. But he did not considered the effect of multiple contingency combinations .

Rao R.S and Rao V.S (2014) described in their literature titled, “Comparison of Various Methods for Optimal Placement of FACTS devices “,Compared various FACTS placement methods . But Overload handling not considered after the FACTS placement.

Rao R.S and Rao V.S (2015) proposed a generalized approach for optimal location of FACTS devices based on total system loss sensitivity indices and real power flow PI sensitivity indices in their article titled ,” A generalized approach for determination of optimal location and performance analysis of FACTS devices“. But multiple contingency not considered and after placement of FACTS devices if the current flow exceeds limit then how to tackle is not stated.

Sheth A, Kotwal C.D and Pujara S (2015) applied heuristic types of procedures for optimum FACTS placement in the literature titled ,”Optimal Placement of TCSC for Improvement of Static Voltage Stability“. But here also multiple contingency and overload conditions are not considered.

Ziae O and Choobineh F (2017) propose a novel decomposition procedure for determining the optimal location of TCSC and their respective size for a network in their article titled ,” Optimal Location Allocation of TCSC Devices on a Transmission Network “. But Overloading and multiple contingency cases are not considered here also.

J. Urdaneta, R. Nadira, and L. G. Perez (1998) uses linear programming technique for optimal relay coordination in their literatura titled ,” Optimal coordination of directional overcurrent relays in interconnected power system “. But problem regarding this technique is the solution will not come unless all the constraints are satisfied.

H. Zeineldin, E. El-Saadany, and M. A. Salama (2006) has done optimal co ordination of overcurrent relays by using Particle swarm optimization in his literature titled ,” Optimal coordination of overcurrent relays using a modified particle swarm optimization “. But there are

two types of problem exist in this approach. First one is mis coordination and other one is lack of solution for relays with both discrete and continuous time setting multipliers (TSMs).

J.Sadeh, V.Aminotojari and M.Bashir (2011) suggested a technique for relay coordination among distance and overcurrent relays using hybrid GA in their literature ,”Optimal coordination of over current and distance relays with hybrid genetic algorithm “. But problem regarding this technique is Slow convergence & fixed over current relay characteristics (no use of intelligent characteristics) although 8 kinds of intelligent overcurrent relay characteristics available in digital relays.

M.Singh, B.K.Panigrahi and A.R.Abhyankar (2013) described a technique for relay coordination using Teaching Learning based Optimization (TLBO) in their literature ,”optimal coordination of directional over-current relays using teaching learning-based optimization (TLBO) algorithm “. But here also they used fixed characteristics (Standard IDMT). Intelligent overcurrent relay characteristics available in digital relays are not used.

1.3 Motivation and Objectives of the Thesis

From the literature survey following observations are made on the research area to motivate :

- I. The various problems faced by power systems due to weak voltage profiles should be reviewed and also the solution for a better, reliable power supply in wide area power systems needed to be tried to achieve.
- II. Designing efficient backup protection scheme capable to support even in case of simultaneous faults in power system.
- III. Proper compensation should be provided in the network to increase power transfer capability, scarcity of reactive power in the network if any and smooth voltage profile etc via fixed capacitor or by using FACTs devices. Now a days , trend is to use FACTs devices more instead of using any fixed capacitor.
- IV. Proper relay coordination should be arranged to ensure a smooth and uninterrupted power supply.

1.4 Contributions

This thesis work has made an effort to develop an improved and reliable wide area protection system which fulfils all the aspects discussed above. The thesis proposes different aspects like fault location, detection, identification techniques; backup protection even in case of simultaneous faults; optimum FACTs placement and improvement of voltage profiles by using series compensation and intelligent relay co-ordination with a novel technique, which converges in fastest CPU elapsed time with respect to other contemporary techniques.

The main contributions are as follows:

1)Strength Of Standard IEEE Power Systems : This work reviews various problems associated with power system protection due to weak voltage profiles and also suggested solution for a better , reliable power supply in wide area power systems. Based on this review work , the strength of the buses are determined from their voltage profiles after running the load flow.

2) Distance relay performance evaluation on series compensated transmission line under faulted conditions- In this work a novel methodology is proposed to identify faulty phases based on correlation factor computation. The proposed method is tested on series capacitor compensated transmission lines (SCCTLs) with their different configurations and contingency combinations. Distance characteristics are also drawn for various zones of protection based on polar plot of impedance, which is helpful in two ways : i) Determination of zone of fault ii) Fault direction estimation based on the value of the angle (or sign of the angle).

3) A Synchrophasor Measurement-Based Fault Locator with Novel Fault Detection Technique- This work presents a numerical algorithm for locating fault in a short transmission line with improved accuracy. This algorithm is independent of the line parameters for locating fault and accuracy of the algorithm is improved by using filtering algorithm. A fault classification approach by use of zero sequence components of power and a faulty phase detection approach by the study of change of phase currents are also presented in this work.

4) An Efficient Fault Locating Technique with Backup Protection Scheme Using Wide Area Measurement for Power System with Simultaneous Faults- This work presents a synchronized phasor measurement-based wide-area backup protection scheme which uses the

magnitude of sequence voltages of buses at a system protection centre to identify the faulted bus closest to the fault and faulted line. The technique is tested for various faults including simultaneous faults in various systems. The study of new backup protection scheme is done on a WSCC-3 machine-9 bus system and an IEEE 14 bus test system.

5) Optimal placement of TCSC and TCPAR using sensitivity analysis –The contributions of the work are manifold. First of all, the network in single and multiple contingency combinations is considered. TCSC and TCPAR are placed using sensitivity analysis keeping constraints as reduction of line losses i.e energy savings. In the proposed technique a practical approach is considered by taking the effect of change of generations. Secondly, it describes the procedure about how to handle the power network during overloading of any line of the system.

6) Optimal Combined Over current and Distance Relays Coordination using Teaching Learning based Optimization- Relays should be organised such a way that every relay should have a backup and Coordination time interval between primary and back up and different zones of the relay should be maintained. In this work, distance and over current relays are used in pair. Relay co-ordination is done on an IEEE 5-bus, 6-bus system, WSCC-3-Machine-9-Bus, IEEE 14-bus and IEEE 30-bus system. Teaching Learning Based Optimization Technique (TLBO), a recent meta-heuristic technique, is used along with incorporation of different intelligent relay characteristics available in digital relay. Results are compared with GA and PSO. Minimization of number of relays using network graph theory is also presented as an extension of the work.

1.5 Organization of the Thesis

The thesis work is organized into eight chapters and presented as follows :

The first Chapter describes an introduction and state of art on several issues of power system protection. Brief introduction of Wide Area Monitoring systems (WAMs) and Phasor measurement unit(PMU) have been presented. The scope of the work has been highlighted and author's contribution in the research area has been summarized.

The second Chapter presents the algorithms for load flow solutions and their advantages, disadvantages; Indian Electricity Rules for permissible fluctuation of voltage; top view of IEEE 57, 118 and 300 bus test systems constructed in Power World software ; improvement of voltage profile and power flows after inserting series capacitor in the IEEE 57

bus test system and strong and weak bus voltages of IEEE 118 and 300 bus test systems after running Newton Raphson Load Flow(NRLF). Based on the review, the strength of the buses are determined from their voltage profiles after running the load flow. Application of NRLF is found to be the best solution among load flow algorithms. Voltage profile, active power transfer capability improvement and mitigation of scarcity of reactive power in power network can be done by inserting series capacitor in the circuit.

A compensated line imposes problems to directional relaying schemes due to Voltage and current inversion situations, operation of metal oxide varistor (MOV) protecting series capacitor and reactance modulation issues. **The third Chapter** presents a work related to distance relay and directional relaying aspect of series compensated transmission line. In this work the behaviour of series compensated EHV transmission lines during faults is simulated. The use of series capacitors for compensating part of the inductive reactance of long transmission lines increases the power transmission capacity. Emphasis is given on the impact of modern capacitor protection techniques (MOV protection).A novel methodology is proposed to identify faulty phases based on correlation factor computation. Under various fault conditions the proposed method is tested for its validation. The proposed method is tested on series capacitor compensated transmission lines (SCCTLs) with their different configurations and contingency combinations and performance is observed with transmission line both end voltage profiles. Distance characteristics are also drawn for various zones of protection. Simulation results show that proposed method has identified correct fault location.

Exact fault location detection is vital for power system restoration and security purposes. The line parameters plays a key role for accurately detecting fault location in a transmission line of a power network. In other fault location algorithms, line parameters used are approximately constant and they varies with weather and loading conditions also. So, an algorithm which is independent of the line parameters, is more accurate , flexible and robust. The **fourth Chapter** presents a work, which proposes a numerical algorithm for locating fault in a short transmission line with improved accuracy. This algorithm is independent of the line parameters for locating fault and accuracy of the algorithm is improved by using filtering algorithm. The performance of the algorithm is tested on several power networks by Simulation carried out by PSCAD/EMTDC. It is found that the accuracy of the algorithm can be further improved by using a Butterworth 2nd order and 4th order filter ,which is used for

the better refinement of collected current and voltage signals and to eliminate unwanted frequency components. A fault classification approach by use of zero sequence components of power and a faulty phase detection approach by the study of change of phase currents are also presented in the work.

The **fifth chapter** presents a synchronized phasor measurement-based wide-area backup protection scheme which uses the magnitude of sequence voltages of buses at a system protection centre to identify the faulted bus closest to the fault and faulted line. The technique is tested for various faults including simultaneous faults in various systems. The scheme is found to be accurate and fast with today's synchronized measurement technology. Analysis using simultaneous faults is a novel contribution in this work. It is expected that this scheme will reduce the number of disastrous blackouts and improve the reliability and security of the power system. The required information is able to distinguish between balanced and unbalanced fault in the system. The study of new back up protection scheme is done on a WSCC-3 machine-9 bus system and an IEEE 14 bus test system. The data is simulated through EMTDC/PSCAD and MATLAB /SIMULINK softwares.

Optimal placement of Flexible AC Transmission System (FACTs) devices are very important for maintaining proper power system performance. The **sixth chapter** presents an optimal placement approach of two well-known FACTs devices, Thyristor controlled series capacitor (TCSC) and Thyristor controlled phase angle rectifier (TCPAR) based on sensitivity analysis. In this method, reduction of line losses and overloading are taken care of. Sensitivity indexes are used to find proper place of FACTs devices in the network. After placing FACTs devices the performance of the network is also analyzed. Which FACTs device is more suitable for the network is also analyzed with the impact of change of generation. Effectiveness of the method is tested on a WSCC-3-Machine-9 bus system and an IEEE 57 bus test system with various single and multiple contingency combinations. The results obtained are accurate and satisfactory. The whole simulation work is done by using Power World 12.0 commercial version.

Relay coordination is an important aspect to maintain proper power system operation and control. Relays should be organized in such a way that every relay should have a backup and Coordination time interval (CTI) between primary and back up and different zones of the relay should be maintained to achieve proper fault identification and fault clearance

Introduction

sequence. The relays should operate in minimum desirable time satisfying all the co-ordination constraints. So, relay coordination is nothing but highly constraint problem. Heuristic techniques are often used to get optimal solution of this kind of problem. In the **seventh chapter** this constraint problem is solved by Teaching learning based optimization(TLBO) on several test systems from IEEE 5 bus to IEEE 30 bus test system. Proper desirable time setting multiplier (TSM) with minimum operating time of relays are calculated. We also incorporated intelligent over current relay characteristics selection to get the desired results in this work. The results seem to be satisfactory as the results obtained from TLBO are comparatively better than so called conventional methods like Genetic Algorithm(GA) and Particle Swarm Optimization (PSO).

Chapter eight presents the conclusions and future scope of research of this whole work.

The appendix and the references are mentioned at the end of the thesis.

Chapter 2

Strength of Standard IEEE Power Systems

Chapter 2

Strength of Standard IEEE Power Systems

2.1 Introduction

Bus is an important component of power system. Weak voltage profile of buses is a serious problem in power network which can harm the security and reliability of power system. Whenever there is a change in load, the system voltage level changes. The demand of reactive power in power system increases with the drop in voltage level. If the reactive power demand is not met, then it leads to further decline in bus voltage resulting in the cascading effect on adjacent power networks. Hence determination of the strength of buses and maintaining the voltage profile within permissible limits becomes essential. This work reviews various problems faced by power systems due to weak voltage profiles and its solution for a better, reliable power supply in wide area power systems. This review work presents algorithms for load flow solutions and their advantages, disadvantages ;Indian Electricity Rules for permissible fluctuation of voltage ; top view of IEEE 57 ,118,300 Bus test system constructed in Power World software ; improvement of voltage profile and power flows after inserting series capacitor in the IEEE 57 bus test system and strong and weak bus voltages of IEEE 118 and 300 bus test systems after running NRLF.

Bus bar in a power system is a metallic strip responsible for conducting electricity in a substation ,electric grid , battery bank or other electrical apparatus. Bus bar is usually made of copper ,brass or aluminium. Bus bar are of variety of shapes.e.g.- flat strips , solid or hollow tubes etc. Bus bar should be robust enough to support its own weight ,mechanical vibrations and earthquakes also. Bus bars are typically placed inside switchyard ,control panels etc. Busbar should have proper insulators . In substations mainly two bus system is used . The concept of two bus system is like that every feeder of the two bus system is connected with two different busbars. e.g- Main bus system and transfer bus system. The main bus is connected to each feeder through a circuit breaker. One bus coupler couples main and transfer bus through a circuit breaker and isolator. Voltage profile in bus bars in Wide Area Systems is an important parameter w.r.t the security and reliability issue of

the power system. Whenever there is a change in load the system voltage level changes. With the drop in voltage level, the reactive power demand increases. If the reactive power demand is not satisfied, then it leads to further decline in bus voltage resulting in the cascading effect on adjacent power systems. So, maintaining the voltage profile within permissible limits becomes necessary and essential [17]. To improve the voltage profile, series capacitor is used in the circuit. It increases active power transfer capability and supply some portion of reactive power also [31]. To control the reactive power synchronous motor is used at distribution level or 132 KV level, shunt inductor is used at 400 KV, 765 KV, 1000KV and 1200 KV at the receiving end substation. Inductor is preferred to account the possible Ferranti effect voltage at light load conditions[32]. Voltage control devices (e.g- Shunt Capacitor, Synchronous motor, FACTs devices) are usually placed at load station. A true load station does not have capability to control the reactive power. Hence, it is called a PQ bus. But a load bus is a reactive power control element and have the capability to maintain voltage profile to control reactive power and maintain voltage profile. This type of bus is called voltage controlled bus [33].

2.1.1 Load Flow Study – Load flow refers to the calculation of (V and δ) complex bus voltages, such that all buses except slack bus subjected to the given loading conditions, enforcing Q limits, tap limits and tie line power flow limits [34].

Usually a centrally located large generating station is selected as slack bus (or swing or reference bus).

Voltage profile or power transfer capability can be improved by inserting capacitor between relatively weak voltage buses of a Wide Area system. This process not only affect the buses between which the capacitor is placed but also has a cascading effect in the whole network. Specially adjacent buses of sending and receiving end sides are mostly affected. By improving the voltage profile the reliability, stability and security of the system is largely improved.

Tajudeen et al., [31] proposed improvement of voltage profile by applying concepts of circuit theory and by Y-admittance matrix on networks. Eigen value decomposition and partitioned Y-admittance matrix determines the location for VAR compensators. Buses associated with smallest Eigen value have dominant influence on entire voltage of network on the basis of inversely proportional relation existing between bus voltage and Eigen values. This

reveals the highly suitable locations for allocating VAR compensators. State variables of VAR compensators are consisted in load flow techniques and hence power flow solution can be used to determine the appropriate compensators sizes [17].

Most of the problems faced by the power system can be resolved by internal relationship among its parameters. Tajudeen et al., [35] have discovered the characteristic indices based on inherent structure using partitioned Y-admittance matrix. Ideal generators, affinity of generator and effect of structure on generator and load electrical attraction regions have contributed for the value of the indices. With the indices generator locations can be specified to inject maximum real power in the power system. For solution of load flow problem, the linear equations can be solved directly by several methods. e.g.- Cramer's rule, Inverse technique, Gauss seidel method, Cholesky method etc.

The several iterative techniques for load flow study are:

- a) Gauss method
- b) Gauss Seidel method
- c) Newton – Raphson method (NR method)
- d) Fast – Decoupled method

Out of the above methods, NR method is used in our work. We feel it is the best out of the lot [33].

2.1.2 Well conditioned and ill-conditioned system- A power system is characterized as, well conditioned system w.r.t good X/R ratio and good convergence characteristics. Usually a well conditioned system having X/R ratio more than 5. Highly mesh connected or interconnected systems usually have all the above properties. Hence they are treated as well-conditioned. But distribution network is highly radial system and it has low X/R ratio and exhibits poor convergence characteristics. Therefore they can be treated as ill-conditioned system [36]. An ill-condition system having X/R ratio maximum 1-2 , or even below 1.

2.1.3 Gauss Method - In Gauss method, initially we have to start with a guess voltage. $(k+1)^{th}$ value of iteration can be calculated using below formula [34]-[37]:

```

graph TD
    a((a)) --> S1["Select highest voltage of the voltage levels of all the buses connected to bus a"]
    S1 --> S2["Find the bus with the selected voltage"]
    S2 --> S3["If voltage compensation is involved in the faulted bus, then do the voltage compensation when required to"]
    S3 --> S4["Apply appropriate relaying algorithm"]
    S4 --> Stop[Stop]
  
```

K is the previous iteration count

K+1 is the present iteration count

In Gauss method, updation of bus voltage is done only at the end of one full iteration. Latest values are not used by Gauss method. Therefore it takes too many iterations to converge. The solution time become prohibitively large. Thus Gauss method is not used in our load flow studies.

2.1.4 Gauss-Seidel Method(GS) : Seidel has overcome the above disadvantage by updating the bus voltage immediately and always uses the latest bus voltage(E_P^{K+1}).

$$E_P^{K+1} = \frac{1}{Y_{PP}} \left[\frac{P_P - jQ_P}{E_P^{K*}} - \sum_{\substack{p=1 \\ p \neq q}}^{p-1} Y_{pq} E_q^{K+1} \right] \quad (2)$$

Now calculate

$$\Delta E_P^{K+1} = E_P^{K+1} - E_P^K \quad (3)$$

$$E_P^{K+1} = E_P^K + \alpha \Delta E_P^{K+1} \quad (4)$$

α is called as acceleration factor.

2.1.5 Significance of acceleration factor : The acceleration factor largely affects the convergence of the algorithm. It is found that the value of α between 1.4-1.7 gives the best voltage through iterations. The impact of various acceleration factors in GS is discussed below [34]-[37]:

$\alpha = 1$: No acceleration is used. So, takes more iteration to converge.

$\alpha = 1.2$: Little acceleration is used. A little bit improvement, convergence is observed.

$\alpha = 1.4-1.7$: Found to be best range to reduce number of iterations. It is best range by trial and error approach.

5 bus system : $\alpha = 1.4$: Converged in 10 iterations.

14 bus system : $\alpha = 1.55$: Converged in 17 iterations.

30 bus system : $\alpha = 1.6$: Converged in 28 iterations.

57 bus system : $\alpha = 1.55$: Converged in 58 iterations.

118 bus system : $\alpha = 1.7$: Converged in 97 iterations.

1040 bus system : $\alpha = 1.7$: Converged in 980 iterations.

$\alpha = 1.8$: Causes very big acceleration which leads to non-linearity and further it causes numerical divergence.

So, α is to be selected by us optimally for a given power system .

In GS-method number of iterations for convergence is proportional to size of the system. So, solution time will be very large for big power systems. Though, GS method is simple in nature ,it cannot be used for real time study of a big system.

2.1.6 PV-Bus treatment : At PQ bus P_p and Q_p are known. So equation(2) can be easily solved to get E_p^{K+1} . For slack bus all the values are referenced value. At PV bus Q_p is not known. It must be

$$Q_{\min} \leq Q_p \leq Q_{\max} \quad (5)$$

Now calculation at PV bus or PV bus treatment is as follows :

At PV bus V_{sp} , Q_{\min} , Q_{\max} , Q_{load} are given

$Q_p = Q_{gen} - Q_{load}$ = Injected reactive power.

In PV bus treatment , we must enforce Q limit w.r.t $Q_{\max,inj}$ and $Q_{\min,inj}$ as we calculate Q_p as injection value .

$$\text{Let } E_p^K = e_p^k + j f_p^k \quad (6)$$

$$\delta_p^k = \tan^{-1} \left(\frac{f_p^k}{e_p^k} \right) \quad (7)$$

$$e_{\text{new}} = V_{SP}(P) \cos(\delta_p^K) \quad (8)$$

$$f_{\text{new}} = V_{SP}(P) \sin(\delta_p^K) \quad (9)$$

$$E_{\text{new}} = e_{\text{new}} + j f_{\text{new}} \quad (10)$$

$$I_{\text{new}} = Y_{pp} E_{\text{new}} + \sum_{q \neq p}^n Y_{pq} E_q^{k+1} \quad (11)$$

$$= Y_{pp} E_{\text{new}} + \sum_{q=1}^{p-1} Y_{pq} E_q^{k+1} + \sum_{q=p+1}^n Y_{pq} E_q^k \quad (12)$$

Complex power injection

$$= E_{\text{new}} I_{\text{new}}^* \quad (13)$$

$$Q_{\text{new}} = \text{Imaginary}(S_{\text{new}}) \quad (14)$$

If $Q_{\text{new}} < Q_{\min,inj} - Q_{\text{new}}$ is violating lower limit

If $Q_{\text{new}} > Q_{\text{max,inj}}$ - Q_{new} is crossing the upper limit

When

$Q_{\text{min,inj}} \leq Q_{\text{new}} \leq Q_{\text{max,inj}}$ - Q_{new} is within Q limits

Q_{min} and Q_{max} are called Hard limits and V_{max} and V_{min} are called soft limits.

In GS method we can enforce the Q limits, that comes under the category of Q-adjusted study. Q-unadjusted study is not possible in GS as in that case Q_{min} and Q_{max} have wide limits, so V_{sp} can easily be maintained.

PV bus is supposed to maintain the specified voltage but when Q_{new} violates the lower limit or upper limit, it will be converted into PQ bus category. Where, the voltage is not allowed to vary as per load conditions.

When Q_{new} are within the limit, the PV bus is having the ability to maintain V_{sp} , and hence maintains the PV bus status.

2.1.7 Merits of the GS Method :

- i) Very simple to understand.
- ii) Easy to write full length program including sparsity aspect.
- iii) It takes less time per iteration. In GS method linear convergence is observed..
- iv) It needs very less memory.
- v) Easy to enforce Q-limits at PV buses.
- vi) Easy to simulate line outage or transformer outage.

In practical power system, a line gets disconnected by opening of circuit breaker at both ends. Electrical disconnection means the impedance is infinity[34]. we put

$$R(K) = 10^{20} \text{ p.u}$$

$$X(K) = 10^{20} \text{ p.u}$$

$$Y_{cp} = 0.0$$

$$Y_{cq} = 0.0$$

and modify appropriate Y_{bus} locations and then run GS method. (Y_{cp}, Y_{cq} are shunt conductances).

vii) Easy to simulate generator outage.

(put $P_{\text{gen}}(i) = 0$ and $V_{\text{sp}}(i) = 1.0$

2.1.8 Demerits of the GS Method :

- i) Number of iterations proportional to the size of the system.

5bus- 10 iterations
 14 bus-17 iterations
 30 bus -28 iterations
 57 bus-56 iterations
 118 bus-98 iterations
 1040bus- 990 iterations

Total solution time is prohibitively large for large power system. GS is not useful for real time applications. We can make use of GS method to have better exposure and experience in load flow solution of power system if it is used for small systems as planning stage studies i.e off-line study.

- ii)It demands good slack bus position (Centrally located big Generating station to be as slack bus).
- iii)Acceleration factor is to be selected by trial and error for optimum value.
- iv)It fails to converge on overload system, ill-condition system ,radial system.

2.2 NR load flow(NRLF) : NR method is proposed by Tinney Peterson (1963). In NR method all buses are updated simultaneously. This becomes a very strong point for good convergence for NR. In power system load flow solutions many of the other algorithms except NR, may fail to converge on ill-conditioned system (X/R ratio low) but NR method, exhibits good convergence (Quadratic convergence characteristics) in all types of power system even loading conditions are ill-conditioned. Thus we normally call NR as parent load flow algorithm[37].NR method can be described by the following equations :

$$\begin{bmatrix} \Delta P \\ \Delta Q \end{bmatrix} = \begin{bmatrix} H & N \\ M & L \end{bmatrix} \begin{bmatrix} \Delta \delta \\ \Delta V/V \end{bmatrix} \quad (15)$$

2.2.1 Merits of NRLF :

- i)NR exhibits quadratic convergence characteristics and converges within 3 iterations for a very high accuracy of 0.0001 p.u for ΔP_{\max} and ΔQ_{\max} .
- ii) No. of iterations are independent of size of the system .

5 bus – 3 iterations
 14 bus – 3 iterations

30 bus – 3 iterations

57 bus – 3 iterations

118 bus – 3 iterations

1040 bus- 3 iterations

iii) It converges on ill-conditioned systems , well conditioned system and overloaded power system.

iv)Easy to simulate line outages and generator outages.

v)Easy to enforce the Q limits (i.e $Q_{adjusted}$ load flow is possible).

vi) NR is not affected by the location of slack bus position.

2.2.2 Demerits of NRLF :

i)Total CPU time is very large. To reduce the total CPU time, we need to use sparsity technique even for Jacobian elements. The modern practice is to use sparsity technique for jacobian of NRLF and make it as a potential algorithm for online load flow solution as well.

2.3 Advanced Newton's Decoupled (NDC) / Fast Decoupled(FDC) Load Flow Method :

Fast Decoupled method is proposed by Brain Stott in 1973. It is an advanced version of NRLF. So, it is called Newton's Decoupled method (NDC) also. Here weak coupling between M and N is assumed. So, it becomes as follows[34]-[37]:

$$\begin{bmatrix} \Delta P \\ \Delta Q \end{bmatrix} = \begin{bmatrix} H & 0 \\ 0 & L \end{bmatrix} \begin{bmatrix} \Delta \delta \\ \Delta V/V \end{bmatrix} \quad (16)$$

$$[\Delta P] = [H] [\Delta \delta] \quad (17)$$

$$[\Delta Q] = [L] \begin{bmatrix} \Delta V \\ V \end{bmatrix} \quad (18)$$

The above relations can be represented as

$$\begin{bmatrix} \Delta P \\ V \end{bmatrix} = [B'] [\Delta \delta] \quad (19)$$

$$\begin{bmatrix} \Delta Q \\ V \end{bmatrix} = [B''] [\Delta V] \quad (20)$$

The above equations(eqn. 19 & 20) are called FDC equations .

2.3.1 Merits of FDC :

- i)Two constant slope matrices (B' , B'') are used in FDC. They need to be formed and decomposed only once. So, large CPU time reduction is observed.
- ii)No. of iterations are independent of system size .

5 bus – 3.5 iterations ($\epsilon=0.0001$ p.u)

Q-unadjusted case:

14 bus -4.5 iterations

30 bus-4 iterations

57 bus-4.5 iterations

118 bus- 4.5 iterations

1040 bus -4.5 iterations

For Q-adjusted case, another 2-3 iterations are required (6-7.5 iterations).

- iii)Total solution CPU time is low. It is very widely used in real time studies.

Any learner should attempt GS method first, then directly FDC and if failed , then should attempt by NR method for load flow solutions.

iv) Sparsity technique can be used easily for B' , B'' formation and also for decomposition.

v) No special guess voltages are required. Flat start assumed ($V= 1+j0$) is correct.

2.3.2 Demerits of FDC :

i) Enforcement of Q-limit is very difficult .

ii)Line outage simulation will change the structure of B' and B'' . They need to be reformed and retriangularised .

2.4 Best Suitable Method for our Work :

FDC exhibits Geometric convergence characteristics. It takes less memory (50% of NR) and total solution CPU time is also very low. But it may exhibit slow convergence or in some cases fail to converge on ill-condition system. Proper selection of slack bus position is required for FDC method. In other words, convergence of FDC is influenced by the location of slack bus but it is not in case of NR. So, NR is the best method among iterative techniques of load flow study.

In our work, we have used Power World 12.0 commercial version to create IEEE 57, IEEE 118 and IEEE 300 Bus system and run NRLF to find relatively weak voltage profile buses in that Wide area systems. Then we placed capacitor of different compensations between weakest buses and again run NRLF. The we find the impact of the capacitor in whole network in terms of sending end voltage, receiving end voltage, active power and reactive power. We compared the results with before and after compensation cases.

2.5 General View About Power World Simulator

Power world simulator is an interactive power system simulation package designed to simulate high voltage power system operation on a time frame ranging from several minutes to several days. The software contains a highly effective power flow analysis package capable of efficiently solving systems of up to 250,000 buses. Power world software is capable of doing load flow study, contingency analysis, fault analysis, sensitivity analysis, optimal power flow analysis etc of network.

2.6 Different Voltage Levels and Permissible Voltage Fluctuations

The voltages are classified into following levels as per IEC (International Electrotechnical commission)[38].e.g.-

- 1) Low Voltage – up to 1000 volts only.
- 2) Medium Voltage – 1KV to 33 KV.
- 3) High Voltage – 33 KV to 245 KV
- 4) Extra High Voltage – above 245 KV
- 5) Ultra High Voltage – above 800 KV

As per Indian Electricity Rules, except with the written consent of the consumer or previous sanction of the state Government a supplier shall not permit the voltage at the point of commencement of the supply as defined under rule 58 to vary from the declared voltage as follows :

- i) In case of low or medium voltage by more than 6%.
- ii) In the case of high voltage, by more than 6 per cent on the higher side or by more than 9 per cent on the lower side.
- iii) In the case of extra high voltage, by more than 10 per cent on the higher side or by more than 12.5 per cent on the lower side.

So, in any test system voltage goes beyond lower or upper limit is a threat for power system. Our work is an effort to maintain a good voltage profile and improved power transfer capability of Wide area power systems.

2.7 Simulated Test Systems

In Power World Simulator 12.0 commercial version we have created IEEE 57, IEEE 118 and IEEE 300 bus test system and then run NRLF to find weakest bus and strongest bus. Then we placed capacitors with different compensations between weak profile buses and observed their impact on the network. Fig 1 is showing constructed IEEE 57 bus test system by using power world software. Fig 2 is showing constructed IEEE 118 bus test system by using power world software. Fig 3 is showing constructed IEEE 300 bus test system by using power world software.

The sources of relevant data for construction of these test systems are shown in Appendix-A.

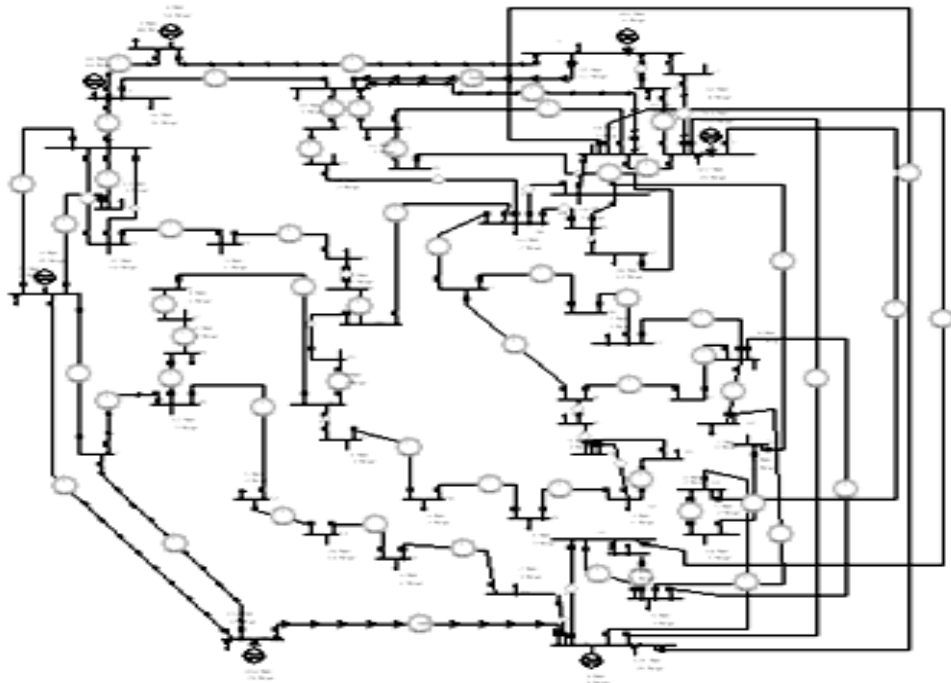


Fig 1 :IEEE 57 Bus Test System in Power World Software(Top View)

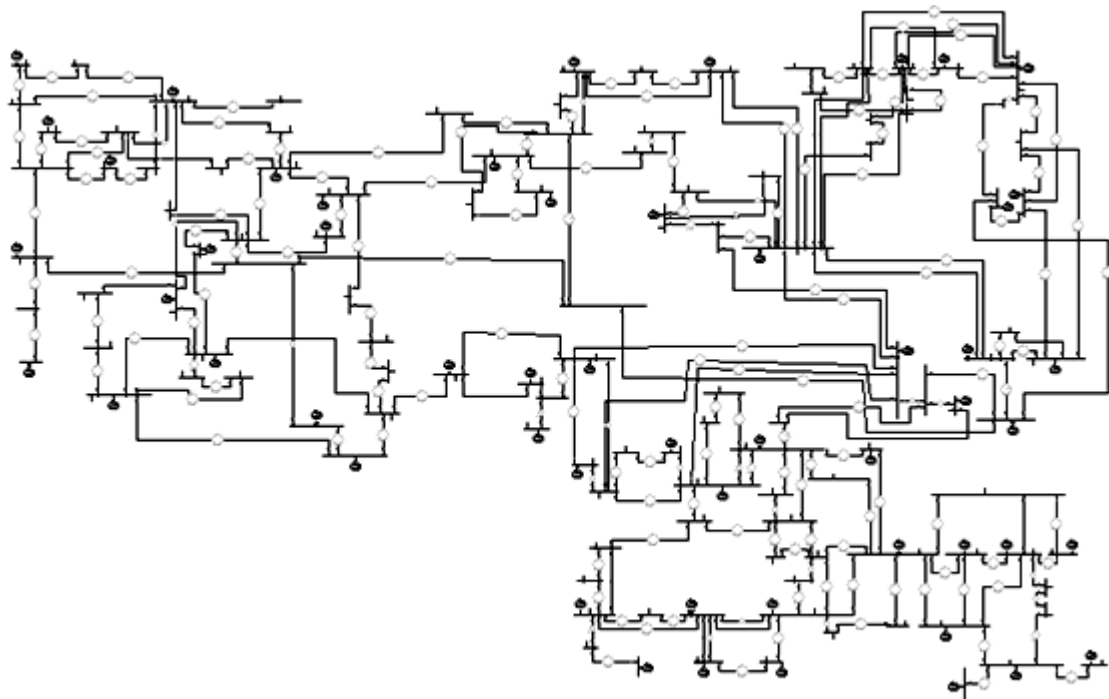


Fig 2 : IEEE 118 Bus Test System in Power World Software(Top View)

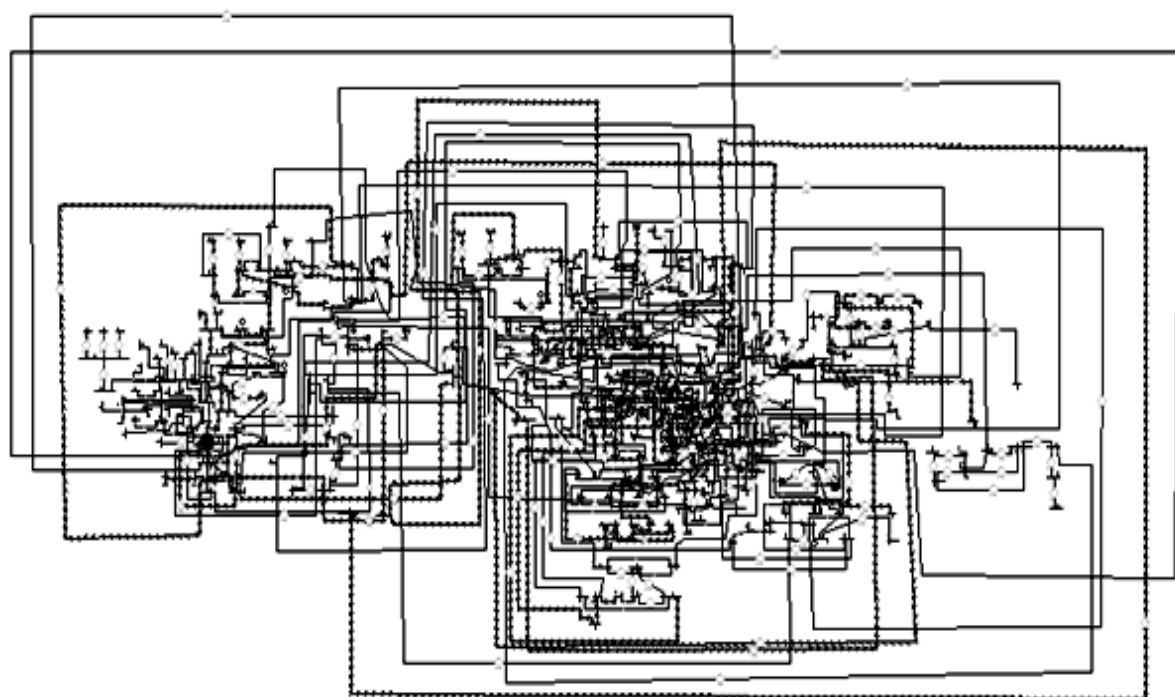


Fig 3 :IEEE 300 Bus Test System in Power World Software(Top View)

2.8 Results

After running NRLF to IEEE 57 Bus system we got Bus 51 is strongest bus having p.u bus voltage 1.01748 p.u and Bus 46 is 2nd strongest bus having p.u voltage 1.01098 p.u. After running the NRLF, we found 10 buses below 0.9 p.u., Which we termed as weak bus or weak voltage bus. The weakest bus we got at Bus no. 31(voltage 0.80779 p.u) and second weakest bus we got at Bus no. 30 (voltage 0.81367 p.u). We placed capacitor between bus 30 and bus 31 and run the NRLF again and listed values of corresponding bus voltages with 10% , 20% ,30% and 40% compensation.

We listed all the corresponding bus voltages (initially considered as weak buses) after placing capacitor in Table –1 and observed the Changes From Table-1. It is clear that after inserting series capacitor in line between bus 30 and bus 31, the voltage profile also changes.

Voltage profile improves towards receiving end and it slightly decreases towards sending end. With the increase of series compensation this effect gradually increases i.e. receiving end voltages gradually increase and sending end voltage gradually decreases. This incident resembles network's Ferranti effect phenomena. We considered up to 40% series compensation because beyond this value may affect network's stability.

Table- 1 Weak Voltage Profile buses of IEEE 57 Bus system (without compensation) : impact on bus voltages after implementing series compensation between bus 30 and bus 31

Bus No.	p.u volt				
	Without compensation	10% compensation	20% compensation	30% compensation	40% compensation
25	0.82652	0.82595	0.82534	0.82472	0.82407
26	0.89969	0.89963	0.89957	0.89950	0.89943
30	0.81367	0.81303	0.81234	0.81166	0.81094
31	0.80779	0.80813	0.80845	0.80880	0.80917
32	0.86481	0.86490	0.86498	0.86507	0.86517
33	0.86884	0.86892	0.86900	0.86908	0.86916
34	0.86884	0.86892	0.86900	0.86908	0.86916
35	0.88058	0.88064	0.88069	0.88075	0.88081
36	0.89445	0.89449	0.89453	0.89457	0.89461
40	0.89260	0.89265	0.89268	0.89272	0.89277

Table- 2 Transmission lines between weak Voltage Profile buses of IEEE 57 Bus system (without compensation) : impact on active and reactive power flow after implementing series compensation between bus 30 and bus 31

From bus	To bus	Active and Reactive Power Flow among Transmission Lines									
		Without compensation		10% Compensation		20% Compensation		30% Compensation		40% Compensation	
		MW	MVAR	MW	MVAR	MW	MVAR	MW	MVAR	MW	MVAR
25	30	2.4	3.7	2.4	3.7	2.3	3.7	2.3	3.8	2.3	3.8
26	27	-8.6	-9.6	-8.6	-9.6	-8.6	-9.6	-8.6	-9.7	-8.6	-9.7
24	25	8.7	9.0	8.7	9.0	8.6	9.1	8.6	9.1	8.6	9.2
30	31	-1.3	1.8	-1.3	1.8	-1.3	1.9	-1.3	1.9	-1.3	1.9
31	32	-7.1	-1.1	-7.1	-1.1	-7.1	-1.0	-7.1	-1.0	-7.1	-1.0
32	33	-8.1	-0.8	-8.8	-0.1	-8.8	-0.1	-8.8	0	-8.8	0
33	34	-12.7	-2.1	-12.6	-2.0	-12.6	-2.0	-12.6	-2.0	-12.6	-1.9
34	32	0.3	2.5	0.3	2.5	0.3	2.5	0.3	2.5	0.3	2.5
34	35	-12.9	-4.5	-12.9	-4.5	-13.0	-4.5	-13.0	-4.4	-13.0	-4.4
35	36	-19.1	-7.5	-19.1	-7.4	-19.1	-7.4	-19.1	-7.4	-19.1	-7.3
36	37	-21.5	-9.7	-21.5	-9.7	-21.5	-9.7	-21.5	-9.7	-21.6	-9.6
36	40	2.2	2.1	2.2	2.1	2.2	2.1	2.2	2.1	2.2	2.1
40	56	2.2	2.1	2.2	2.1	2.2	2.1	2.2	2.1	2.2	2.1

Table –3 : Strong and Weak Buses of IEEE 118 and IEEE 300 Bus system

Test System	Strong Buses		Weak Buses	
	Bus No.	Bus Voltage (p.u)	Bus No.	Bus Voltage (p.u)
IEEE 118 Bus	10	1.05	53	0.94404
	25	1.05	63	0.94963
	65	1.05	76	0.94300
	66	1.05	118	0.94826
	1	3.48586	43	1.03408
IEEE 300 Bus	22	3.53707	44	1.84137
	140	3.95060	257	1.03408
	141	4.04742	266	2.18921
	144	4.22221	288	2.19425

From the above Table-2, it is clear, after inserting series capacitor reactive power deficit in the circuit improves. The negative MVAr tends to go towards zero. Active power transfer capability is also improved. Table-3 describes strong and weak buses of IEEE 118 Bus and IEEE 300 Bus systems. IEEE 118 Bus system obeys the Indian Electricity Rules of voltage fluctuations and all the p.u voltage values are within permissible range of high voltage. IEEE 300 bus systems results are more fluctuating. But with the use of series capacitor, the voltage profile can be improved similar to IEEE 57 bus system.

2.9 Summary

In this chapter, the several problems associated with wide area power flow due to weak voltage profiles are reviewed. Based on the review , it can be said that the strength of the bus can be determined from its voltage profile after running the load flow. And in this context application of NRLF is the best solution. Voltage profile improvement , active power transfer capability improvement and mitigation of scarcity of reactive power in the power network can be done by inserting series capacitor in the circuit. This review has given an insight about strongest and weakest bus of the system, most suitable algorithm for the solution of load flow problem, different problems faced by power systems due to weak voltage profile and scarcity of reactive power in the network and their solution for a better voltage – reactive power balance for a reliable and secured operation of wide area power systems.

Chapter 3

Distance Relay Performance Evaluation on Series Compensated Transmission Line under Faulted Conditions

Chapter 3

Distance Relay Performance Evaluation on Series Compensated Transmission Line under Faulted Conditions

3.1 Introduction

A compensated line imposes problems to directional relaying schemes due to Voltage and current inversion situations and operation of metal oxide varistor (MOV) protecting series capacitor, reactance modulation issues. In this chapter the behaviour of series compensated EHV transmission lines during faults is simulated. The use of series capacitors for compensating part of the inductive reactance of long transmission lines increases the power transmission capacity. Emphasis is given on the impact of modern capacitor protection techniques (MOV protection). A novel methodology is proposed to identify faulty phases based on correlation factor computation. Under various fault conditions the proposed method is tested for its validation. The proposed method is tested on series capacitor compensated transmission lines (SCCTLs) with their different configurations and contingency combinations and performance is observed with transmission line both end voltage profiles. Distance characteristics are also drawn for various zones of protection. Simulation results show that proposed method has identified correct fault location.

use of series capacitors for compensating inductive reactance of long transmission lines increases the power transmission capacity. It also increases transient stability margins, optimizes load-sharing between parallel transmission lines and reduces system losses [39]. Transmission line compensation implies a modification in the electrical characteristic of the transmission line with the objective of increase power transfer capability .

Fast and accurate determination of a fault in electrical power system is a vital part in power restoration. In Power system majority of the faults are happened to be single line to ground fault. Other important types of faults are LLG, LLL, LL, LLLG faults. The presence of the capacitor in the circuit immediately after a fault is very important,

because it helps in improvement the transient stability of the system. Also in case of unbalanced faults, only the protection devices of the faulted phases operate leaving the capacitor of the other phases on line. It is indispensable to be able to model such devices in a fault analysis program and predict the level of short circuit currents as well as the energy absorbed by the conducting MOV.

Some of the advantages of series compensation of transmission line are listed below:

- 1) Reduces line voltage drop.
- 2) Limits load-dependant voltage drops.
- 3) Influences load flow in parallel transmission lines.
- 4) Increases power transfer capability
- 5) Highly effective in maintaining the desired voltage profile along the transmission line interconnecting two busses of the ac system and providing support to the end voltage of radial lines in the face of increasing power demand.

This chapter proposes a novel methodology to identify faulty phases of a transmission line which is tested on a series compensated transmission line through PSCAD/EMTDC simulation. This faulty phase identification algorithm gives better result compare to detection of faulty phase by imposing the tolerance limit method and the polar plot analysis gives more insight about the zone of the fault and chance of mal-operation.

3.2 Series Capacitor Effect On Distance Measurement:

Distance relays are designed to perform correctly on a resistive/inductive system. When series capacitors are introduced, the normal voltage/current relationships are affected, especially when the fault levels are not sufficient to flash-over the gaps or to produce significant conduction in the MOV's [40] .

3.3 Single And Multi-Phase Fault Detection :

Linear correlation coefficient r , measures the strength and the direction of a linear relationship between two variables. It is a measure of how similar the two signals or variables are. The mathematical formula for computing r is:

$$r = \frac{n \sum AB - (\sum A)(\sum B)}{\sqrt{n(\sum A^2 - (\sum A)^2)} \sqrt{n(\sum B^2 - (\sum B)^2)}} \quad (1)$$

Where n is the number of pairs of data. The value of r is such that $-1 \leq r \leq +1$. The + and - signs are used for positive linear correlations and negative linear correlations, respectively.

Positive Correlation: If A and B have a strong positive linear correlation, r is close to +1. An r value of exactly +1 indicates a perfect positive fit. Positive values indicate a relationship between A and B variables such that as values for A increases, values for B also increase.

Negative Correlation: If A and B have a strong negative linear correlation, r is close to -1. An r value of exactly -1 indicates a perfect negative fit. Negative values indicate a relationship between A and B such that as values for A increase, values for B decrease.

No-Correlation: If there is no linear correlation or a weak linear correlation, r is close to 0. A value near zero means that there is a random, nonlinear relationship between the two variables. r is a dimensionless quantity; It does not depend on the units employed. A Perfect Correlation of ± 1 occurs only when the data points all lie exactly on a straight line. If $r = +1$, the slope of this line is positive. If $r = -1$, the slope of this line is negative.

A correlation greater than 0.8 is generally described as *strong*, whereas a correlation less than 0.5 is generally described as *weak*. These values can vary based upon the type of data being examined. A study utilizing scientific data may require a stronger correlation than a study using social science data. These statistical concepts will be used for detection of the phases involves fault.

Algorithm for Proposed method:

Step1: Start

Step2: Sample the faulted voltage or current waveform during fault duration.

Step3: From the samples find out greatest change of current or least change in voltage containing sample.

The phase which containing greatest change of current or least change in voltage must contain fault. The change is considered to eliminate ZCD (Zero Crossing Detector) Problem.

Now check for whether two or more phases contain fault or not. This paper is concentrated particularly on the aspect when two or more phases contain fault or not. The computational steps as continues:

Step4 :Take I_a, I_b, I_c or V_a, V_b, V_c sample data during fault time and store it in three different variables A,B,C.

Step5: Now compute correlation between A&B,B&C,C&A.

Step6: Stop

If at least two values comes between -0.5 to -1 then all the phases involves fault(LLL or LLLG fault), or if any one value comes between -0.5 to -1 then that two phases involve with fault. Test results obtained from the algorithm are enlisted in Table 1 and Table 2 . Fig 1 shows the flow chart of the algorithm proposed.

Table 1
Test System-Series Capacitor Compensated Transmission Line with Protection Unit

Analysis with current variable: Fault Created at 140 KM distance. Faulted time (0.34-0.38sec).Series compensation 40% employed.

Type of fault created	r_{ab}	r_{bc}	r_{ca}	Faulty phases identified
LLL	0.14002289	-0.84169	-0.6524	All faulty
AB-G	-0.51618	-0.49752	-0.4861	A,B faulty
LLLG	-0.77963	-0.99386	-0.9938	A,B,C faulty
Ph-CA	0.4555593	-0.455791	-0.9999	A,C faulty

Table 2
Analysis with Voltage variable: Fault Created at 140 KM distance. Faulted time (0.34-0.38sec).Series compensation 20% employed.

Type of fault created	r_{ab}	r_{bc}	r_{ca}	Faulty phases identified
LLLG	-0.77959	0.723784	-0.99386	A,B,C faulty
Ph-CA	-0.46896	0.790685	-0.92395	C,A faulty
LLL	-0.54237	0.492593	-0.93517	A,B,C faulty

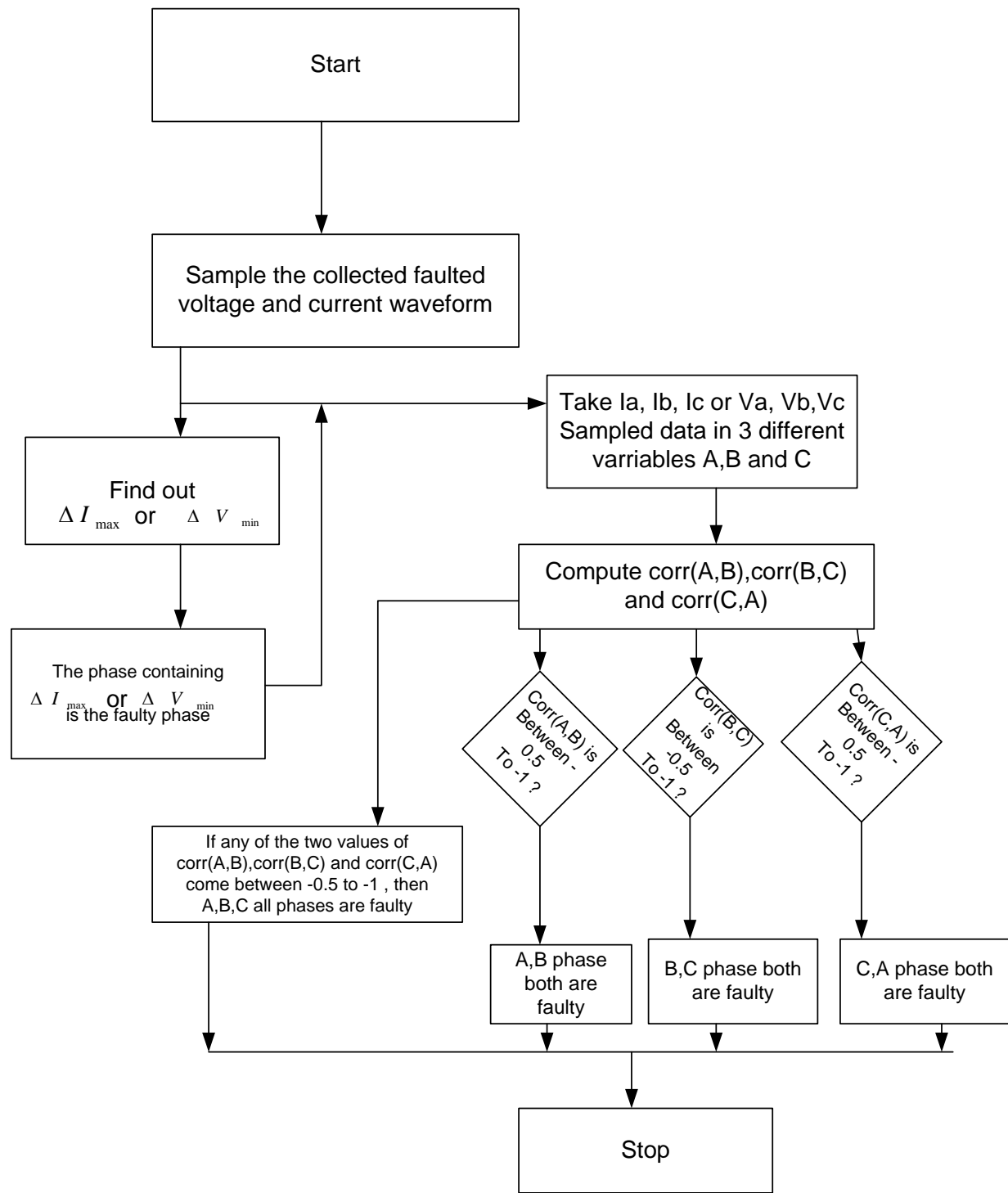


Fig 1 : Flow chart of the proposed faulty phase detection algorithm

3.4 Implementation

Fault location is computed using faulted voltage and current samples that described as below:

$$\text{Fault impedance } Z_f = \frac{V_f}{I_f} \text{ Ohm} \quad (2)$$

$$\text{Fault Location } d = \frac{Z_f}{Z_1} \quad (3)$$

Empirical formula of fault current

$$I_{F_i} = \frac{I_{S_i} + I_{R_i} \cosh(\gamma_i l) - \frac{V_{R_i}}{Z_{C_i}} \sinh(\gamma_i l)}{\cosh(\gamma_i l d)} \quad (4)$$

Fault Voltage

$$V_{F_i} = V_{R_i} \cosh(\gamma_i l(1-d)) - Z_{C_i} I_{R_i} \sinh(\gamma_i l(1-d)) \quad (5)$$

Fault loop equation

$$V_F(d) - R_F I_F(d) = 0 \quad (6)$$

More the length increases the algorithm for fault location identification gives more accurate value. In case of fault impedance, during healthy state positive sequence impedance (Z_1 Ohm/Km) present in the system and the value is given in the paper. V_f and I_f are obtained from the sampling of the waveforms after creation of different faults at different lengths.

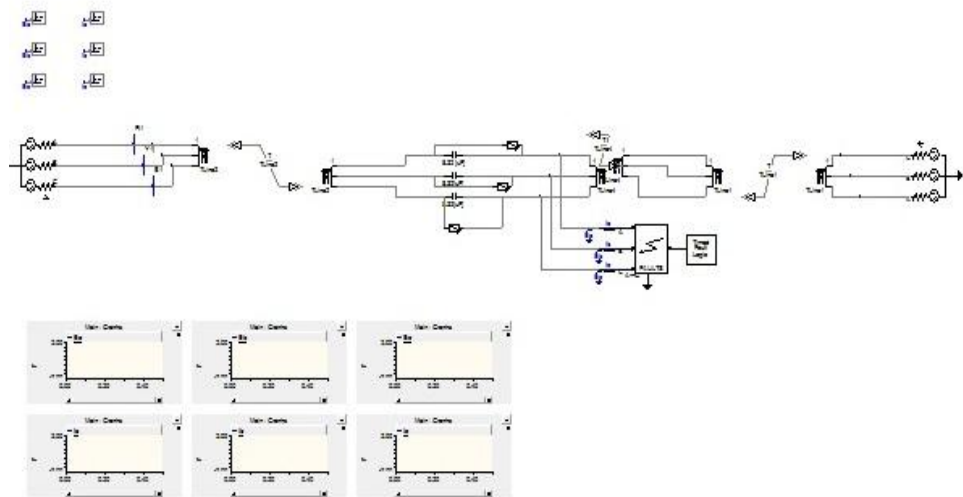


Fig 2: PSCAD implementation of series capacitor compensated transmission line

Test system(Fig 2)is simulated using PSCAD/EMTDC software and test different cases with varying fault location, varying compensation, varying fault resistance, varying fault duration etc. Then calculated and plotted faulted wave forms and R&X curves(ref. Fig.3 to Fig.13). Data sampling frequency maintained here 4KHZ and system frequency maintained here 50 HZ. Test system data is shown in Appendix-B.



Fig 3: Performance of the test system during a Ph-B-G fault at 40% line length

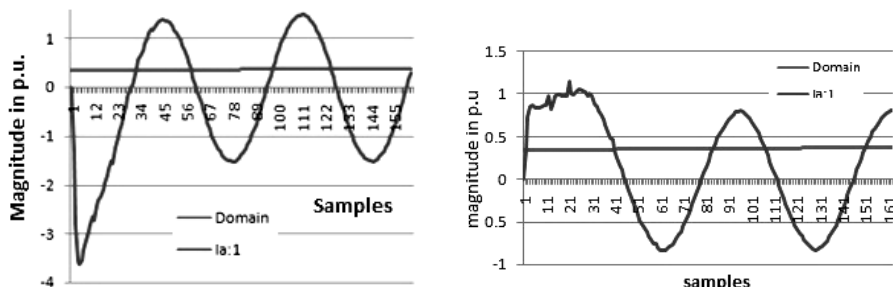


Fig 4: Performance of the test system during a Ph-AB-G fault at 40% line length

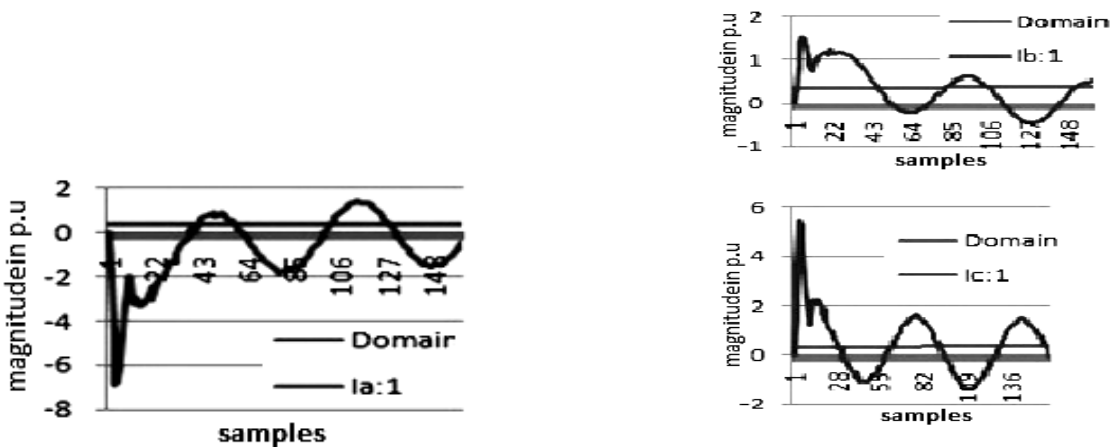


Fig 5: Performance of the test system during a LLL fault at 40% line length

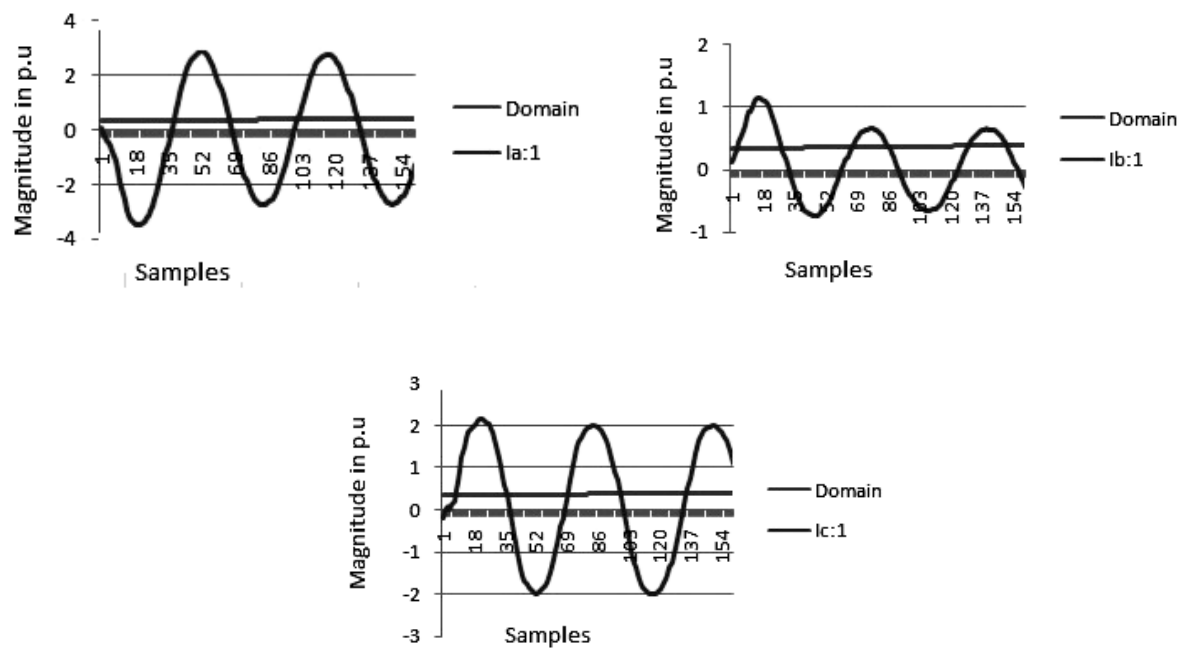


Fig 6: Performance of the test system during a LLLG fault at 40% line length

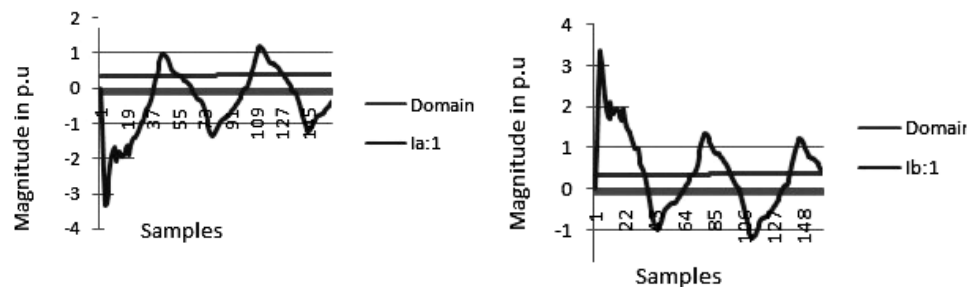


Fig 7: Performance of the test system during a LL fault at 40% line length

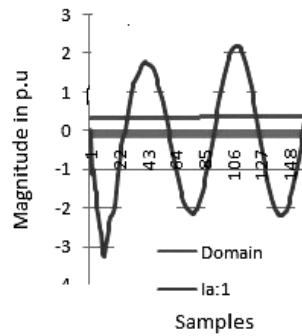


Fig 8: Performance of the test system during a AG fault at 40% line length

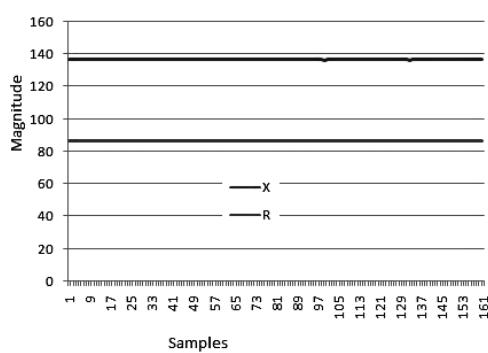


Fig 9: Variations of R & X in p.u during a b-g fault

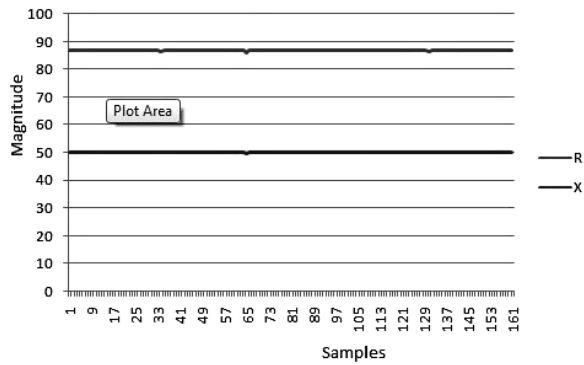


Fig 10: Variations of R&X in p.u During a bc-g fault

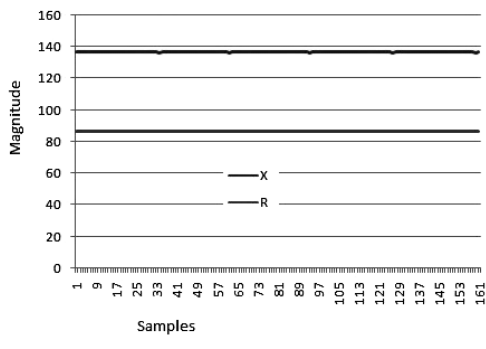


Fig 11: Variation of R&X in p.u during a LLLG fault

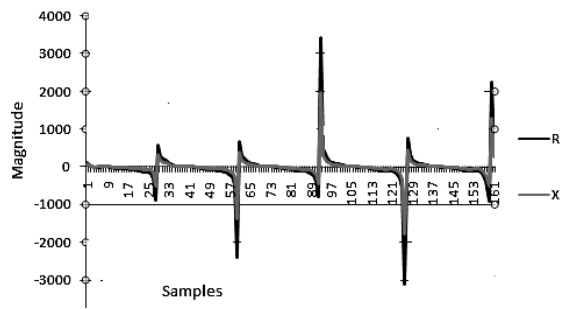


Fig 12: Variations of R&X in p.u during a LL fault

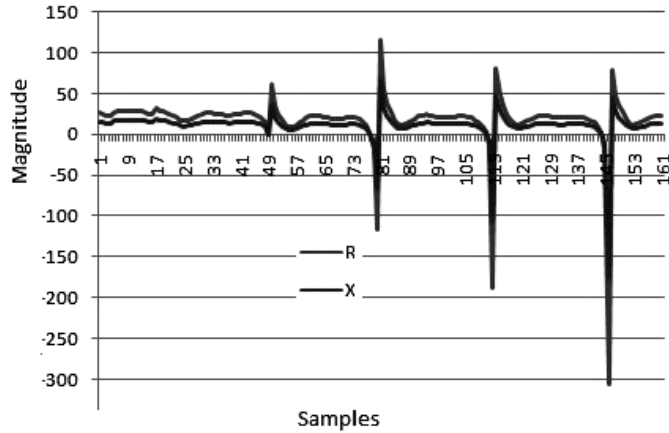


Fig 13: Variations of R&X in p.u during a LLL fault

During fault, from the available voltage and current samples data corresponding resistance and reactance parameters are estimated to plot the impedance characteristics and to confirm the zone where the fault has located. R and X values are shown in Table 3 ,Table 4 and Table 5.

Table3

Calculation of R&X for a BC-G fault:

Z(units)	R(units)	X(units)
99.91033	86.52234	49.95516
99.93408	86.54291	49.96704
99.94821	86.55515	49.97411
99.95479	86.56085	49.97739
99.95831	86.5639	49.97916
99.96272	86.56772	49.98136
99.96037	86.56568	49.98018
99.96443	86.5692	49.98221
99.96637	86.57088	49.98319

Table 4

Calculation of R&X for a B-G fault :

Z(units)	R(units)	X(units)
99.93755	86.54592	49.96877
99.93737	86.54576	49.96869
99.93712	86.54555	49.96856
99.93663	86.54512	49.96831
99.93924	86.54738	49.96962
99.94398	86.55149	49.97199
99.94644	86.55362	49.97322
99.95059	86.55721	49.9753
99.95314	86.55942	49.97657

Table 5

Calculation of R&X for a LL fault

Z(units)	R(units)	X(units)
129.1968	111.8844	64.59838
361.101	312.713	180.55
1015.94	879.807	507.972
2767.65	2396.78	1383.82
3951.639	3422.119	1975.819
3588.58	3107.71	1794.29
894.3192	774.4805	447.1596
2604.014	2255.076	1302.007
1063.61	921.087	531.806

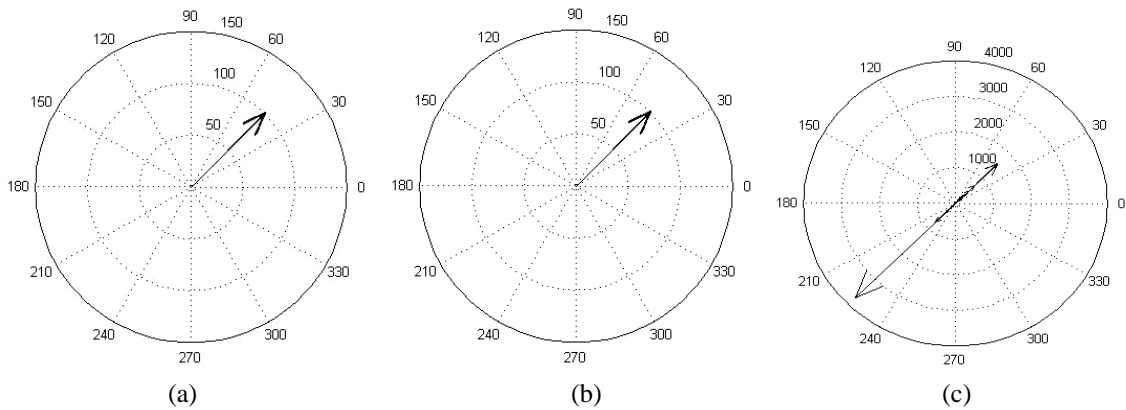


Fig14: Fault Impedance locus during (a) LG fault (b) LLG fault (c) LL fault

The fault impedance characteristics for different types of faults are plotted on R-X plane(ref. Fig 14). Here it is considered up to magnitude 50 unit circle as Zone1, up to 100 unit circle as zone2 and beyond this magnitude as zone3. From the above characteristics it is clear that the

fig14(a) LG fault and fig14(b) LLG fault both located at Zone2. But fig14(c) is located at Zone3. So, in fig14(c) case there may be a possibility for involvement of load encroachment problem and distance relay may give a trip signal to the circuit breaker. From the angle values (sign of the angles), fault direction estimation is also possible in case of polar plot based analysis of fault impedance locus.

3.5 Implementation of the above method in case of a communication link failure :

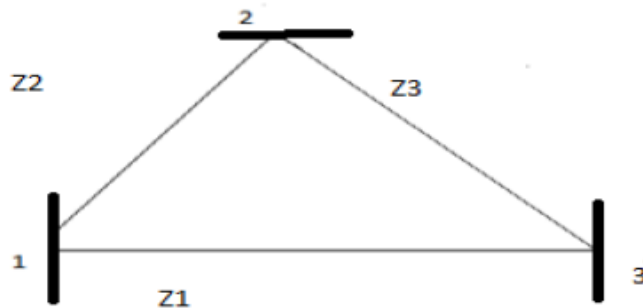


Fig 15 : Data extraction during a communication link failure of a 3-phase system

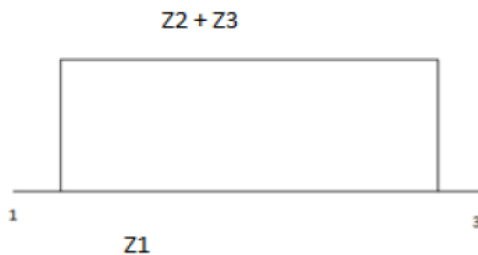


Fig 16 : Equivalent Circuit for Data Extraction when Link 2 fails for the above 3-Phase system

Consider, the case of implementing this method in case of a larger system, where data or samples of voltage or current wave forms are coming from PMUs or Wide Area measurement systems. Suppose link 2 of the above system (ref. Fig. 15) fails and link 1 and link 3 are active.

In that case the data can be extracted in the following ways :

Let us consider link i voltage is V_i

Link i current is I_i

And impedance Z_i where $i \in \{0, 1, 2, \dots, n\}$

Then in case of communication link 2 failure, there will be two parallel paths in the system between 1 to 3 for the above system(same as Fig.16)

Path 1-2-3 and path 1-3

So, Z_2 & Z_3 will be in series which will be parallel with Z_1

So, Total impedance offered between 1 & 3 point will be

$$Z = Z_1 \parallel (Z_2 + Z_3) \quad (7)$$

$$Z = \frac{Z_1(Z_2 + Z_3)}{(Z_1 + Z_2 + Z_3)} \quad (8)$$

So, if the net voltage difference between path 1& 3 is V

Then net current flowing through the path is

$$I = \frac{V}{Z} \quad (9)$$

So, according to the current dividers rule, current flowing in the path 1-2-3 is

$$I_2 = \left(\frac{Z_1}{Z_1 + Z_2 + Z_3} \right) * I \quad (10)$$

$$I_2 = \left(\frac{Z_1}{Z_1 + Z_2 + Z_3} \right) * \frac{V}{Z} \quad (11)$$

$$I_2 = \left(\frac{Z_1}{Z_1 + Z_2 + Z_3} \right) * \frac{V(Z_1 + Z_2 + Z_3)}{Z_1(Z_2 + Z_3)} \quad (12)$$

$$= \frac{V}{(Z_2 + Z_3)} \quad (13)$$

So, between 1-2 link Sample voltage will be

$$= \frac{V * Z_2}{(Z_2 + Z_3)} \quad (14)$$

Between 2-3 link sample voltage will be

$$= \frac{V * Z_3}{(Z_2 + Z_3)} \quad (15)$$

Now, the application of the above method proposed here is possible.

3.6 Validity of the above Method During Transient conditions of PMUs :

The method will work fine during transient conditions. e.g- power swing or electromagnetic transients etc. As the method depends on correlation factor calculation, which

is a measure of how two signals are changing together. So, there is no problem with cycle to cycle or sample to sample comparison which happens in case of power swing due to frequency variation of power other than voltage or current signal[41].

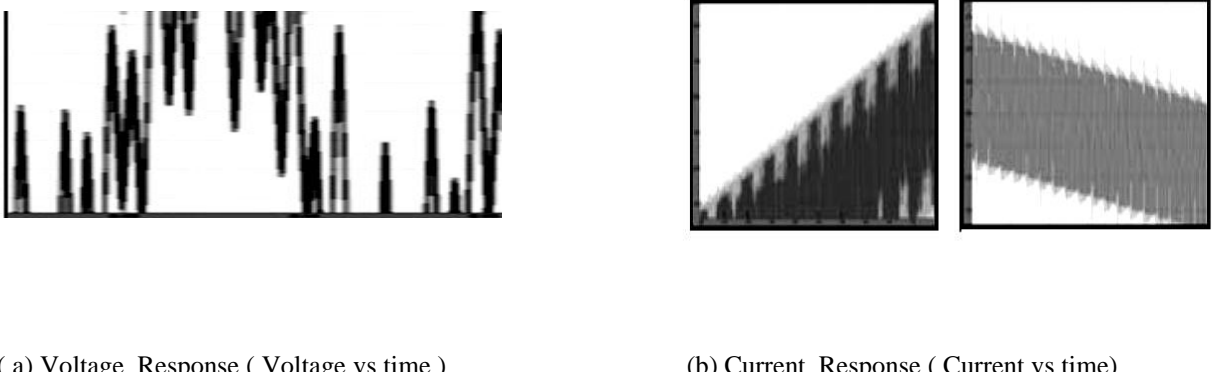


Fig 17 : Transient Response from PMUs

A typical Voltage and current response is shown in Fig. 17 (a) & (b).

3.7 Stability of the Method :

The method is based on correlation coefficient calculation between two signals. It is totally depend on the sampling process of the signal. It is not having direct relation with fault levels or phase angles. Entirely the method depends on the features of the samples extracted from the voltage or current signals. So, it is stable and also not going to affect the stability of the system.

3.8 Comparative Analysis :

Table 6
Comparative analysis with other works

Ref [21]	Proposed Work
Fault phase detection not achieved	We have achieved fault detection part
This method is mainly applicable to low impedance fault	This method is applicable irrespective of impedance of the fault
Percentage error is more in case of distance more than 50%	Percentage error is less and irrespective of fault distance

3.9 Summary

The main results regarding MOV protected series capacitor compensated transmission line, obtained by the fault simulation can be summarized as follows:

The variation of R&X is less during ground faults, compared to the phase faults. From the figures it is evident during a bg fault, the maximum value of R&X is confined in the order of 140 unit(ref.Fig.9), while in the case of a Phase-B to Phase-CG fault, the variation is of the order of 90 units(ref. Fig. 10) and during a LLLG fault the variation is of maximum 140 unit(ref. Fig.11). But in case of phase faults, it is more than two times of ground faults. In case of LL fault, it comes beyond 1000 unit(ref. Fig. 12) and LLL fault it is coming beyond 300 units in negative half (ref. Fig 13).

From polar plot of the fault impedance, it can be concluded which zone the locus is confined and whether distance relay is going to generate any trip signal to circuit breaker or not and if there is any chance for evolving load encroachment problem or not and also the direction of fault is upstream or downstream based on the sign of the angle(angle sign positive-fault direction upstream i.e left side of transmission line, angle sign negative-fault direction downstream i.e right side of transmission line). Faulty phases can be identified when two or more phases involves fault using correlation statistical operator.

Several special cases have been discussed in the context of the Work. e.g- implementation of the proposed method in case of a communication link failure in the system, the transient performance issues of the PMUs etc. The stability of the proposed method with respect to the system stability is also addressed.

This work is having vivid contributions w.r.t protection of series compensated transmission line. First of all a novel methodology is proposed for phase detection of fault based on correlation factor computation, is very simple and effective in correctly predicting the phase of the fault and it is further extended to the analysis of polar plot which is helpful in the assessment of system internal state. It can judge the state of the fault with fault direction estimation as well as any chance of mal-operation of the system. Eventually this methodology is helpful not only for predicting of fault but also for the condition monitoring of the system which can lead its increase in security and reliability .

This faulty phase identification algorithm gives better result compare to detection of faulty phase by imposing the tolerance limit method and the polar plot analysis gives more insight about the zone of the fault, direction of fault and chance of mal-operation. Thus this work is commendable w.r.t the protection of series compensated transmission line .

Chapter 4

**A Synchrophasor Measurement-Based Fault Locator
with Novel Fault Detection Technique**

Chapter 4

A Synchrophasor Measurement-Based Fault Locator with Novel Fault Detection Technique

4.1 Introduction

Fast and accurate fault detection and location is vital from the aspect of power system security and restoration. Algorithms which provide essential analysis for locating the fault of overhead transmission line is an important part of protection schemes. Fault locator, which helps to locate accurate fault location with appropriate fault location algorithm (FLA), is also an important and essential component of such protection schemes. It calculates the distance to the fault from a given reference point. Outage times can be reduced and service to consumers restored more quickly ,if the location of the fault can be determined accurately [12].

Several fault location algorithm has been developed from the past. Some of them use data from single line terminal ,some of them use data from multiple terminals , some of them use synchronized data sampling from terminals, and some of them use other techniques like travelling wave based methods or ANN , Fuzzy logic based methods etc. Single-end methods use local measurements of current and voltage at one terminal of the faulted line [42–43].With the emergence of communication technologies, double end fault location method using synchronized or unsynchronized data samples from both terminals of a transmission line has been employed [44]. Single Terminal Fault location algorithms (STFLA) calculate impedance seen from the local terminals and then use line parameters to calculate the fault distance. The accuracy of the algorithm is largely affected by the zero sequence component of the line and fault resistance [45]. Two terminals FLA are relatively more accurate than STFLA as they are not affected by fault resistance but disadvantage of these methods is they need a mean to gather data from both terminals at one location prior to be analyzed [12]. Speed of these algorithms are less than STFLA. Three-end and multi-end methods are extensions of double-end methods [46–47]. These methods identify the faulted sections by multi-end measurements first and then locate the fault along the identified section by the double-end methods. Fault location of a transmission line by travelling wave based methods and impedance based

methods draws the attention of the researchers increasingly [48-49]. The measurement may also not available at faulted line terminal rather it may be available in buses distant from the faulted line [48]. In [50] a method is described which requires data from both ends of the line requires synchronized sampling. In [51] a technique is presented for estimating fault location which requires unsynchronized data sampling at both ends of the transmission line. [52] presents a fault location technique which incorporates analysis of data during circuit breaker operation. [53] Investigates the malfunctioning of the circuit breaker and their impact on hidden failure. During a 3-phase circuit breaker operation all the three phases may not open simultaneously. The individual zero crossing of each phase may be displaced by certain degree, accordingly several discrete states known as inter-pole states may arise due to this phenomena which may affect the desired result or accurate fault location. Selection of window size for extracting fundamental frequency may also affect the accuracy of the algorithm. e. g- The use of full cycle, fractional cycle or multiple cycle of waveform for extracting fundamental components may affect the results also. In [54] a PMU based fault location method is discussed for series compensated line which uses sequence components of voltages and currents and Islanding technique of power network to detect fault in a series compensated transmission line inside a power network. In [55] a fault location technique is presented which uses voltage and current phasors computed from two or three line terminals.

A common feature or essence of these various FLA are, they requires the knowledge about the system parameters like – line length , line parameters (R,L etc) and appropriate equation for computation of fault distance. But the line parameters may vary depending upon different loading ,weather conditions, aging etc which may of course affect the accuracy of the algorithm. So, an algorithm is needed which is independent of line parameters and thus which will be more accurate, robust and flexible. In [56],[57],[58] proposed fault location algorithms do not require line parameters to locate fault. [56] & [57] Algorithms uses voltage and current data and avoided the necessity of data sampling synchronization. However those parameters having limitations to locate symmetrical fault.

There are two FLA s are presented in [58]. First one uses both pre-fault and fault data and then uses iterative technique to locate fault. The second one uses fault data to locate asymmetrical faults only. In [12] an FLA is derived which uses data from both ends of the line with assuming synchronized data sampling for all kinds of the fault. However, the algorithm

does not need synchronized data sampling to locate symmetrical three-phase faults. Further, since it is developed in the phasor-domain, it does not require a very high sampling frequency.

In this chapter we worked further on this algorithm and proposed a measure to improved the accuracy of the above algorithm. The objective of the chapter is to enhance the accuracy of the above algorithm with appropriate data extraction procedure. A fault classification approach by use of zero sequence components of power and a faulty phase detection approach by the study of change of phase currents are also presented in the chapter.

4.2 Proposed fault location algorithm

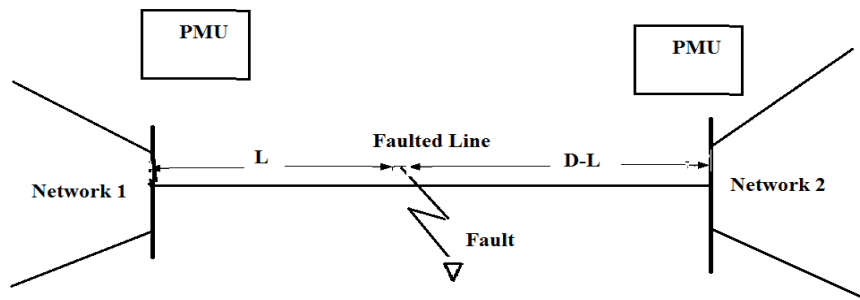


Fig 1: Single Line Diagram of Simulated Faulted Power Network

4.2.1 Asymmetrical Fault :

LG , LLG ,LL are asymmetrical faults. During asymmetrical fault, the fault location algorithm (FLA) is derived here. Assume an asymmetrical fault is taken place in the transmission line at L km length from the sending end of the transmission line, and total line length is considered as D Km.

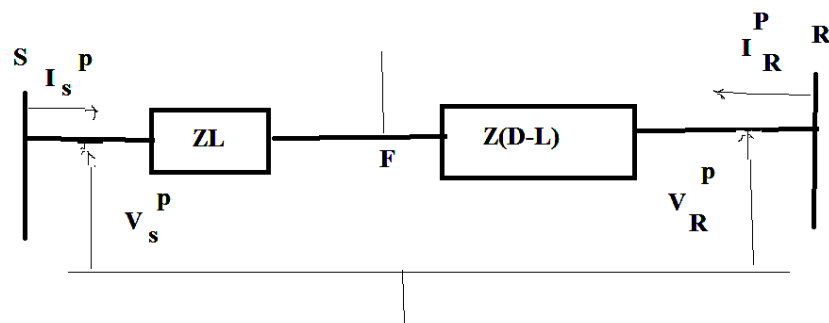


Fig 2: Equivalent Positive Sequence Network of Faulted Line

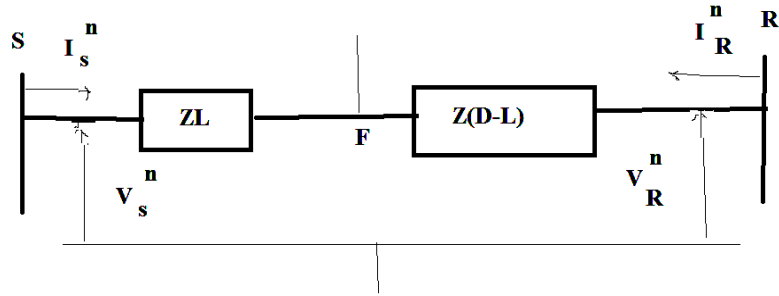


Fig 3: Equivalent Negative Sequence Network of Faulted Line

Assuming line length less than equals to 100 Km(short transmission line), the shunt conductance and shunt capacitance of a transmission line can be neglected. A faulted line is shown in Fig 1. Fault location is denoted by F in Fig 2 & Fig 3. D is the total line length and L is the faulted length from reference point i.e sending end. S denotes sending end and R denotes receiving end. s subscript denotes a sending end variable and R subscript denotes a receiving end variable. p superscript denotes positive sequence variable and n superscript denotes a negative sequence variable. Voltage and current samples are synchronously sampled here in both the line terminals. Corresponding Phasors are calculated by using standard signal processing techniques with the help of voltage and current samples after passing them consecutively through a Second order Butterworth filter and FFT block. From Fig 2 & Fig 3 it can be written-

$$V_S^P - ZL I_S^P = V_R^P - Z(D-L) I_R^P \quad (1)$$

$$V_S^n - ZL I_S^n = V_R^n - Z(D-L) I_R^n \quad (2)$$

By solving equation (1) & (2) we get

$$ZL = \frac{(V_S^P - V_R^P) I_R^n - (V_S^n - V_R^n) I_R^P}{(I_S^P I_R^n - I_S^n I_R^P)} \quad (3)$$

$$Z(D-L) = \frac{(V_S^P - V_R^P) I_S^n - (V_S^n - V_R^n) I_S^P}{(I_S^P I_R^n - I_S^n I_R^P)} \quad (4)$$

Fault distance is L & total line length is D. Fault distance can be expressed as a percentage of total length-

$$\%L = 100 \times \left(\frac{L}{D} \right) \quad (5)$$

Equation (5) can be rewritten as-

$$\%L = 100 \times \left(\frac{ZL}{ZL + Z(D - L)} \right) \quad (6)$$

From equation (3),(4) and (6) , it can be written as

$$\%L = 100 \times \frac{(V_S^P - V_R^P)I_R^n - (V_S^n - V_R^n)I_R^P}{(V_S^P - V_R^P)(I_S^n + I_R^n) - (V_S^n - V_R^n)(I_S^P + I_R^P)} \quad (7)$$

4.2.2 Symmetrical Fault :

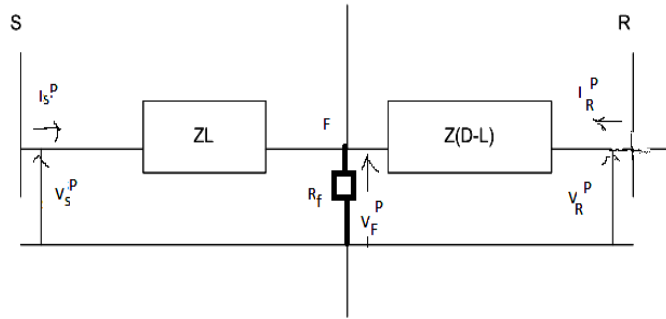


Fig 4 : Equivalent positive sequence circuit for Symmetrical Fault

In case of symmetrical faults , only positive sequence network is present , no negative or zero sequence network. R_f denotes fault resistance and V_F^P is fault voltage. From Fig 4 we are getting the following equations :

$$V_S^P - ZL I_S^P - V_F^P = 0 \quad (8)$$

$$V_R^P - Z(D - L) I_R^P - V_F^P = 0 \quad (9)$$

From Equation (8),(9) & (5),(6) we get-

$$\%L = 100 \times \frac{(V_S^P - V_F^P)I_R^P}{(V_S^P - V_F^P)I_R^P + (V_R^P - V_F^P)I_S^P} \quad (10)$$

The proposed algorithm does not need to know any fault type or line parameters. The presence of negative sequence current determines difference between symmetrical and asymmetrical fault. The flow chart of the proposed algorithm is shown in Fig 5.

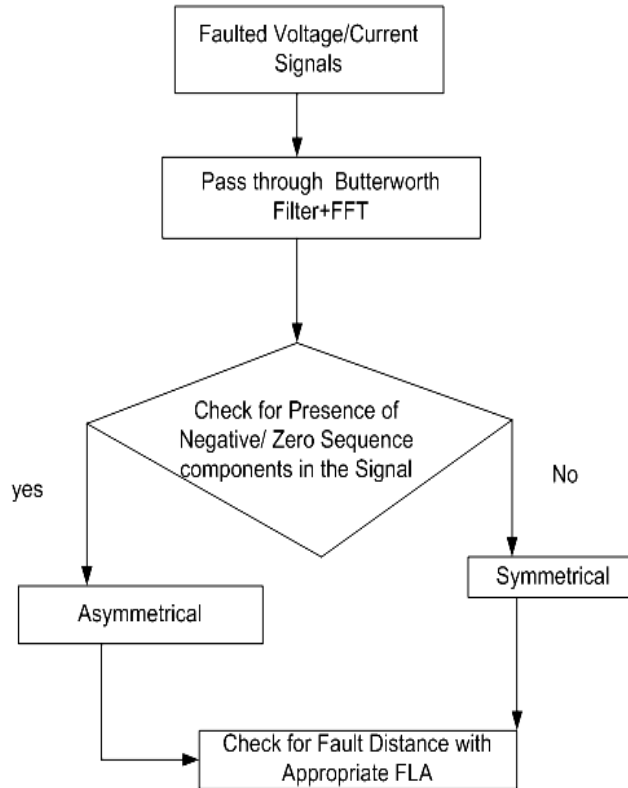


Fig 5 : Flow Chart of the Proposed Algorithm

4.3 Results and Discussions :

Test results of the algorithm is carried out on a 400 KV , 100 Km long overhead transmission line using PSCAD / EMTDC software. Multiple cases of symmetrical and asymmetrical faults were carried out. All the parameters used here are same as reference [12]. The test system data are shown in Appendix-C. The FLA results for both kinds of fault are listed in Table-1 and Table –2.

4.3.1 Asymmetrical Faults : Asymmetrical faults (LG,LLG ,LL etc) faults were simulated at the various points of the line. Fault initiation time $t = 0.2$ sec. Sampling frequency $f_s = 4$ KHz. It is assumed all the phasors are ideally synchronized ($\phi = 0^0$). Using the voltage current samples unknown fault locations has been calculated. The results related to asymmetrical faults are listed in Table 1.

Table 1: %Errors in Asymmetrical Fault Distance Calculation

Fault type	Fault Resistance (Ω)	Fault Distance (Km)	% error before using Butterworth filter	% error after using Butterworth 2 nd order filter
AG	0.01	40	0.10925	0.02125
ABG	0.01	65	0.0471	0.0424
BCG	100	60	0.0471	0.01406
ABG	0.01	30	0.1136	0.068
ABG	2	30	0.2063	0.1165
ABG	0.1	20	0.1453	0.075
AB	100	75	0.4221	0.3893
ABG	0.01	75	0.3875	0.3333

Different results are generated with varying faults and varying fault resistance R_f . Fault location percentage error is calculated as a percentage of full line length.

$$\% \text{Error} = (I_{\text{calculated}} - I_{\text{exact}}) \times \frac{100}{D} \quad (11)$$

4.3.2 Symmetrical Faults : Symmetrical faults(LLL and LLLG) are simulated and calculated fault distance by using the FLA. Fault Location errors are listed in Table2. Other parameters remain same as asymmetrical fault.

Table 2 %Errors in Symmetrical Fault Distance Calculation

Fault type	Fault Resistance (Ω)	Fault Distance (Km)	% error before using Butterworth filter	% error after using Butterworth 2 nd order filter
LLLG	0.01	80	0.0496	0.0011
LLL	0.25	35	0.1679	0.0033
LLL	2	60	2.008	0.02496
LLLG	100	30	0.2063	0.1165
LLLG	100	50	1.4914	0.7539
LLL	1	75	1.324	0.1382
LLL	1	10	0.9390	0.4104

4.3.3 Improved accuracy using higher order filter :

With the use of higher order filter, better refinement in voltage and current signals can be achieved and unwanted frequency components can be eliminated with better accuracy. As a result better accuracy in the above fault location algorithm can be achieved. The only disadvantage of using higher order filter is ,with the increase of order of the filter the size and

cost of the filter will also increase and that will affect the economy of the process. So, it is suggested to optimize the accuracy with economy of the process. In Table 3 the comparison of percentage error with Butterworth 2nd and Butterworth 4th Order filter is shown in context to proposed methodology. It is suggested that for all calculations the first half cycle samples of voltage and currents of the faulted duration can be ignored as they are contaminated by dc offset signals which can affect the accuracy of the algorithm.

Table 3 Comparison of % error of fault distance with Butterworth 2nd and Butterworth 4th Order filter

Fault type	Fault Resistance (Ω)	Fault Distance (Km)	% error after using Butterworth 2 nd order filter	% error after using Butterworth 4 th order filter
ABG	0.1	15	0.6113	0.4548
ABG	0.01	75	0.3333	0.07989
LLLG	0.01	80	0.0011	0.000705
LLL	0.01	40	0.03125	0.0049
BCG	0.1	15	0.6007	0.3011
AG	1	40	0.26	0.234
LLL	2	75	0.2204	0.1108
AB	100	75	0.3893	0.1455

4.3.4 Application of the Methodology in case of a series compensated transmission line :

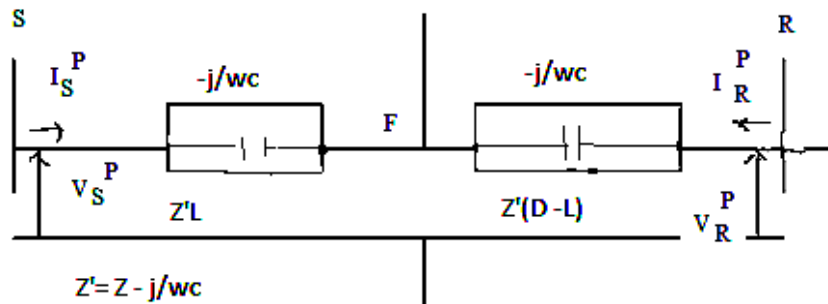


Fig 6 : Equivalent Positive Sequence Network in case of series-compensation involved

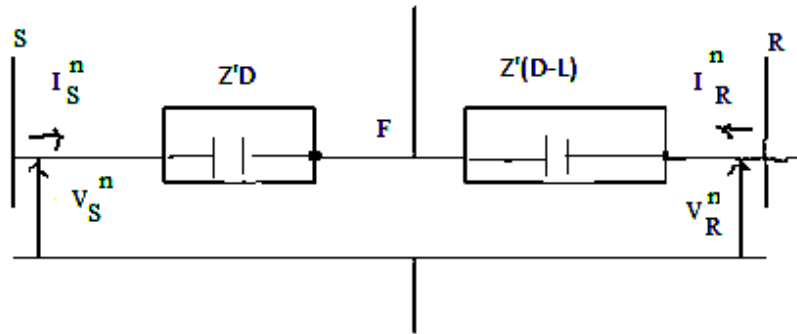


Fig 7: Equivalent Negative Sequence Network in case of series-compensation involved

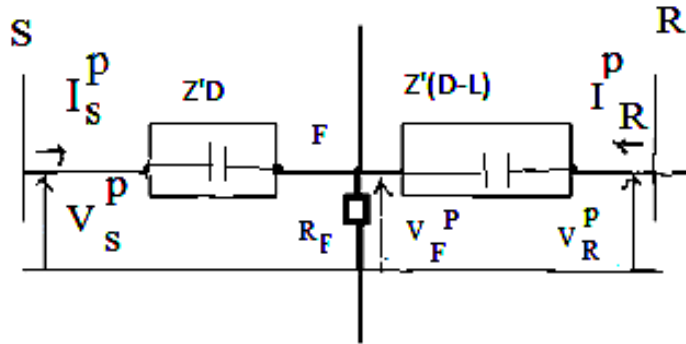


Fig 8 : Equivalent Positive Sequence Network for Symmetrical fault calculation in case of series-compensation involved

Here we are considering the line having series capacitor c per unit length. In that case the equivalent networks needed for derivation of the FLA will be as above Fig 6,7 & 8. In that case we can derive the above FLA by substituting Z' instead of Z in the equations (1) to (10). Where $Z' = (Z - j\omega c)$. Rest of the calculations are same as above. Assumption to use this FLA in case of series compensation involved in transmission line is the capacitor is assumed to be distributed throughout the line. Hence we can derive two lumped capacitors in the model for calculation. One capacitor is upto faulted point from sending end side and another from faulted point upto receiving end side of the transmission line.

4.4 Classification of fault :

Fault can be classified as Symmetrical and asymmetrical w.r.t presence of negative and zero sequence current or voltage. Presence of positive sequence current or voltage

only (no negative / zero sequence) indicates that the fault is a symmetrical fault i.e LLL or LLLG fault. LLL or LLLG fault is almost identical. Due to balanced nature of fault there will be no current flowing through neutral wire. But in practical case there might be existence of a small current flow in the neutral wire which can distinguish LLLG and LLL type fault. Asymmetrical faults can be distinguished through study of its active and reactive power profile due to zero sequence fault voltage and current. From the theory zero sequence component of Power during fault.

$$S_{f0} = V_{f0} I_{f0}^* \quad (12)$$

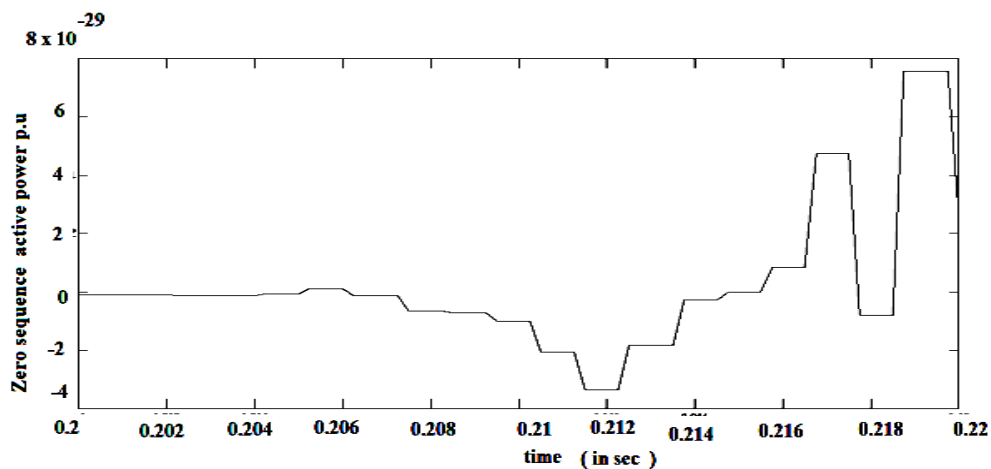
Zero Sequence Active Power during fault can be written as

$$P_{f0} = \text{Real} (V_{f0} I_{f0}^*) \quad (13)$$

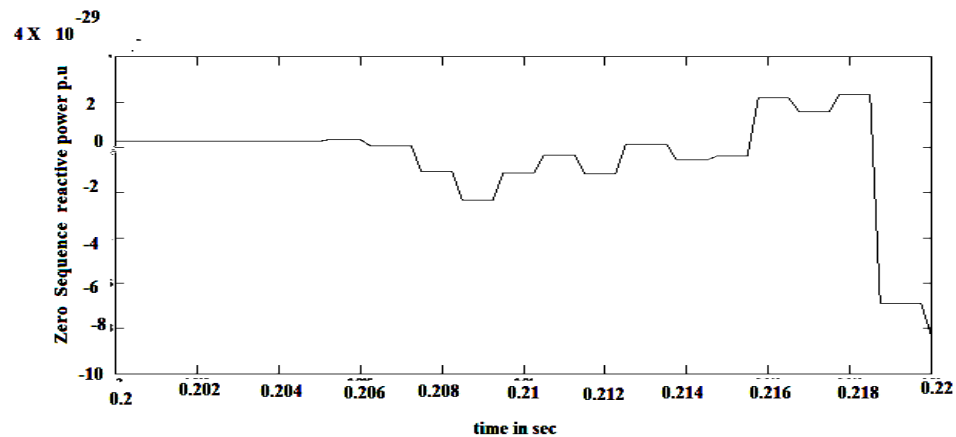
Zero Sequence Reactive power during fault can be written as

$$Q_{f0} = \text{Imaginary} (V_{f0} I_{f0}^*) \quad (14)$$

In the below Fig 9 (a,b) , Fig 10(a,b) , Fig 11(a,b) , Zero sequence active and reactive power profile are Studied during different Kinds of asymmetrical faults like – LL ,LLG and LG faults. From the study of the below figures it is clear that the Zero Sequence Power components in case of a LL fault is almost negligible (almost in the order of 10^{-29} p.u). So, from the study of Zero Sequence components of power during fault we can easily distinguish a LL fault from LLG and LG fault.

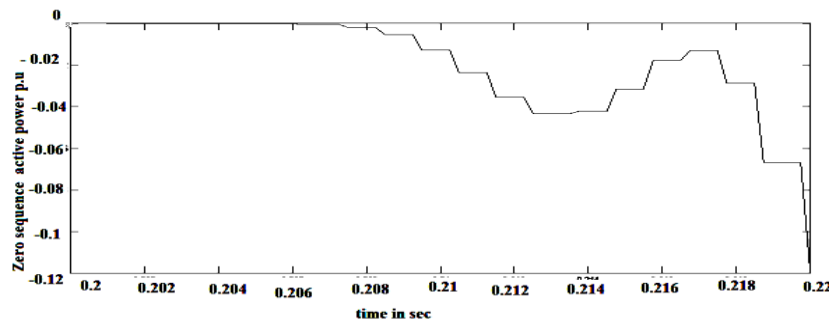


(a) Zero Sequence Active Power vs time during LL fault

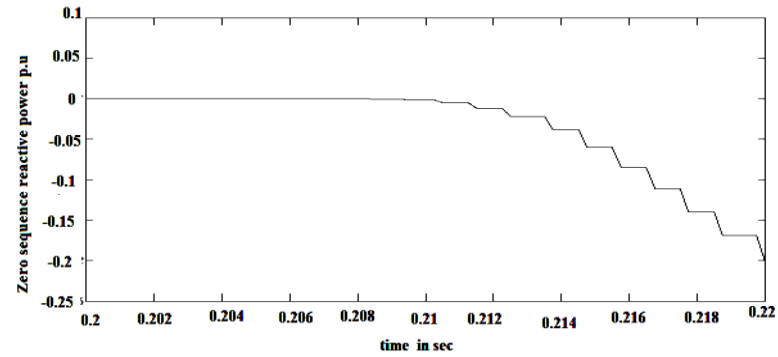


(b) Zero Sequence Reactive Power vs time during LL fault

Fig 9 (a,b): Profile of Active and reactive power during LL fault



(a) Zero Sequence Active Power vs time during LLG fault



(b) Zero Sequence Reactive Power vs time during LLG fault

Fig 10 (a,b): Profile of Active and reactive power during LLG fault

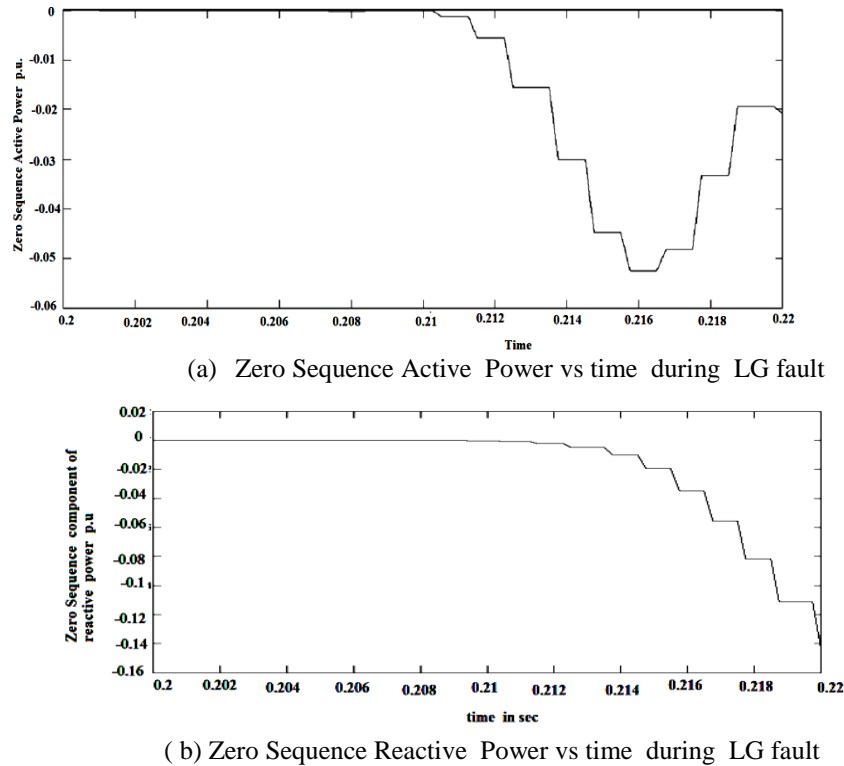


Fig 11 (a, b): Profile of Active and reactive power during LG fault

Now to distinguish between a LLG and a LG fault we will again study their Zero Sequence component power profiles during fault. It is seen from the study that Zero sequence components of power that during an LLG fault the values are more compare to an LG fault. Thus we can distinguish between a LLG and a LG fault.

$$P_{f0LG} < P_{f0LLG} \quad \&& \quad Q_{f0LG} < Q_{f0LLG} \quad (15)$$

Fig 12 shows the flow chart for classification of the asymmetrical faults.

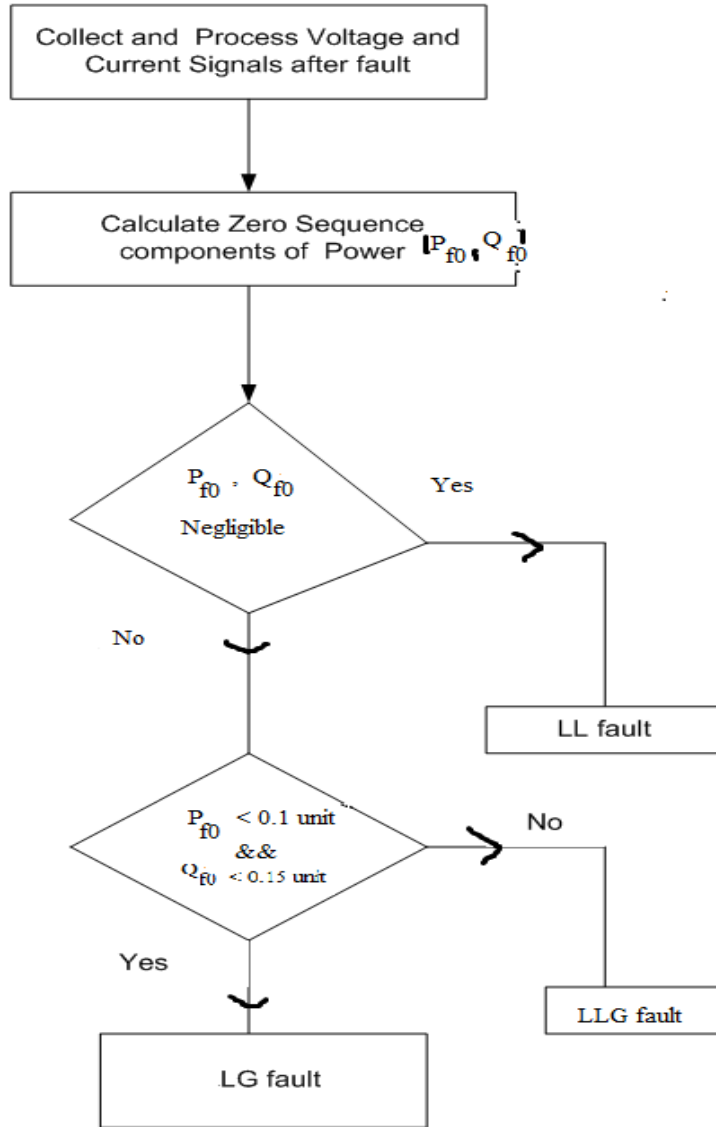


Fig 12 : Flow Chart for classification of asymmetrical fault

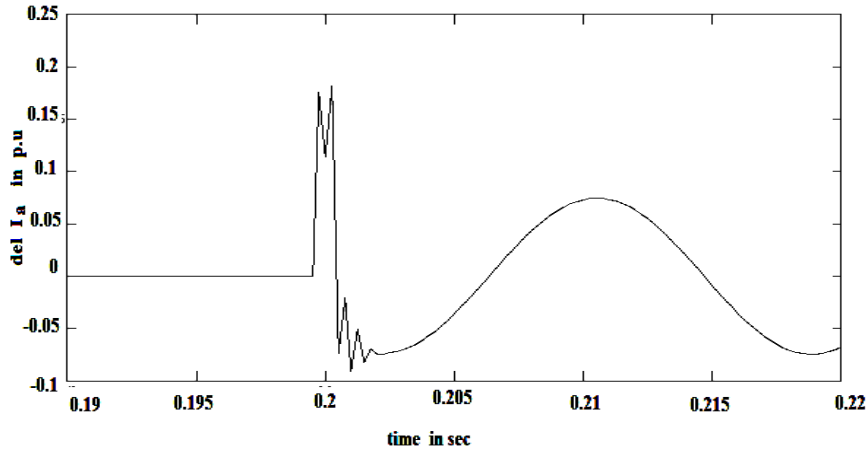
4.5 Detection of Phases of fault :

Faulty phases can be identified by the study of the change in phase current characteristics. To study the said behaviour, different types of faults are created with fault duration 0.02 sec with initiation of fault at 0.2 sec. Change in phase current is captured from 0.19 sec-0.22 sec.

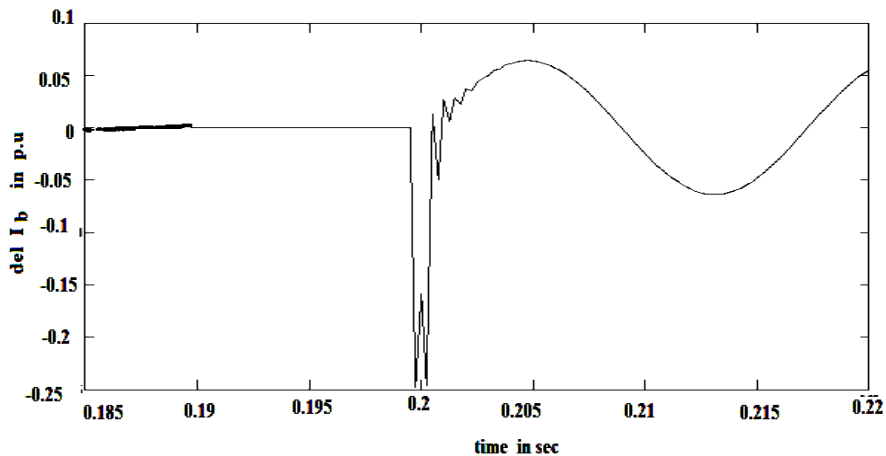
$$\Delta(I_a)_k = (I_a)_{k+1} - (I_a)_k \quad (16)$$

$$\Delta(I_b)_k = (I_b)_{k+1} - (I_b)_k \quad (17)$$

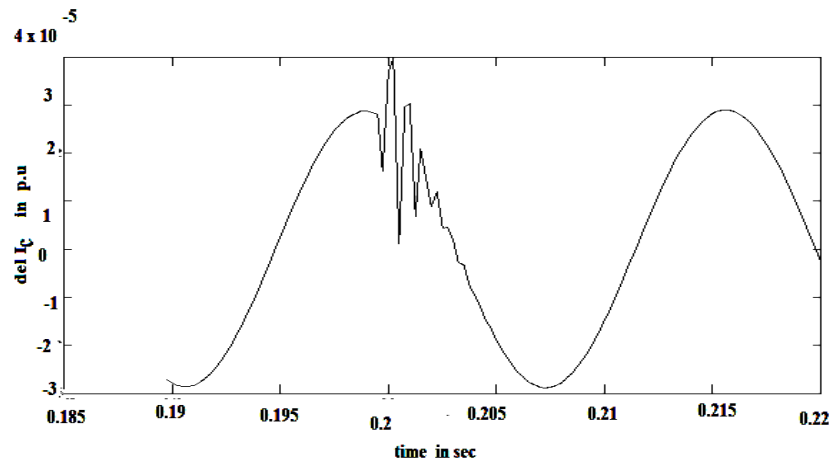
$$\Delta(I_c)_k = (I_c)_{k+1} - (I_c)_k \quad (18)$$



(a) ΔI_a vs time plot in case of an ABG fault



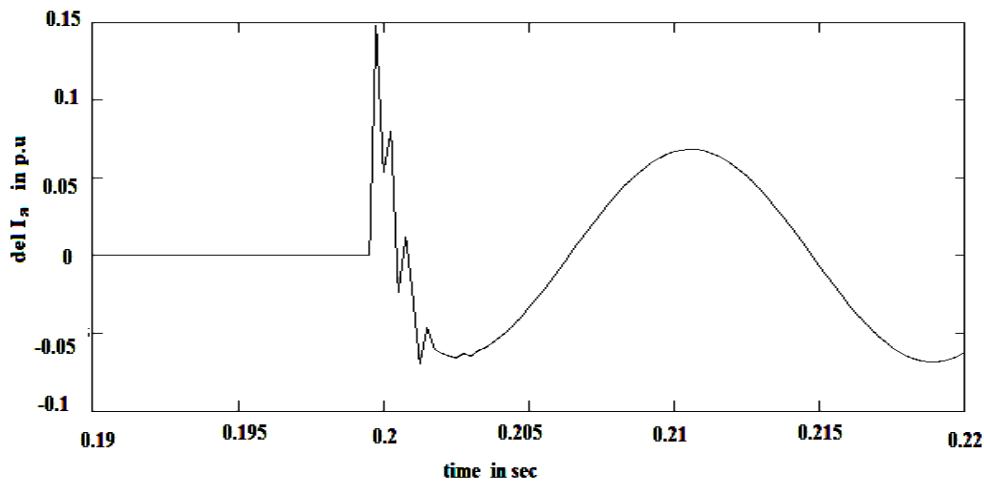
(b) ΔI_b vs time plot in case of an ABG fault



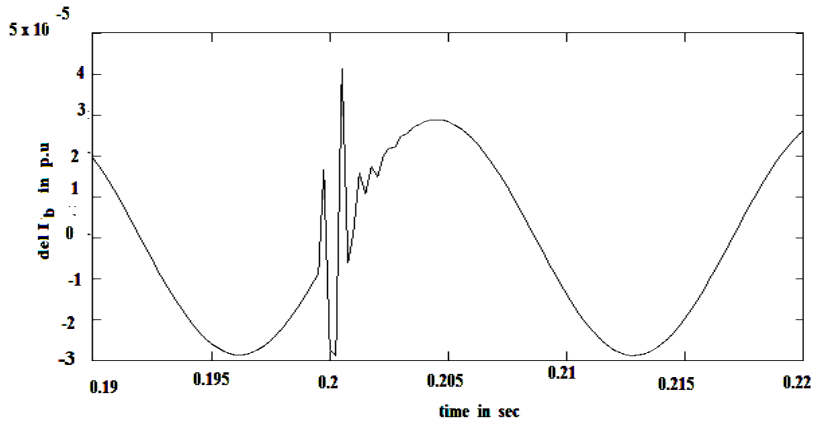
(c) ΔI_c plot vs time in case of an ABG fault

Fig 13 (a,b,c): ΔI_a , ΔI_b , ΔI_c vs time plot in case of an LLG fault

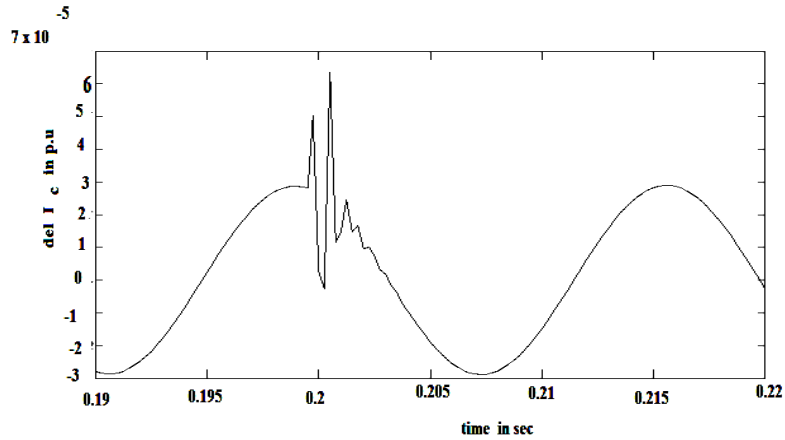
From the Fig 13(a,b,c) , it is clear that in case of faulty phases (Ph-A & Ph- B), there is a sharp change in change of phase current waveform at the time of fault inception (absolute value around 0.2 unit at 0.2 sec). Whereas the change is almost negligible (in the order of 10^{-5} unit) at the same time in case of healthy phase(Ph-C). Similar Characteristics can be generated in case of a LL fault to detect the faulty phase.



(a) ΔI_a vs time plot in case of an AG fault



(b) ΔI_b vs time plot in case of an AG fault



(c) ΔI_c vs time plot in case of an AG fault

Fig 14 (a,b,c): ΔI_a , ΔI_b , ΔI_c vs time plot in case of an LG fault

From Fig 14(a,b,c) it is clear that there is a sharp change in phase current in case of faulty phase (Ph-A , at 0.2 sec, ΔI_a value is around 0.15 unit),whereas for healthy phases (Ph-B & Ph-C) this change is almost negligible (order of 10^{-5} unit) at the same time. So, to detect faulty phases and healthy phases the following condition can be imposed:

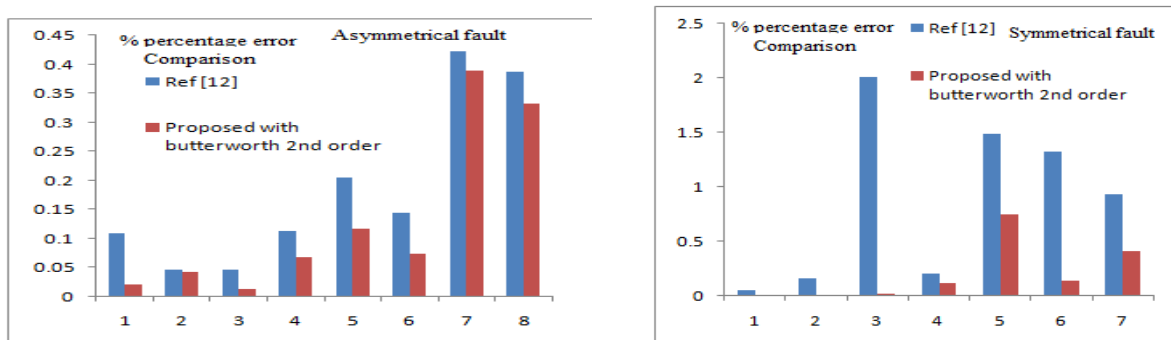
When $ABS(\Delta I) > ABS(\Delta I_{threshold})$, a fault is detected in the phase. (19)

$\Delta I_{threshold}$ should be properly chosen to solve the problems. In this work its value was chosen ± 0.1 unit. In case of symmetrical faults all the three phases are faulty.

4.6 Advantages of the proposed algorithm :

The work done prior to this work on the same problem(i.e designing transmission line parameter independent fault locator) are very little. This work have several strong features that leads the proposed approach to supersede other techniques developed prior to this work. First of all, almost all the techniques developed prior to this work addressing the same problem have certain limitations in locating symmetrical or asymmetrical faults but the proposed technique is capable of detecting and locating both symmetrical and asymmetrical faults. Second of all, some of the techniques developed prior to the proposed technique use iterations to get the desired solution which is lengthy and time consuming. But the proposed technique does not use iterations. It uses direct expressions. The proposed technique is advanced over [12],as it uses appropriate filtering technique for signals to improve accuracy of the algorithm. It also shows with the use of higher order filters the accuracy of the algorithm can be improved further. Third important point in this respect is the proposed algorithm can further classify faults which all the previous algorithms cannot do. Even the proposed technique can predict the faulty phase also. Proposed fault classification and faulty phase detection methods are very simple, accurate and fast. The proposed technique does not affect the system stability or fault level and it works fine in case of transient network conditions also. So, this technique is better than other developed techniques prior to it addressing the same problem.

4.7 Comparative Analysis :



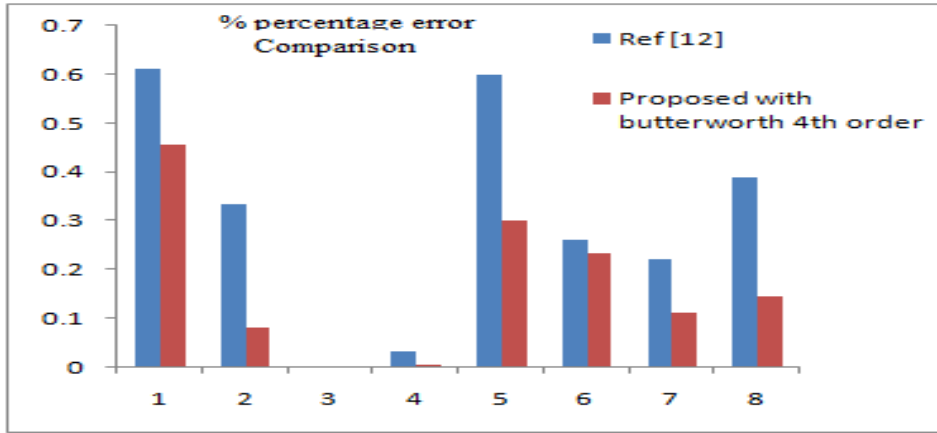


Fig 15: Comparison of percentage error in fault distance calculation in various cases with Ref[12] method

Fig 15 shows the comparison of percentage error in fault distance calculation in various cases with Ref[12] method and it is found that accuracy in fault distance calculation is improved through our approach rather than previous approach.

4.8 Summary

In this chapter a flexible, robust improved FLA is presented, which can work in the absence of any information of system parameters. Proposed algorithm can be applied in case of both symmetrical and asymmetrical faults and the use of filtering technique with FFT will increase the performance of the proposed algorithm. This algorithm can be applied during the presence of capacitor(series compensation) and contingency conditions of the network also. It remains unaffected by fault and arc resistances. The work is extended by improving accuracy of the algorithm further by using 4th Order Butterworth filter, application in series compensated transmission line, classification of faults by using active and reactive power components of zero sequence power during fault and faulty phase detection by study of change in phase current profiles. All the studies are carried out in the chapter by PSCAD simulation model of the test system and found to be accurate and fast.

Chapter 5

An Efficient Fault Locating Technique with Backup Protection Scheme Using Wide Area Measurement for Power System with Simultaneous Faults

Chapter 5

An Efficient Fault Locating Technique with Backup Protection Scheme Using Wide Area Measurement for Power System with Simultaneous Faults

5.1 Introduction

Protection of power systems is important for stable and uninterrupted operation of power network. Maloperation of traditional back up protection schemes (e.g-Zone3 maloperation) causes many catastrophic phenomenon like cascaded tripping in power systems. So, some defensive mechanism are needed for taking care of such failures in power systems and to increase their security and reliability. Due to hugeness and complexity of Modern power systems, they are controlled, monitored and protected by Wide Area Measurement Systems (WAMS). WAMS increases the efficiency and reliability of power networks and prevent the chance of blackouts and cascading failures in tandem. A synchronized phasor measurement-based wide-area backup protection scheme is presented in the chapter where the magnitude of sequence voltages of buses at a system protection centre are used to identify the faulted area, bus closest to the fault and faulted line. The proposed method is tested for several faults including simultaneous faults in power systems also. This technique is found to be Reliable, accurate and fast with contemporary synchronized measurement based technology. It is expected that numerous disastrous blackouts, cascaded tripping of power networks can be avoided and reliability and security of the power systems can be improved by the scheme. The study of new and improved back up protection scheme is done on a WSCC-3 machine-9 bus and an IEEE 14 bus test system. The data is simulated through EMTDC/PSCAD and MATLAB /SIMULINK software.

In general local voltage or current measurements are used in conventional back up protection schemes used for power networks which find obstacle in distinguishing the fault from heavy loading conditions [67]. Maloperation of back up protection during stressed conditions causes the cascaded tripping. Wide area interconnection leads to huge number of blackouts throughout the world.

Recent advancements in technology draws significant attention for the utilization of the synchronized phasor measurement unit (PMU) based wide-area measurement system (WAMS) for power system protection [68]-[69]. Emergence of new technologies like smart electric grid increased the safety and reliability power networks and mitigates the more serious consequences like blackouts, cascaded tripping of power networks and other power outages. Thus they help to continue safe, reliable and continuous power supply.

The largest power outage in history happened in India on 30th and 31st July 2012. The outage affected 22 states in Northern, Eastern and Northeast India. About 32000MW of generating capacity was taken offline in the outage. Several factors responsible for the blackout were:

- i) Weak inter-regional power transmission due to multiple existing outages.
- ii) Drastically increase in loading on 400 kV Binna-Gwalior-Agra power link.
- iii) Inadequate response by State Load Dispatch Centres (SLDCs). This outage affects most of the population of India (about 620 million).
- iv) Loss of 400 kV Binna-Gwalior link due to mal-operation of the protection system [70].

The wide-area backup protection (WABP) based on faulted line identification (FLI) is an interesting topic of research in recent days due to several reasons. First of all a good backup protection can increase the security and reliability of power system. Second of all, a good backup protection can ensure a stable and uninterrupted flow of power. Thus, it reduces power outage and loss of production in plants. The proposed technique can overcome the limitations of conventional backup protection and allows faster operation since it does not need coordination among different zones.

Different WABP schemes for FLI are discussed [71-75]. In [71], a WABP is proposed that compares the positive-sequence voltage magnitude at each bus during the fault to identify the closest bus to the fault. Positive-sequence current angles of all lines connecting the selected bus are used to detect the line having fault. In [72] the residual vector of a Synchrophasor based state estimator, used in a supervisory system, is proposed to improve security of an existing remote backup protection scheme. A supervisory and an agent-based ad-hoc backup relay protection scheme based on a network infrastructure and communication are proposed in [73].

A WABP scheme based on the fault steady-state component of voltages and currents is proposed for Faulted line identification in [74]. In that method, subsets of buses, called protection correlation regions (PCRs), are formed on the basis of network topology and PMU placement. The steady-state component of differential currents in each region is used to identify the PCR with the fault. A WABP algorithm based on the fault component voltage distribution is proposed in [75]. In this scheme, the faulted voltage at one terminal of the line is estimated by the measured values of faulted voltage and current at other terminals, and the faulted line is identified based on the ratio of estimated values to measured values. A faulted area detection technique is also used to accelerate the faulted line identification task. In [2]-[70], synchronized phasor measurement based back up protections are suggested but those schemes deal with only one fault at a time occurred in a power network. But faults or contingencies in a power network is not an isolated issue. In fact more than one fault or contingencies can occur in a power network, especially in a Wide area network, at a time or simultaneously. But nothing is discussed about power systems behaviour if more than one fault or contingencies occurred in power network simultaneously, in any of the above methods. In this chapter, the method discussed is an advanced version of the method discussed in [2], which is modified and extended up to describing the behaviour of power systems during simultaneous faults.

A series capacitor with Metal Oxide Varistor creates problems to distance relaying based transmission-line protection. Typical problems associated with relays have been addressed in [76]-[77] which include several critical phenomenon like voltage/current inversion, sub harmonic oscillations, and additional transients caused by the air-gap operation [78]. Performances of available WABP schemes [71-75] have not been evaluated for series-compensated lines and may find limitation for such lines. This chapter proposes a WABP scheme where angle information between voltage and current at both ends of a line is used for faulted line identification. The scheme is found to be accurate for the compensated and uncompensated line from the evaluation for a 400-kV, 9-bus system and IEEE 14 bus test system with simultaneous faults also. In this chapter several cases have been studied to justify the proposed technique.

5.2 Phasors of Nominal Frequency Signals :

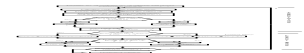
Nominal frequency means desired central frequency. In case of a signal, the desired

central frequency is the same as source or generation frequency. If it deviates from desired central frequency, then it is called off-nominal.

Let us consider a constant input signal $x(t)$, with nominal frequency f_0 [72]. It is sampled at a sampling frequency Nf_0 . The sampling angle $\phi = 2\pi/N$, and the phasor estimation is done below :

$$X(t) = X_m \cos(2\pi f_0 t + \phi)$$

The N data samples of this input $X_n : \{n=0,1,2,\dots,N-1\}$ are



$$\begin{aligned}
 X_c^{n-1} &= \frac{\sqrt{2}}{N} \sum_{n=0}^{N-1} X_n \cos(n\Phi + \delta) \\
 &= \frac{\sqrt{2}}{N} \sum_{n=0}^{N-1} X_m \cos(n\Phi + \delta) \cdot \cos(n\Phi) \\
 &= \frac{\sqrt{2}}{N} X_m \sum_{n=0}^{N-1} [\cos \delta \cdot \cos^2 n\Phi - \frac{1}{2} \sin \delta \cdot \sin(2n\Phi)] \\
 &= \frac{X_m}{\sqrt{2}} \cos \delta
 \end{aligned} \tag{1}$$

$$\begin{aligned}
 \text{Similarly, } X_s^{n-1} &= \frac{\sqrt{2}}{N} \sum_{n=0}^{N-1} X_n \sin(n\delta) \\
 &= -\frac{X_m}{\sqrt{2}} \sin \delta
 \end{aligned} \tag{2}$$

$$\text{The Phasor } X^{N-1} = X_c^{n-1} - jX_s^{n-1}$$

$$\begin{aligned}
 &= \frac{X_m}{\sqrt{2}} [\cos \delta + j \sin \delta] \\
 &= \frac{X_m}{\sqrt{2}} e^{j\delta}
 \end{aligned}$$

5.2.1 Calculation of Protection criterion values :

Assume a voltage or current having orthogonal components X_{1c} and X_{1s} [70-72].

$$\text{Signal } X_1(n) = X_{1c} + jX_{1s} \tag{3a}$$

$$X_1(n) * X_1(n)^* = X_{1m}^2 = X_{1c}^2 + X_{1s}^2 \quad (3b)$$

$$X_{1m} = \sqrt{(X_{1c}^2 + X_{1s}^2)} \quad (3c)$$

5.2.2 Calculation of Power :

Suppose Voltage signal is denoted by $U_{1n} = U_{1c} + jU_{1s}$ (3d)

Current Signal is denoted by $i_{1n} = i_{1c} + ji_{1s}$

$$\text{So, Power } S = U_{1n} * i_{1n}^* \quad (3e)$$

$$\begin{aligned} &= (U_{1c} + jU_{1s}) * (i_{1c} - ji_{1s}) \\ &= (U_{1c} * i_{1c} + U_{1s} * i_{1s}) + j(U_{1s} * i_{1c} - U_{1c} * i_{1s}) \end{aligned} \quad (3f)$$

$$\text{Active Power } P = 0.5(U_{1c} * i_{1c} + U_{1s} * i_{1s}) \quad (3g)$$

$$\text{Reactive Power } Q = 0.5(U_{1s} * i_{1c} - U_{1c} * i_{1s}) \quad (3h)$$

5.3 Proposed Method :

The main purpose of this proposed technique is to improve wide area monitoring and system event analysis. The proposed technique is useful for monitoring and control of large power networks like plants, transmission lines and significant control points of the grid [2]. Synchro-phasor using phasor measurement unit provides all significant measurements required for the operation including voltage magnitudes, phase angles and frequency. The rate of data sampling is maintained at 4kHz. Channel plot step in project settings of EMTDC/PSCAD is kept at 250 micro-seconds.

The Proposed Technique is follows:

Algorithm:

Step1: Start

Step2: Collect all data from all PMUs and PDCs in real time.

Step 3: Obtain minimum positive sequence voltage magnitude or maximum negative or zero sequence magnitude (v_k)

Step4: Compare with the threshold value. If it is less than minimum positive sequence voltage magnitude or more than maximum negative or zero sequence magnitude value, then there is no fault in the system. Otherwise, area or bus k is the nearest to the fault go to Step5 and Proceed

Step5 : Check whether it is a balanced fault or unbalanced fault.

The negative- and zero-sequence voltages are used to identify unbalanced faults [2]. For these faults, the pickup criterion is defined as,

$$V_{m2} \geq K_2 V_n \quad U \quad V_{m0} \geq K_0 V_n \quad (4)$$

Where V_{m2} & V_{m0} are the negative and zero sequence components of the waveform of m^{th} bus and V_n is the rated voltage of the bus. K_2 and K_0 are the constants. In this work, the thresholds of K_2 and K_0 are set at 0.1 for an unbalanced fault. The reason of choosing low threshold settings are that the combined information of negative and zero-sequence voltage magnitudes could improve the sensitivity of pickup criterion during a high-resistance earth fault[2].

If unbalanced fault condition is not satisfied then the substation will check for balanced fault criterion:

$$V_{m1} \leq K_1 V_n \quad (5)$$

V_{m1} is the positive sequence voltage of m^{th} bus. K_1 is a constant whose value is kept 0.6 in this work. Higher threshold for the balanced fault is chosen in order to avoid frequent pickup of the WABP system under normal switching condition of the power system. If it is as high as 0.8 or 0.9 then even any load fluctuation also can generate trip signal and if it is as low as 0.1 or 0.2 also then in case of many faults, trip signal may not be generated[2]. So, a moderate value 0.6 is chosen.

Step6: Compute absolute angle difference of all lines connected to bus or area k .

Step7: Obtain highest value line of phase angle.

Step8: The j^{th} line connected to area k is faulted line.

Step9: Authentication if series capacitor compensation involved in the faulted line: Check

$$g_{2s}, g_{2s'}, g_{2R} \text{ all } > 0 \quad (6) \quad \text{for an unbalanced fault.}$$

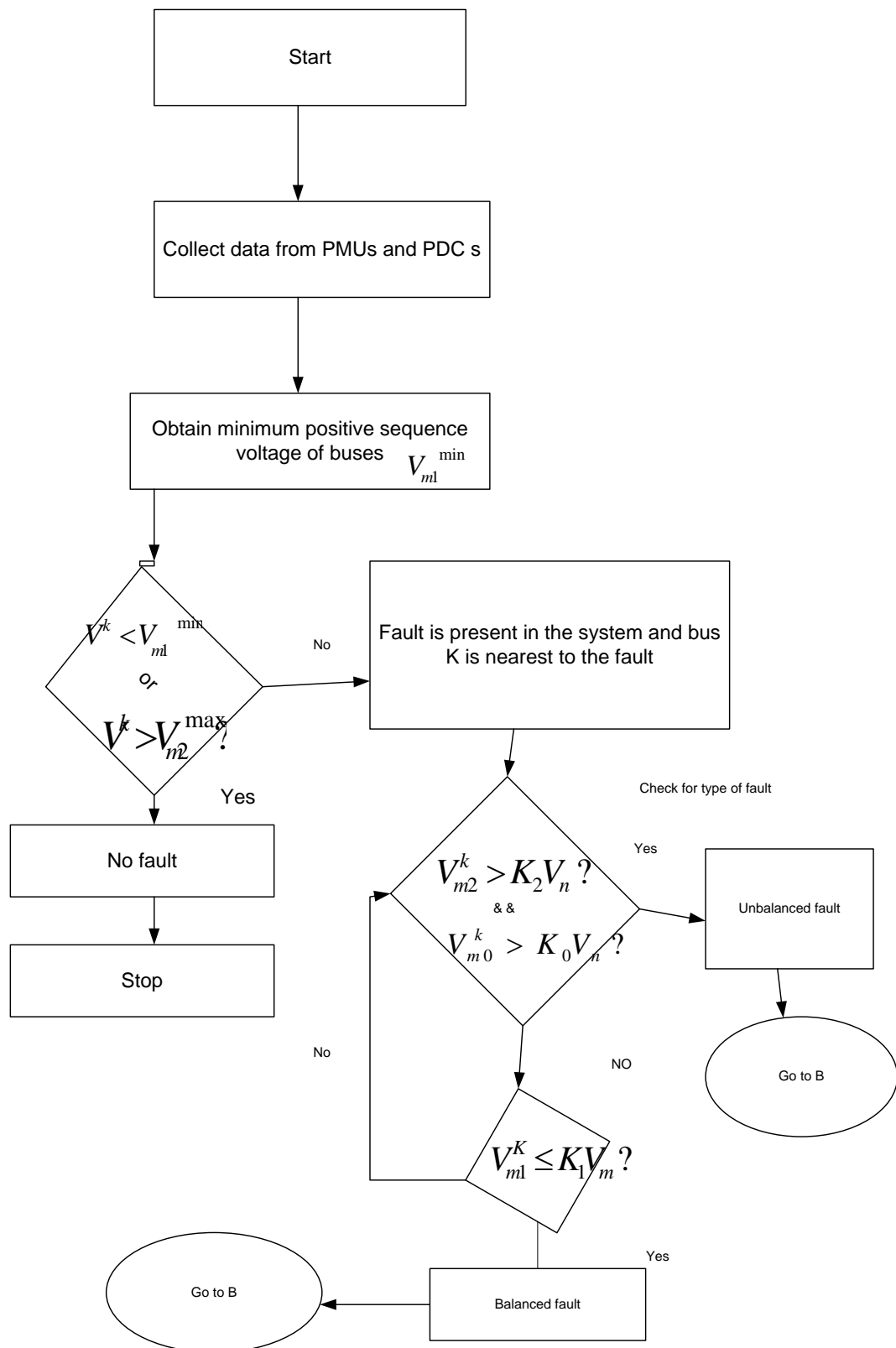
Check,

$$g_{1s}, g_{1s'}, g_{1R} \text{ all } > 0 \quad (7) \quad \text{for a balanced fault.}$$

Step10 : Relaying algorithm

Step11 : Stop

Flow chart of the proposed method is shown in Fig 1.



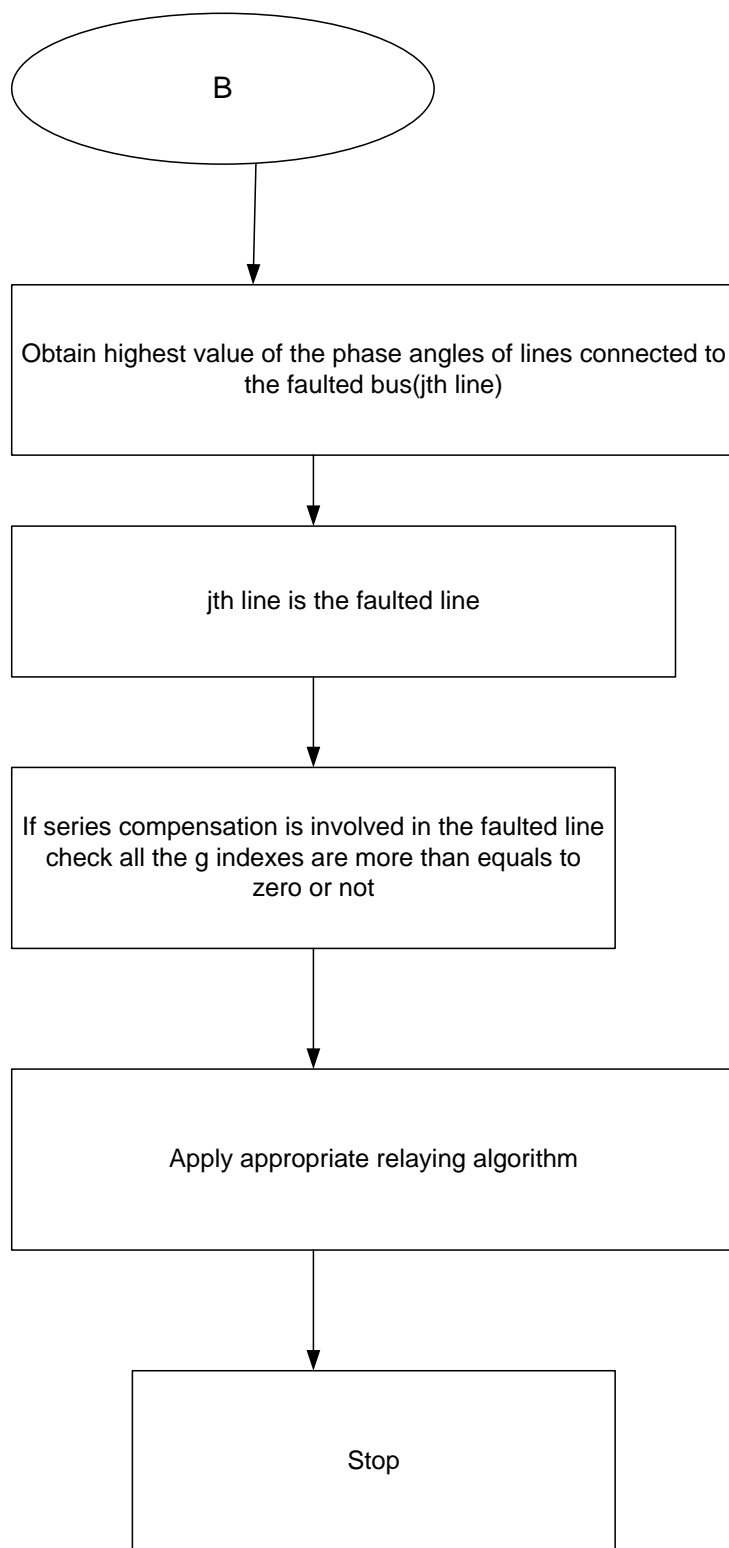


Fig1 : Flow chart of the proposed method

5.4. Case Studies

5.4.1 WSCC-3 Machine-9 Bus System Applications

The proposed Wide Area Measurement Back up protection (WABP) algorithm is tested for a WSCC 3-Machine-9 bus system (same as Fig 2). Using EMTDC/PSCAD and MATLAB/SIMULINK software simulations are carried out for different types of fault and even simultaneous faults in different branches of the system (both balanced and unbalanced faults). The data sampling rate is maintained at 4 KHz throughout. Solution time step is kept at 50 microsecond and channel plot step is kept 250 micro seconds in project settings of EMTDC / PSCAD for capturing data (in case used EMTDC/PSCAD for WSCC-3-Machine-9 bus system simulation).

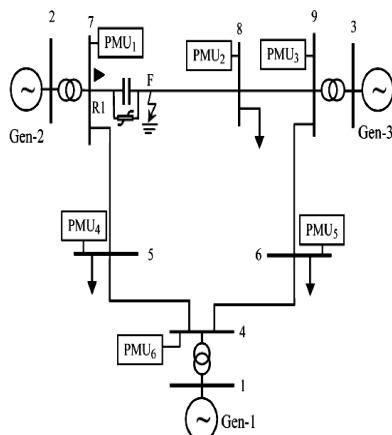


Fig.2. Single Line Diagram of WSCC-3Machine-9bus system with PMUs

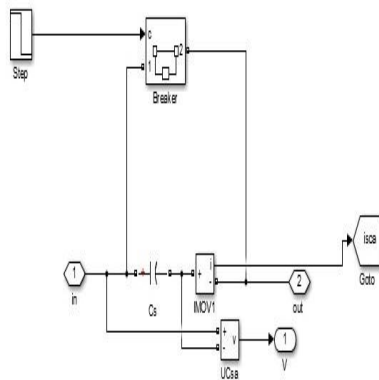


Fig.3. Simulink Design of MOV Circuit with different protections

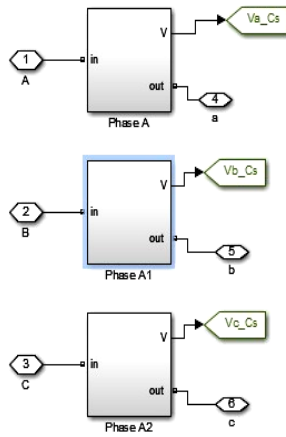


Fig.4. Simulink Design of Data Acquisition system

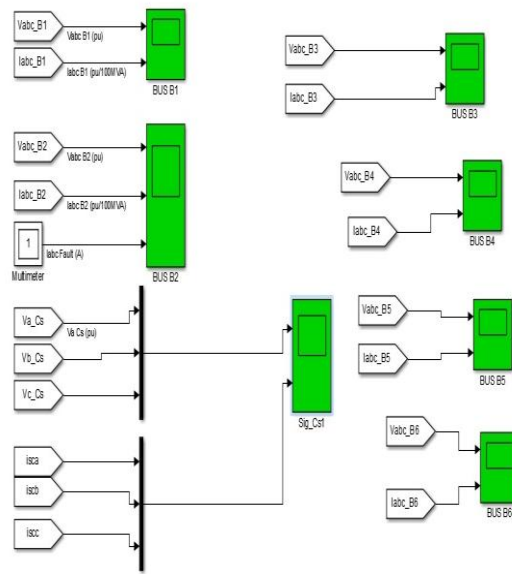


Fig. 5. Design of Data Acquisition with Simulink

Fig.6 is showing Simulink implementation of WSCC-3-Machine-9 bus system and Fig.7 is showing PSCAD implementation of 9 bus system. Fig.3, Fig.4 and Fig.5 are showing different internal protections and arrangement of data acquisition by Simulink software required for the work.

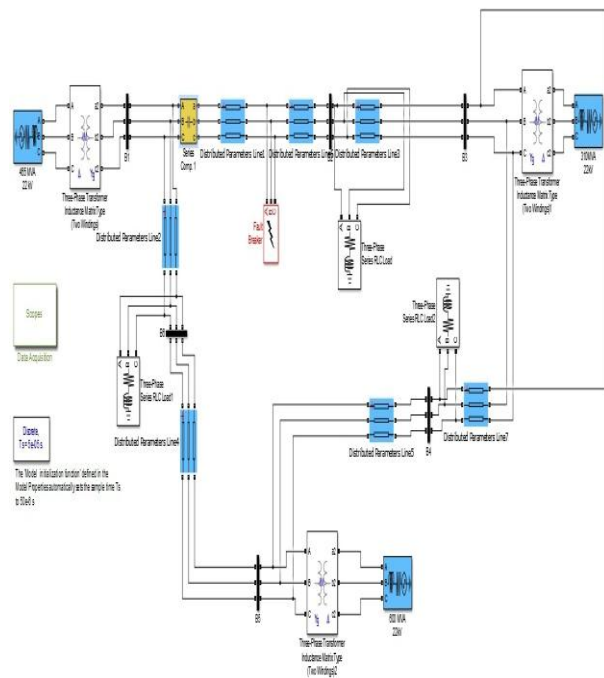


Fig.6. Simulink Implementation of 9 bus system

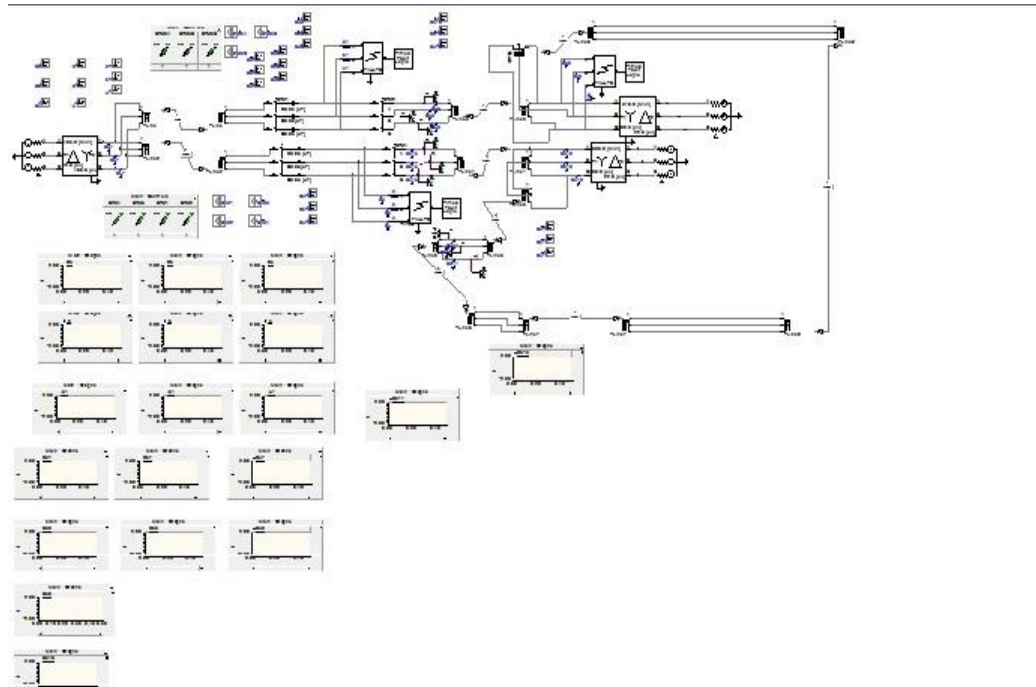


Fig.7. PSCAD Implementation of 9 bus system

5.4.1.1 Unbalanced Fault Case:

5.4.1.1 Case-1: LG Fault :

An LG fault (AG-type) is created at 0.34 sec on line 5-7 at a distance of 30 km from bus-5 for 0.04 sec. A capacitor is used in Line 5-7 with 40% compensation. The waveform got from different buses are studied below:

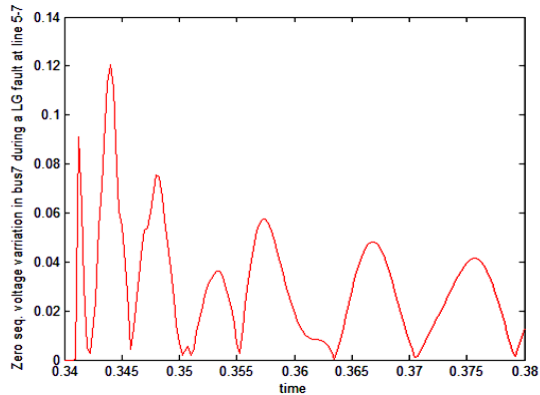


Fig.8(a). Zero Sequence Voltage Profile at bus7

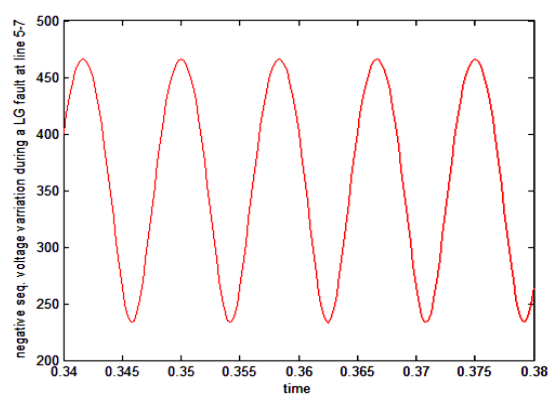


Fig 8(b):Negative Sequence Voltage Profile at bus5

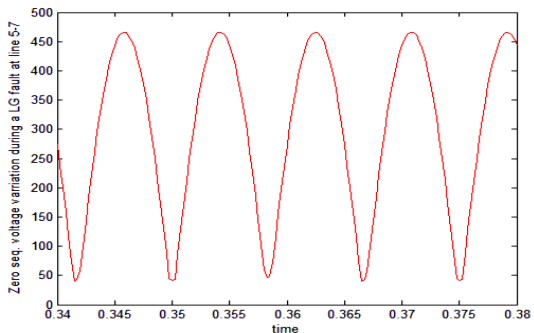


Fig.8(c). Zero Sequence Voltage Profile at bus5

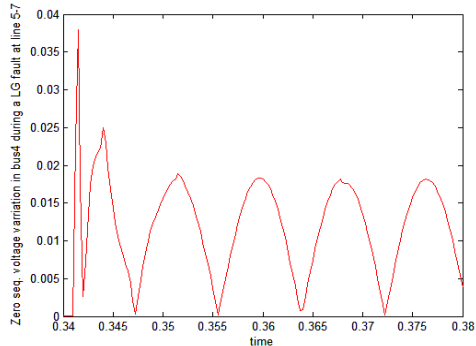


Fig.8(d). Zero Sequence Voltage Profile at bus4

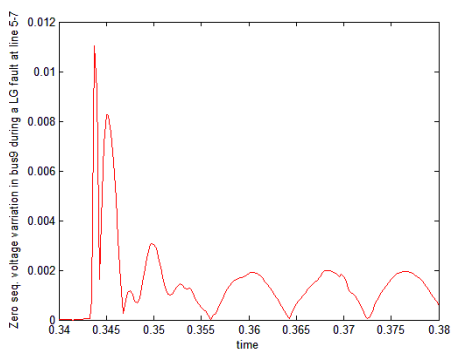


Fig.8(e). Zero Sequence Voltage Profile at bus9

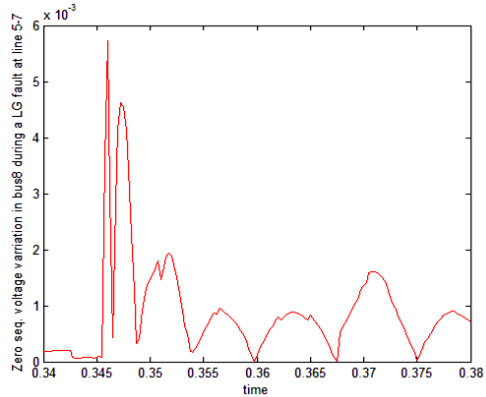


Fig.8(f). Zero Sequence Voltage Profile at bus8

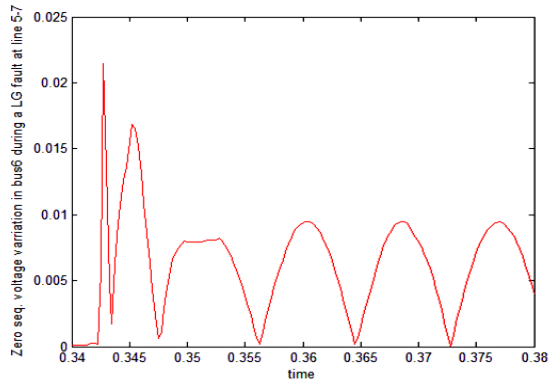


Fig.8(g). Zero Sequence Voltage Profile at bus6

The observation of the figures 8(a), 8(b), 8(c), 8(d), 8(e), 8(f), 8(g) clearly shows it satisfies the equation (4), the pickup condition for unbalanced fault as:

$$K_2 V_n = 40 \text{ KV} \quad K_0 V_n = 40 \text{ KV}$$

Bus 5 zero sequence voltage profile having maximum voltage magnitude among other buses in the network. So, the bus 5 data satisfies the criterion for an unbalanced fault and as bus 5 having maximum zero sequence magnitude, Bus5 is closest to the fault.

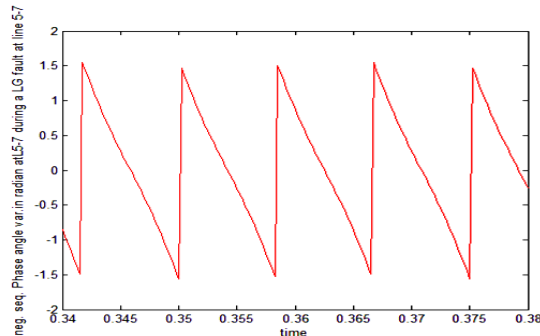


Fig.9(a). Phase Variation Line 5-7

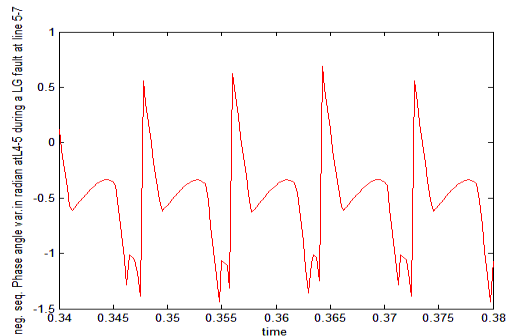


Fig.9(b). Phase Variation Line 4-5

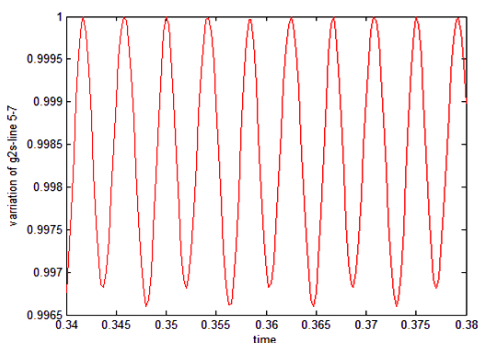


Fig.10(a). g_{2s} profile during LG fault

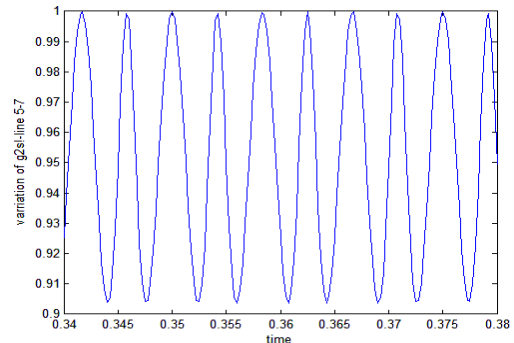


Fig.10(b). g_{2s}^{-1} profile during LG fault.

Two lines are adjacent to bus5. Line 5-7 and Line 4-5. The negative sequence phase variation is shown for those two lines are in figure 9(a), 9(b). The phase variation is expressed in radian. It is seen the variation of phase lies between $-\pi/2$ to $+\pi/2$ or -90degree to +90 degree.

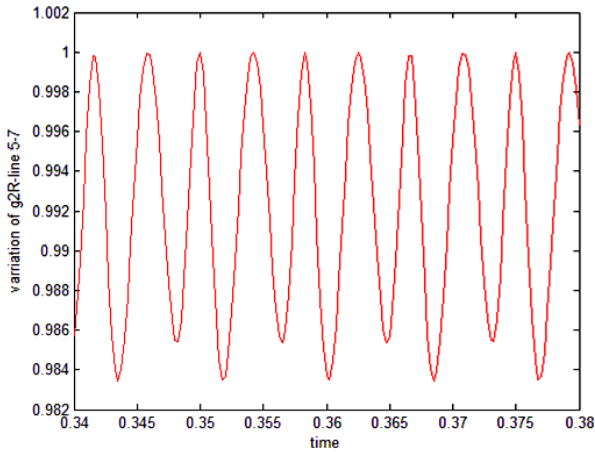


Fig.10(c). g_{2R} profile during LG fault

From the figures 9(a), 9(b) and 10(a), Fig.10(b), Fig.10(c), it is clear that line 5-7 is satisfying the equation (6), hence the criterion and authentication of an unbalanced fault. So, line 5-7 is the faulted line.

5.4.1.1.2 Case-2: LLG Fault :

A double line-to-ground fault (ABG-type) is created at 0.34 s on line 5-7 at a distance of 30km from bus-5 for 0.04 sec. A capacitor is used in Line 5-7 with 40% compensation.

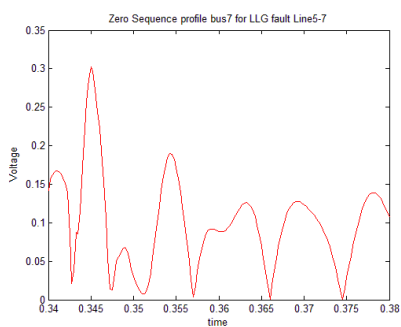


Fig11(a)zero Sequence Voltage Profile at bus7

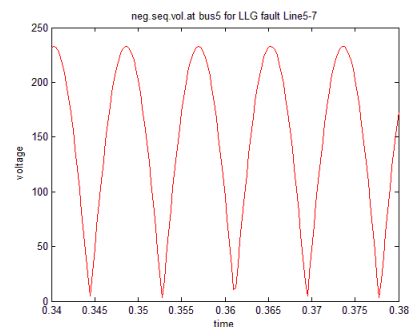


Fig11(b)negative Sequence Voltage Profile at bus5

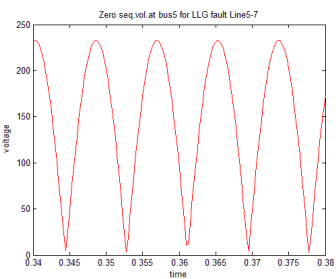


Fig11(c)Zero Sequence Voltage Profile at bus5

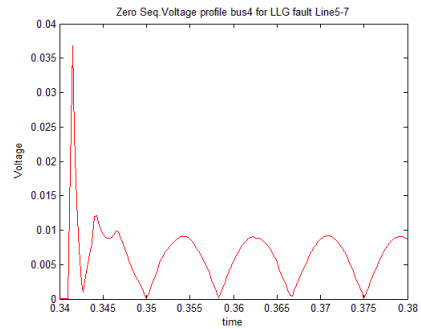


Fig11(d)Zero Sequence Voltage Profile at bus4

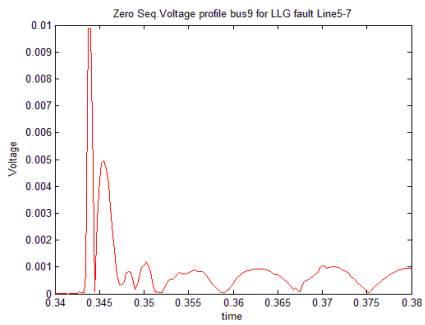


Fig 11(e)Zero Sequence Voltage Profile at bus9

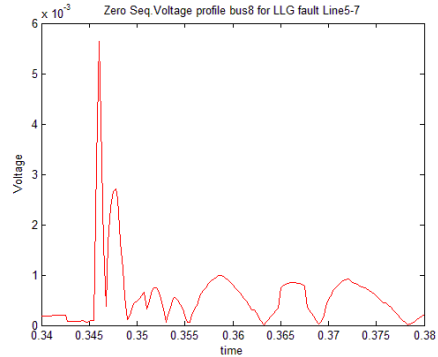


Fig 11(f)Zero Sequence Voltage Profile at bus8

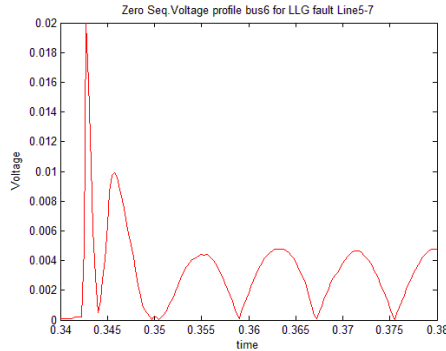


Fig11(g)Zero Sequence Voltage Profile at bus6

The observation of the figure no.11(a),11(b),11(c),11(d),11(e),11(f),11(g) clearly shows it satisfies equation 4, the pickup condition for unbalanced fault as:

$$K_2 V_n = K_0 V_n = 40KV$$

Bus 5 zero sequence voltage profile having maximum voltage magnitude among other buses in the network. However depending on source, load and measurement errors in each substation some samples may deviate from the pickup criteria. So, the bus 5 data satisfies

the criterion for an unbalanced fault and as bus 5 having maximum zero sequence magnitude, Bus5 is closest to the fault. All the voltages are expressed in KV.

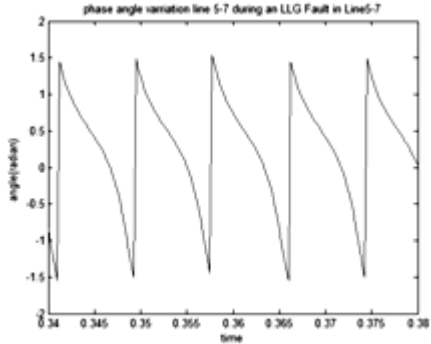


Fig 12(a) Phase variation of line 5-7

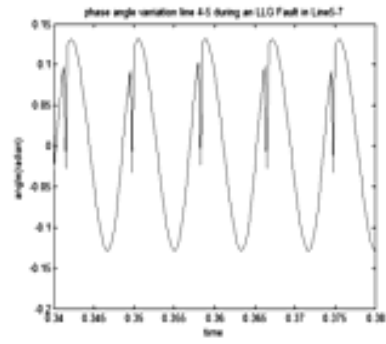


Fig 12(b) Phase variation of line 4-5

Two lines are adjacent to bus 5, line 5-7 and line 4-5. The phase variations of those lines are shown in Fig 12(a) and Fig 12(b). The variations are expressed in radians. It is seen that the variations of the phase lies between $-\pi/2$ to $+\pi/2$ (-90degree to + 90 degree).

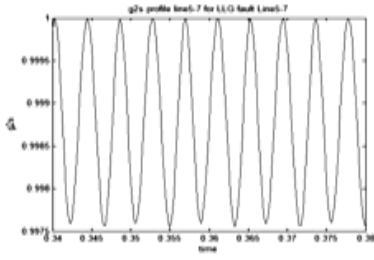


Fig 13(a): g_{2s} profile

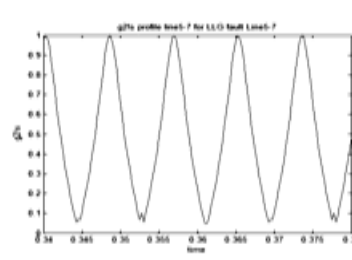


Fig 13(b): g_{2s} profile

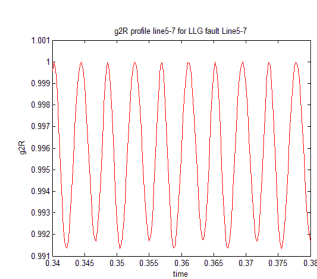


Fig 13(c) g_{2R} profile

Fig 13(a ,b,c):g index profiles during a LLG fault

From the figure 12(a),12(b) and 13(a),13(b),13(c) it is clear that line 5-7 is satisfying equation (6) also, hence the criterion and authentication of an unbalanced fault. So, line 5-7 is the faulted line.

5.4.1.2 Balanced Fault Case:

5.4.1.2.1 Case-1: LLL Fault :

a 3-phase fault is created at 0.34 s on line 5-7 at a distance of 30km from bus-5 for 0.04 sec. After collecting all data, the following analysis has been done:

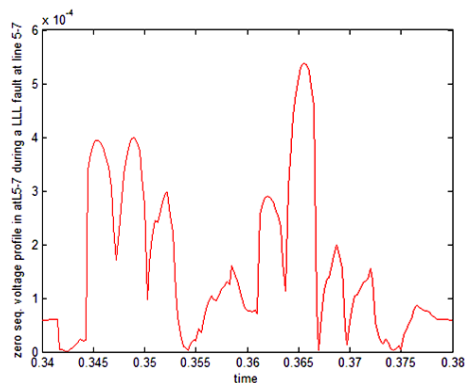


Fig.14(a). Zero Sequence Voltage Profile at bus5.

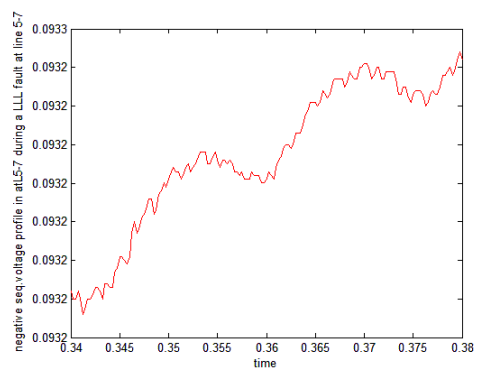


Fig.14(b). Negative Sequence Voltage Profile at bus5.

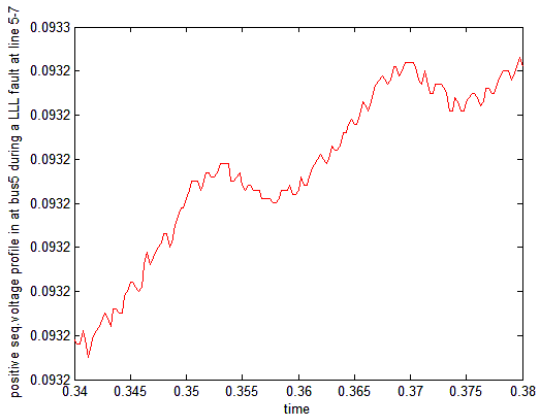


Fig.14(c). Positive Sequence Voltage Profile at bus5.

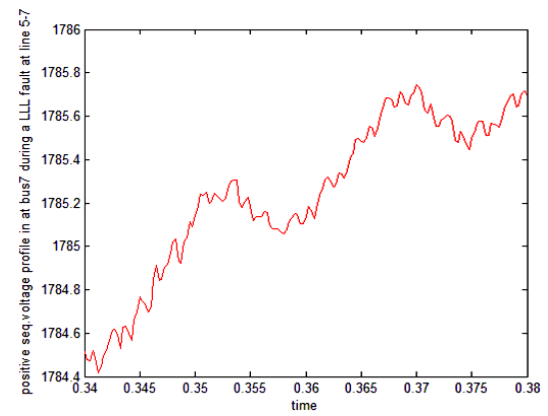


Fig.14(d). Positive Sequence Voltage Profile at bus7.

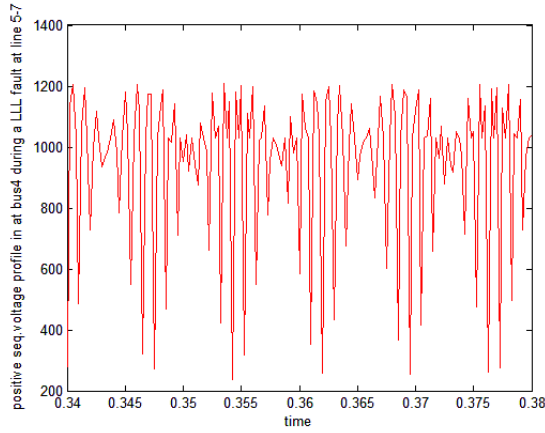


Fig.14(e). Positive Sequence Voltage Profile at bus4.

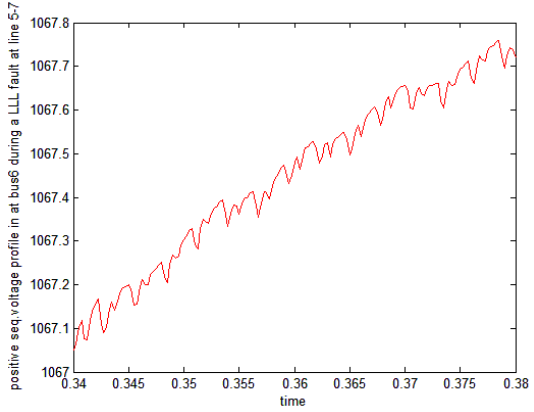


Fig.14(f).Positive Sequence Voltage Profile at bus6.

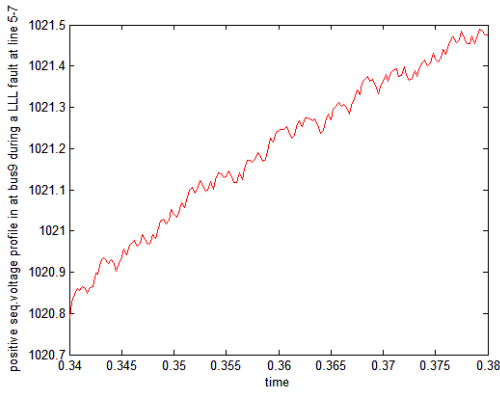


Fig.14(g).Positive Sequence Voltage Profile at bus9

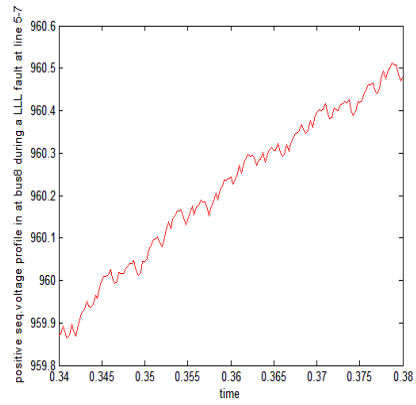


Fig.14(h). Positive Sequence Voltage Profile at bus8.

All the units of voltage are expressed in Kilo Volt (KV) here and time in second. The observation of the figure 14(a), 14(b), 14(c), 14(d), 14(e), 14(f), 14(g), 14(h) clearly shows it does not satisfy equation (4), the pickup condition for unbalanced fault.

$$\text{as } V_{m2} \leq K_2 V_n \text{ && } V_{m0} \leq K_0 V_n$$

$$K_2 V_n = 40 \text{ KV} \quad K_0 V_n = 40 \text{ KV}$$

But it satisfies equation (5), the pickup criterion of a balanced fault as:

$$K_1 V_n = 240 \text{ KV.}$$

and minimum value of positive sequence voltage exist in bus5. So, bus 5 can be considered as bus nearest to the fault.

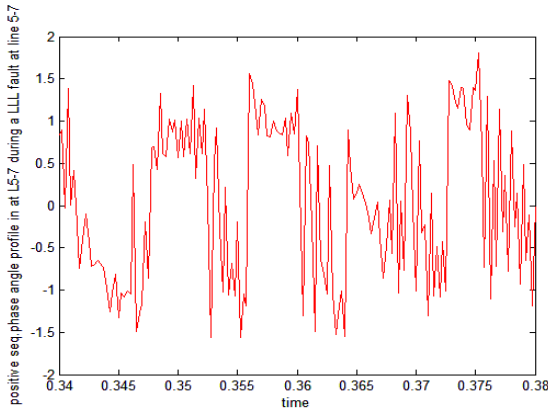


Fig.15(a). Phase Variation Line 5-7.

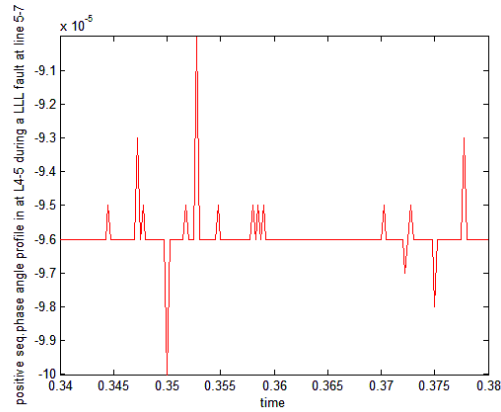


Fig.15(b).Phase Variation Line 4-5.

From the figures 15(a), 15(b), 15(c) and 16(a), 16(b), 16(c) it is clear that line 5-7 is satisfying equation (7), and hence the criterion and authentication of an balanced fault. So, line 5-7 can be considered as the faulted line.

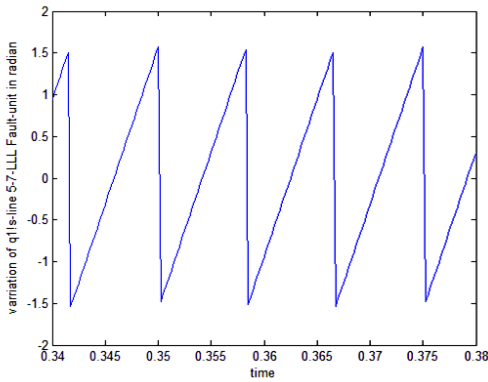


Fig.15(c). Variation of q_{1s} for Line 5-7

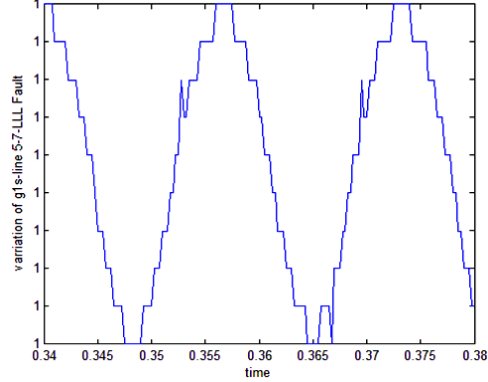


Fig.16(a). g_{1s} profile during LLL fault.

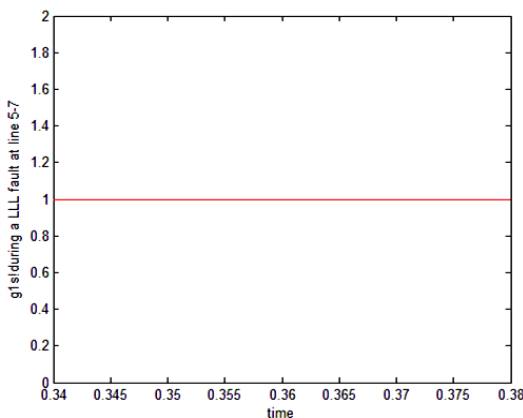


Fig.16(b). g_{1s}' profile during LLL fault.

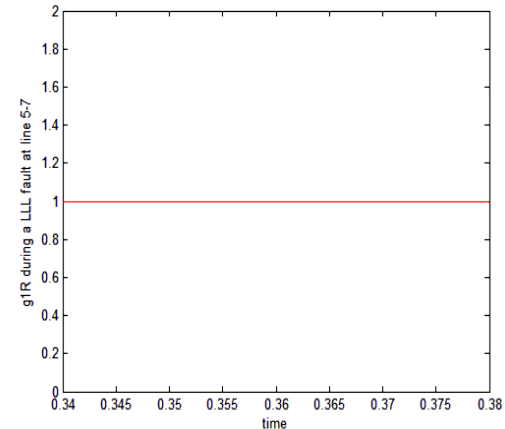


Fig.16(c). g_{1R} profile during LLL fault

5.4.1.2.2 Case-2: LLLG Fault :

a LLLG fault is created at 0.34 s on line 5-7 at a distance of 30km from bus-5 for 0.04 sec. After collecting all data, the following analysis has been done :

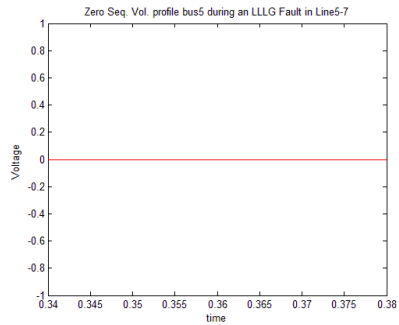


Fig 17(a) Zero Sequence Voltage Profile at bus5

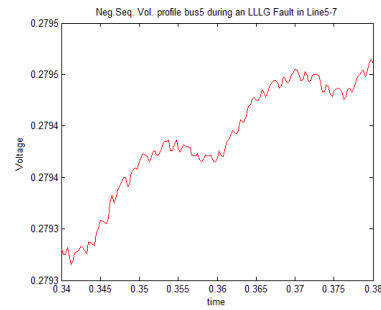


Fig 17(b):Negative Sequence Voltage Profile at bus5

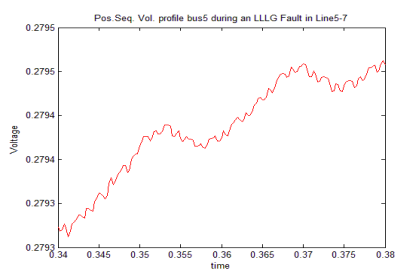


Fig 17(c)Positive Sequence Voltage Profile at bus5

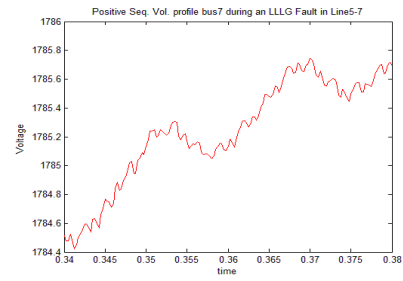


Fig17(d)Positive Sequence Voltage Profile at bus7

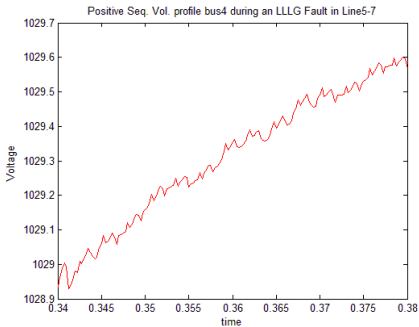


Fig17(e)Positive Sequence Voltage Profile at bus4

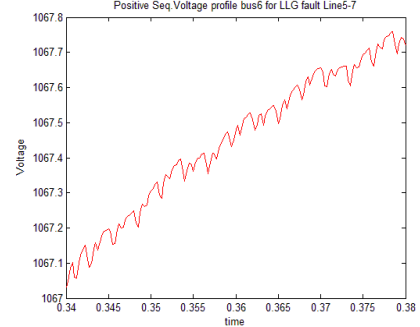


Fig17(f)Positive Sequence Voltage Profile at bus6

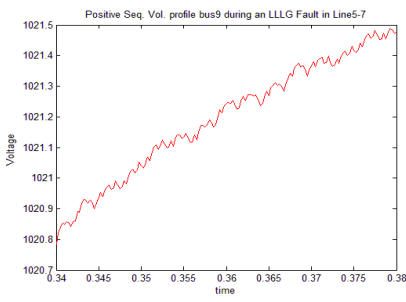


Fig17(g)Positive Sequence Voltage Profile at bus9

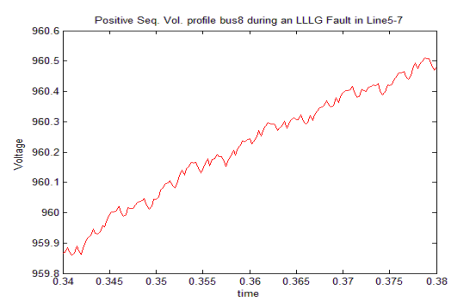


Fig17(h)Positive Sequence Voltage Profile at bus8

All the units of voltage are expressed in KV here. Time is expressed in second. The observation of the figures 17(a) to 17(h) clearly shows it does not satisfy equation (4),the

pickup condition for unbalanced fault as $V_{m2} \leq K_2 V_n$ && $V_{m0} \leq K_0 V_n$
 $K_2 V_n = K_0 V_n = 40KV$

But it satisfies equation(5), the pickup criterion of a balanced fault as $K_1 V_n = 240KV$

And minimum value of positive sequence voltage exist in bus5. So, bus 5 is considered as bus nearest to the fault.

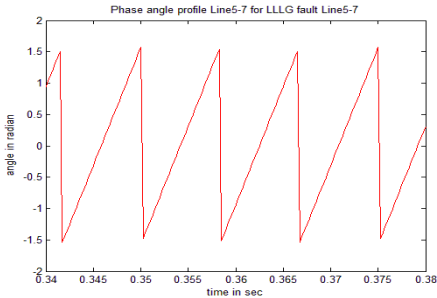


Fig 18(a) :Phase Variation Line 5-7

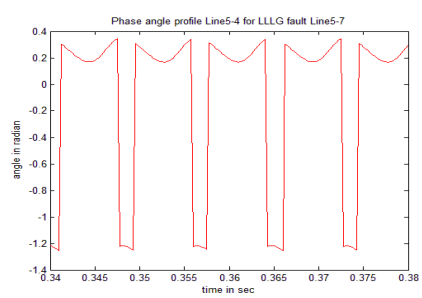


Fig 18(b):Phase Variation Line 4-5

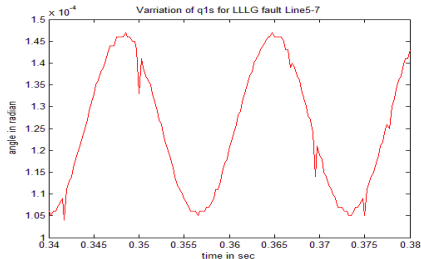


Fig 18 (c)Variation of \mathcal{O}_{1s} for Line 5-7

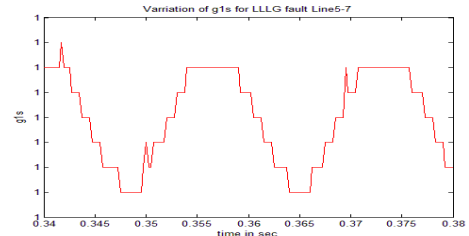


Fig 19(a): g_{1s} profile during LLLG fault

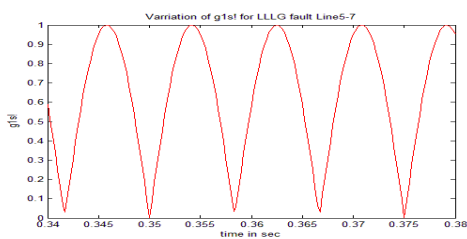


Fig 19(b): g_{1s} profile during LLLG fault

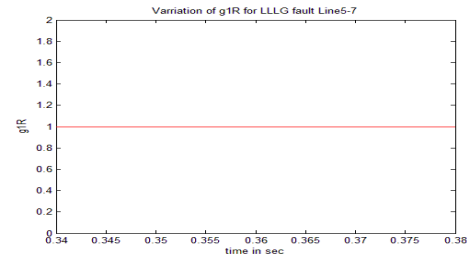


Fig 19(c) g_{1R} profile during LLLG fault

From the figures 18(a), 18(b), 18(c) and 19(a), 19(b), 19(c), it is clear that line 5-7 is satisfying equation(7), hence the criterion and authentication of an balanced fault. So, line 5-7 is the faulted line.

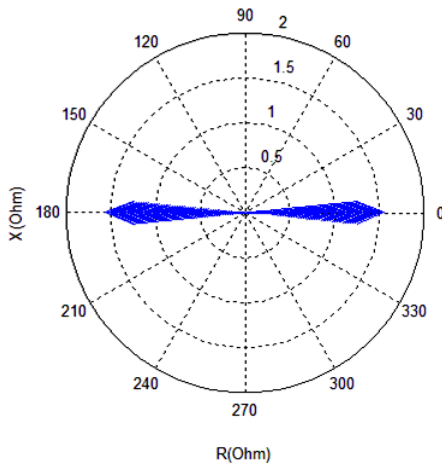


Fig. 20(a). During an LG fault

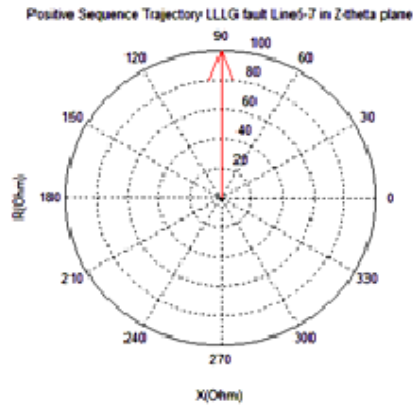


Fig 20(b): During an LLLG fault

Fig 20 : Positive Sequence Impedance Trajectory in $Z-\phi$ plane

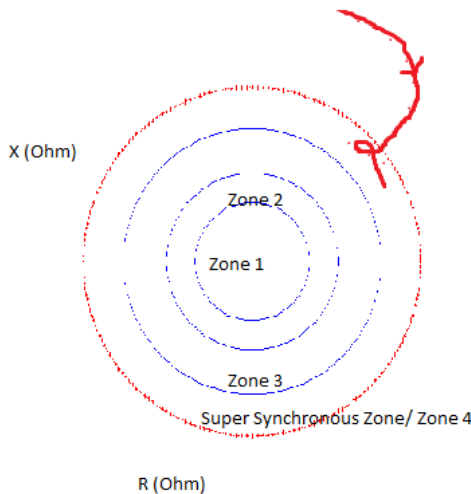


Fig.21. Positive Sequence Impedance Trajectory in $Z-\phi$ plane enters super synchronous zone (zone 4).

The positive sequence impedance of the test system seen by the relaying point during the fault is plotted in the impedance plane (Fig 20(a) and Fig 20(b)). From the trajectory of the fault impedance, it can be concluded which zone the locus is confined and whether distance relay is going to generate any trip signal to circuit breaker or not and if there is any chance for evolving load encroachment problem or not. Fig.21 is showing another case of analysis of system behavior through analysis of impedance trajectory. Here we are considering another circle apart from 3 circles of 3-zone characteristics of relay, encircling zone 3 or relay characteristics. We are calling it as super synchronous zone or zone 4 of the relay. Zone 4

boundary is chosen very nearer to the boundary of zone 3 but greater than zone 3 circle boundary. If from the study of impedance characteristics of a system, we found that impedance trajectory entered in zone 4 or super synchronous zone of the relay characteristics then the system can be distinguished as prone to fault or prone to generate trip signal to the circuit breaker of the system. So, it can be said that, the system needs precaution. From the sign of the angle values of impedances, fault direction estimation is also possible(upstream or downstream part of the transmission line). This analysis can be used in case of condition based monitoring of the system to increase its reliability or security of operation. Thus the impedance trajectory is very helpful in judging several critical conditions of power systems including power swing or dynamic loading conditions (load encroachment etc), fault prone conditions etc.

5.4.1.3 Simultaneous Fault Case :

Protection of power systems or occurrence of faults in a power network is not an isolated task. It may happen simultaneously. So, now the new WABP algorithm is tested under the condition of occurrence of simultaneous faults across the power network. And here also it is found that it is having immunity to support simultaneous occurrence of faults phenomena.

5.4.1.3.1 Simultaneous Faults at different buses :

5.4.1.3.1.1 Case 1: Bus5 and Bus9 both involved with LLL fault:

a LLL fault is created at 0.34 s on line 5-7 at a distance of 30km from bus-5 for 0.04sec and at the same time another LLL fault is created at line 8-9 at 0.35sec for 0.04 sec. The wave forms obtained from this case is studied below :

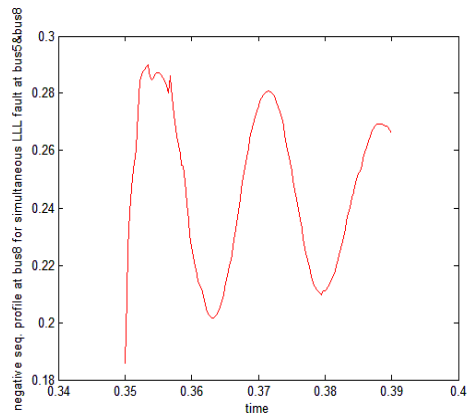


Fig.22(a). Negative Sequence Profile at bus8.

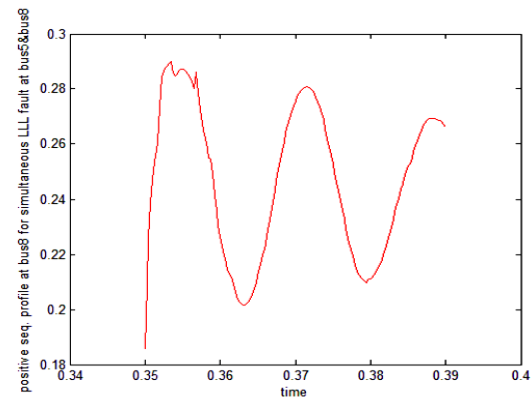


Fig.22(b). Positive Sequence Voltage Profile at bus8.

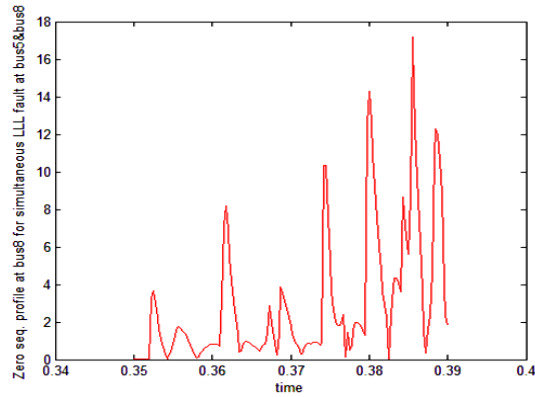


Fig.22(c). Zero Sequence Voltage Profile at bus8.

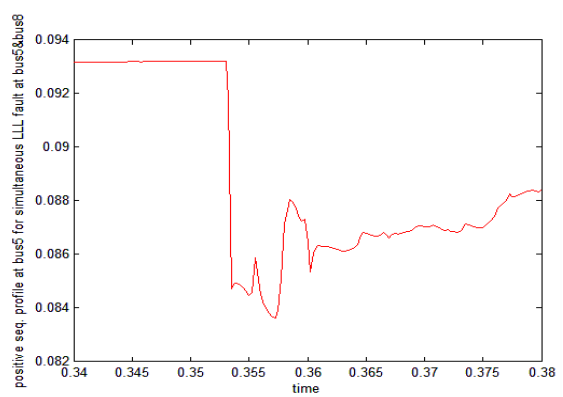


Fig.23(a). Positive Sequence Voltage Profile at bus5.

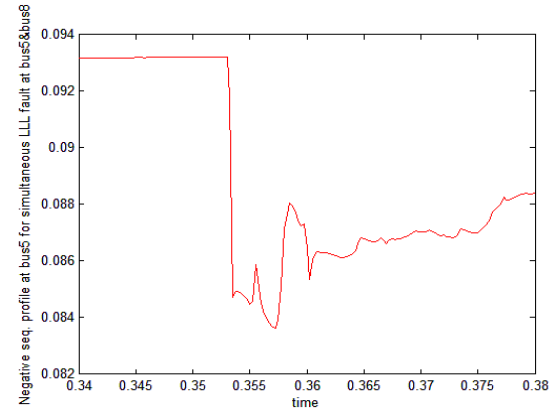


Fig.23(b). Negative Sequence Profile at bus5.

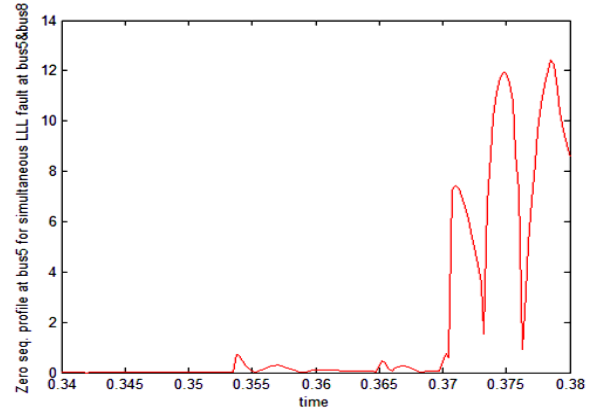


Fig.23(c). Zero Sequence Voltage Profile at bus5

From the sequence voltage (positive, negative and zero) profiles at both the buses, it is evident both the buses individually satisfying the pickup criterion for a balanced fault.

5.4.1.3.1.2 Case 2: Bus5 with LLL and Bus9 with LLG Fault:

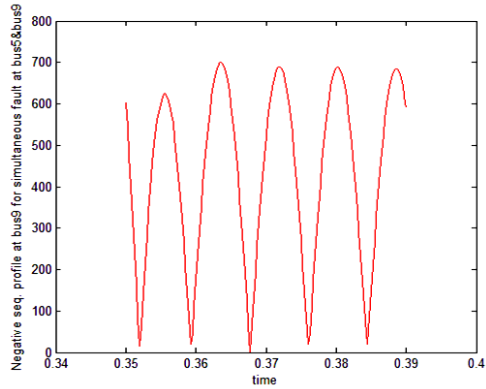


Fig.24(a). Negative Sequence Profile at bus9

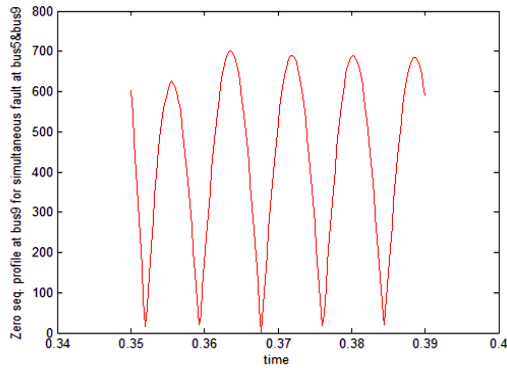


Fig.24(b). Zero Sequence Profile at bus9.

Here also both the sequence voltage profiles will satisfy their individual fault pick up criterion. However depending on source, load and measurement errors in each substation and circumstances some samples may deviate from the pickup criteria. During critical conditions of power systems like- load encroachment and power swing conditions, the positive sequence impedance may enter zone 3 of relay which can cause undesired tripping of lines. But in those cases FLI criterion will not satisfy and thus such events will declare as a non-fault situation by the scheme. Thus WABP Scheme mitigates the problem raised during critical conditions of power network (e.g-load encroachment and power swing conditions). So, this scheme works fine for zone 3 protection support also.

5.4.1.3.1.3 Case 3: Bus5, Bus 8 and and Bus9 with balanced Fault:

Fig 25(a) and 25(b) are showing the voltage profiles at bus5 .

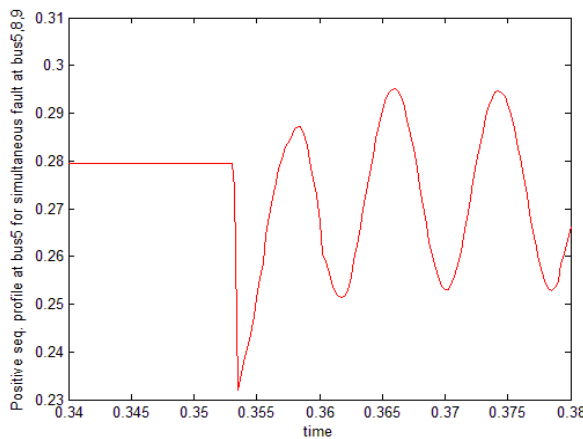


Fig 25(a) Zero Sequence Voltage bus5

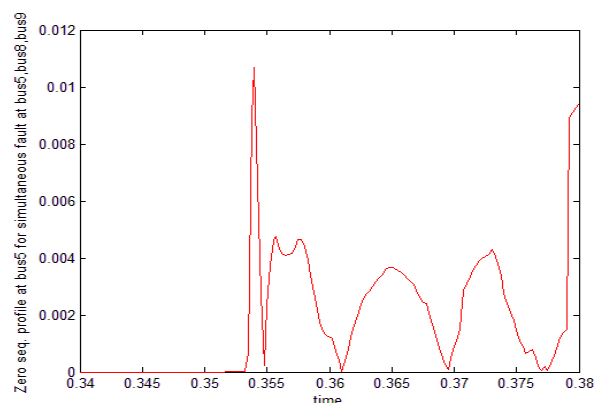


Fig25(b)Positive Sequence Voltage bus5

5.4.1.3.2 Sources of error/ Limitation : Simultaneous Faults at different Lengths of the same Line :

5.4.1.3.3.1 Case 1: LG and LLL Fault in Line 5-7: Possibility1

A-G fault is created at Line 5-7 at 0.32 sec for 0.04 sec at 30KM distance from bus 5 and at the same time another fault is created on the same line and almost at the same distance (within 1km)for 0.34 sec for 0.04 sec which is a 3-phase fault. Now the fault voltage profile from 0.32 sec to 0.38 sec for bus 5 is indicated as follows:

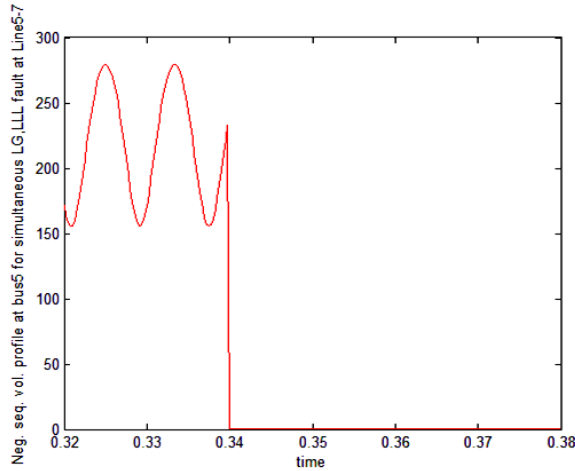


Fig.26(a). Negative Sequence Profile at bus5

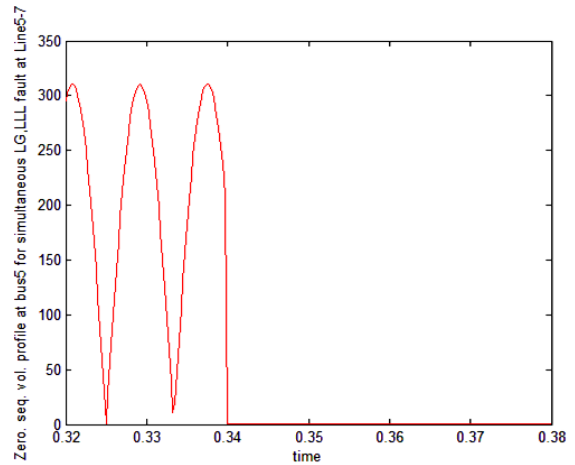


Fig.26(b). Zero Sequence Profile at bus5

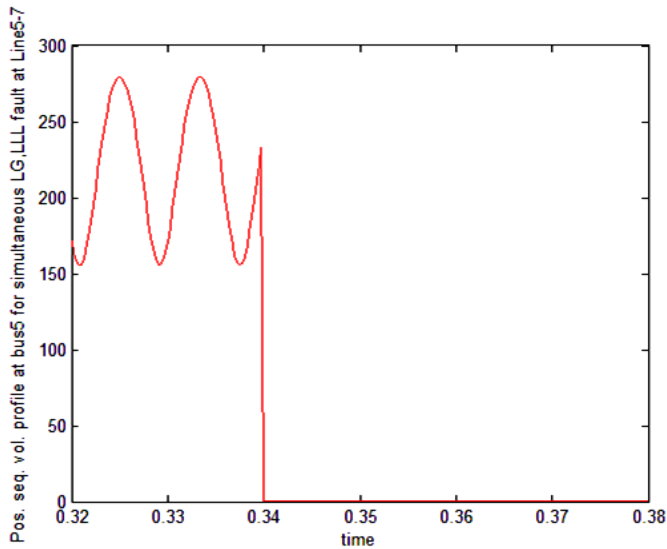


Fig.26(c). Positive Sequence Profile at bus5

From the above figure no. 26(a), 26(b), 26(c), it is clear that resultant waveforms having two parts.

- i) up to 0.32-0.34 sec ,it is obeying the pickup criterion of an unbalanced fault and
- ii) 0.34-0.38 sec, the waveforms are obeying the pickup criterion for a balanced fault.

Theoretically, the wave should have three parts, 0.32-0.34 sec. unbalanced fault, 0.34-0.36 sec both balanced and unbalance fault exist in the line and 0.36-0.38 sec balanced fault exist in the line. Here the circuit is obeying superposition theorem of network. As 3-phase fault is the most severe fault in the circuit, it nullifies the effect of an unbalanced fault and predominates.

So, with this scheme if some balanced fault is indicating, it may contain some percentage of simultaneous unbalanced faults also, in the line as faults in power system is not an isolated issue. This scheme is showing unbalanced fault means the line contains unbalanced faults only but in case of balanced fault, the line may contain some percentage of unbalanced faults also.

5.4.1.3.3.2 Case 2: LG and LLL Fault in Line 5-7: Possibility2

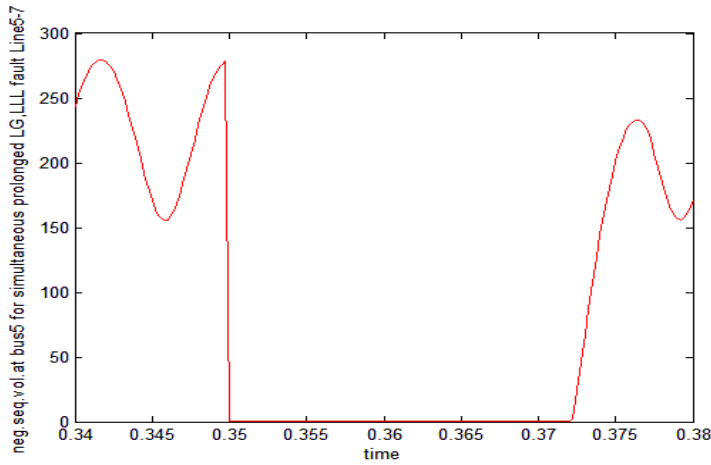


Fig.27. Negative Sequence Profile at bus5.

Fig.27 is another case study, where an A-G fault is created at 0.34 sec for 0.04 sec on line 5-7 at 30KM distance, at the same time another close in fault which is a 3-phase fault by nature is created on the same line at 0.35 sec for 0.02sec (between 0.35-0.37 sec). Same as previous case, between 0.35-0.37 sec, the balanced fault predominates and suppressed the effect of unbalanced A-G fault and once the balanced fault is cleared, between 0.37-0.38 sec, the effect of unbalanced fault is again seen. Thus output is a composite figure in nature. So, in the presence of a balanced fault, the effect of unbalanced fault cannot be distinguished as LLL fault predominates with respect to its degree of severity than LG fault. LLL is the most severe fault, however most occurred fault in power system is LG fault. Around over 70% fault occurred in the power systems are generally LG fault and a perfect symmetrical fault occurred in a power system is seen to be very rare.

So, existence of Simultaneous faults in the same line is confirmed with logic shown below.

- i) Balanced + Unbalanced- Output Balanced
- ii) Balanced+ Balanced- Output Balanced

- iii) Unbalanced + Balanced- Output Balanced
- iv) Unbalanced +Unbalanced –Output Unbalanced

The above four postulates can be represented in a form of truth table as Table-1 :

Table –1 : Simultaneous fault logic

Balanced	Unbalanced	Output Balanced
High	X	High
Low	High	Low

X – Indicates don't care condition.

With the existing scheme, it is difficult to distinguish the simultaneous faults in a same line which involves both balanced and unbalanced type of faults. Moreover, depending on the several parameters and constraints of the power system like - source strength, demand of load and other errors in measurement and operation, some samples may deviate from their own pick up criterion sometimes.

5.4.2 Application on an IEEE-14 Bus System

The method discussed above is also tested on an IEEE-14 bus system to prove its effectiveness. The test system (ref. Fig 28) is constructed by using PSCAD software (ref. Fig.29). Different cases are simulated on this test system to show the effectiveness of the proposed method.

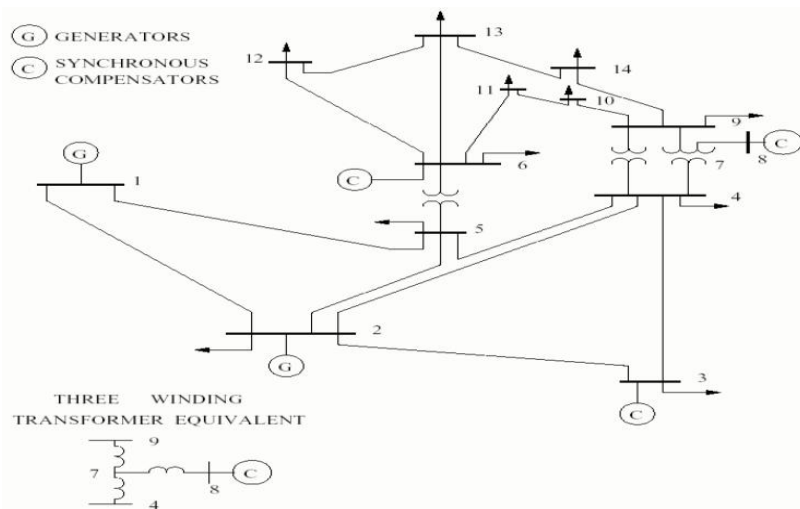


Fig 28: Single Line Diagram of an IEEE-14 bus test system

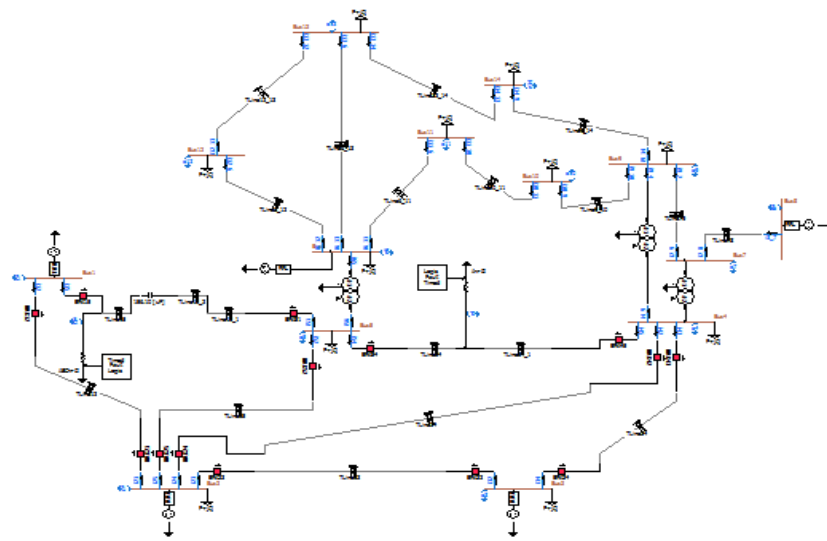
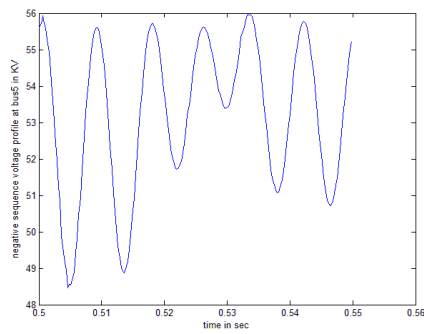


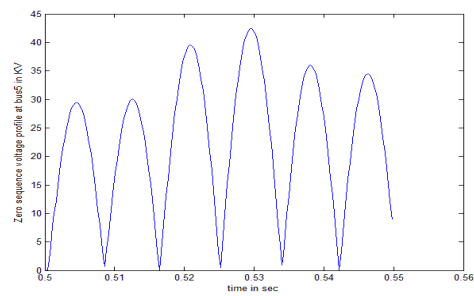
Fig 29: PSCAD Implementation of IEEE 14 bus system

5.4.2.1 Case-1: LG fault :

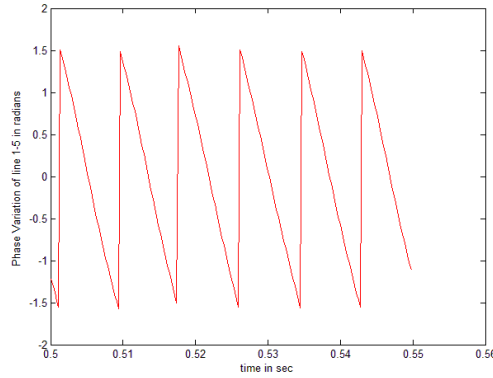
A Phase A-G fault is created at line 1-5 at 0.5 sec for 0.05 sec duration at a distance 50Km from bus1 (33.87 Km from bus 5). A capacitor with 40% compensation is used in line 1-5. The bus nominal voltages are 138 KV. From the analysis of its sequence component voltages and phase angles it is found that bus5 is satisfying the bus closest to the fault and unbalanced fault pick up criteria as $K_2 V_n = K_0 V_n = 13.8$ KV. Bus 5 is connected with line 1-5, line 4-5 and line 5-6. Among them line 1-5 has highest value of phase angle. So, line 1-5 is the faulted line. The sequence voltages and phase angle variations are shown in Fig 30 (a,b,c). All g index values are also found to be positive. So, it is satisfying the authentication of unbalanced fault also.



(a) Negative Sequence Voltage profile at bus 5



(b) Zero Sequence Voltage profile at bus 5

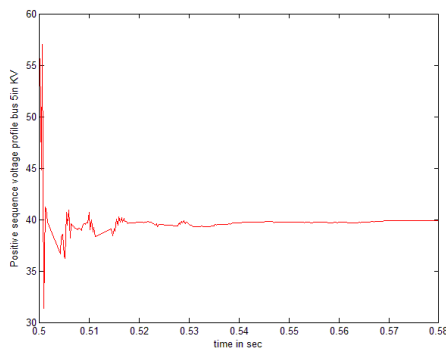


(c) Phase angle variation of line 1-5

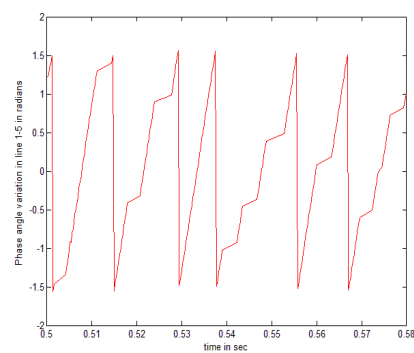
Fig 30(a,b,c): Sequence Voltage profiles at bus 5 and phase angle variation in line 1-5

5.4.2.2 Case-2: **LLL G fault :**

A LLLG fault is created at line 1-5 at 0.5 sec for 0.05 sec duration at a distance 50Km from bus1 (33.87 Km from bus 5). A capacitor with 40% compensation is used in line 1-5. The bus nominal voltages are 138 KV. From the analysis of its sequence component voltages and phase angles, it is found that bus5 is satisfying the bus closest to the fault and balanced fault pick up criteria as $K_1 V_n = 82.8$ KV. Bus 5 is connected with line 1-5, line 4-5 and line 5-6. Among the line 1-5 has highest value of phase angle. So, line 1-5 is the faulted line. The sequence voltage and phase angle variations are shown in Fig 31(a,b). All g index values are also found to be positive. So, it is satisfying the authentication of balanced fault also.



(a) Positive Sequence Voltage profile at bus 5



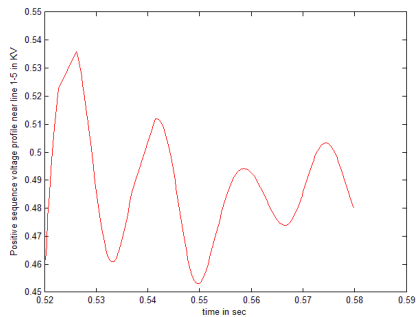
(b) Phase angle variation of line 1-5

Fig 31(a,b): Sequence Voltage profile at bus 5 and phase angle variation in line 1-5

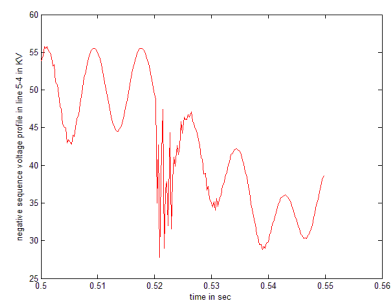
5.4.2.3 Case-3: Simultaneous Faults :

5.4.2.3.1 Line 1-5 with LLLG fault and Line 5-4 with LG fault:

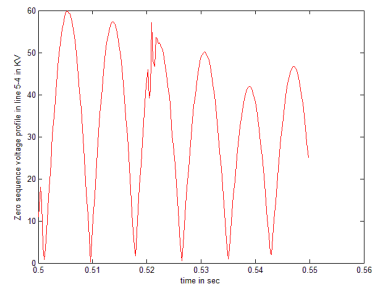
A LLLG fault is created at 50 Km distance from bus 5 at line 1-5 at 0.52 sec for 0.06 sec duration and a LG close in fault is created at line 5-4 at 0.5 sec for 0.05sec duration. From the sequence voltages and phase angle variation analysis, it is found that each line will satisfy their own individual fault pick up criteria. The sequence voltage profiles and phase angle variations are shown in Fig 32(a,b,c,d,e).



(a) Positive sequence voltage profile at line 1-5



(b) Negative sequence voltage profile at line 5-4



(c) Zero sequence voltage profile at line 5-4 (d) Phase angle variation of line 5-4 (e) Phase angle variation of line 1-5

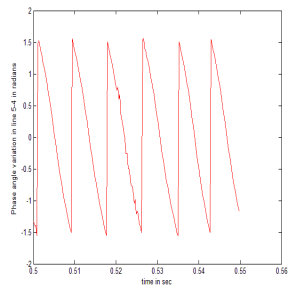
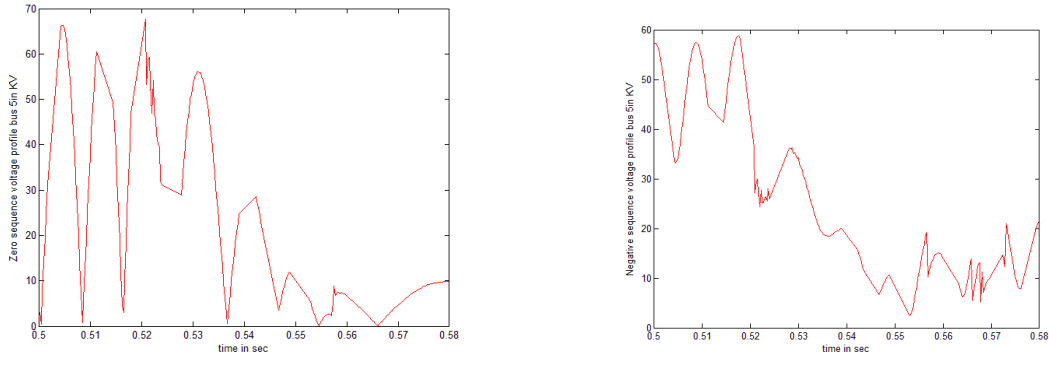


Fig 32(a,b,c,d,e): Sequence Voltage profiles and phase angle variations

5.4.2.3.2 Simultaneous faults at different Lengths of the same Line :

An AG fault is created at line 1-5 in close in distance at a time 0.5 for 0.05 sec duration and a LLLG fault is created in the same line at a distance 20 Km from bus 1 at 0.52 sec for 0.06 sec duration. The composite fault voltage sequence waveforms are shown in Fig 33(a,b).



(a) Zero sequence voltage profile at line 1-5

(b) Negative sequence voltage profile at line 1-5

Fig 33(a,b): Sequence Voltage profiles in line 1-5 when simultaneous AG and LLLG fault exist in the line

From the composite waveform it is clear that from 0.5-0.52 sec unbalanced fault pick up criterion is satisfying and from 0.52-0.58 sec, balanced fault pick up criterion is gradually predominating. The only difference with 9bus case studies is , in case of 9bus , whenever there exist a balanced and unbalanced fault in the system, the balanced fault starts to predominate immediately but in case of IEEE 14 bus system balanced fault starts to predominate gradually. The cause of this change can be explained as the influence of the length or size of the system which introduces a delay in the predomination of balanced fault. The delay can be further increased if the methodology is tested for more higher and larger test systems.

5.5 Discussions

5.5.1 Reduction of PMUS :

We need voltage data of the whole system for analysis of the methodology. But placing PMUs in each bus to capture data is a costly affair specially in case of a larger system. Here, an Integer Linear Programming (ILP) is used to solve the PMU placement problem. The results obtained are presented in the Table 2 shown below. Our objective is to make the system complete observable with minimum number of PMUs. The minimum number of PMUs to make the system complete observable is roughly 1/3 rd of the total number of buses exist in the system except zero injection buses[78]-[83].

Table –2 : PMU locations to obtain complete observability under normal operating conditions in test systems

System	Location of PMUs in bus no.	Number of PMUs
WSCC-3-machine-9bus	4 ,6 ,8	3
IEEE 14 bus	2,6,8,9	4

5.5.2 Stability of the method :

This method will work fine even in the transient conditions of the network. It is not depending on fault level. The method is totally depending on extracted voltage and current samples. So, the method is stable and not going to affect the stability of the system.

5.6 Comparative analysis

Table –3 : Comparison with other work

Properties	Ref [2]	Proposed Work
Total no. of PMUs used to capture data	6	3
No. of faults considered	Single fault at a time	Extended to simultaneous faults
Test system used	WSCC-3-Machine-9-Bus system	Extended to IEEE 14 bus system also
Super Synchronous Zone	The concept is not used	Here the concept used for alarming purpose

5.7 Summary

A Novel WABP scheme based on synchronized phasor measurements is proposed in this chapter. The sequence components of voltage, phase angles and the sign of cosine of the angle between voltage and current at both ends of a line is utilized to identify the faulted area and faulted branch. Simulation results for the nine-bus and IEEE 14bus power system show that the method performs correctly during several faults in systems, including simultaneous faults also.

Apart from the simple setting principle, the scheme has the ability to distinguish the fault from load encroachment and power swing and can mitigate the shortcomings of the conventional backup protection scheme. It is helpful to prevent blackouts. Thus with the context of today's backup protection schemes, the scheme described here is commendable.

Chapter 6

Optimal Placement of TCSC and TCPAR using Sensitivity Analysis

Chapter 6

Optimal Placement of TCSC and TCPAR using Sensitivity Analysis

6.1 Introduction

Optimal placement of Flexible AC Transmission System (FACTS) devices are very important for maintaining proper power system performance. This chapter presents an optimal placement approach of two well-known FACTS devices, Thyristor controlled series capacitor (TCSC) and Thyristor controlled phase angle rectifier (TCPAR) based on sensitivity analysis. In this method, reduction of line losses and overloading are taken care of. Sensitivity indexes are used to find proper place of FACTS devices in the network. After placing FACTS devices the performance of the network is also analyzed. Which FACTS device is more suitable for the network is also analyzed with the impact of change of generation. Effectiveness of the method is tested on a WSCC-3-Machine-9 bus system and an IEEE 57 bus test system with various single and multiple contingency combinations. The results obtained are accurate and satisfactory. The whole simulation work is done by using Power World 12.0 commercial version.

The Flexible Alternating Current Transmission System(FACTS) devices are very important for the improvement of the power system security. The objectives of using these FACTS devices are to bring the system under control and increase the power transfer capability through the lines. However, these devices have to be located optimally to reduce the capital investment.

With the expansion of power network, several financial, social and technical problems are also increasing. Efforts have been made to utilize existing electric power systems optimally. Line flows and losses are increasing in power system due to consistent increase in energy demand. These issues lead to the system security and stability problems. All these problems can be solved by the use of FACTS devices [84]. FACTS devices are capable to control power flow both in steady state as well as in dynamic state [85]. Using controllable series capacitors, losses can be reduced and stability margin can be increased. Thus energy can be saved for proper

utilization. FACTS devices such as TCSC, TCPAR, UPFC, IPFC and OUPFC can be used to change power flow in the lines by changing their parameters to achieve various objectives[86]. FACTS devices are capable of controlling steady state power flow as well as system parameters in dynamic state [87-88]. Due to the advancements in power electronics industry, FACTS devices have become cost effective [89]-[90]. In order to get maximum economic benefits, FACTS devices should be placed at optimal locations.

Several approaches are proposed in the literature for optimizing location and parameter settings of the FACTS devices. The most popular technique used for FACTS placement problem is the heuristic types of procedures applied for optimal FACTS location. Examples of heuristic types of procedures applied to the FACTS placement are found in reference [91]-[92].

S.N.Singh et al.[84] have developed models for optimal location of FACTS devices for congestion management. S.N.Singh et al.[85] suggested a sensitivity analysis for placing FACTS devices and reduction in real power flow performance index to enhance security of power system. R.Srinivasa Rao et al.[89] developed a generalized approach for optimal location of FACTS devices based on total system loss sensitivity indices and real power flow PI sensitivity indices. They have considered the effect of change of generation and comparison of various methods also in their work. But they did not consider the effect of *different contingency combinations* in the system while placement of TCSC, as well as which is the best suitable choice among FACTS devices to deal the problem.

S.C.Srivastava et al [90] suggested a novel approach to locate TCSC and UPFC for improving power system steady state operation. S.Parida et al. [86] developed a novel methodology for combined location of TCPAR and TCSC using a Mixed integer linear programming (MILP) approach in the deregulated electricity environment. The technique was based on DC load flow (DCLF) equations taking constraints on generation, line flow, TCPAR and TCSC parameters, power angle, and a number of FACTS controllers. The system loadability has been determined without and with combined optimal location of FACTS controllers. H.M.Ravi Kumar et al.[87] presented a three step procedure to decide number, location and optimal settings of TCSC to eliminate overloads on transmission lines under network contingencies. But *multiple contingency cases* are still untouched in this work also. H.I.Shaheen et al.[88] used GA and PSO for finding optimal location and settings of TCSC. In Reference [94] the authors propose a novel decomposition procedure for determining the

optimal location of TCSC and their respective size for a network. In Reference [95] authors propose a multi-objective optimization based FACTs device placement approach. In Reference [96] authors propose a mixed-integer linear programming based approach for optimal placement of TCSC. In reference [97] authors suggested a technique which iteratively minimizes the operating points of the FACTs devices to enhance the security. In Reference [98] authors used line flow based (LFB)equations to find the optimal locations and settings of a TCSC. However it shows that LFB equations are invalid for modelling meshed networks. Therefore application of LFB equations in FACTs location allocation problem is limited.

This chapter presents a generalized approach to determine the optimal location of TCSC and TCPAR. The approach is based on sensitivity analysis which is subjected to reduction of line losses i.e. energy savings. The contributions of the paper are manifold. First of all we consider the network in single and multiple contingency combinations. We placed TCSC and TCPAR using sensitivity analysis keeping constraints as reduction of line losses i.e energy savings. In our proposed technique we consider a practical approach by taking the effect of change of generations. Secondly, it describes the procedure about how to handle the power network during overloading of any line of the system.

We utilized the WSCC-3-Machine-9-bus system and IEEE 57 Bus test systems to demonstrate the effectiveness of the proposed procedure and to develop new insights into the optimal placement problem of TCSC and TCPAR. The remainder of the chapter is organized as follows :

Section2 and 3 describes the mathematical modelling of TCSC and TCPAR. Section 4 and 5 describes the optimal placement of TCSC and TCPAR with results. Section 6 describes the discussions. Finally in section-7, we have summarized the whole chapter with conclusions and comments.

6.2 Modelling of TCSC

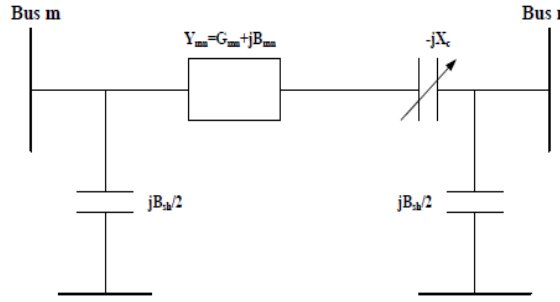


Fig.1 : Transmission line modelling with TCSC

The transmission line with TCSC modelled as static reactance ($-jx_c$) is shown in Fig 1. The power flow equations from bus m to bus n (P_{mn} and Q_{mn}) and from bus n to bus m (P_{nm} and Q_{nm}) are given by following equations [16] :

$$P_{mn} = -V_m V_n [G_{mn} \cos \delta_{mn} + B_{mn} \sin \delta_{mn}] + V_m^2 G_{mn} \quad (1)$$

$$Q_{mn} = -V_m V_n [G_{mn} \sin \delta_{mn} - B_{mn} \cos \delta_{mn}] - V_m^2 (B_{mn} + B_{sh}) \quad (2)$$

$$P_{nm} = -V_n V_m [G_{mn} \cos \delta_{mn} - B_{mn} \sin \delta_{mn}] + V_m^2 G_{mn} \quad (3)$$

$$Q_{nm} = -V_n V_m [G_{mn} \sin \delta_{mn} + B_{mn} \cos \delta_{mn}] - V_m^2 (B_{mn} + B_{sh}) \quad (4)$$

The active power loss in the line is given by

$$P_{lk} = -2V_m V_n G_{mn} \cos \delta_{mn} + (V_m^2 + V_n^2) G_{mn} \quad (5)$$

$$\text{Here } G_{mn} = \frac{r_{mn}}{r_{mn}^2 + (x_{mn} - x_c)^2} \quad (6)$$

$$B_{mn} = \frac{-(x_{mn} - x_c)}{r_{mn}^2 + (x_{mn} - x_c)^2} \quad (7)$$

6.3 Modelling of TCPAR

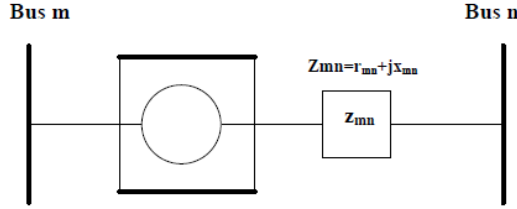


Fig. 2 : Modelling of TCPAR

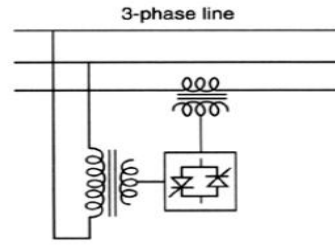


Fig. 3: Simple model of TCPAR /TCPST

TCPAR means Thyristor controlled phase angle regulators. With the phase shift of TCPAR, power flows and losses can be compensated. This device is also called TCPST (Thyristor controlled phase shifting transformer). The device is required for power control damping of oscillations and transient stability. TCPAR/ TCPST can be modelled (ref. Fig 2 and Fig 3) by using following equations[16] :

$$P_{mn} = -V_i V_j A [G_{mn} \cos(\delta_{mn} + \Phi) + B_{mn} \sin(\delta_{mn} + \Phi)] + V_m^2 A^2 G_{mn} \quad (8)$$

$$Q_{mn} = -V_i V_j A [G_{mn} \sin(\delta_{mn} + \Phi) - B_{mn} \cos(\delta_{mn} + \Phi)] - V_m^2 A^2 B_{mn} \quad (9)$$

$$P_{nm} = -V_i V_j A [G_{mn} \cos(\delta_{mn} + \Phi) - B_{mn} \sin(\delta_{mn} + \Phi)] + V_m^2 A^2 G_{mn} \quad (10)$$

$$\text{A} = \sec(\Phi) \quad (11)$$

$$A = \sec(\Phi) \quad (12)$$

The real power loss

$$P_{lk} = -2V_m V_n A G_{mn} \cos(\delta_{mn} + \Phi) + V_m A^2 G_{mn} + V_n^2 G_{mn} \quad (13)$$

6.4 Optimal placement of TCSC/TCPAR

The optimal placement of TCSC/ TCPAR may be based on one of the following objectives described below :

- i) Reduction of real power loss of a particular line-k (P_{lk}).
- ii) Reduction of total system real or / and reactive power loss.
- iii) Reduction in real power flow performance index.
- iv) Minimization of total generation cost.
- v) Minimization of total system real power loss and total generation cost simultaneously .

The first three approaches are based on sensitivity analysis based approach .

6.4.1. Line loss sensitivity indices

Line loss sensitivity factor for calculation of optimal location of TCSC and TCPAR is based on differential approach. The factors are given by following equations :

$$a_1 = \frac{\Delta P_{lk}}{\Delta X_{ck}} \quad \text{for TCSC placement} \quad (14)$$

$$a_2 = \frac{\Delta P_{lk}}{\Delta \Phi_k} \quad \text{for TCPAR / TCPST placement} \quad (15)$$

X_{ck} is TCSC reactance and Φ_k is phase angle shift produced by TCPAR / TCPST

6.4.2. Criteria for optimal placement of TCSC/TCPAR

The criteria for optimal placement of TCSC / TCPAR are as follows :

- i) The device should be placed in a line which has least sensitivity with respect to the magnitude of static reactance.
- ii) The device should be placed in a line which has largest absolute value of the sensitivity with respect to the phase angle.
- iii) The device should not be placed in the line containing generation buses, even if the sensitivity is the highest.
- iv) The terminal end bus must not have a switched shunt connected to it.
- v) Multiple devices sending end on same bus are allowed.

6.4.3. The terms of sensitivity factors

From equation (1) to (13) following terms can be obtained:

$$\frac{\Delta P_m}{\Delta X_{ck}} = (V_m^2 - V_m V_n \cos \delta_{mn}) \frac{\Delta G_{mn}}{\Delta X_{ck}} - V_m V_n \sin \delta_{mn} \frac{\Delta B}{\Delta X_{ck}} \text{ when } X_{ck} = 0 \quad (16)$$

$$\frac{\Delta P_n}{\Delta X_{ck}} = (V_m^2 - V_m V_n \cos \delta_{mn}) \frac{\Delta G_{mn}}{\Delta X_{ck}} + V_m V_n \sin \delta_{mn} \frac{\Delta B}{\Delta X_{ck}} \text{ when } X_{ck} = 0 \quad (17)$$

$$\frac{\Delta P_m}{\Delta \Phi_k} = -V_m V_n (G_{mn} \sin \delta_{mn} - B_{mn} \cos \delta_{mn}) \text{ when } \Phi_k = 0 \quad (18)$$

$$\frac{\Delta P_n}{\Delta \Phi_k} = -V_m V_n (G_{mn} \sin \delta_{mn} + B_{mn} \cos \delta_{mn}) \text{ when } \Phi_k = 0 \quad (19)$$

6.5 Results

Various test cases are checked with single and multiple contingency conditions with WSCC-3-Machine-9 bus system(ref. Fig 4) and IEEE-57 bus test system. Various test cases results are listed in Table- 1, Table-2 ,Table -3,Table-4 and Table-5.

6.5.1.WSCC-3-Machine-9 Bus System Cases

The test system is constructed by using Power World 12.0 Commercial version. The Newton Raphson load flow (NRLF) is run in the test system in base case (without change of compensation and without contingency) condition. Then the different types of single and multiple contingencies are created in the system and then again NRLF is run in the system. Then the different indexes are calculated as per formula from the available data in two different run cases. eg: For showing one calculation, we are choosing the example of line 7-8 arbitrarily. As per Table-1, the base case real power loss in case of line 7-8 was 0.26 p.u and at contingency was 0 p.u. So,

$$\Delta P_{lk} = (0 - 0.26) \text{ p.u}$$

= -0.26 p.u. In the said case, change in line reactance is 0.0288 p.u (decrease). So,

$\Delta X_{ck} = -0.0288 \text{ p.u}$.So, for line 7-8 as per Table1

$$a_1 = \frac{\Delta P_{lk}}{\Delta X_{ck}} = \frac{-0.26}{-0.0288} = 9.0278$$

Here one thing is needed to be mentioned that before placement of TCSC , while calculating the a_1 index, we will consider the line reactance change to produce the change of real power loss. i.e- ΔP_{lk} is the change of real power loss in the line(lk) while the line reactance is varied by ΔX_{ck} and after placement of TCSC, the ΔX_{ck} term can be calculated from TCSC reactance.

In case of TCPAR, the calculation of a_2 can be done from change of real power loss (ΔP_{lk}) in the line with respect to change in difference in bus angle magnitudes ($\Delta\Phi_k$) before placement of TCPAR and after the placement of TCPAR the change of angle values can be obtained from TCPAR itself.

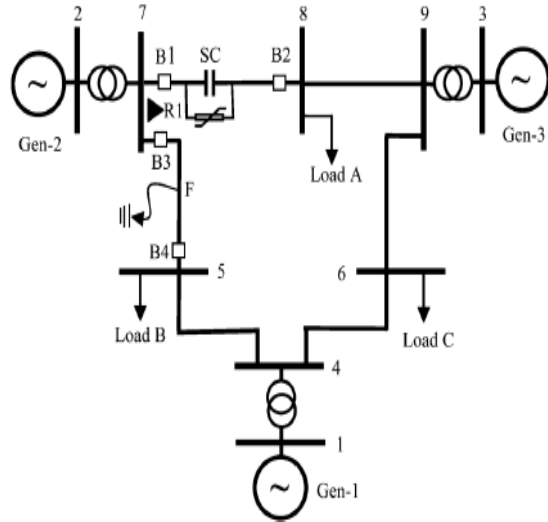


Fig. 4: Single line diagram of a WSCC-3-Machine -9-bus system

For showing one calculation of a_2 , we are choosing the example of line 7-8 arbitrarily. As per Table-3, the base case real power loss in case of line 7-8 was 0.26 unit and at contingency was 0.2 unit. So,

$$\Delta P_{lk} = (0.2 - 0.26) \text{ p.u}$$

$$= -0.06 \text{ p.u}$$

And in the said case change in phase angle shift obtained from TCPAR is 0.39 p.u (increase). So,

$$\Phi_k = 0.39 \text{ p.u} \text{ So, for line 7-8 as per Table3}$$

$$a_2 = \frac{\Delta P_{lk}}{\Delta\Phi_k} = \frac{-0.06}{0.39} = -0.1538$$

Fig 5 to Fig 8 show some graphical plots (bus voltage profile and real power loss) to see the effect of FACTs devices (TCSC) with and without on a WSCC-3-Machine -9bus system. Fig 9 to Fig 12 show the same in case of an IEEE 57 bus system. In both the cases we are observing the voltage profile smoothens and real power loss decreases in the presence of

FACTs device (TCSC). Table- 1 shows FACTs (TCSC) placement under single contingency condition and Table-2 (TCSC) , Table-3 (TCPAR) show under multiple contingency condition in case of 9 Bus system.

Table-4 and Table-5 shows IEEE 57 bus applications . Table-4 listed the results of TCSC placement and Table-5 shows the results of TCPAR placement.

6.5.1.1 TCSC Placement

Table-1 : Line 8-9 under contingency (single contingency case)

Line	Base case real power loss(p.u) (P _{base})	Real power loss at contingency (p.u) (P _{contingency})	ΔP_{lk} (p.u) = (P _{contingency} - P _{base})	Change in line reactance (p.u) (ΔX _{ck})	$a_1 = \frac{\Delta P_{lk}}{\Delta X_{ck}}$	Remarks
2-7	-	-	-	-	not required	Connected to generation bus . So, violating the criteria.
7-8	0.26	0	-0.26	-0.0288	9.0278	
5-7	2.11	8.99	6.88	-0.0644	-106.832	
8-9	-	-	-	-	-	Under contingency
3-9	-	-	-	-	not required.	Connected with generation bus. So, violating the criteria.
6-9	0.14	23.24	23.10	-0.068	-339.706	Proper place for TCSC Placement. Run NRLF after placement of TCSC .In case of any violations,% compensation to be adjusted.
4-5	0.06	8.86	8.8	-0.0386	-227.647	
4-6	0.04	10.83	10.79	-0.0392	-275.815	
4-1	-	-	-		not required.	Connected to generation bus. So, violating the criteria

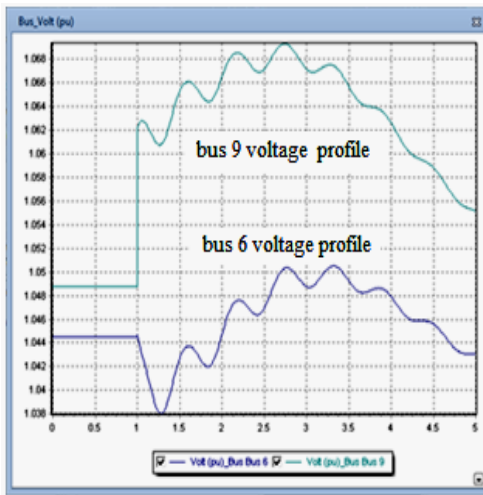


Fig.5: Voltage profile before placement of TCSC

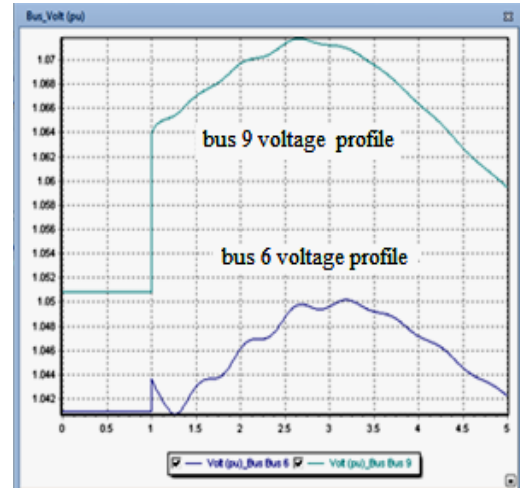


Fig.6 : Voltage profile after placement of TCSC

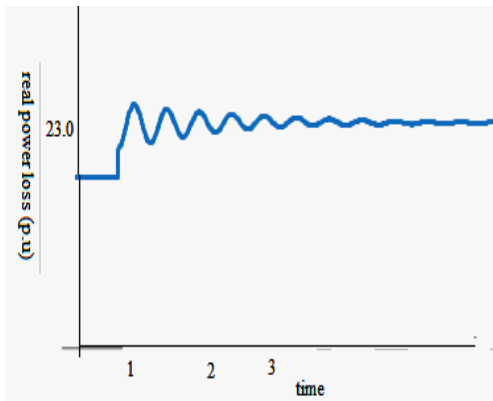


Fig.7: real power loss in line 6-9 before TCSC placement

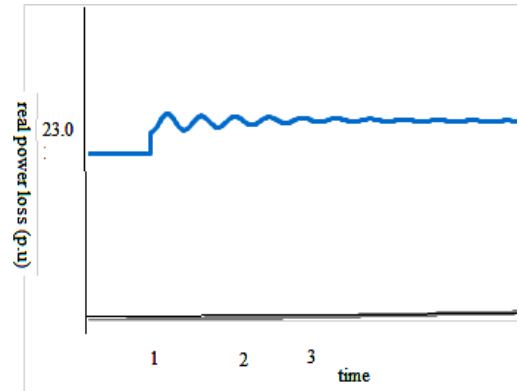


Fig.8: real power loss in line 6-9 after TCSC placement

Table-2 : Line 8-9 and Line 3-9 under contingency (Multiple contingency case)

Line	Base case real power loss (p.u) (P_{base})	Real power loss at contingency (p.u) ($P_{contingency}$)	ΔP_{lk} (p.u) =($P_{contingency}$ - P_{base})	Change in line reactance (p.u) (ΔX_{ck})	$a_1 = \frac{\Delta P_{lk}}{\Delta X_{ck}}$	Remarks
2-7	-	-	-	-	Calculation not required.	Connected to generation bus. So, violating the criteria of optimal placement of TCSC.
7-8	0.26	0	-0.26	-0.0288	9.0278	
5-7	2.11	19.16	17.05	-0.0644	-264.75	Proper place for TCSC Placement. Run NRLF after placement of TCSC. In case of any violations, % compensation to be adjusted.
8-9	-	-	-	-	-	Under contingency
3-9	-	-	-	-	-	Connected with generation bus and it is under contingency
6-9	0.14	17.98	17.84	-0.068	-262.5	.
4-5	0.06	2.36	2.3	-0.034	-67.647	
4-6	0.04	6.94	6.9	-0.0368	-187.5	
4-1	-	-	-	-	Calculation not required	Connected to generation bus. So, violating the criteria of optimal placement of TCSC.

6.5.1.2. TCPAR / TCPST Placement

Table-3 : Line 4-6 and Line 4-5 under contingency (Multiple contingency case)

Line	Base case real power loss(p.u) (P_{base})	Real power loss at contingency (p.u) ($P_{contingency}$)	ΔP_{lk} (p.u) =($P_{contingency}$ - P_{base})	Change in phase angle shift(p.u) $\Delta\Phi_k$		Remarks
2-7	-	-	-	-	Calculation not required.	Connected to generation bus. So, violating the criteria of optimal placement of TCPAR.
7-8	0.26	0.2	-0.06	0.39	-0.1538	
5-7	2.11	3.35	1.24	-3.31	-0.3746	Proper place for TCPAR Placement. Run NRLF after placement of TCPAR .In case of any violations,% compensation(or proper angle) to be adjusted
8-9	0.32	0.21	-0.11	-5.34	0.0206	
3-9	-	-	-	-	Calculation not required.	Connected to generation bus . So, violating the criteria of optimal placement of TCPAR.
6-9	0.14	0.13	-0.01	-1.11	0.009	
4-5	-	-	-	-	-	Under contingency
4-6	-	-	-	-	-	Under contingency
4-1	-	-	-	-	Calculation not required.	Connected to generation bus. So, violating the criteria of optimal placement of TCPAR.

6.5.2 IEEE-57 Bus Application

6.5.2.1 TCSC Placement

Table –4 : Line 1-2 under contingency(Single contingency case)

Line	Base case real power loss(p.u) (P _{base})	Real power loss at contingency (p.u) (P _{contingency})	ΔP_{lk} (p.u) = (P _{contingency} - P _{base})	Change in line reactance (p.u) (ΔX_{ck})	$a_1 = \frac{\Delta P_{lk}}{\Delta X_{ck}}$	Remarks
1-2	-	-	-	-	-	Under contingency
4-18	0.18	0.11	-0.07	-0.02564	2.73	
6-7	-	-	-	-	not required.	Connected to generation bus. So, violating the criteria of optimal placement of TCSC
7-29	0.14	0.13	-0.01	-0.03392	0.295	
11-43	0	0		-0.0612	0	
13-49	7.89	8.4	0.51	-0.01736	-29.38	Proper place for TCSC Placement. Run NRLF after placement of TCSC. In case of any violations, % compensation to be adjusted.

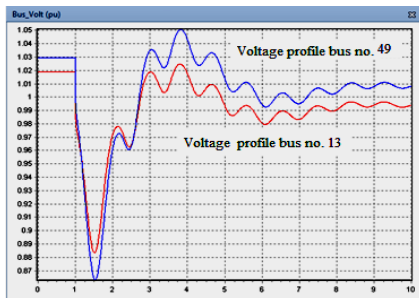


Fig.9 : Voltage profile before placement of TCSC

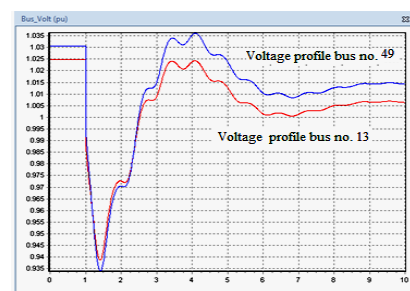


Fig.10 : Voltage profile after placement of TCSC

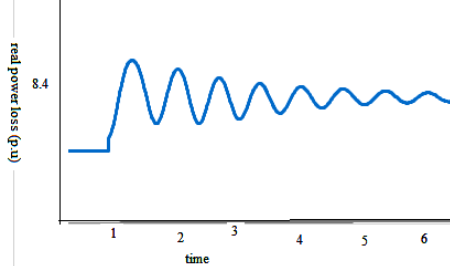


Fig.11: real power loss in line 13-49 before TCSC placement

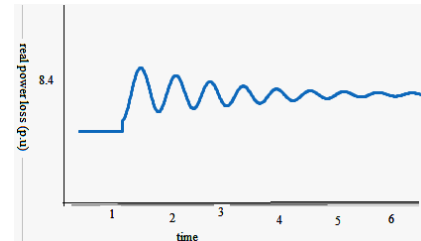


Fig.12: real power loss in line 13-49 after TCSC placement

6.5.2.2 TCPAR Placement

Table –5: Line 24-26 and Line 37-38 under contingency (Multiple contingency case)

Line	Base case real power loss(p.u) (P_{base})	Real power loss at contingency (p.u) ($P_{contingency}$)	ΔP_{lk} (p.u) =($P_{contingency}$ - P_{base})	Change in phase angle shift(p.u) $\Delta\Phi_k$	$a_2 = \frac{\Delta P_{lk}}{\Delta\Phi_k}$	Remarks
1-2	-	-	-	-	Calculation not required.	Connected to generation bus . So, violating the criteria of optimal placement of TCPAR.
4-5	0.17	0.16	-0.01	-0.08628	0.1159	
6-7	-	-	-	-	Calculation not required.	Connected to generation bus. So, violating the criteria of optimal placement of TCPAR.
10-12	0.27	0.3	0.03	-0.013	-2.308	
13-49	7.89	7.57	-0.32	-0.010145	31.542	Proper place for TCPAR Placement. Run NRLF after placement of TCPAR. In case of any violations,% compensation to be adjusted.
14-15	1.07	1.14	0.07	0.14112	0.496	
24-26	-	-	-	-	-	Under contingency
26-27	0.04	0.34	0.3	2.0027	0.1498	
37-38	-	-	-	-	-	Under contingency
46-47	0.06	1.12	1.06	2.0076	0.528	
56-57	0.05	0.13	0.08	-1.4286	-0.056	

6.6 Discussion

6.6.1 Treatment of Network after placing TCSC/ TCPAR

After placing FACTs device in proper place, we will run the NRLF and observe any line is violating the limit or not. In case any line is violating any limit, then we need to adjust the percentage compensation of the overloaded line. Here one thing need to be mentioned that the line is provided with up to 30% overload backup support. So, our objective will be to bring the

line with in 30% overload. Refer to Table-2 multiple contingency case after placing TCSC in line 5-7 and then running load flow we get the result same as Fig13. Here we can see line 2-7 is congested with 45% overload and line 6-9 is congested with 43% overload. We are neglecting line 5-7(1% overload < 30%). Then we can vary percentage compensation to adjust the network within limit like shown in Fig14 and Fig15. First we compensated line 2-7 by 40% and run the load flow again. Still line 2-7 is showing 40% overload and line 6-9 is showing 44% overload (ref. Fig14). Now we compensate line 2-7 and line 6-9 both by 50% and run the load flow again. Now we can see both the lines(line 2-7 and line 6-9) are within limit (within 30% overload)(ref. Fig 15).

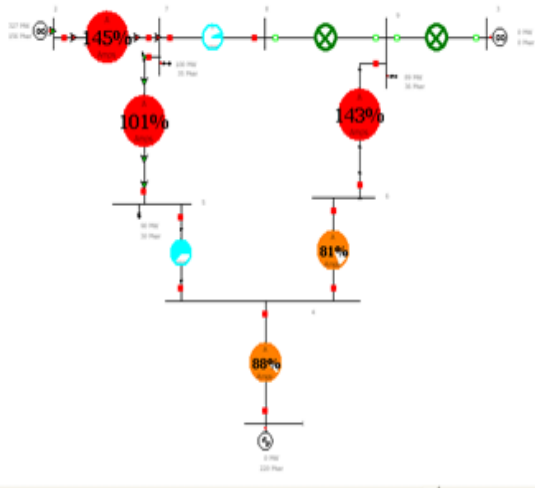


Fig.13 : NRLF result after placing TCSC in line 5-7

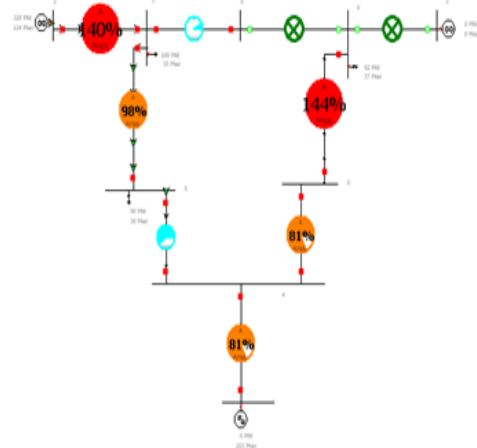


Fig.14: NRLF result after 40% compensation in line 2-7

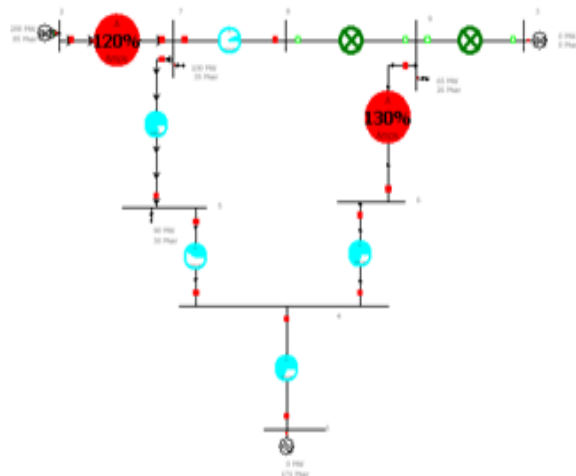


Fig.15: NRLF result after 50% compensation in line 2-7 and Line 6-9

6.6.2.TCSC or TCPAR Which FACT device is more appropriate for network and Impact of Generation

Both TCSC and TCPAR are useful for power system to maintain proper performance of the network. TCSC varies its percentage compensation and firing angle to maintain network performance and TCPAR usually gives negative phase shift to a line in a network to minimize losses etc and maintaining proper power system performance. But TCPAR is very sensitive to the phase angle shift. If phase shift exceeds certain limits, it can produce even black out of the whole system. But such conditions does not occur in case of TCSC. So, it can be said TCPAR is more vulnerable than TCSC. So, TCSC is more appropriate FACT device than TCPAR. Fig 16 shows the screen shot of the simulation when TCPAR exceeds -58 degree phase shifts in line 6-9. Here it is showing complete black out of the system.

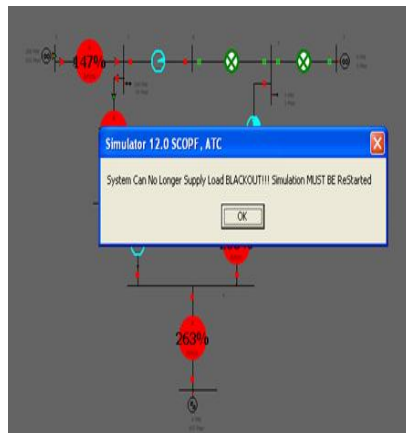


Fig. 16 : NRLF result after TCPAR phase shift exceeds -58degree in line 6-9

Now, to study the effect of variation of generation in this method to determine the optimal location of the FACTs device, the generation has been rescheduled to 45 MW from 85 MW at bus 3 and 130 MW from 163 MW at bus 2. Results are listed in Table-6. Comparing with Table-3, we can say line 8-9 and line 6-9 are not much affected with respect to change in sensitivity index. In case of line 7-8 and line 5-7, sensitivity index increased but optimal place for TCPAR placement remains same(line 5-7) (refer to Table-6).

Table-6 : Line 4-6 and Line 4-5 under contingency (Multiple contingency case)

Line	Base case real power loss(p.u) (P_{base})	Real power loss at contingency (p.u) ($P_{contingency}$)	ΔP_{lk} (p.u) =($P_{contingency}$ - P_{base})	Change in phase angle shift(p.u) $\Delta\Phi_k$	$a_2 = \frac{\Delta P_{lk}}{\Delta\Phi_k}$	Remarks
2-7	-	-	-	-	not required.	Connected to generation bus. So, violating the criteria .
7-8	0.62	0.65	0.03	0.161	0.1863	
5-7	2.73	3.4	0.67	0.161	4.1615	Proper place for TCPAR Placement. Run NRLF after placement of TCPAR. In case of any violations,% compensation(or proper angle) to be adjusted
8-9	0.82	0.83	0.01	0.161	0.0621	
3-9	-	-	-	-	Calculation not required.	Connected to generation bus . So, violating the criteria of optimal placement of TCPAR.
6-9	0.001	0.001	0	0.0001	0	
4-5	-	-	-	-	-	Under contingency
4-6	-	-	-	-	-	Under contingency
4-1	-	-	-	-	not required.	Connected to generation bus. So, violating the criteria.

6.6.3 Advantages of using the technique

This method is very useful as it is developed on consideration of reduction of real power loss(P_{lk}) of lines. It is very simple and useful in case of both single and multiple contingency conditions. This method explains how to treat the network after the placement of the FACTS devices and also works fine with respect to change of generation. It is transparent with both heavy and light loads. So, the technique is very useful and advantageous compare to other contemporary techniques .

To prove the superiority of our work, we have compared in with Ref.[16] method. The comparison is listed in Table-7.

Table-7 : Comparison of the methods

Reference [16]Method	Proposed Method
This method is used for only small test systems. e.g- 5 bus and IEEE 14bus system.	Our work extends for larger test systems. e.g- WSCC-3-machine-9 bus and IEEE 57 bus test system
This method is used for only single contingency case studies.	This work extends for even multiple contingency case studies.
This method is unable to handle overloading cases of lines after FACTs placement through single method.	This method can handle overloading cases of lines through single approach.

6.7 Summary

An optimal FACTs device placement method based on sensitivity analysis is developed in this chapter. The differential of real power loss is taken with respect to FACTs device control parameters (TCSC reactance and TCPAR phase angle). Calculation of indexes are also shown in this chapter with examples. After placing TCSC or TCPAR, the NRLF is run using Power World simulator. If there is no overload condition observed, then the result is correct. But in case, if any violation of limit is taken place, then how to treat the condition that is also discussed in this chapter. Apart from that a rigorous analysis is done about the more suitable FACTs device between TCSC and TCPAR for the power network in this chapter. The effect of changes in generation and advantages of using the proposed technique are also discussed in the chapter. A comparison with other method is also discussed in this context. Analysis using multiple contingency cases is novel in this chapter and in future extension of the work can be, to be implemented on larger wide area systems(e.g-IEEE 118 bus , IEEE 300 bus systems or practical systems like Northern Regional Power Grid or Southern Regional Power Grid etc.) with more number of contingency combinations(e.g- different lines, generators and buses etc.). It is expected that this analysis will be helpful for industry practitioners, for choosing appropriate FACTs device for their work.

Chapter 7

**Optimal Combined Over current and Distance Relays
Coordination using Teaching Learning based
Optimization**

Chapter 7

Optimal Combined Over Current and Distance Relays Coordination using Teaching Learning based Optimization

7.1 Introduction

Relay coordination is an important aspect to maintain proper power system operation and control. Relays should be organized in such a way that every relay should have a backup and Coordination time interval (CTI) between primary and back up and different zones of the relay should be maintained to achieve proper fault identification and fault clearance sequence. The relays should operate in minimum desirable time satisfying all the co-ordination constraints. So, relay coordination is nothing but highly constraint problem. Heuristic techniques are often used to get optimal solution of this kind of problem. In this chapter, this constraint problem is solved by Teaching learning based optimization(TLBO) on several test systems. e.g-IEEE 5 bus, 6 bus, WSCC-3-Machine-9bus, IEEE 14 bus and IEEE 30 bus test system. Proper desirable time setting multiplier (TSM) with minimum operating time of relays are calculated. We also incorporated intelligent over current relay characteristics selection to get the desired results in this work. The results seem to be satisfactory as the results obtained from TLBO are comparatively better than so called conventional methods like Genetic Algorithm(GA) and Particle Swarm Optimization (PSO) for all the test systems studied here from small to big.

During fault conditions , these relays must operate quickly isolating the faulted section of the network and allows for continued operation of the healthy circuits. If primary relay meant for clearance of the fault fails, backup relay must operate after providing for sufficient time discrimination for the operation of primary relays. Hence the operation of back up relays must be coordinated with those of the operation of the primary relays. The flexible settings of the relays (e.g- plug setting , Time multiplier setting and possibly selection of suitable time-current operating characteristics), must be set to achieve the desired objectives.

Over current and distance relays are often used for protection of power system. Now a days this scheme is used in almost all sub-transmission system. To achieve better co ordination , a distance with a distance, an over current with a over current relay and an over current relay

with a distance relay must be coordinated. One of them will act as main relay and another one as back up. Proper co-ordination time interval should be maintained between them.

The study of co-ordination of relays was first done among over current relays. Initially it is done by using linear programming method including simplex, two-phase simplex and dual simplex methods[99]-[102]. But the problem regarding using these methods is the solution will not come unless all the constraints are satisfied.

So, people gradually started to use intelligent and meta-heuristic approaches which gives optimal solution instead of exact solution meeting all the constraints criteria. In ref.[103], optimal co-ordination is done by Genetic Algorithm. Ref.[104] shows optimal co-ordination by using Particle swarm optimization and Ref.[105] shows the time co-ordination by using evolutionary algorithm. But these schemes are having two types of problems. First one is mis-coordination and other one is lack of solution for relays with both discrete and continuous time setting multipliers (TSMs). The problems are resolved in [106] by adding a new expression with the objective function. All the above discussed methodologies are done by using over current relays and the relay characteristics are assumed to be fixed. While in digital relays different over current relay characteristics can be selected. So, the algorithm for relay co-ordination should be capable of selecting the best fitting characteristics of over current relays to have optimal co-ordination.

Ref.[107] shows relay co-ordination with an hybrid GA algorithm which is helpful in relay coordination of over current and distance relays. Ref.[11] shows relay co-ordination using GA and intelligent relay characteristics selection. Ref. [108]-[110] shows relay coordination using TLBO for small systems but all of them used fixed characteristics (Standard IDMT). None of them used different intelligent characteristics available in digital relays.

In this chapter, we are using Teaching learning based optimization (TLBO) for distance and over current relay coordination with intelligent over current relay characteristics selection. Relay co-ordination using TLBO and with intelligent over current relay characteristics is a novel contribution in this chapter. The method is more simple and reliable than previous methods used. We have taken several test systems to test this methodology including IEEE 5 bus, 6 bus, WSCC-3-Machine-9 bus, IEEE 14 bus and IEEE 30bus test system and implement the discussed method. The results seem to be satisfactory.

7.2 Teaching Learning based Optimization (TLBO)

TLBO is an algorithm inspired by teaching learning process. It is proposed by Rao et al. [111]. The learning process will be done through two stages such as teacher stage and learner stage. While modeling the algorithm, the group of learners was modeled as population; subjects opted by learners were modeled as design variables. Here, learners result becomes the fitness value. After iteration, the best solution inside the population becomes teacher. And, the constraints of optimization problem become design variables [111]-[114].

7.2.1 Teacher Stage

The first stage is the teacher stage. As all of us know teacher teaches students and increases the mean of their marks depending upon their capability. Assume that there are 'm' number of subjects (i.e. design variables), 'n' number of learners (i.e. population size, $k = 1, 2, \dots, n$) and the mean result of the learners is $M_{j,i}$ in a particular subject 'j' ($j = 1, 2, \dots, m$). The best overall result considering all the subjects together obtained in the entire population of learners can be considered the result of the best learner, k_{best} . However, since the teacher is usually considered a highly learned person who trains learners so that they can have better results, after iteration, the best learner will be considered as teacher. The difference between the existing mean result of each subject and the corresponding result of the teacher for each subject is given by

$$\text{Difference_Mean}_{j,k,i} = r_i(X_{j,k_{best},i} - T_F M_{j,i}) \quad (1)$$

Where $X_{j,k_{best},i}$ is the result of the best learner (i.e., teacher) in subject j. T_F is the teaching factor, which decides the value of the mean to be changed, and r_i is the random number in the range [0, 1]. The value of T_F can be either 1 or 2. The value of T_F is decided randomly with equal probability as follows:

$$T_F = \text{round}[1 + \text{rand}(0,1)\{2 - 1\}] \quad (2)$$

T_F is not a parameter of the TLBO algorithm. The value of T_F is not given as an input to the algorithm, and its value is randomly decided by the algorithm using Eq. (2). After conducting a number of experiments on many benchmark functions, the algorithm was concluded to perform better if the value of T_F was between 1 and 2. However, the algorithm was found to perform much better if the value of T_F is either 1 or 2. Hence, the teaching factor is suggested to take a value of either 1 or 2 depending on the rounding up criteria given by Eq.(2) to simply the

algorithm. Based on the Difference_Mean_{j,k,i}, the existing solution is updated in the teacher phase according to the following expression:

$$X'_{j,k,i} = X_{j,k,i} + Difference_Mean_{j,k,i} \quad (3)$$

Where $X'_{j,k,i}$ is the new value of $X_{j,k,i}$. Accept $X'_{j,k,i}$ if it improves the value of the function. After teacher stage, all fitted values will be given as input to the learner stage. So, it means the learner stage depends on teacher stage.

7.2.2 Learner Stage

Learner phase is the second part of the algorithm. Learners boost up their knowledge by interactions among themselves. A learner learns new things if the other learner has more knowledge than him or her. Considering a population size of 'n', the learning phenomenon of this phase is expressed below.

Randomly select two learners P and Q such that $X'_{total-P,i} \neq X'_{total-Q,i}$ (where, $X'_{total-P,i}$ and $X'_{total-Q,i}$ are the updated values of $X_{total-P,i}$ and $X_{total-Q,i}$ respectively at the end of teacher phase)

$$X''_{j,P,i} = X'_{j,P,i} + r_i(X'_{j,P,i} - X'_{j,Q,i}), \text{If } X'_{total-P,i} < X'_{total-Q,i} \quad (4)$$

$$X''_{j,P,i} = X'_{j,P,i} + r_i(X'_{j,Q,i} - X'_{j,P,i}), \text{If } X'_{total-P,i} > X'_{total-Q,i} \quad (5)$$

Accept $X''_{j,P,i}$ if it gives a better function value.

Optimal Combined Over current and Distance Relays Coordination using Teaching Learning based Optimization

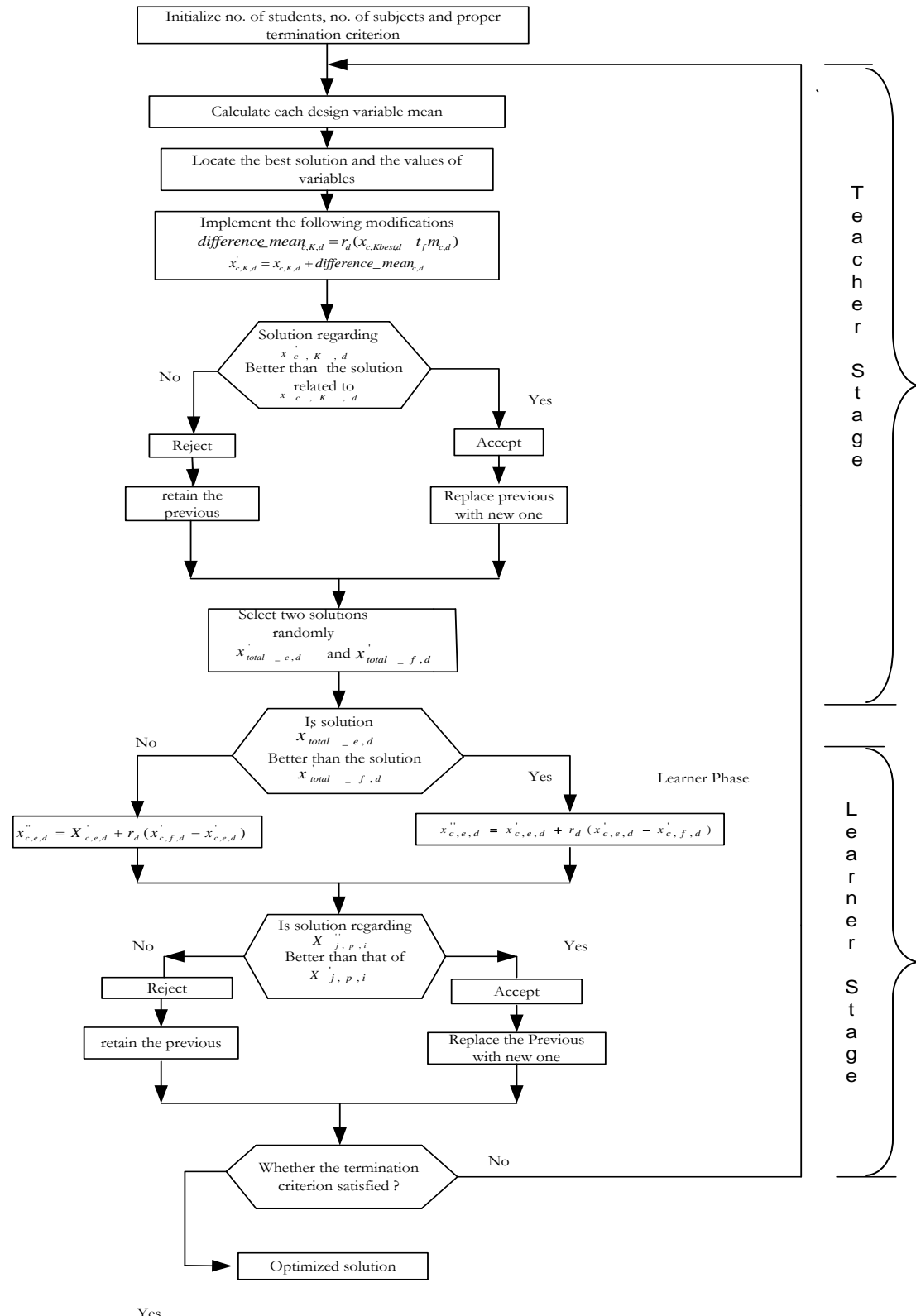


Fig 1: Flowchart of TLBO algorithm

7.3 Problem Statement

To achieve better protection, it is common to use both distance and over current relays as main and back up relays respectively, in power transmission protection scheme. In this situation, it is necessary to coordinate these two types of relays simultaneously that makes the problem harder to find a global operating point.

$$\text{Fitness function} = \min(\alpha \sum_{i=1}^n t_i + \beta \sum_{i=1}^n |T_{DIOCi} - |T_{DIOCi}| + \lambda \sum_{i=1}^n |T_{OCDi} - |T_{OCDi}| + \delta \sum_{i=1}^n |T_{OCi} - |T_{OCi}|) \quad (6)$$

Where

$$T_{OCi} = T_{ocbackupi} - T_{ocmaini} - CTI' \quad (7)$$

$$T_{DIOCi} = T_{oci} - T_{z2i} - CTI' \quad (8)$$

$$T_{OCDi} = T_{z2i} - T_{oci} - CTI' \quad (9)$$

T_{oc} is the operating time of over current relay and T_{z2} is the operating time of 2nd zone of the distance relay $\alpha, \beta, \lambda, \delta$ are penalty factors.

7.4 Constraints

The several constraints need to be satisfied to obtain optimal co-ordination and settings are as follows :

7.4.1 Co-ordination constraints

It is described as follows(ref. Eq.(12) and Eq.(13)):

$$T_{z2backup} - T_{ocmain} \geq CTI' \quad (12)$$

$$T_{ocbackup} - T_{z2main} \geq CTI' \quad (13)$$

The typical value of coordination time interval(CTI) is between 0.2 to 0.3 sec.

7.4.2 Relay Characteristics

The over current relay characteristics are typically of below nature(ref. Eq.(14)):

$$t = TSM \left(\frac{K}{M^\alpha - 1} + L \right) \quad (14)$$

t = time of operation of the relay TSM = Time setting multiplier. K , L and α are constants. They varies characteristics to characteristics. M is the ratio between short circuit current I_{sc} and pick up current I_p of the relays.

Coordinating time interval in each cases is supposed to be 0.25 sec. Eight types of intelligent over current relay characteristics are obtained from Ref.[11].

7.4.3 Pick-up current constraints

Pick up current is having a limit. The relay co-ordination problem is highly dependent on the value of the pickup current of the relays. The limits of pick up current can be expressed as below[15](ref. Eq. (15)):

$$I_{p_{\min}} \leq I_p \leq I_{p_{\max}} \quad (15)$$

7.4.4 TSM constraints

TSM is supposed to be continuous and can take any value between 0.05-1.1. Mathematically it can be expressed as below (ref.Eq.(16)):

$$TSM_{\min} \leq TSM \leq TSM_{\max} \quad (16)$$

7.4.5 Constrains on relay operating time

Limits on time of operation of relay(t_{op}) can be expressed as(ref. Eq.(17)):

$$t_{op\min} \leq t_{op} \leq t_{op\max} \quad (17)$$

Minimum operation time of relay is 0.1 sec and maximum depends on the requirement of the user.

7.4.6. Constraints on PSM :

Plug setting multiplier (PSM) should be within range. Mathematically it can be expressed as follows (ref. Eq. (16)).

$$PSM_{\min} \leq PSM \leq PSM_{\max} \quad (16)$$

7.5 Test Results

The methodology has been tested on several test systems. e.g- IEEE 5 bus, 6 bus , WSCC 3 Machine 9 Bus , IEEE 14 bus and IEEE 30 bus system.

7.5.1 IEEE 5 bus system Results :

The proposed methodology has been implemented here using IEEE 5 Bus Test system. Test system data is obtained from Appendix-F. The relay arrangement for the above mentioned power system is shown in Fig 2. The directional mho relays are used here. Over current relays are arranged using time graded protection scheme with IDMT (Inverse definite minimum time) characteristics.

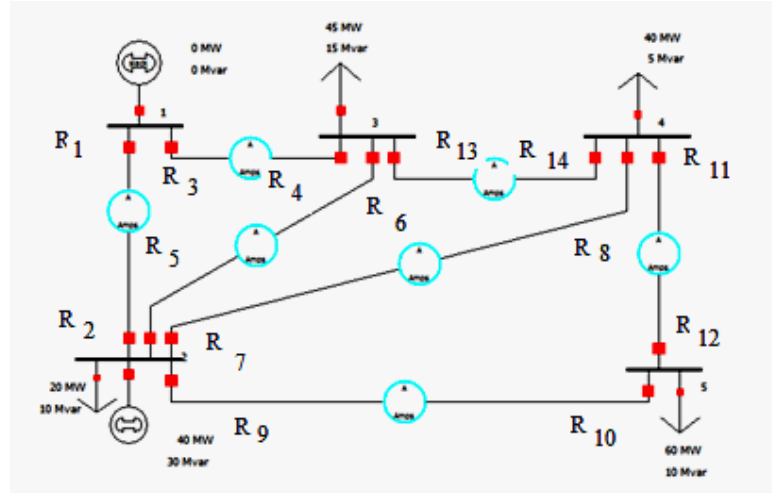


Fig 2: Relay arrangement for IEEE-5 Bus System

The main and back up relay pairs for the above IEEE 5 Bus system are shown in Table 1.

Table 1 : Main and backup relay pairs

Sl. No.	Main over current and distance relays	Back up over current and distance relays	Sl. No.	Main over current and distance relays	Back up over current and distance relays
1.	R ₁	R ₄	9.	R ₉	R ₁
2.	R ₂	R ₁₀	10.	R ₁₀	R ₁₁
3.	R ₃	R ₂	11.	R ₁₁	R ₁₃
4.	R ₄	R ₁₄	12.	R ₁₂	R ₉
5.	R ₅	R ₈	13.	R ₁₃	R ₃
6.	R ₆	R ₁₄	14.	R ₁₃	R ₅
7.	R ₇	R ₆	15.	R ₁₄	R ₇
8.	R ₈	R ₁₃	16.	R ₁₄	R ₁₂

The information regarding pick up current settings are given in Table 2. The value of pick up current of each over current relay is assumed approximately to be 1.25 times of the relevant maximum load in approximated integer form. The short circuit current data are shown in Table

3. From Table-1, it is found that relay no. 13 and 14 are having better protection reliability as both of them have two back up relays.

Table 2 : Pickup current values of the Relay

Relay number(R_i)	Load Current(amps)	Pick up Current(amps)
1	386	483
2	383	479
3	177	221
4	177	221
5	90	113
6	93	116
7	132	165
8	160	200
9	240	300
10	242	303
11	24	30
12	22	28
13	72	90
14	70	88

Table 3 : Short Circuit Current data for main and back up relays

Main Relay(R_i)	Back up Relay(R_i)	Main relay short circuit current (amps)	Back up relay short circuit current(amps)
1	4	684	97
2	10	790	18
3	2	1060	561
4	14	721	443
5	8	1151	34
6	14	761	443
7	6	1151	31
8	13	661	481
9	1	1176	502
10	11	374	272
11	13	858	481
12	9	709	708
13	3	602	326
13	5	602	280
14	7	561	377
14	12	561	184

The objective function is found on the basis of trial and error. The objective of choosing objective function is to reduce the time of operation of relay. When $|T_{DLOCi}|$ is positive then the second term of objective function is becoming zero but when $|T_{DLOCi}|$ is negative then the second term is additive with the objective function and increasing its value. Since it is a minimization problem, the chance of survival of such fitness value is mitigated by this approach. As per coordination constraints $|T_{DLOCi}|$ value should be always greater than equals to zero. Its value can be negative only in case of mis-co-ordination. So, with such approach the

chance of mis-coordination problem is almost nullified. The same kind of explanation can be given for choosing the third and fourth term of the fitness function also.

Table 4: Output Table (IEEE 5-bus system) in terms of second zone operation time, TSM and no. of selected intelligent overcurrent relay characteristics

Relay (R_i)	Second Zone operation time (T_{z2})(sec)	TSM	No. of selected Characteristic
1	0.9997	0.05	7
2	0.5946	0.05	7
3	0.3503	0.0985	3
4	0.4724	0.08073	2
5	0.4327	0.1467	2
6	0.3465	0.0949	2
7	0.3102	0.1373	3
8	0.3668	0.0634	2
9	0.3454	0.0747	3
10	0.2956	0.05	1
11	0.3640	0.1803	2
12	0.4855	0.2314	2
13	0.3218	0.1356	3
14	0.2628	0.10465	3
Average Value	0.42488	0.107013	-
Fitness value	100	-	-

The output results are obtained by applying the TLBO (Teaching learning based optimization) for a network shown in Fig 2. TSMs and over current relay characteristics selected by TLBO are shown in Table 4. TSMs are assumed as continuous (0.05-1.1) in all the

cases. The time of operation of relays in each case are also shown in the Table 4. The various outputs for IEEE 5 bus test system are shown pictorially from Fig 3 to Fig 7.

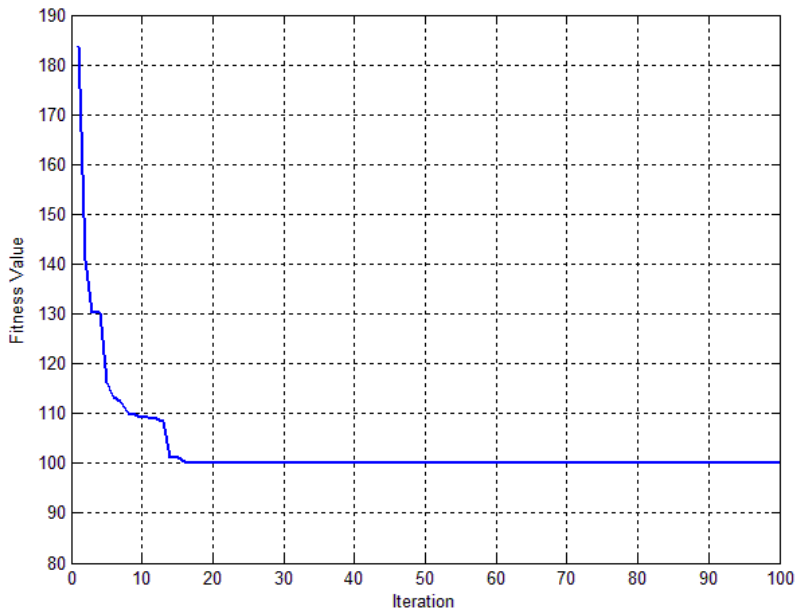


Fig 3 : Convergence characteristics of the TLBO algorithm for IEEE 5 bus system

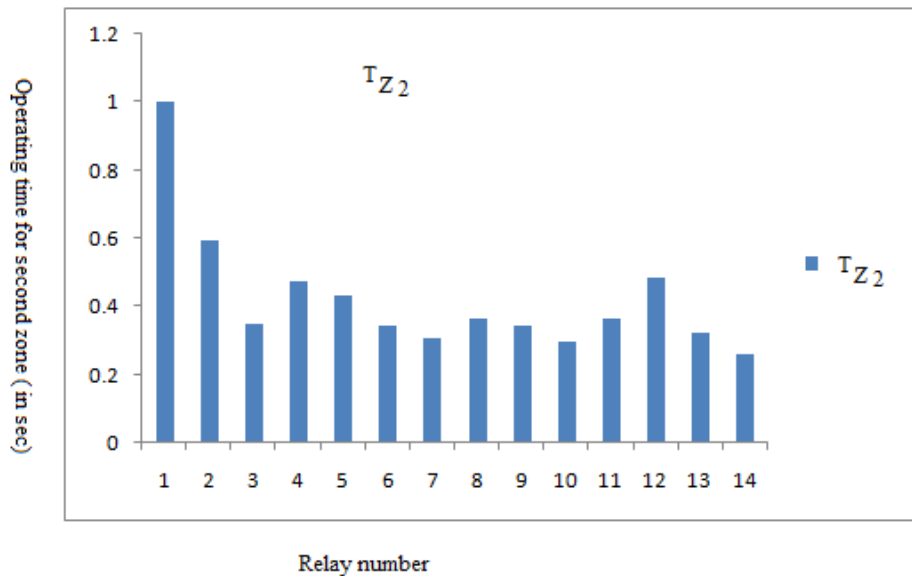


Fig 4 : Comparison of operating time of second zone of relays for IEEE 5 bus system

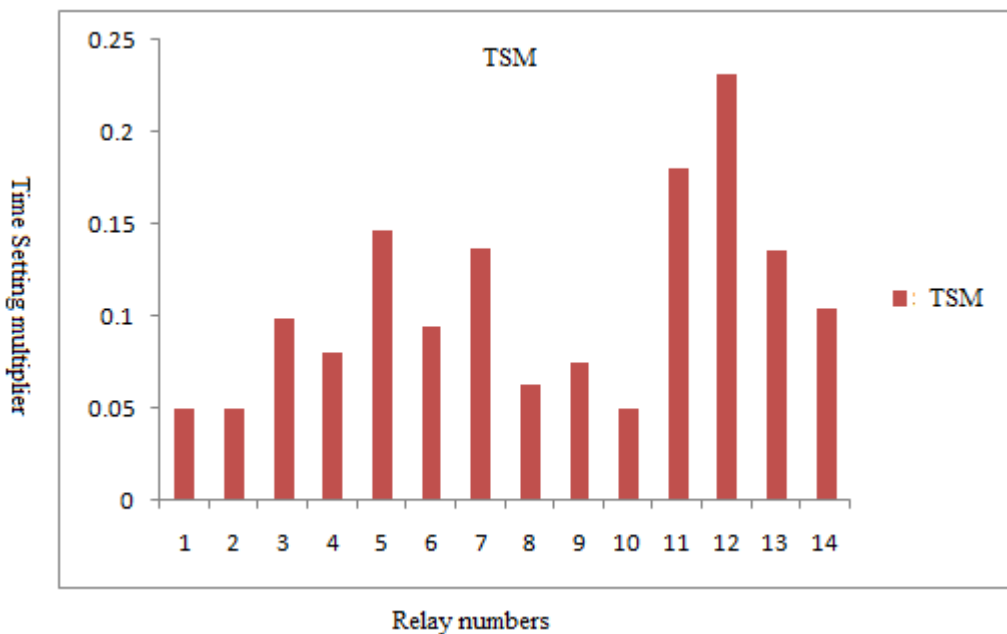


Fig 5 : Comparison of optimum Time setting multipliers of relays for IEEE 5 bus system

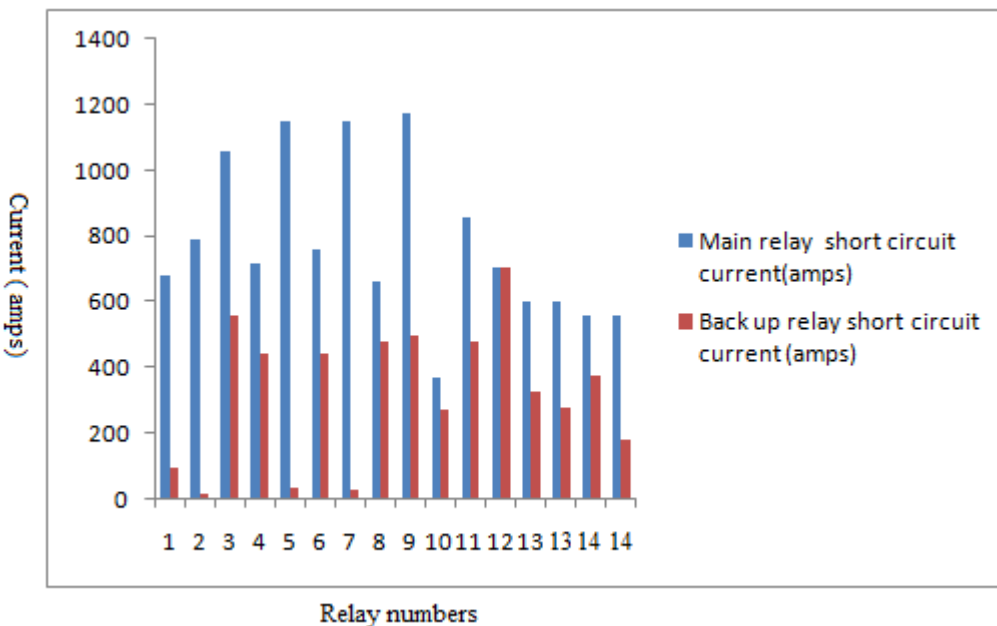


Fig 6 : Comparison of short circuit currents of main and backup relays for IEEE 5 bus system

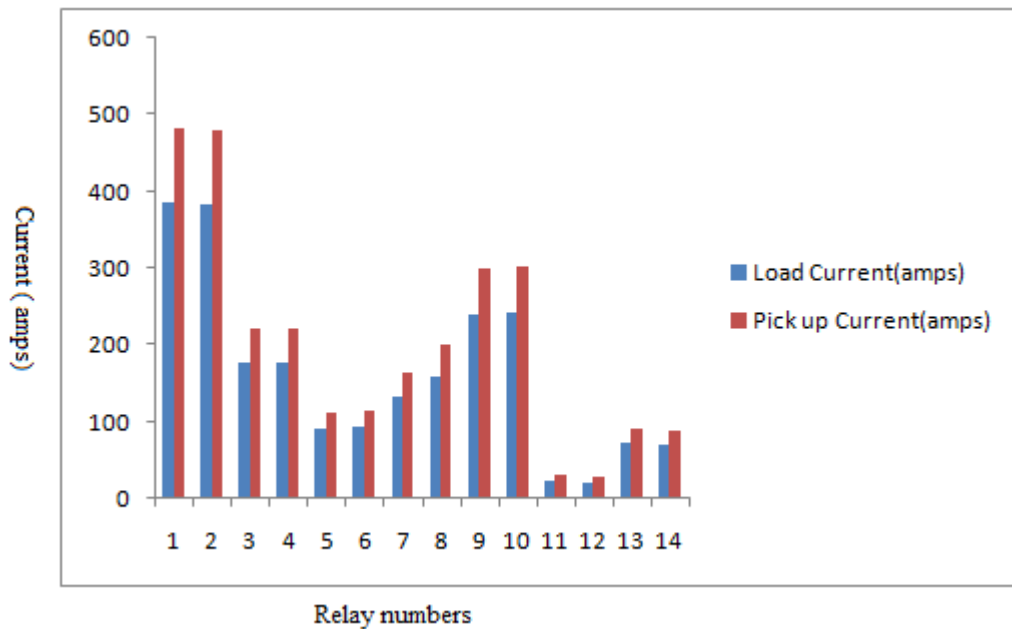


Fig 7 : Comparison of load currents and pick up currents of various relays for IEEE 5- bus system

7.5.2 6 bus system Results :

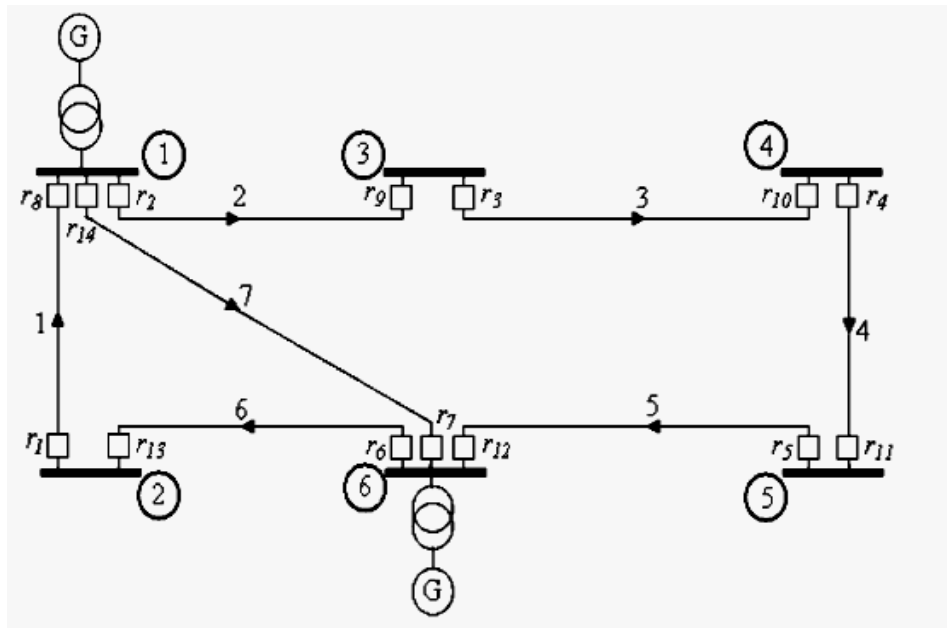


Fig.8:Relay arrangement for 6 Bus System

Table-5: Main and backup relay pairs with short circuit data

Main Relay(r _i)	Back up Relay(r _i)	Short circuit current of main relay (amps)	Short circuit current of back up relay (amps)
r ₂	r ₁	5428	828
r ₁₄	r ₁	4184	816
r ₃	r ₂	3505	3505
r ₄	r ₃	1769	1769
r ₅	r ₄	1103	1103
r ₆	r ₅	4936	340
r ₇	r ₅	4184	337
r ₁	r ₆	2682	2682
r ₂	r ₇	5428	1571
r ₈	r ₇	4933	1563
r ₁₃	r ₈	2492	2492
r ₈	r ₉	4933	340
r ₁₄	r ₉	4184	337
r ₉	r ₁₀	1174	1174
r ₁₀	r ₁₁	2589	2589
r ₁₁	r ₁₂	3655	3655
r ₇	r ₁₃	4184	816
r ₁₂	r ₁₃	5431	828
r ₆	r ₁₄	4936	1565
r ₁₂	r ₁₄	5431	1573

Total number of relays used here is 14. From Table-5, it is found that relays r₂,r₆,r₇,r₈,r₁₂,r₁₄ are having better protection reliability compare to other relays, as they have more than one backups.

Critical fault location-There is a minimum length of the line, below which the relay is unable to protect the line. If the fault point is too close to the relaying point, the relay may fail to operate. The relay will operate if the following condition is satisfied [115] :

$$\frac{Z_s}{Z_L} \leq \left(\frac{E}{V} - 1 \right) \quad (18)$$

Z_s is the source impedance behind the relay, Z_L is the line impedance from the relaying point to the fault point, E is the line input voltage (or normal secondary C.T voltage), V is the

voltage at relay location. Critical fault location is that point, which is the minimum distance of the line to make the relay to start work. In that point the following condition is satisfied :

$$\frac{Z_s}{Z_L} = \left(\frac{E}{V} - 1 \right) \quad (19)$$

In critical fault location, the discrimination time is zero i.e

$$T_b - T_m = CTI \quad (20)$$

Usually the critical fault location is situated within 12% length of each transmission line.

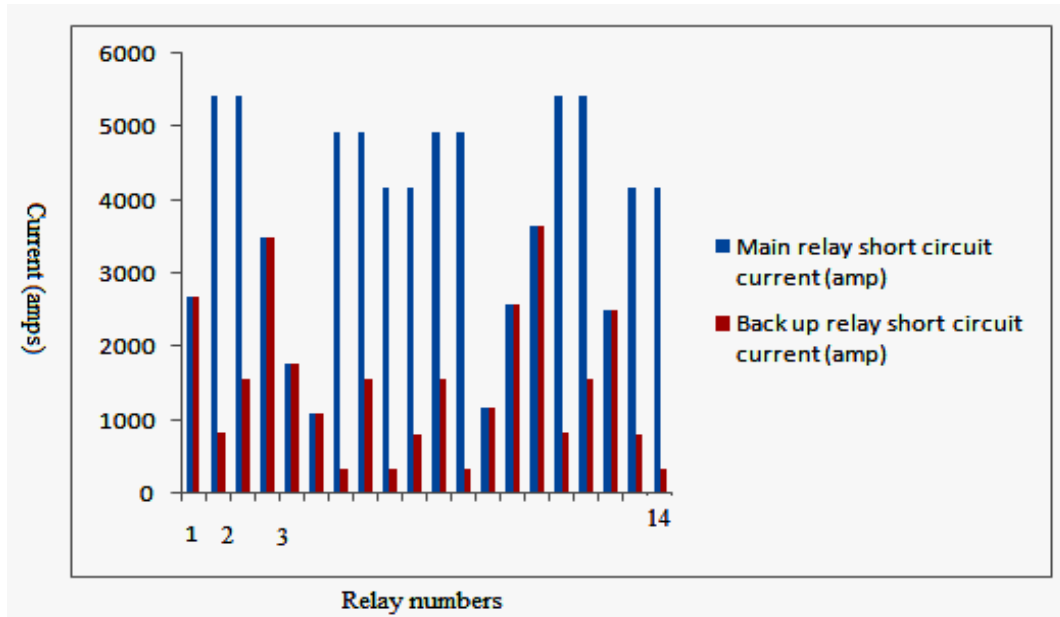


Fig. 9: Comparison of short circuit currents of main and backup relays

Table-6: Pick up current values of the relay

Relay number(r_i)	Load Current(amps)	Pick up Current(amps)
r_1	104	125
r_2	166	200
r_3	125	150
r_4	180	200
r_5	129	137
r_6	114	137
r_7	141	162
r_8	109	137
r_9	118	135
r_{10}	110	137
r_{11}	135	162
r_{12}	122	137
r_{13}	125	150
r_{14}	166	200

By applying TLBO (Teaching learning based optimization) in the network of Fig 8 the output results are obtained. TSMs and over current relay characteristics which are selected by TLBO are shown in Table-7. The time of operation of relays in each case are also shown in the table(Table-7). The various outputs from this work are shown pictorially from Fig.9 to Fig.12.

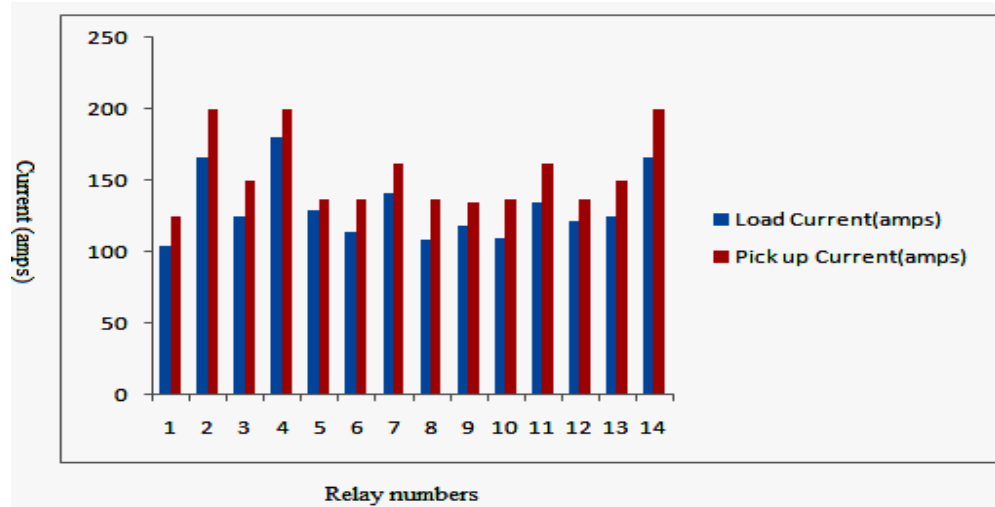


Fig.10: Comparison of Load current and pick up current of various relays

Table-7: Output table for type of characteristics and TSM selection

Relay (r _i)	Second Zone operation time (T _{z2})(sec)	TSM	No. of selected Characteristic
1	0.537	0.242567	2
2	0.4987	0.243110	2
3	0.5482	0.254736	2
4	0.6027	0.191837	3
5	0.5333	0.162270	3
6	0.5693	0.302211	2
7	0.4984	0.239195	2
8	0.5806	0.308156	2
9	0.537	0.169566	3
10	0.6233	0.269546	6
11	0.5872	0.269727	2
12	0.5365	0.292676	2
13	0.5333	0.220228	2
14	0.4942	0.221336	2
Average Value	0.54855	0.24194	-
Fitness value	120.664	-	-

Justification on incorporating different intelligent overcurrent relay characteristics: From Table-7, it is observed that the TLBO applied to the test system used mainly no.2 intelligent characteristics (10 out of 14 relays are using no. 2— standard inverse characteristics). But the selection of types of characteristics depends on several factors. e.g- Short circuit data , load and pick up current data, fault location, type of fault etc. Here, in this particular case ,no.2(Standard inverse) characteristics is frequently used. But the other characteristics also have equal importance when the types of faults or location or size of the test system(specially higher order test system) will change.

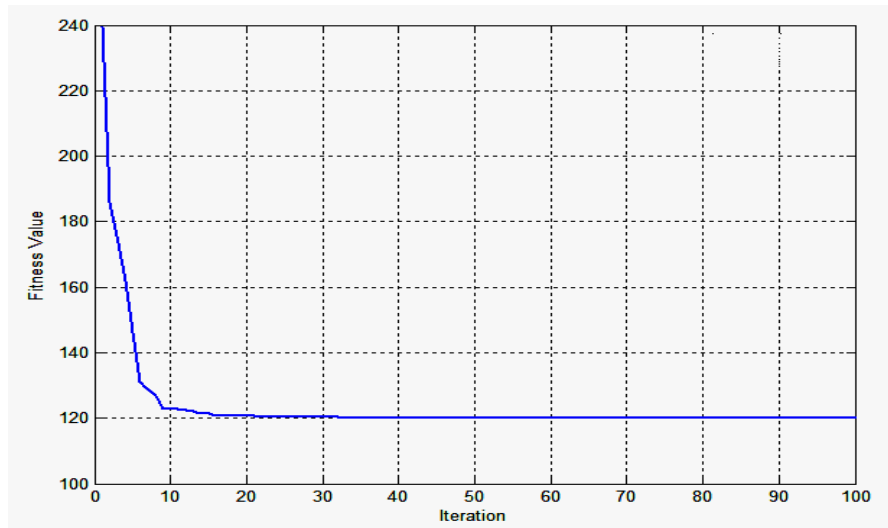


Fig.11: Convergence characteristics of the TLBO algorithm

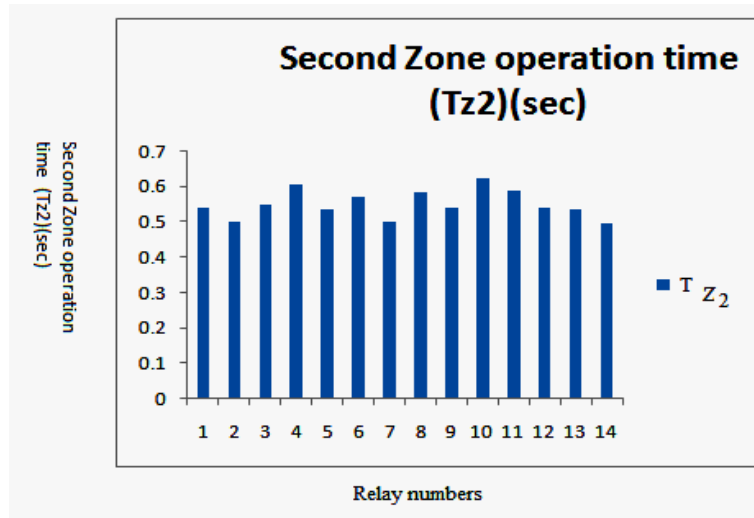


Fig.12: Comparison of operating time of second zone of relays

7.5.3 WSCC 3 Machine 9 bus system Results :

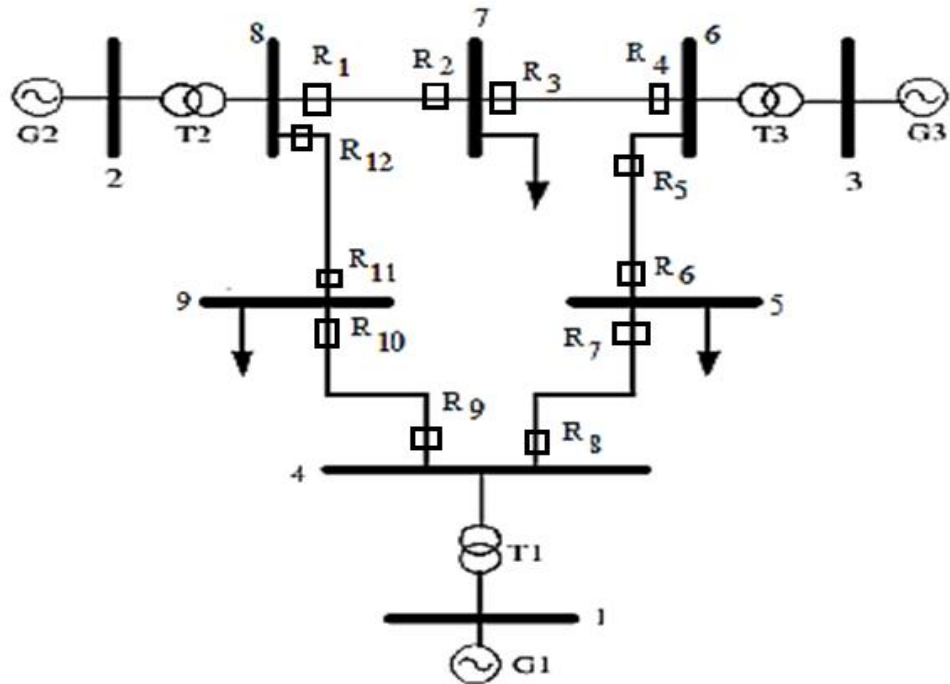


Fig.13:Relay arrangement in WSCC-3-Machine-9-Bus System

Table-8: Main and backup relay pairs

Main over current and distance relays	Back up over current and distance relays
R ₃	R ₁
R ₅	R ₃
R ₇	R ₅
R ₉	R ₇
R ₁₁	R ₉
R ₁	R ₁₁
R ₁₂	R ₂
R ₁₀	R ₁₂
R ₈	R ₁₀
R ₆	R ₈
R ₄	R ₆
R ₂	R ₄

Table-9: Pick up current values of the Relay

Relay number(R_i)	Load Current(amps)	Pick up Current(amps)
1	176	220
2	175	210
3	57	70
4	25	30
5	148	185
6	146	180
7	40	50
8	16	20
9	68	85
10	10	12
11	225	270
12	230	285

Table-10: Short Circuit Current data for main and back up relays

Main Relay(R_i)	Back up Relay(R_i)	Main relay short circuit current (amps)	Back up relay short circuit current(amps)
1	11	705	315
2	4	247	256
3	1	515	510
4	6	466	294
5	3	290	140
6	8	300	316
7	5	294	285
8	10	943	250
9	7	578	70
10	12	373	364
11	9	295	318
12	2	686	245

Table-11: Output Table

Relay (R _i)	Second Zone operation time (T _{z2})(sec)	TSM	No. of selected Characteristic
1	0.5215	0.0878	2
2	0.5505	0.0717	1
3	0.33913	0.1597	3
4	0.5673	0.2285	2
5	0.5472	0.19856	1
6	0.6110	0.25226	1
7	0.310426	0.13028	4
8	0.6022	0.3446	2
9	0.3222	0.13843	3
10	0.4848	0.24638	2
11	0.70456	0.050	1
12	0.3332	0.0727	7
Average Value	0.49117	0.16507	-
Fitness value	75		

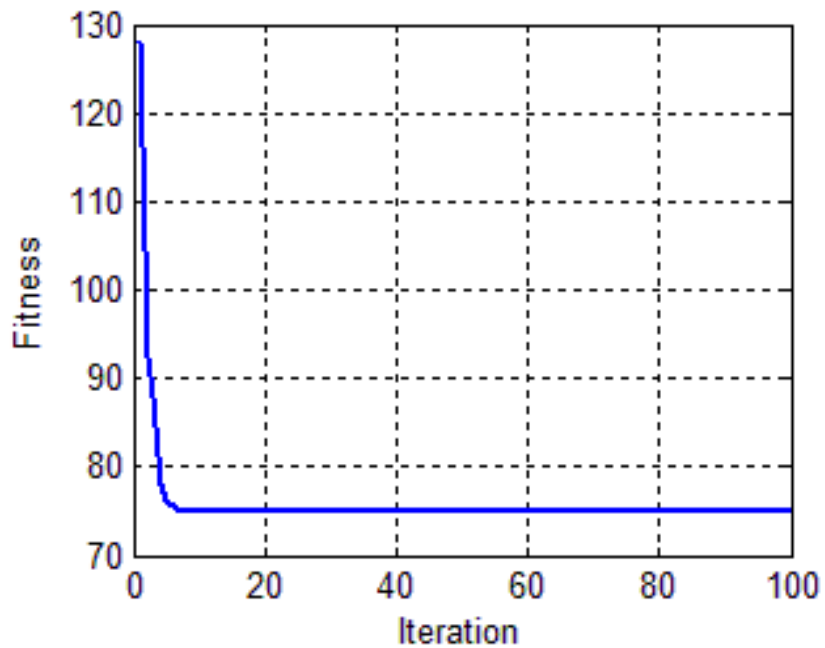


Fig.14: Convergence curve of the TLBO algorithm

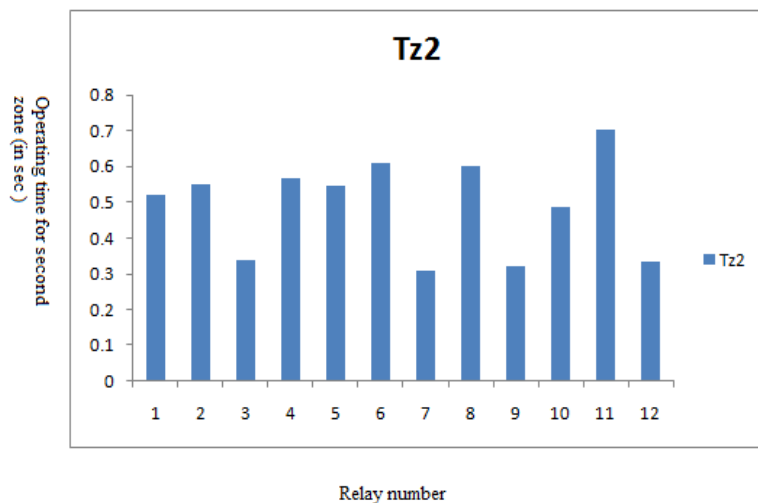


Fig.15: Comparison of operating time of second zone of relays

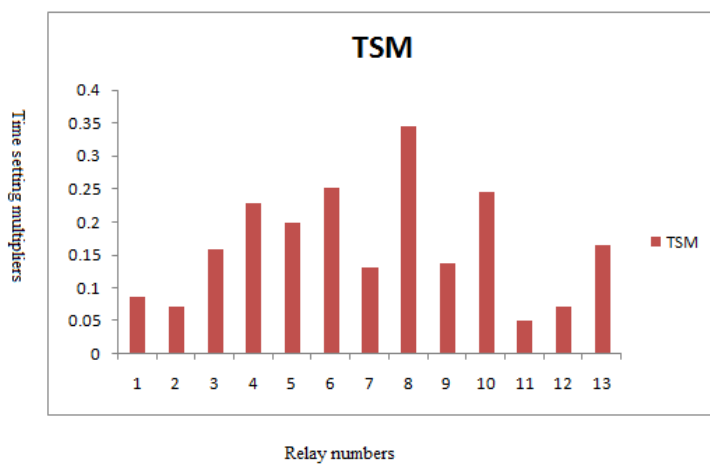


Fig.16: Comparison of optimum Time setting multipliers of relays

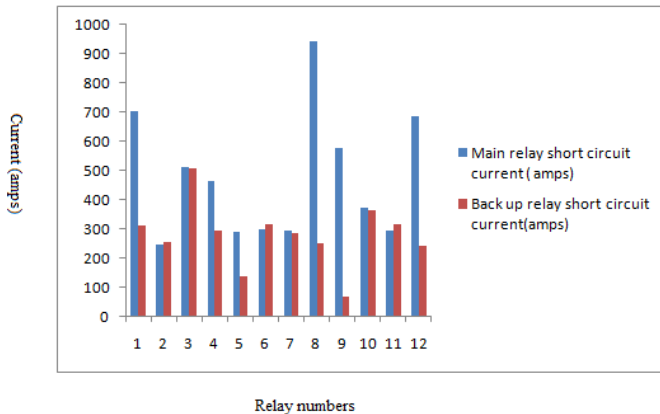


Fig.17: Comparison of short circuit currents of main and backup relays

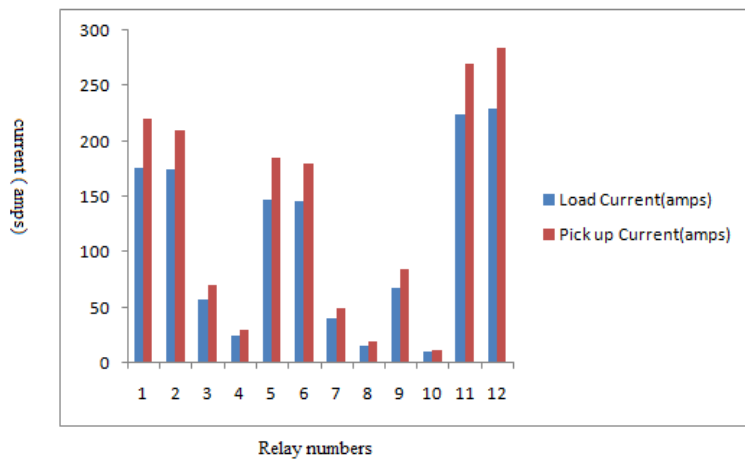


Fig.18: Comparison of Load current and pick up current of various relays

In Fig 16 , the 13th TSM value indicates the average TSM value of all the twelve used relays in the test system.

7.5.4 IEEE 14 bus system Results :

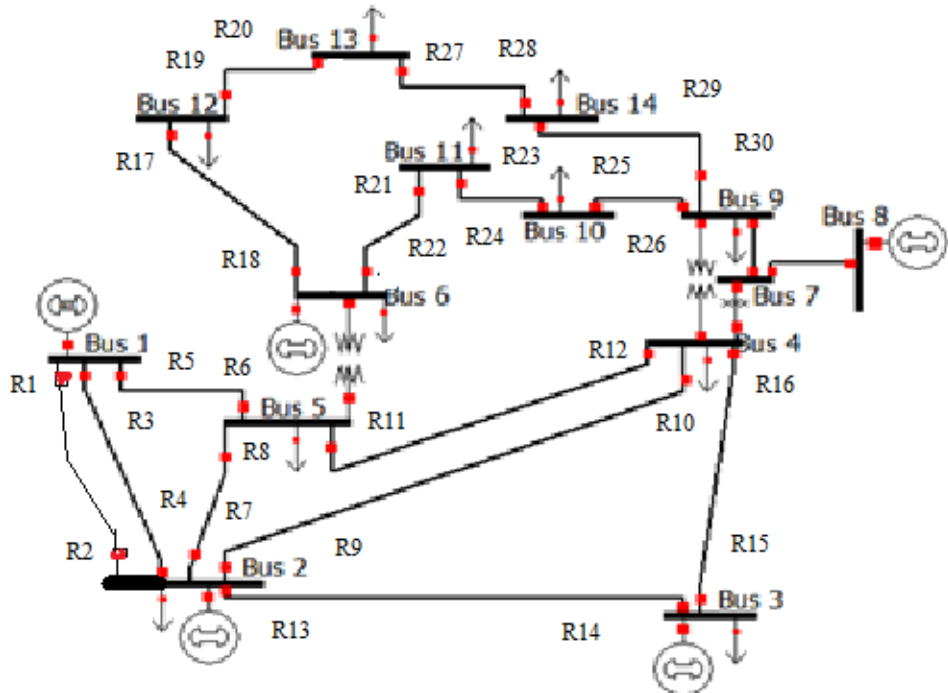


Fig.19.Relay arrangement in IEEE 14 Bus System

The main and back up relay pairs with short circuit current data are shown in Table 12.

Table 12. Main and backup relay pairs with Short Circuit Current data

Main Relay(R_i)	Back up Relay(R_i)	Main relay short circuit current (amps)	Back up relay short circuit current(amps)
R_1	R_6	1494	125
R_2	R_{14}	621	268
R_3	R_6	1494	125
R_4	R_{10}	621	260
R_4	R_8	621	281
R_5	R_2	3393	338
R_5	R_4	3393	338
R_6	R_{12}	1716	880
R_6	R_7	1716	678
R_7	R_3	2732	1816
R_8	R_5	703	788
R_9	R_3	2753	132
R_{10}	R_{11}	1766	1088
R_{11}	R_5	1109	795
R_{12}	R_{15}	1380	464
R_{12}	R_9	1380	699
R_{13}	R_1	2774	1820
R_{14}	R_{16}	1118	795
R_{15}	R_{13}	1249	925
R_{16}	R_{11}	2004	1092
R_{17}	R_{20}	415	415
R_{18}	R_{21}	1419	270
R_{19}	R_{18}	565	565
R_{20}	R_{28}	996	267
R_{21}	R_{24}	528	528
R_{22}	R_{17}	1189	35
R_{23}	R_{22}	641	641
R_{24}	R_{26}	921	921
R_{25}	R_{23}	377	377
R_{26}	R_{29}	1239	168
R_{27}	R_{19}	913	186
R_{28}	R_{30}	608	608
R_{29}	R_{27}	406	406
R_{30}	R_{25}	1327	264

From the above Table 12, it is found that relay R_4 , R_5 , R_6 , R_{12} having more protective reliability as they have two backups.

Table 13. Pick up current values of the Relay

Relay number(R_i)	Load Current(amps)	Pick up Current(amps)	Relay number(R_i)	Load Current(amps)	Pick up Current(amps)
1	312	390	16	100	125
2	310	388	17	32	40
3	312	390	18	32	40
4	310	388	19	8	10
5	298	373	20	8	10
6	298	373	21	32	40
7	166	208	22	32	40
8	166	208	23	16	20
9	224	280	24	16	20
10	224	280	25	26	33
11	260	325	26	26	33
12	260	325	27	24	30
13	294	368	28	24	30
14	294	368	29	40	50
15	100	125	30	40	50

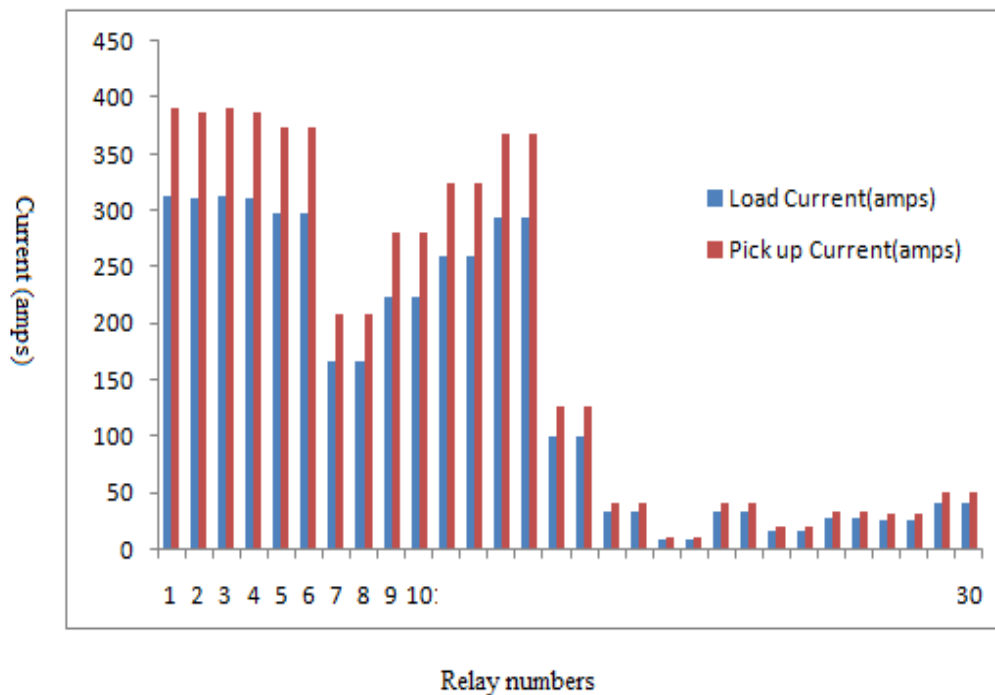


Fig.20. Comparison of Load current and pick up current of various relays

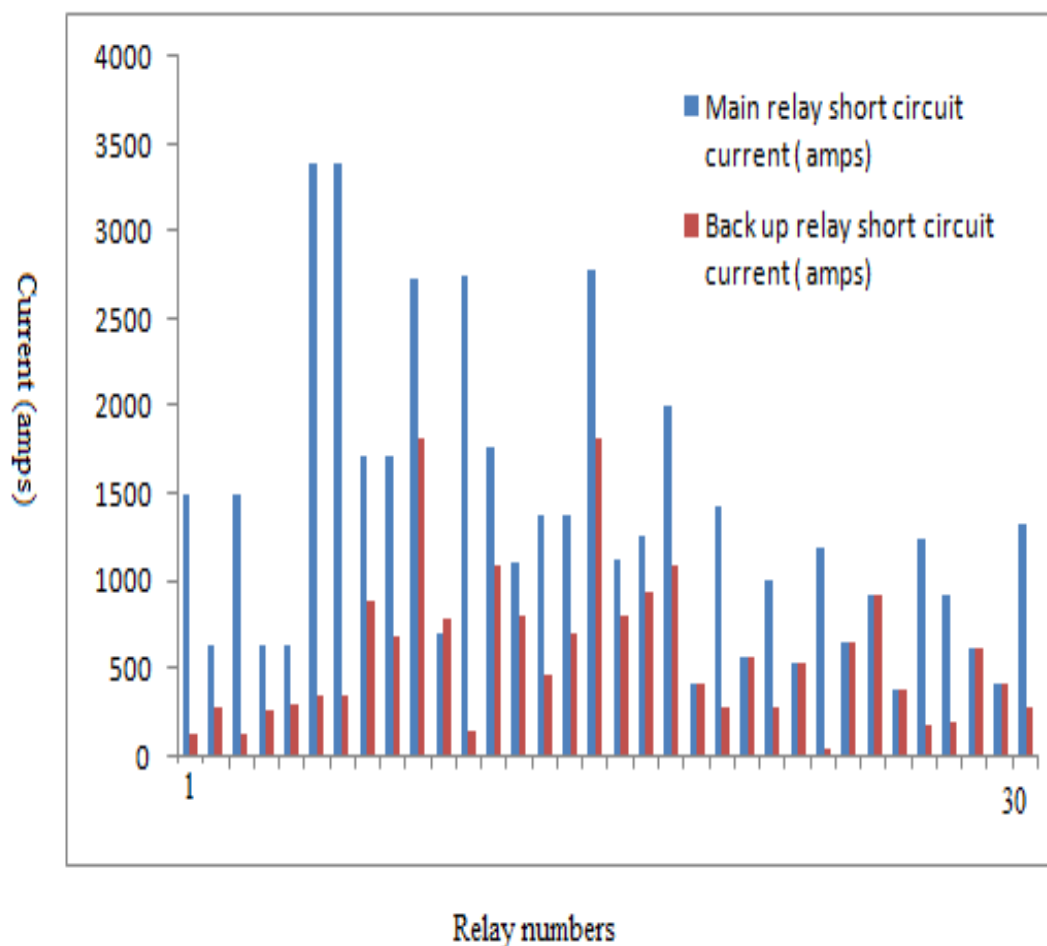


Fig.21. Comparison of short circuit currents of main and backup relays

Table 14. Output Table

Relay (R _i)	Second Zone operation time (for distance relay)(T _{z2})(sec)	TSM (for over current relay)	No. of selected Characteristic
1	0.42825	0.0898	3
2	0.27816	0.05	6
3	0.5388	0.113	3
4	0.27816	0.05	6
5	0.4546	0.1465	2
6	0.5249	0.14	3
7	0.5353	0.2822	2
8	0.44928	0.0792	3
9	0.4505	0.1505	2
10	0.3067	0.12057	3
11	0.44658	0.0798	3
12	0.4662	0.1121	3
13	0.2736	0.1325	3
14	0.45	0.07225	2
15	0.45	0.15142	2
16	0.38253	0.18996	8
17	0.4537	0.15513	2
18	0.4514	0.23845	2
19	0.4569	0.2743	2
20	0.4178	0.3434	5
21	0.4501	0.1704	2
22	0.4502	0.2256	2
23	0.45	0.2308	2
24	0.4521	0.25697	2
25	0.4566	0.16278	2
26	0.4569	0.24553	2
27	0.4569	0.23077	2
28	0.45	0.19935	2
29	0.2625	0.13844	3
30	0.4518	0.21868	2
Average Value	0.427682	0.16822	-
Fitness Value	211.4055	-	-

From Table 13 and Table 14 , it is observed that in case of relays with less pick up current , Characteristic 2 (Standard Inverse) is more suitable.

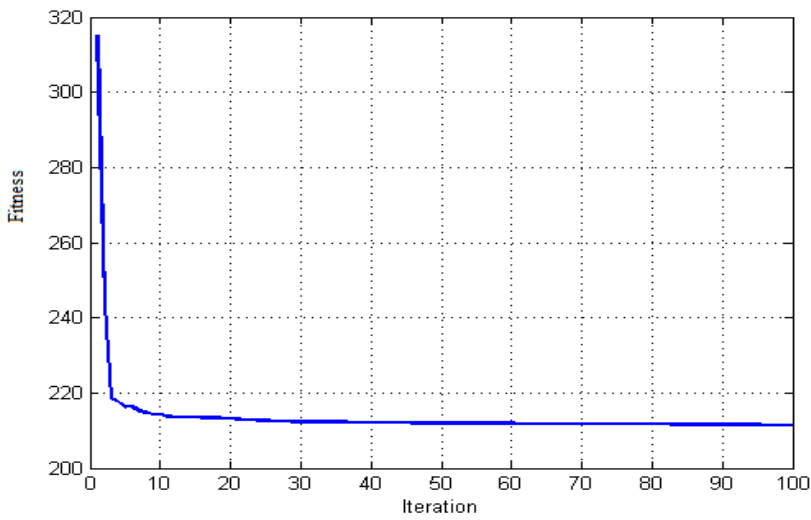


Fig.22. Convergence curve of the TLBO algorithm

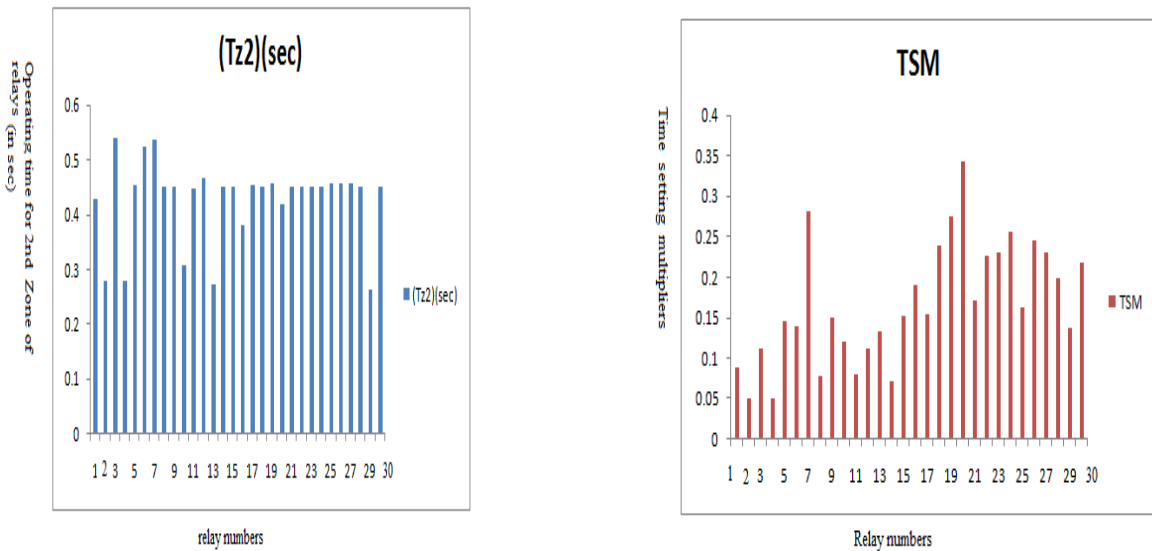


Fig.23. Comparison of operating time of second zone of relays

Fig.24. Comparison of optimum TSM of relays

7.5.5 IEEE 30 bus system Results :

To test the methodology, an IEEE 30 Bus system has been selected. Test system data are obtained from Appendix-F. The relay arrangements are shown for this power system as per Table 15. The mho directional relays are used here. Over current relays are arranged using time graded protection scheme with IDMT (Inverse definite minimum time) characteristics.

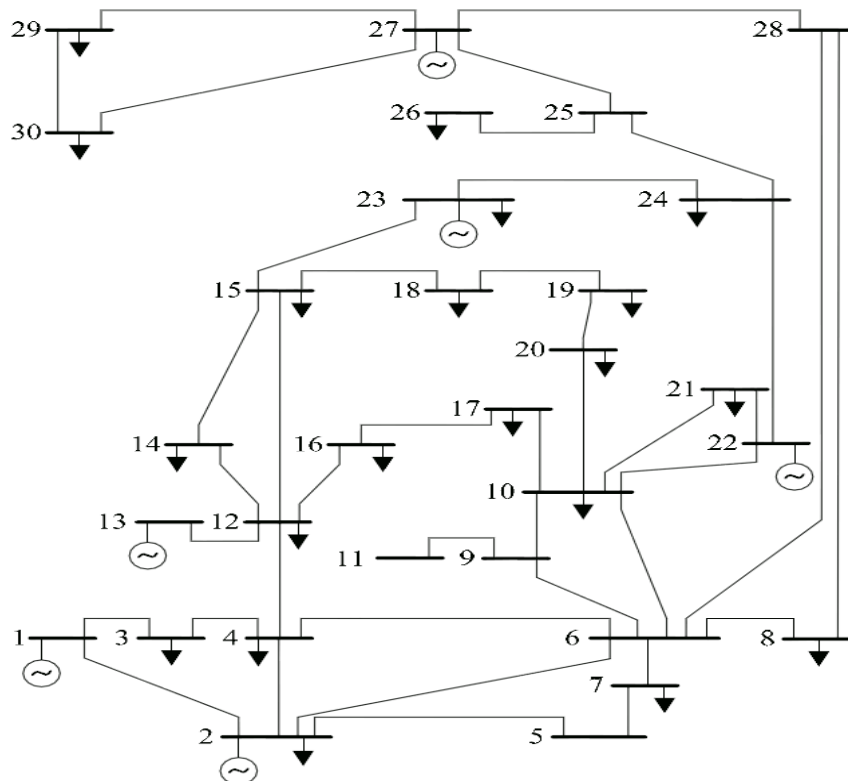


Fig 25: IEEE-30 Bus System

Table 15: Relay arrangement for IEEE 30 bus system

Sl. No.	Branch data from bus no.	Branch data to bus no.	Relay no. (R_i) adjacent to from bus	Relay no. (R_i) adjacent to to bus
1	1	2	1	2
2	1	3	3	4
3	2	4	5	6
4	3	4	7	8
5	2	5	9	10
6	2	6	11	12
7	4	6	13	14
8	5	7	15	16
9	6	7	17	18
10	6	8	19	20
11	6	9	-	-
12	6	10	-	-
13	9	11	-	-
14	9	10	-	-
15	4	12	-	-
16	12	13	-	-
17.	12	14	21	22
18.	12	15	23	24
19.	12	16	25	26
20.	14	15	27	28
21.	16	17	29	30
22.	15	18	31	32

Table 15: Relay arrangement for IEEE 30 bus system (Contd.)

Sl. No.	Branch data from bus no.	Branch data to bus no.	Relay no. (R_i) adjacent to from bus	Relay no. (R_i) adjacent to to bus
23	18	19	33	34
24.	19	20	35	36
25.	10	20	37	38
26.	10	17	39	40
27.	10	21	41	42
28.	10	22	43	44
29.	21	22	45	46
30.	15	23	47	48
31.	22	24	49	50
32.	23	24	51	52
33.	24	25	53	54
34.	25	26	55	56
35.	25	27	57	58
36.	28	27	-	-
37.	27	29	59	60
38.	27	30	61	62
39.	29	30	63	64
40.	8	28	65	66
41.	6	28	67	68

The main and back up relay pairs for IEEE 30 bus system are shown in Table 16

Table 16 : Main and backup relay pairs for IEEE 30 bus system

Sl. No.	Main over current (o/c) and distance relays	Back up over current and distance relays	Sl. No.	Main over Current(o/c) and distance relays	Back up over (o/c) and distance relays
1	R ₁	R ₄	22	R ₁₇	R ₁₁
2	R ₂	R ₁₀	23	R ₁₈	R ₁₅
3	R ₃	R ₂	24	R ₁₉	R ₆₈
4	R ₄	R ₈	25	R ₂₀	R ₆₆
5	R ₅	R ₁₀	26	R ₂₁	R ₂₆
6	R ₆	R ₁₄	27	R ₂₂	R ₂₈
7	R ₇	R ₃	28	R ₂₃	R ₂₆
8	R ₈	R ₁₄	29	R ₂₄	R ₃₂
9	R ₉	R ₁	30	R ₂₅	R ₂₂
10	R ₉	R ₁₂	31	R ₂₅	R ₂₄
11	R ₉	R ₆	32	R ₂₆	R ₃₀
12	R ₁₀	R ₁₆	33	R ₂₇	R ₂₁
13	R ₁₁	R ₁₀	34	R ₂₈	R ₄₈
14	R ₁₂	R ₁₈	35	R ₂₉	R ₂₅
15	R ₁₃	R ₇	36	R ₃₀	R ₃₉
16	R ₁₃	R ₅	37	R ₃₁	R ₂₃
17	R ₁₄	R ₁₈	38	R ₃₂	R ₃₄
18	R ₁₄	R ₁₁	39	R ₃₃	R ₃₁
19.	R ₁₅	R ₉	40	R ₃₄	R ₃₆
20.	R ₁₆	R ₁₇	41	R ₃₅	R ₃₃
21.	R ₁₇	R ₁₃	42	R ₃₆	R ₃₇

Table 16 : Main and backup relay pairs for IEEE 30 bus system(Contd.)

Sl. No.	Main over current (o/c) and distance relays	Back up over current and distance relays	Sl. No.	Main over Current(o/c) and distance relays	Back up over (o/c) and distance relays
43	R ₃₇	R ₄₀	62	R ₅₂	R ₄₉
44	R ₃₈	R ₃₅	63	R ₅₃	R ₄₉
45	R ₃₉	R ₄₄	64	R ₅₄	R ₅₈
46	R ₃₉	R ₃₈	65	R ₅₄	R ₅₆
47	R ₄₀	R ₂₉	66	R ₅₅	R ₅₈
48	R ₄₁	R ₄₄	67	R ₅₆	-
49	R ₄₂	R ₄₆	68	R ₅₇	R ₅₃
50	R ₄₃	R ₄₀	69	R ₅₈	R ₆₂
51	R ₄₃	R ₄₂	70	R ₅₈	R ₆₀
52	R ₄₄	R ₅₀	71	R ₅₉	R ₆₂
53	R ₄₄	R ₄₅	72	R ₆₀	R ₆₄
54	R ₄₅	R ₄₁	73	R ₆₁	R ₆₀
55	R ₄₆	R ₄₃	74	R ₆₂	R ₆₃
56	R ₄₇	R ₂₇	75	R ₆₃	R ₅₉
57	R ₄₈	R ₅₂	76	R ₆₄	R ₆₁
58	R ₄₉	R ₄₃	77	R ₆₅	R ₁₉
59	R ₅₀	R ₅₄	78	R ₆₆	R ₆₇
60	R ₅₀	R ₅₁	79	R ₆₇	R ₂₀
61	R ₅₁	R ₄₇	80	R ₆₈	R ₆₅

Table 17 : Pick up current values of the Relays

Relay number(R_i)	Load Current(amps)	Pick up Current(amps)	Relay number(R_i)	Load Current(amps)	Pick up Current(amps)
1	720	900	18	165	206
2	716	895	19	133	166
3	362	453	20	132	165
4	363	454	21	136	170
5	184	230	22	136	170
6	185	231	23	317	396
7	353	441	24	317	396
8	352	440	25	132	165
9	346	433	26	132	165
10	345	431	27	29	36
11	253	316	28	29	36
12	253	316	29	66	83
13	320	400	30	66	83
14	319	399	31	105	131
15	82	103	32	105	131
16	87	109	33	48	60
17	166	208	34	48	60

From Table 16, it is found that relay R_{13} , R_{14} , R_{17} , R_{25} , R_{39} , R_{43} , R_{44} , R_{50} , R_{54} , R_{58} are having two backups. So, they are having better protection reliability compare to other relays in present in the network. R_9 is having three backups. So it is having best protection reliability among all the relays present in the power network. One more significant observation from the table is R_{56} is having no separate back up. Because it is connected to an isolated branch connecting branch 25-26. In such case, R_{55} , second and third zone will act as a backup for R_{56} . R_{58} can be observed by second zone of R_{57} also. R_{54} can be observed by R_{58} or R_{56} . The

information regarding pick up current settings are shown in Table 17. The value of pick up current of each over current relay is assumed roughly 1.25 times of the relevant maximum load in approximated integer form. The short circuit current data are shown in Table 18.

Table 17 : Pick up current values of the Relays (Contd.)

Relay number(R_i)	Load Current(amps)	Pick up Current(amps)	Relay number(R_i)	Load Current(amps)	Pick up Current(amps)
35	124	155	52	37	46
36	124	155	53	40	50
37	163	204	54	40	50
38	163	204	55	73	91
39	116	145	56	73	91
40	116	145	57	82	103
41	313	391	58	82	103
42	313	391	59	110	138
43	149	186	60	110	138
44	149	186	61	125	156
45	39	49	62	125	156
46	39	49	63	65	81
47	98	123	64	65	81
48	98	123	65	3	4
49	110	138	66	17	21
50	110	138	67	81	101
51	37	46	68	81	101

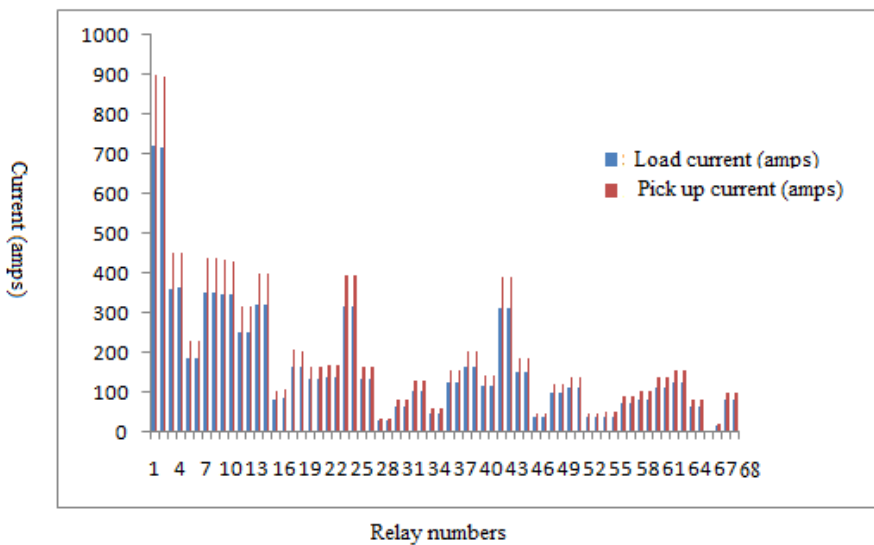


Fig 26 : Comparison of Load currents and pick up currents of Various relays

Table 18 : Short Circuit Current data for main and backup relays

Main Relay(R_i)	Back up Relay(R_i)	Main relay short circuit current (amps)	Back up relay short circuit current(amps)
1	4	1270	522
2	10	1929	421
3	2	1869	1296
4	8	1536	1536
5	10	2134	436
6	14	1959	1219
7	3	723	718
8	14	2045	1232
9	1	2140	915
9	12	2140	458
9	6	2140	385
10	16	1279	736
11	10	2078	435

Table 18 : Short Circuit Current data for main and backup relays (Contd.)

Main Relay(R_i)	Back up Relay(R_i)	Main relay short circuit current (amps)	Back up relay short circuit current(amps)
12	18	2138	404
13	7	1283	530
13	5	1283	513
14	18	1856	411
14	11	1856	492
15	9	1334	817
16	17	1347	1343
17	13	2194	806
17	11	2194	492
18	15	744	744
19	68	2158	115
20	66	825	257
21	26	1689	269
22	28	496	239
23	26	1523	269
24	32	684	244
25	22	1484	60
25	24	1484	235
26	30	594	594
27	21	633	633
28	48	1257	244
29	25	731	731
30	39	1065	1065

Table 18 : Short Circuit Current data for main and backup relays (Contd.)

Main Relay(R_i)	Back up Relay(R_i)	Main relay short circuit current (amps)	Back up relay short circuit current(amps)
31	23	1210	774
32	34	475	475
33	31	633	633
34	36	654	654
35	33	466	466
36	37	787	787
37	40	1612	274
38	35	1608	163
39	44	1501	84
39	38	1501	158
40	29	415	415
41	44	1648	80
42	46	915	624
43	40	1681	274
43	42	1681	118
44	50	1031	308
44	45	1031	727
45	41	911	911
46	43	789	483
47	27	1215	197
48	52	449	449
49	43	1215	481
50	54	590	248

Table 18 : Short Circuit Current data for main and backup relays (Contd.)

Main Relay(R_i)	Back up Relay(R_i)	Main relay short circuit current (amps)	Back up relay short circuit current(amps)
50	51	590	342
51	47	664	664
52	49	898	650
53	49	988	650
54	58	449	449
54	56	449	0.068
55	58	924	449
56	55 ^{2nd & 3rd zone}	0.35	0.35
57	53	481	481
58	62	654	0.098
58	60	654	7
59	62	975	3
60	64	158	158
61	60	971	5
62	63	214	214
63	59	406	406
64	61	309	309
65	19	2040	1505
66	67	1617	1497
67	20	2489	488
68	65	565	442

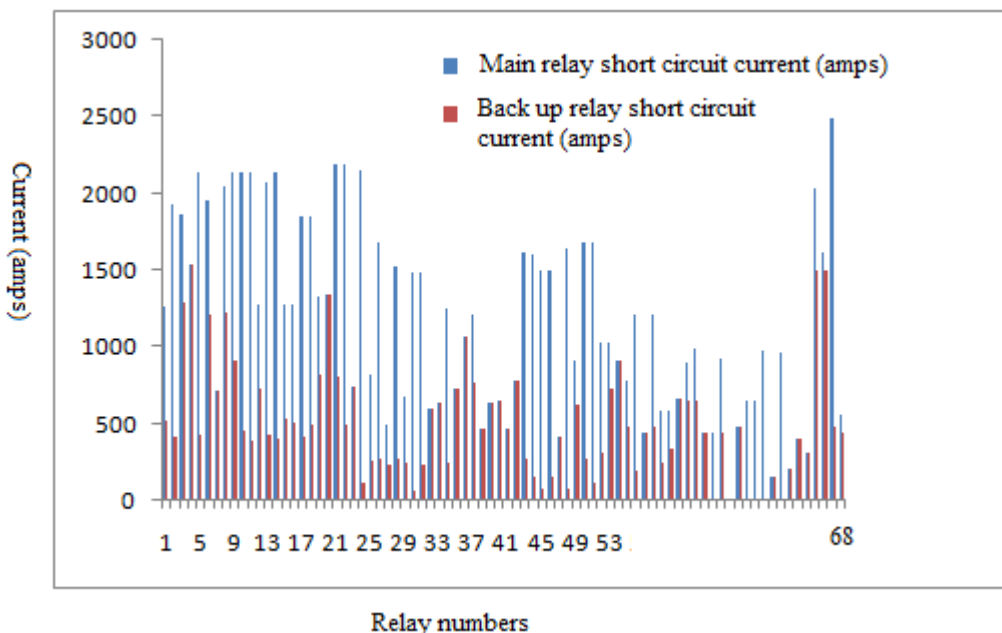


Fig 27 : Comparison of short circuit currents of main and backup relays for IEEE 30 bus system

The outputs are shown in Table 19.

Table 19 : Output Table (IEEE 30 bus system) for TSM and intelligent characteristics selection

Relay (R _i)	Second Zone operation time (for distance relay)(T _{z2})(sec)	TSM (for over current relay)	No. of selected Characteristic
1	0.989	0.05	7
2	0.5479	0.1126	2
3	0.3993	0.09245	3
4	0.4499	0.07943	3
5	0.4501	0.1465	2
6	0.2828	0.15672	3
7	0.581	0.05	7
8	0.3897	0.10035	4
9	0.3562	0.1043	4
10	0.2988	0.0885	8

Table 19 : Output Table (IEEE 30 bus system) for TSM and intelligent characteristics selection (Contd.)

Relay (R _i)	Second Zone operation time (for distance relay)(T _{z2})(sec)	TSM (for over current relay)	No. of selected Characteristic
11	0.3305	0.1234	3
12	0.2889	0.1399	3
13	0.4501	0.076	2
14	0.3706	0.10025	3
15	0.45	0.169	2
16	0.5016	0.1854	2
17	0.4929	0.17	2
18	0.4327	0.0837	3
19	0.4503	0.1693	2
20	0.3503	0.1051	4
21	0.45	0.151	2
22	0.2609	0.0695	8
23	0.4165	0.0878	3
24	0.349	0.05	7
25	0.456	0.1453	2
26	0.4336	0.0835	3
27	0.3645	0.05	5
28	0.4501	0.2368	2
29	0.2514	0.1454	3
30	0.3616	0.1683	7
31	0.45	0.12994	2
32	0.4313	0.0839	3
33	0.4501	0.1551	2
34	0.4932	0.3617	3

Table 19 : Output Table (IEEE 30 bus system) for TSM and intelligent characteristics selection (Contd.)

Relay (R _i)	Second Zone operation time (for distance relay)(T _{z2})(sec)	TSM (for over current relay)	No. of selected Characteristic
35	0.2508	0.0715	8
36	0.3429	0.1062	4
37	0.2654	0.1357	3
38	0.2658	0.1355	3
39	0.45	0.1538	2
40	0.6997	0.1064	2
41	0.2942	0.1631	8
42	0.2684	0.0551	7
43	0.4613	0.1484	2
44	0.4501	0.1121	2
45	0.45	0.1935	2
46	0.4519	0.1844	2
47	0.4503	0.1508	2
48	0.4294	0.0843	3
49	0.2938	0.281	4
50	0.3904	0.09473	3
51	0.2767	0.6237	1
52	0.4043	0.0624	5
53	0.2688	0.3735	3
54	0.45	0.1443	2
55	0.4527	0.1535	2
56	0.4502	0.05	2
57	0.494	0.1343	3
58	0.2539	0.1248	4

Table 19 : Output Table (IEEE 30 bus system) for TSM and intelligent characteristics selection (Contd.)

Relay (R_i)	Second Zone operation time (for distance relay)(T_{z2})(sec)	TSM (for over current relay)	No. of selected Characteristic
59	0.2867	0.1288	3
60	0.4605	0.05	1
61	0.2677	0.1197	3
62	0.4523	0.05	2
63	0.3492	0.1053	4
64	0.433	0.09029	3
65	0.45	0.4269	2
66	0.45	0.2918	2
67	0.45	0.2127	2
68	0.2971	0.1125	4
Average Value	0.406504	0.141944	-
Fitness Value	490.697	-	-

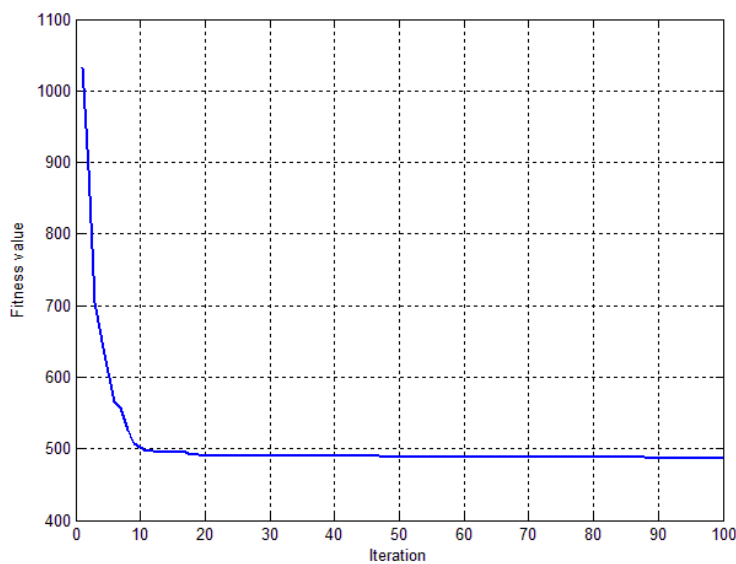


Fig 28 : Convergence characteristics of the TLBO algorithm for IEEE 30 bus system

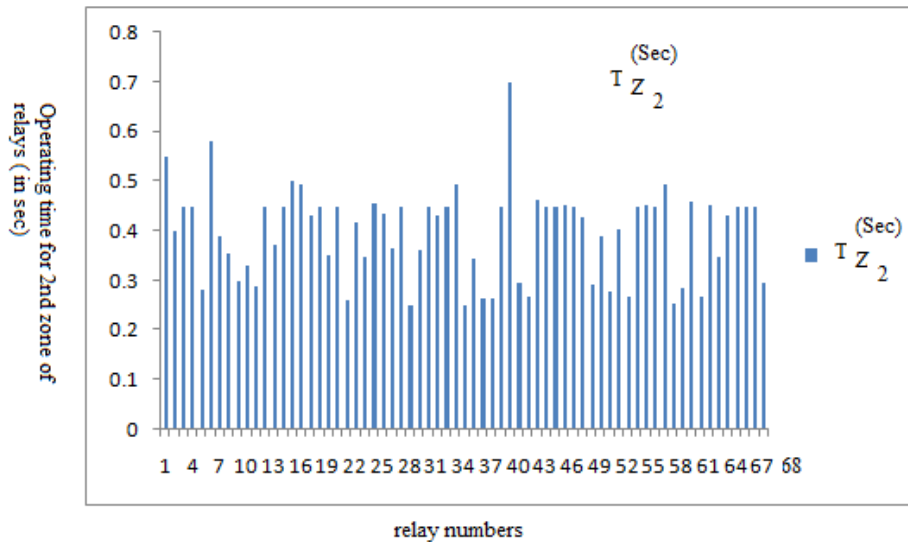


Fig 29 : Comparison of operating time of second zone of relays for IEEE 30 bus system

From Table 17 and Table 19, it is observed that in case of relays with less pick up current, Characteristic 2 (Standard Inverse) is more suitable. Figure 26 to Figure 30 shows various outputs obtained from the test case for IEEE 30 bus system.

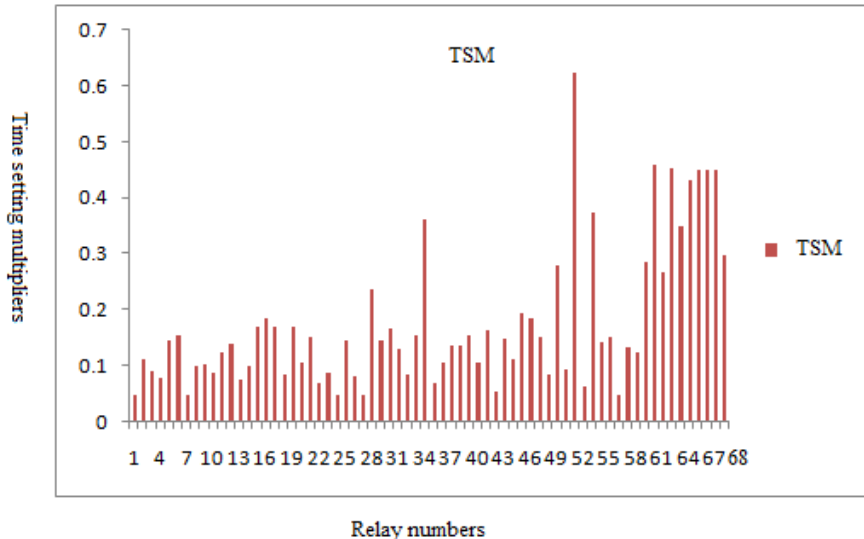


Fig 30 : Comparison of optimum Time setting multipliers of relays for IEEE 30 bus system

7.6 Advantages of this Technique

The discussed method is superior than previous methods used, in many respects. Firstly, the method is simple and reliable. Secondly, the method is capable of reducing mis-coordination

chances. Thirdly, the method is capable to handle both discrete and continuous time setting multiplier (TSM) cases. Fourthly, the method uses the different intelligent over current relay characteristics available in digital relays to reduce the time of operation. The algorithm is finding the minimum optimum value of relay operation satisfying all the constraints optimally from a look up table created in the memory during execution using the intelligent characteristics. Fifthly, the problem is converging very fast and in least CPU elapsed time than other methods. From our work we have shown, both in case of a small and a big test system, the problem is converging in less than 20 iterations by using this method and in least CPU elapsed time(ref. Table 20 to Table 24). Thus it is saving computational time, as well as the memory requirements needed for the program. The comparison of performance of this algorithm with contemporary other techniques like GA,PSO is shown in Subsection 7.7.

7.7 Comparative Study with GA and PSO

TLBO does not use any algorithm specific control parameter for finding global optimum solution. This property of this algorithm is an huge advantage over contemporary other optimization techniques. GA (Genetic algorithm) uses mutation rate, selection rate and cross over probability. PSO(Particle Swarm Optimization) uses inertia weight, social and cognitive parameters. The proper tuning of these parameters are very important for the performance of these optimization algorithms. TLBO does not need such kind of parameters. It only needs population size and number of generations for working. So, TLBO becomes highly consistent optimization algorithm. It converges very fast and superior compare to GA and PSO.

Fast convergence w.r.t number of iterations taken to converge the fitness function may often be deceptive. Because one iteration can take different time spans to compute for different meta-heuristic techniques subject to different constraints. So, ideally one should consider the total CPU elapsed time for convergence as a parameter to decide the fast convergence irrespective of number of iterations to converge. Among these three(GA,PSO and TLBO) algorithms, TLBO is converging in least CPU elapsed time as per Table-20 to Table-24. So, it is the fastest among them.

7.7.1 IEEE 5 bus case :

Table 20 : Comparative study with GA and PSO(IEEE 5 bus)

Attributes	TLBO	GA	PSO
Number of iterations to converge	17	10	24
Average time per iteration(Sec) taken	0.0038	0.013	0.0063
Total time taken to converge (CPU elapsed time)(sec)	0.0646	0.13	0.1512

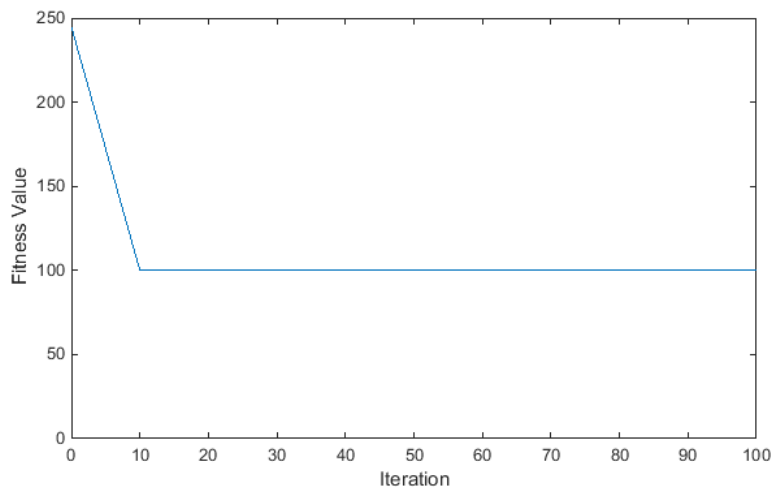


Fig 31: Convergence characteristics using GA(IEEE 5 bus)

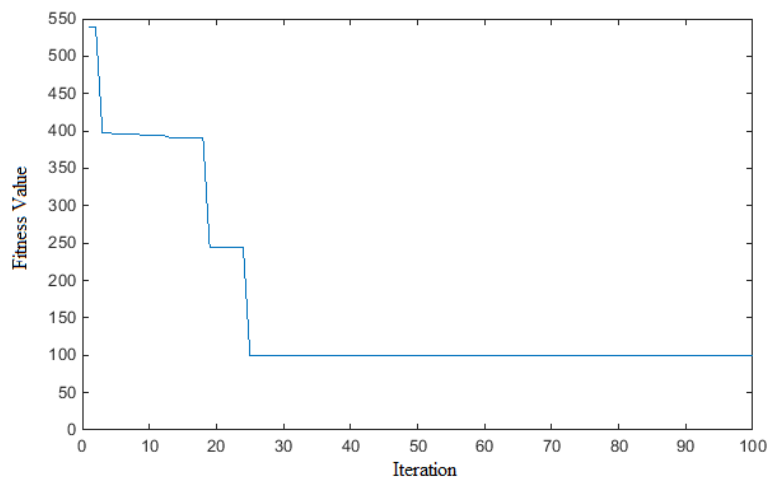


Fig 32: Convergence characteristics using PSO(IEEE 5 bus)

7.7.2 6 bus case :

Table-21: Comparison of results obtained by using GA,PSO and TLBO with respect to process speed

Attributes	GA	PSO	TLBO
Number of iterations to converge	20	8	16
Average time per iteration(Sec) taken	0.00955	0.0304	0.00438
Total time taken to converge (CPU elapsed time)(sec)	0.191	0.243	0.07

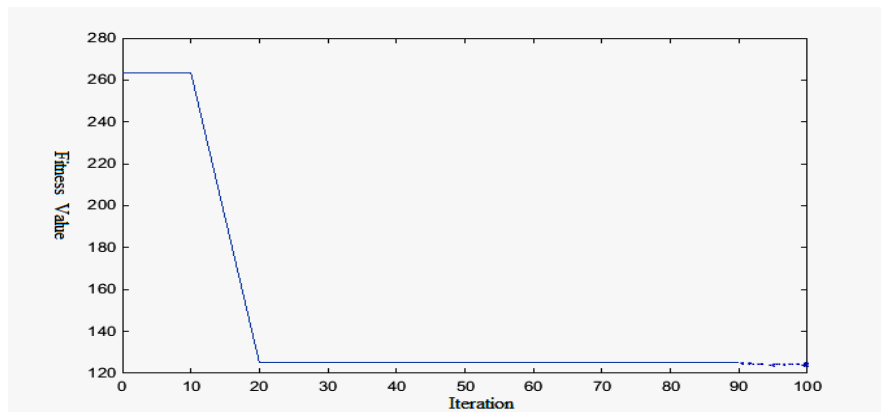


Fig.33: Convergence characteristics using Genetic Algorithm(GA)

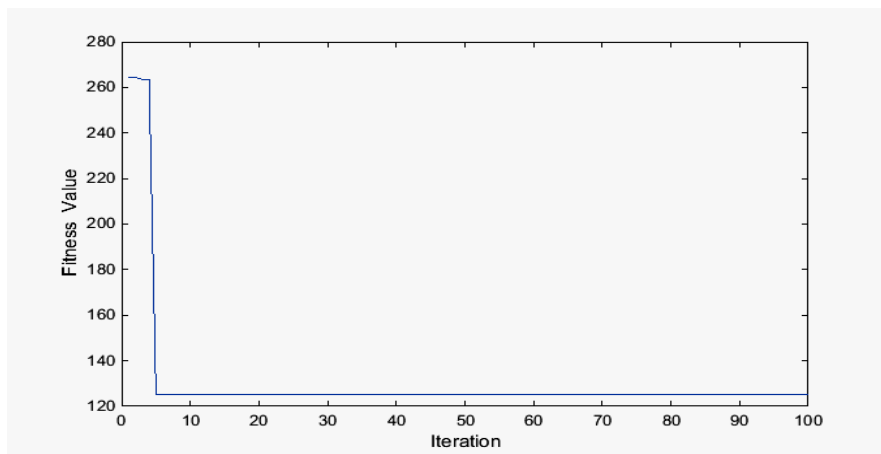


Fig.34: Convergence characteristics using Particle Swarm Optimization(PSO)

7.7.3 WSCC 3 Machine 9 bus case :

Table 22 : Comparative study with GA and PSO(WSCC 3 Machine 9 bus)

Attributes	GA	PSO	TLBO
Number of iterations to converge	21	19	15
Average time per iteration(Sec) taken	0.00626	0.00833	0.00404
Total time taken to converge (CPU elapsed time)(sec)	0.13138	0.15822	0.0606

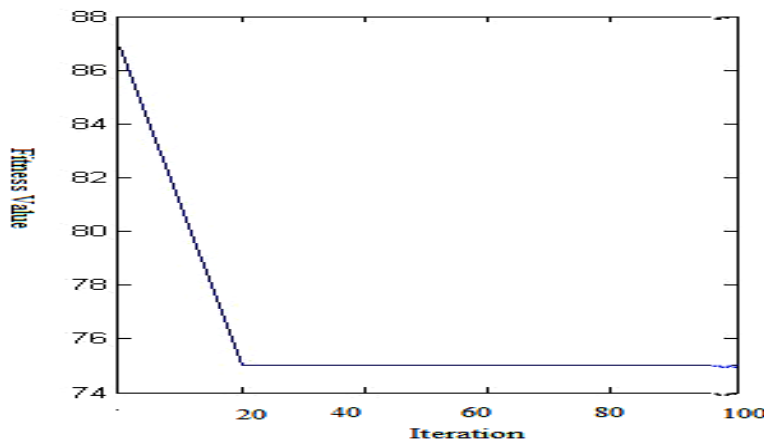


Fig.35: Convergence curve using Genetic Algorithm(GA)

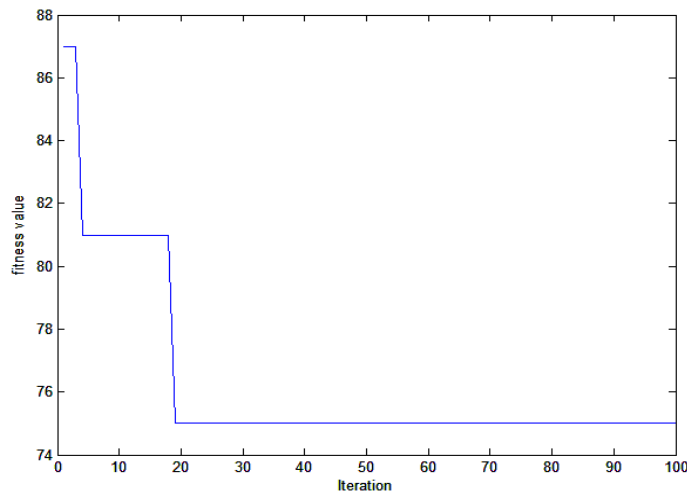


Fig.36: Convergence curve using Particle Swarm Optimization(PSO)

7.7.4 IEEE 14 bus case :

Table 23. Comparative Study with GA and PSO

Attributes	TLBO	GA	PSO
Number of iterations to converge	12	10	34
Average time per iteration(Sec) taken	0.0078	0.0139	0.0054
Total time taken to converge (CPU elapsed time)(sec)	0.0936	0.139	0.1836

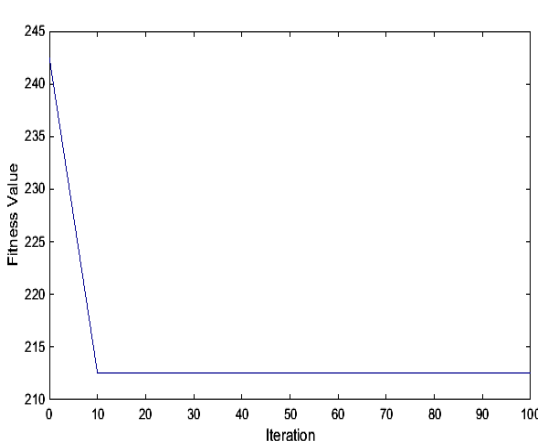


Fig.37. Convergence curve using GA

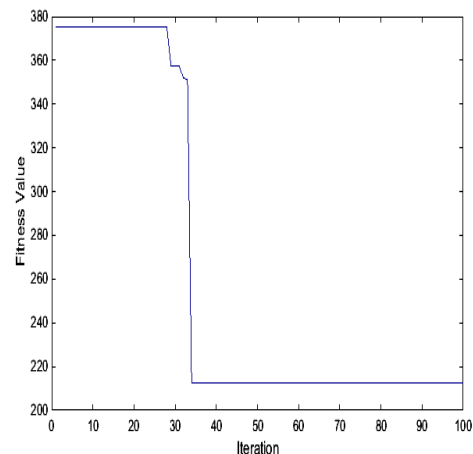


Fig.38. Convergence curve using PSO

7.7.5 IEEE 30 bus case :

Table 24 : Comparative study with GA and PSO(IEEE 30 bus)

Attributes	TLBO	GA	PSO
Number of iterations to converge	20	20	19
Average time per iteration(Sec) taken	0.0138	0.0144	0.016
Total time taken to converge (CPU elapsed time)(sec)	0.276	0.288	0.304

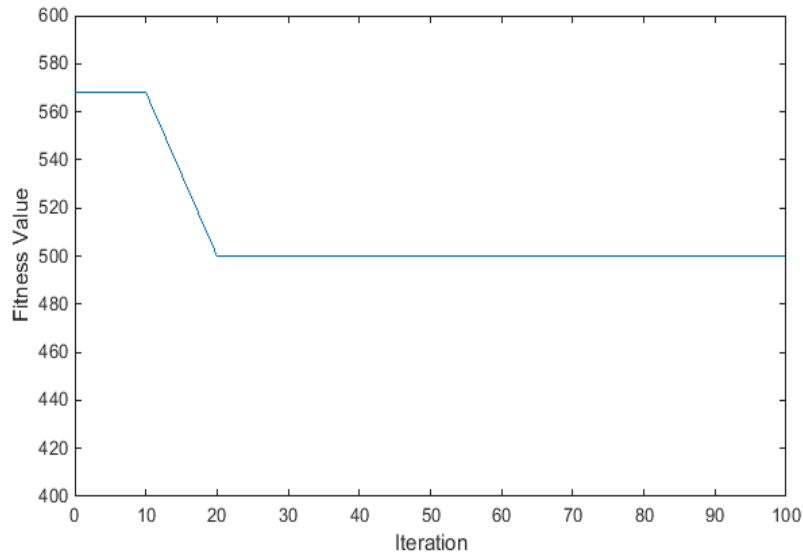


Fig 39: Convergence characteristics using GA(IEEE 30 bus)

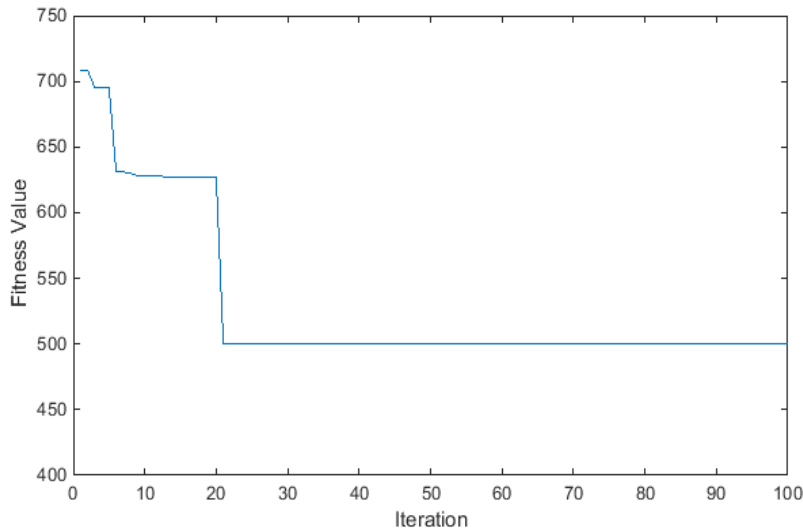


Fig 40: Convergence characteristics using PSO(IEEE 30 bus)

7.8 Discussions

7.8.1 *Minimization of the number of relays*

The complexity of the co-ordination problem increases in multiple loop system which share some relays. Hence we have to find one common acceptable setting for relays , which share multiple loops, so, that their co-ordination in individual loops is achievable. The number of

such relays should be kept to minimum, so that we make minimum assumptions on relay settings in co-ordination of loops. Such relays are called minimum break point relays. There can be multiple choices to minimum break point relays [116]-[121]. In this subsection we will concentrate on computation of minimum break point set of relays based on critical element finding and network graph theory.

7.8.1.1 Procedure

For obtaining minimum break point set of relays, we follow a technique, which is the combination of simulation and by using network graph theory. The procedure is as follows:

7.8.1.1.1 Finding critical element of the network

Critical elements are such elements of a network(bus , transmission line), which if removed , the complete network will be suffering from blackout. Specially in case of big systems, its effect is huge. Such critical elements should be always protected by relays. The critical elements obtained from power world simulation are as follows for the used test systems in the work. Table 25 shows critical elements of different test systems used here.

Table 25 : Critical Elements of Network

Test system	Critical buses	Critical lines
IEEE 5 bus	-	-
6 bus	-	-
WSCC 3 Machine 9 bus	-	-
IEEE 14-bus	2	1-2
IEEE 30-bus	2,6	1-2

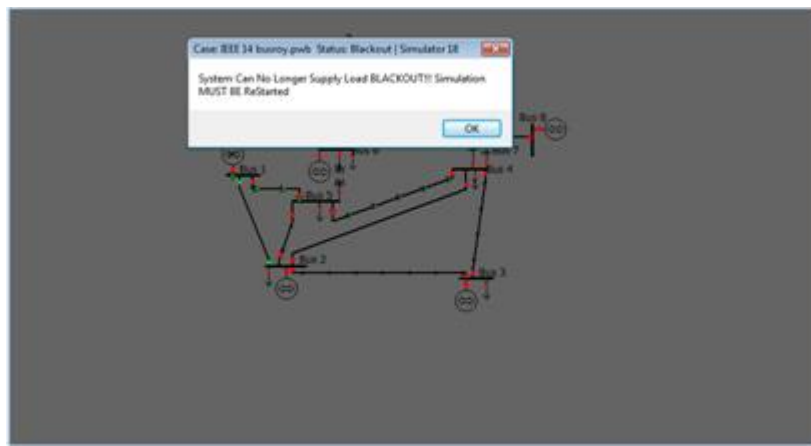


Fig 41: Power World Simulation of IEEE 14 bus system when critical line 1-2 is under contingency

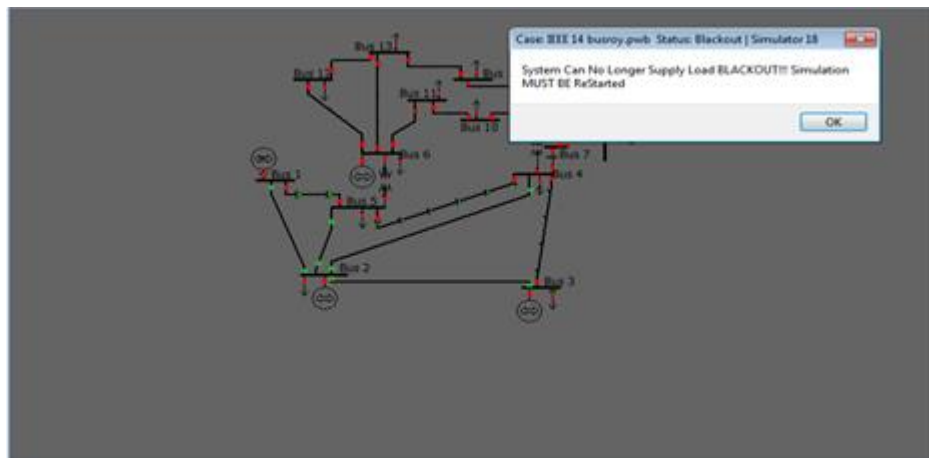


Fig 42 : Power World Simulation of IEEE 14 bus system when critical bus 2 is under contingency

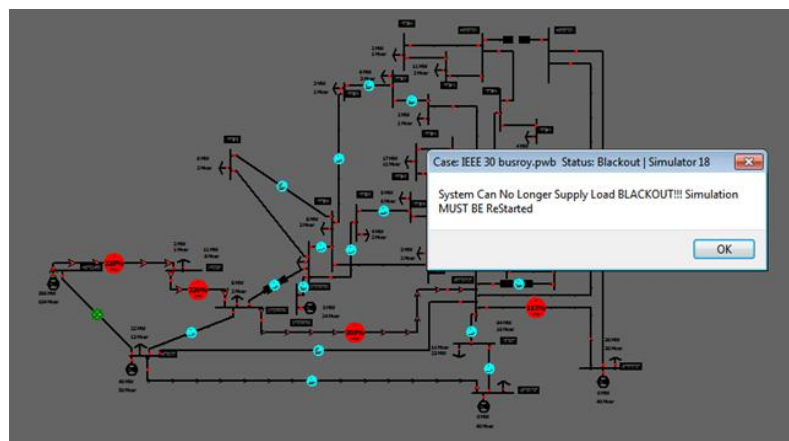


Fig 43 : Power World Simulation of IEEE 30-bus when critical line 1-2 is under contingency

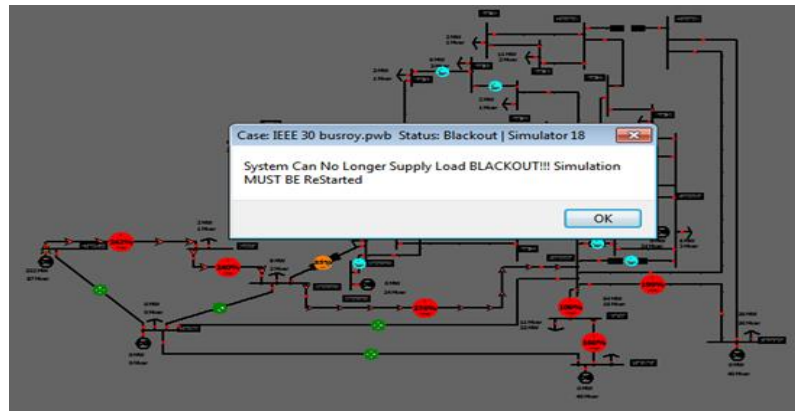


Fig 44 : Power World Simulation of IEEE 30-bus when critical bus 2 is under contingency

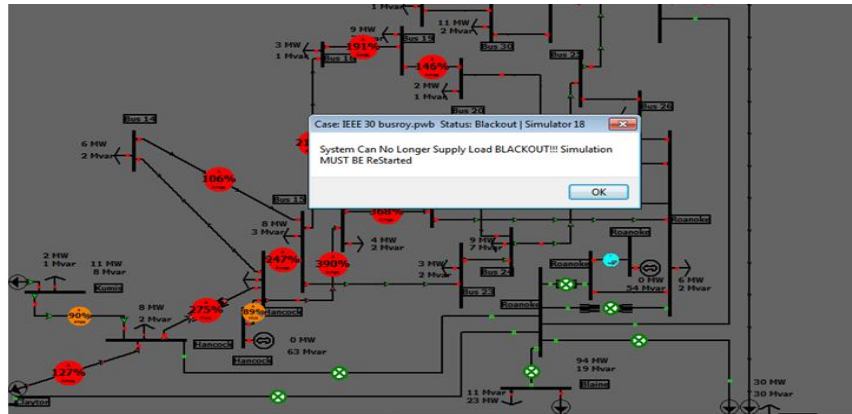


Fig 45 : Power World Simulation of IEEE 30-bus when critical bus 6 is under contingency

Fig 41 to Fig 45 shows the simulation when the critical elements of IEEE 30 bus system are under contingency.

7.8.1.1.2 Apply Network Graph Theory

For rest of the network, the Minimum break point set relays can be determined from LU factorization of reduced and permuted incidence matrix. L-matrix indicates minimum break point sets [116]. Table 26 , shows the minimum break point set obtained for the test systems. Here one thing is needed to be mentioned that ,a network may have multiple minimum break point set solutions. Here we have shown just one possible solution for minimum break point set. The procedure of finding MBPS after securing critical elements of a network safe is as follows :

- Form incidence matrix.

- ii)Reduced and permuted incidence matrix.
- iii)Decompose it into LU factorization. [116]
- iv)Determine MBPS with L

Table 26 : Minimum break point set of the network

IEEE Test system	Minimum break point set Relay no. (R_i)
IEEE 5 bus	2,3,6,7,9,12,14
IEEE 14 bus	1,2,4,5,7,9,13,15,18,20,29
IEEE 30 bus	1,6,8,9,11,12,14,17,19,23,27,37, 39,41,46,49,52,59,64,65,67

7.9 Summary

This chapter focused on optimal coordination of directional and over current relays. The problem statement and various constraints to be satisfied are already presented in the chapter. Teaching learning based optimization (TLBO), which is a modern meta-heuristic technique is applied to solve the problem. The optimum time of operation, TSM, pick up currents of relays are calculated for an IEEE 5 bus system and IEEE 30 bus system. All the constraints are found within desirable range. Which intelligent over current characteristics are required to get the desired result are also selected. Coordination time interval is taken 0.25 sec for each cases. The protection settings seems to be satisfactory for the discussed power networks as they are performing better compare to contemporary other meta-heuristic techniques like GA and PSO. Iteration time increases with the system size increases , although the number of iterations for convergence remains more or less the same irrespective of the size of the system. As an extension of this relay coordination work, a relay number minimization technique is introduced based on finding critical element of the network and network graph theory in the later part of this chapter.

Chapter 8

Conclusions and Scope for Future work

Chapter 8

Conclusions and Scope for Future work

Protection of power system is an important aspect for reliable and smooth operation of power network. If proper protection arrangements are not provided, the whole power network can even suffer complete black out. Black out will cause inconvenience and huge financial losses. So, the several issues related to power system protection should be studied thoroughly to ensure security of the power network. Among the several important issues of protection of power system the following issues are very much important:

Power system fault analysis, distance relaying, back up protection, Optimal FACTs devices placement , relay coordination etc. These all aspects are essential to keep power system in healthy state and continue uninterrupted power supply to the network. From the literature survey reported that in spite of the global improvement of technology, modern power system still lacks efficient distance protection scheme, advanced back up protection scheme sustainable to even in case of simultaneous faults exists in the system, advanced FACTs placement technique, improved relay coordination technique etc aspects. In view of the above context, this thesis presents research work on several issues of power system protection. This thesis work has made an effort to develop an improved and reliable wide area protection system which fulfils all the aspects for reliable operation. The thesis work is summarized in section 8.1 as follows.

8.1 Conclusions

Thesis introductory part, importance and its organization are discussed in Chapter-1. Chapter 2 reviews various problems faced by power systems due to weak voltage profiles and also the solution for a better, reliable power supply in wide area power systems is tried to be achieved.

Chapter 3 proposes a faulty phase detection algorithm based on correlation coefficient computing method which enhances the performances of the distance relay. Then a polar plot of impedance based analysis is suggested to know the system fault details and fault direction. The

work is extended further considering the application of the methodology during communication failure and performance during transient conditions of PMUs.

Chapter 4 suggests a synchrophasor measurement based fault locator which is capable of locating fault, classification of fault and faulty phase detection and compared with previous methods used for improved accuracy. The methodology is tested on a two terminal transmission line.

Chapter 5 presents an efficient and improved back up protection scheme which is capable to support during simultaneous fault conditions also. The scheme utilizes angle information between voltages and currents and sequence voltage data to identify the bus nearest to the fault and faulted line. The technique is implemented on a WSCC 3 Machine 9 bus system and an IEEE 14 bus test system. In addition to that the number of PMUs utilized is restricted which definitely helps the economy of implementing the method. The PMU number minimization is suggested via utilizing a linear programming technique and the results are presented there.

Chapter 6 presents an optimal placement technique of TCSC and TCPAR. The technique is observed with various contingency combinations. After placement of the TCSC or TCPAR in the desired location, if any line overloading is taken place in current flow, then how to tackle the situation is presented there. The work is further extended to check the impact of changes in generation and changes in angle shift in bus angles.

Chapter 7 presents an intelligent overcurrent and distance relays coordination technique by using TLBO and intelligent over current relay characteristics which is proved to be fastest with respect to CPU elapsed time rather than the other contemporary techniques like GA and PSO. The work is further extended by suggesting a relay minimization technique by using critical elements of the network and network graph theory. The process is tested by utilizing several test systems from small to big.

8.2 Scope for Future Work

Any research never ends without leaving open window for further research, hence the thesis work incite with the scope for further research on following issues;

- FACTs placement can be carried out in the presence of distributed energy sources and renewable energy with different penetrating level.

- Relay coordination can be carried out for higher test systems and effect of series compensation can be monitored in the TSM values, PS values and other settings.
- All the discussed issues can be done on higher test systems and preferably on practical test systems (e.g-NRPG, SRPG, INDIAN GRID etc.).
- Relay coordination can be done by using Jaya algorithm which is more recent than TLBO and compare the results.
- Filtering of signals can be further improved to get more accurate results in case of fault detection techniques.
- The distance relay scheme used has impedance method for fault location in long transmission lines. The series compensation is bound to create serious problems with the fault location as it will change the impedance of transmission line. Using numerical distance relay with impulse type fault location and synchrophasor is desirable in future. This may be an interesting topic of research in future to explore further.
- The segregation of simultaneous existence of balanced and unbalanced faults in the same line may be another aspect of future work.
- Relay coordination considering the effects of discrimination time may be another future scope of this thesis work.
- Finally hardware or prototype implementation of all the techniques may be another aspect of the future work, which will enable the practical implementation of this work in real life.

References

- [1] MK Jena , S R Samantaray and B K Panigrahi," A New Wide- Area Backup Protection Scheme for Series-Compensated Transmission System", *IEEE Systems Journal*, Issue 99,August,2015.
- [2] P K Nayek ,A K Pradhan and P Bajpai," Wide-Area Measurement- Based Backup Protection for Power Network with Series Compensation", *IEEE Transactions on Power Delivery* , Vol.29, No. 4 ,pp.1970-1977,Aug 2014
- [3] J.D. Ree, V. Centeno, J.S. Thorp, and A.G. Phadke, "Synchronized phasor measurement applications in Power systems, "IEEE Transactions on Smart Grid, Vol.1, No.1, pp.20–27, June 2010
- [4] J.M.Tripathi, Adhishree , Ram Krishan , Optimal coordination of overcurrent relays using gravitational search algorithm with DG penetration, Presented in *6th IEEE Power India International Conference*,5-7 December, Delhi, India, 2014.
- [5] P Jena and A.K.Pradhan," Directional Relaying During Single-Pole Tripping Using Phase Change in Negative- Sequence Current", *IEEE Transactions on Power Delivery* , Vol.28 ,No.3, July 2013
- [6] P Jena and AK Pradhan , "Directional Relaying in the Presence of a Thyristor-Controlled Series Capacitor", *IEEE Transactions on Power Delivery*,Vol.28 ,No. 2 ,April 2013
- [7] S R Samantaray , "A Data- Mining Model for Protection of FACTS-Based Transmission Line", *IEEE Transactions on Power Delivery* ,Vol.28, No.2 ,April 2013.
- [8] Pratim Kundu, Ashok Kumar Pradhan , "Wide area measurement based protection support during power swing", *Electrical Power and Energy Systems* ,63 (2014) 546–554
- [9] Z Moravej, J D Ashkezari and M Pazoki , "An effective combined method for symmetrical faults identification during power swing", *Electrical Power and Energy Systems* ,64(2015)24-34.
- [10]J Khodaparast and M Khederzadeh , "Three Phase Fault Detection During Power Swing by Transient Monitor ", *IEEE Transaction on Power System* , Vol.30 ,No.5 ,Sept. 2015
- [11] R.M.Chabanloo et. al., "Optimal Combined Over Current and Distance Relays Coordination Incorporating Intelligent Over Current Relay Characteristics Selection ",*IEEE Transactions on Power Delivery*, Vol.26, No. 3,pp.1381-1391, July,2011.
- [12]V Terzija , Z M.Radojevic and G Preston , "Flexible Synchronized Measurement Technology-Based Fault Locator", *IEEE Transactions on Smart Grid*,Vol.6 ,Issue 2 , pp. 866-873,March 2015.
- [13] P.K Nayak, A.K Pradhan, and P. Bajpai, "A Fault Detection Technique for the Series-Compensated Line During Power Swing", *IEEE Transactions on Power Delivery*, vol. 28,no. 2, April 2013,pp.714-722.
- [14] Ali.H.Al Mohammed, M.A. Abido, "A Fully Adaptive PMU-Based Fault Location Algorithm for Series compensated Lines", *IEEE Transactions on Power Systems*, Vol.29, No.5, September 2014, pp.2129-2137.

[15] A.G. Phadke and J.S. Thorp, *Synchronized Phasor Measurements and Their Applications*. New York: Springer, 2008

[16] Rao R.S and Rao V.S ,”Comparison of Various Methods for Optimal Placement of FACTs devices”, *IEEE International Conference on Smart Electric Grid, Guntur , India ,2014.*

[17] D.V.Shiv Sharma et al.,” A wide area prospective on power system protection : A State-of-art”, Presented in *IEEE International Conference on Energy, Power and Environment Towards Sustainable Growth*, 12-13 June,2015, NIT Meghalaya

[18] M.Lohith et. al.,” A novel approach for transmission line fault location using synchrophasor measurement”, Presented in *IEEE International Conference on Energy, Power and Environment Towards Sustainable Growth*, 12-13 June,2015, NIT Meghalaya.

[19] Y.Atlas et al. ,” Adaptive protection scheme for a distribution system considering grid-connected and islanding modes of operation”, *Energies* , Vol.9 ,Issue 5 ,article no. 378 , doi:[10.3390/en9050378](https://doi.org/10.3390/en9050378)

[20] L.Huchel, H.H.Zeineldin and E.F.E Saadany ,” Protection coordination index enhancement considering multiple DG locations using FCL “, *IEEE Transactions on Power Delivery* , Vol.32, No.1 ,pp. 344-350 , February 2017

[21]Tirath Pal S.Bains and Mohammad R.Dadash Zadeh,” Challenges and recommendations for fault location in series compensated transmission lines”, *PES General Meeting*, National Harbor, MD, USA,27-31 July ,2014.

[22]Altuve H.J, Joseph B.M and Alexander G.E,” Advances in series -compensated line protection “, *63rd Annual conference for protective relay Engineers*, Atlanta ,Georgia, April 22-24,2009.

[23] M.Ojaghi and R.Ghahremani,” Piece–wise linear characteristic for coordinating numerical overcurrent relays”, *IEEE Transactions on Power Delivery*, Vol.32,No.1,pp.145-151, February 2017.

[24]Vahedipour Z and Daneshian B,” On the solution of ill-conditioned systems of linear equations ” ,*Journal of Expert Systems* , Vol. 2 , No.1,pp 119-122,2013.

[25] Vanishree J and Ramesh V,” Voltage profile improvement in power system – a review “, *IEEE International conference on Advances in Electrical Engineering (ICAEE)*, 9-11 Jan ,2014,Vellore.

[26]Vyas B ,Maheswari R.P and Das B ,” Protection of series compensated transmission line : Issues and state of art “, *Electric Power System Research* , Vol.107,pp 93-108, February,2014

[27]J. Izykowski, E. Rosolowski, P.balcerek, M.Fulczyk and M. M. Saha,” Accurate non iterative fault location algorithm utilising two-end unsynchronized measurements”, *IEEE Transactions on Power Delivery*, vol. 26, no. 2 ,pp547-555, Apr. 2011.

[28] J. Izykowski, E. Rosolowski, P. Balcerk, M. Fulczyk, M.M. Saha, “Fault location on double-circuit series-compensated lines using two-end unsynchronized measurements,” *IEEE Transactions on Power Delivery*, vol. 26, no. 4, pp. 2072-2080, Oct. 2011.

[29] R. Rubeena, M.R. D. Zadeh, T.P.S. Bains, "An Accurate Offline Phasor Estimation for Fault Location in Series Compensated Lines," *IEEE Transactions on Power Delivery*, Vol.29,Issue:2, April 2014.

[30]C. W. Liu, K. P. Lien, C. S. Chen, and J. A. Jiang, "A universal fault location technique for -terminal transmission lines", *IEEE Tranactions on Power Delivery* , vol. 23, no. 3, pp. 1366–1373, Jul. 2008.

[31] Tajudeen H. Sikiru, Adisa A. Jimoh, Yskandar Hamam, John T. Agee and Roger Ceschi, " Voltage profile improvement based on network structural characteristics", *IEEE Transactions on Power Systems*, 2012.

[32] Tagare D.M ,”Reactive Power Management “, *Tata McGraw-Hill Publishing Company Limited* , India ,2007.

[33] Wadhwa C.L ,”Electrical Power Systems”, *New Age International Publishers*,India, 1983.

[34] Kothari D.P and Nagrath I.J ,” *Modern Power System Analysis* “,Tata Mc-Graw Hill , India,2003.

[35] Tajudeen H. Sikiru , Adisa A. Jimoh, John T. Agee,” Inherent structural characteristic indices of power system networks”, *Electrical Power and Energy Systems*, vol. 47, pp.218–224, December 2013.

[36]Vahedipour Z and Daneshian B,” On the solution of ill-conditioned systems of linear equations ” , *Journal of Expert Systems* , Vol. 2 , No.1,pp 119-122,2013.

[37] Grainger J.J and Stevenson W.D ,”Power System Analysis “, *Mc-Graw Hill* , U.S.A,1994

[38] Gupta J.B ,”A Course in Power Systems “,11th edition ,*Katson Books* ,India,2011 .

[39] Trad o., Ratta G., and Torres M., "Experiences in Setting Protection of Series Capacitor Compensated Lines," *Proceedings of the International Conference on Power System Transients (IPST'01)*, pp. 1-6, June 2001.

[40] Roy S ,Babu P.S,” Power swing protection of series compensated transmission line with novel fault detection technique “, *IEEE International Conference on Green Computing, Communication and Electrical Engineering [ICGCCEE]*. 2014, 6–8 March, Coimbatore.

[41] Pal T , Bains S and Zadeh M.R.D,” Enhanced Phasor Estimation Technique for Fault Location in Series-Compensated Lines”, *IEEE Transactions on Power Delivery* ,Vol.30,No.4,pp. 2058-2060,August 2015 .

[42] M. Djuric, Z. Radojevic, and V. Terzija, Distance protection and fault location utilizing only phase current phasors, *IEEE Transactions on Power Delivery* , vol. 13, no. 4, pp. 1020–1026, Oct. 1998.

[43] L.Huchel and H.H.Zeineldin, “Planning the coordination of directional overcurrent relays for distribution systems considering DG”, *IEEE Transactions on Smart Grid* , Vol. 7 , No. 3, pp.1642-1649, May 2016.

[44] A. T. Johns and S. Jamali, Accurate fault location technique for power transmission lines, *Proceedings of Instrumentation. Electrical Engineering , Generation., Transmission. Distribution.*, vol.137, no. 6, pp. 395–402, Nov. 1990.

[45] *IEEE Guide for Determining Fault Location on AC Transmission and Distribution Lines*, IEEE Standard C37.114TM-2004, 2005.

[46] R. K. Aggarwal, D. V. Coury, A. T. Johns, and A. Kalam, A practical approach to accurate fault location on extra high voltage teed feeders, *IEEE Transactions on Power Delivery.*, vol. 8, no. 3, pp. 874–883 Jul.1993.

[47] C. W. Liu, K. P. Lien, C. S. Chen, and J. A. Jiang, A universal fault location technique for -terminal ($N \geq 3$) transmission lines, *IEEE Tranactions on Power Delivery* , vol. 23, no. 3, pp. 1366–1373, Jul. 2008.

[48] M. Korkali, H. Lev-Ari, and A. Abur, “Traveling-wave-based fault location technique for transmission grids via wide-area synchronized voltage measurements”, *IEEE Transactions on Power Systems* , vol. 27, no. 2, pp. 1003–1011, May 2012.

[49] M. Korkali and A. Abur, “Optimal deployment of wide-area synchronized measurements for fault-location observability”, *IEEE Transactions on Power Systems* , vol. 28, no. 1, pp. 482–489, Feb. 2013.

[50] A. Gopalakrishnan, D. Hamai, M. Kezunovic, and S. McKenna, “Fault location using the distributed parameter transmission line model”, *IEEE Transactions on Power Delivery* , vol. 15, no. 4, pp. 1169–1174, Oct. 2000.

[51] D. Novosel, D. G. Hart, E. Udren, and J. Garity, “Unsynchronized two terminal fault location estimation”, *IEEE Transactions on Power Delivery* , vol. 11, no. 1, pp. 130–138, Jan. 1996.

[52] L. Ji, C. Booth, A. Dysko, F. Kawano, and G. Baber, “Improving fault location by analysis of electric parameters during circuit breaker operation”, presented at the 17th Power System Computation Conference , Stockholm, Sweden, 2011.

[53] S. Tamronglak, S. Horowitz, A. Phadke, and J. Thorp, “Anatomy of power system blackouts: Preventive relaying strategies”, *IEEE Transactions on Power Delivery* , vol. 11, no. 2, pp. 708–715, Apr. 1996.

[54] C.-S. Yu, C.-W. Liu, S.-L. Yu, and J.-A. Jiang, “A new PMU-based fault location algorithm for series compensated lines”, *IEEE Transactions on Power Delivery*, vol. 17, no. 1, pp. 33–46, Jan. 2002.

[55] A. Girgis, D. Hart, and W. Peterson, “A new fault location technique for two- and three-terminal lines”, *IEEE Transactions on Power Delivery* , vol. 7, no. 1, pp. 98–107, Jan. 1992.

[56] Y. Liao and S. Elangovan, “Unsynchronized two-terminal transmission line fault-location without using line parameters”, *IEEE Proceedings of Generation Transmission and Distribution.*, vol. 153, no. 6, pp. 639–643, Nov. 2006.

[57] Y. Liao, “Transmission line fault location algorithms without requiring line parameters”, *Electrical Power Components and Systems* , vol. 36, no. 11, pp. 1218–1225, Nov. 2008.

[58] Y. Liao and N. Kang, “Fault-location algorithms without utilizing line parameters based on the distributed parameter line model”, *IEEE Transactions on Power Delivery* , vol. 24, no. 2, pp. 579–584, Apr. 2009.

[59] S.N.Muneswar, R.Hasabe, D.Shelar, P.Kose, “A new adaptive PMU based protection scheme for interconnected transmission network system”, *2014 International Conference on Circuit, Power and Computing Technologies [ICCPCT]*, 20-21 March 2014 ;Nagercoil, India, IEEE, pp.179- 183.

[60] S.Gajare and A.K.Pradhan , “An accurate fault location method for multi-circuit series compensated transmission lines” , *IEEE Transactions on Power Systems* , vol. 32 , no.1 , pp 572-580 , Jan. 2017 .

[61] G.Feng and A.Abur ,” Fault location using wide area measurements and sparse estimation”, *IEEE Transactions on Power Systems* , vol.31 , no.4 ,pp.2938-2945 , July 2016 .

[62] S.Azizi , M.S.Pasand and M.Paolone , Locating faults on untransposed , meshed transmission networks using a limited number of synchrophasor measurements , *IEEE Transactions on Power Systems* , vol.31 ,no. 6 ,pp.4462-4472 , Nov. 2016.

[63] P.K.Nayek, A.K.Pradhan and P.Bajpai , “A three terminal line protection scheme immune to power swing” , *IEEE Transactions on Power Delivery*, vol.31, no.3 ,pp.999-1006 , June 2016 .

[64] S.A.Lavand and S.A.Soman , “Predictive analytic to supervisory zone1 of distance relay using synchrophasors” , *IEEE Transactions on Power Delivery* , vol.31 ,no.4 ,pp.1844-1854 , Aug. 2016 .

[65] J. Ma , C.Liu and J.S.Thorp , “A wide-area backup protection algorithm based on distance protection fitting factor” , *IEEE Transactions on Power Delivery* , vol.31 ,no.5 ,pp.2196-2205 , Oct. 2016.

[66] J. Ma , X.Yan,B.Fan ,C.Liu and J.S.Thorp , “A novel protection scheme for a single-phase-to-ground fault based on voltage phase comparison” , *IEEE Transactions on Power Delivery* , vol.31 ,no.5 ,pp.2018-2027 ,Oct. 2016.

[67] S.Horowitz and A. G.Phadke, “Third zone revisited”, *IEEE Transactions on Power Delivery* , vol. 21, no. 1, pp. 23–29, Jan.2006.

[68] J. D. Ree,V. Centeno,J. S. Thorp, and A. G. Phadke, “Synchronized phasor measurement applications in Power systems,” *IEEE Transactions on Smart Grid*, vol. 1, no. 1, pp. 20–27, June 2010.

[69] A. G. Phadke and J. S. Thorp, ” Synchronized Phasor Measurements and Their Applications”, New York: *Springer*, 2008.

[70]S.N.Muneswar, R.Hasabe, D.Shelar, P.Kose, “ A New Adaptive PMU based Protection Scheme for Interconnected Transmission Network System”, *International conference on Circuit , Power and Computing Technologies*, 2014.

[71] M. M. Eissa, M. E. Masoud, and M.M.M. Elanwar, “A novel backup wide area protection technique for power transmission grids using phasor measurement unit,” *IEEE Transactions on Power Delivery*, vol. 25, no. 1, pp. 270–278 , Jan. 2010.

[72] P. V. Navalkar and S. A. Soman, “Secure remote backup protection of transmission lines using synchrophasors”, *IEEE Transactions on Power Delivery*, vol. 26, no. 1, pp. 87–96, Jan. 2011.

[73] H. Lin, S. Sambamoorthy, S. Shukla, J. Thorp, and L Mili, “Ad-hoc vs. supervisory wide area backup relay protection validated on power/network co-simulation platform,” presented at the *17th Power System Computation Conference*, Stockholm, Sweden, Aug. 22–26, 2011.

[74] J. Ma, J. Li, J. S. Thorp, A. J. Arana, Q. Yang, and A. G. Phadke, “A fault steady state component-based wide area backup protection algorithm,” *IEEE Transactions on Smart Grid*, vol. 2, no. 3, pp. 468–475, Sep. 2011.

[75] Z. He, Z. Zhang, W. Chen, O. P. Malik, and X. Yin, “Wide-area backup protection algorithm based on fault component voltage distribution,” *IEEE Transactions on Power Delivery*, vol. 26, no. 4, pp. 2752–2760, Oct. 2011.

[76] B. Kasztenny, “Distance protection of series-compensated lines problems and solutions,” presented at the *28th Annual Western Protection Relay Conference*, Spokane, WA, USA, Oct. 22–25, 2001.

[77] D. Novosel, A. G. Phadke, M.M. Saha, and S. Lindahl, “Problems and solutions for microprocessor protection of series compensated lines”, In *Proceedings of Conference on Development on Power System. Protection.*, 1997, pp. 18–23.

[78] W. Rebizant, J. Szafran and A. Wiszniewski, Digital signal processing in power system protection and control, *Springer*, Poland, 2011.

[79] T. Routtenberg, Yao Xie, R.M. Willett, Lang Tong, “PMU Based Detection of Imbalance in Three-Phase Power Systems”, *IEEE Transactions on Power Systems*, Vol.30, no.4, July 2015, pp.1966-1976.

[80] Ali.H.Al Mohammed, M.A. Abido, “A Fully Adaptive PMU Based Fault Location Algorithm for Series compensated Lines”, *IEEE Transactions on Power Systems*, Vol.29, no.5, September 2014, pp.2129-2137.

[81] I. Kamwa, S.R. Samantaray, G. Joos, “Wide Frequency Range Adaptive Phasor and Frequency PMU Algorithms”, *IEEE Transactions on Smart Grid*, Vol.5, no.2, March 2014, pp.569-579.

[82] P. Kundu, A.K. Pradhan, “Online identification of protection element failure using wide area measurements”, *IET Generation, Transmission and Distribution*, 2015, Vol.9, Issue 2, pp. 115-123.

[83] Emily R Fernandes et al., “Application of a phasor-only state estimator to a large power system using real pmu data”, *IEEE Transactions on Power System*, Vol.32, No.1, January 2017, pp.411-420.

[84] David A.K and Singh S.N, “Congestion Management by Optimizing FACTS Device Location”, *Proceedings of International conference on EUDRPE*, London, 4-7 April, 2000, pp.23-28.

[85] Singh S.N, “Location of FACTS devices for enhancing power systems security”, *The Conference on LESCOPE*, Canada, pp.162-166, July 11-13, 2001.

[86]Chanan S, Kumar A and Parida S ,”Combined Optimal Location of FACTs Controllers and Loadability Enhancement in Competitive Electricity Markets”, *Proceedings of IEEE PES Summer Meeting* , San Francisco, 12-16 June, 2005.

[87] Sundar K.S and Ravi Kumar H.M,” Enhancement of power system performance using TCSC”, *Power System Technology and IEEE Power India Conference* ,2008. POWERCON 2008,pp.12-15

[88] Shaheen H.I, Rashed and Cheng D.H.J ,”Evolutionary optimization techniques for optimal location and parameter setting of TCSC under single line contingency”, *Power and Energy Society General Meeting-Conversion and delivery of Electrical Energy in the 21st Century* ,IEEE. ,July 2008 .pp. 20-24

[89] Rao R.S and Rao V.S,” A generalized approach for determination of optimal location and performance analysis of FACTs devices”, *Electric Power and Energy Systems* , Vol.73,pp.711-724,2015.

[90] Srivastava S.C, Singh S.N and Singh J.G ,” Placement of FACTS Controllers for Enhancing Power System Loadability”, *IEEE Power India Conference* , New Delhi, 2006.

[91]Ghahremani E and Kamwa I ,” Optimal Placement of Multiple-type FACTs Devices to Maximize Power System Loadability using a Generic Graphical User Interface”, *IEEE Transactions on Power Systems* , Vol. 28, No.2 ,pp.764-778, May 2013.

[92]XiaS, Chan K.W , Bai X and Guo Z,” Enhanced Particle Swarm Optimization applied for Transient Angle and Voltage Constrained Discrete Optimal Power Flow with Flexible AC Transmission System”, *IET Generation , Transmission , Distribution* , Vol.9 ,No.1 ,pp.61-74,2015 .

[93]Sheth A, Kotwal C.D and Pujara S,” *Optimal Placement of TCSC for Improvement of Static Voltage Stability* ,” *NUICONE* , 5th Nirma University International Conference on Engineering, Nov.2015.

[94] Ziae O and Choobineh F ,” Optimal Location Allocation of TCSC Devices on a Transmission Network “, *IEEE Transactions on Power Systems* , Vol.32 ,No.1,pp.94-102, January 2017.

[95] Ara A.L, Kazemi A and Niaki S,” Multi-Objective Optimal Location of FACTs Shunt-Series Controllers for Power System Operation Planning “, *IEEE Transactions on Power Delivery* , Vol.27 ,No.2 , pp. 481-490, Apr. 2012.

[96]Ziae O and Choobineh F ,” Thyristor-Controlled Switched Capacitor Placement in Large Scale Power Systems via Mixed-interger linear Programming and Taylor Series Expansion “, *Proceedings of PES General Meeting Conference Exposition*, July 2014.

[97] Khan I , Mallick M.A , Rafi M and Mirza M.S ,” Optimal Placement of FACTs Controller Scheme for Enhancement of Power System Security in Indian Scenario “ , *Journal of Electrical Systems and Information Technology* , Vol.2 , Issue 2 ,pp. 161-171 , Sept. 2015.

[98] Farivar M and Low S ,”Branch Flow Model Relaxations and Convexification : Part-I”, *IEEE Transactions on Power System*,Vol.28 , No. 3,pp.2554-2564 ,Aug. 2013.

[99] L. G. Perez, R. Nadira, and A. J. Urdaneta, "Optimal coordination of directional overcurrent relays in interconnected power system" *IEEE Transactions on Power Delivery*, Vol. 3, No 3, Jul.1998

[100] A. J. Urdaneta, H. Restero, J. Sanchez, and J. Fajardo, "Coordination of directional overcurrent relays timing using linear programming," *IEEE Transactions on Power Delivery*, vol. 11, no. 1, pp. 122–129, Jan. 1996

[101] B. Chattpadhyay, M. S. Sachdev, and T. S. Sidhu, "An on-line relay coordination algorithm for adaptive protection using linear programming techniques," *IEEE Transactions on Power Delivery*, vol. 11, no. 1, pp. 165–173, Jan. 1996.

[102] H. Askarian Abyaneh and R. Keyhani, "Optimal co-ordination of overcurrent relays in power system by dual simplex method," presented at the *AUPEC Conference*, Perth, Australia, 1995

[103] C. W. So, K. K. Li, K. T. Lai, and K. Y. Fung, "Application of genetic algorithm for overcurrent relay coordination," in *Proceedings of Instrumentation Electrical Engineering Conference Developments in Power System Protection*, Mar. 25–27, 1997, pp. 66–69.

[104] H. Zeineldin, E. El-Saadany, and M. A. Salama, "Optimal coordination of overcurrent relays using a modified particle swarm optimization," *Electric Power System Research.*, vol. 76, no. 11, Jul. 2006.

[105] C. W. So and K. K. Li, "Time coordination method for power system protection by evolutionary algorithm," *IEEE Transactions on Industrial Applications*, vol. 36, no. 5, pp. 1235–1240, Sep./Oct. 2000.

[106] F. Razavi, H. Askarian Abyaneh, M. Al-Dabbagh, R. Mohammadi, and H. Torkaman, "A new comprehensive genetic algorithm method for overcurrent relays coordination," *Electric Power System Research.*, vol. 92, no. 9, Apr. 2008.

[107] J.Sadeh, V.Aminotojari and M.Bashir , " Optimal coordination of over current and distance relays with hybrid genetic algorithm", in proceedings of *10th International conference on Environment and Electrical Engineering*, IEEE,Rome, Italy,8-11 May,2011.

[108] M.Singh, B.K.Panigrahi and A.R.Ahyankar , " optimal coordination of directional over-current relays using teaching learning-based optimization (TLBO) algorithm ", *Electrical Power and Energy Systems*, Vol.50,pp.33-41, March 2013.

[109] A.A.Kalage and N.D.Ghawghawe , " Optimum coordination of directional overcurrent relays using modified adaptive teaching learning based optimization algorithm", *Intelligent Industrial System*, Vol.2, Issue 1,pp.55-71, March 2016.

[110] D.Saha , A.Dutta , B.K.Saha Roy and P.Das," Optimal coordination of DOCR in interconnected power systems", Presented in *IEEE 2nd International Conference on Control, Instrumentation, Energy and Communication*,28-30 Jan.,2016, Kolkata, India

[111] R.V.Rao and G.G.Wagmare , " A comparative study of a teaching–learning-based optimization algorithm on multi-objective unconstrained and constrained functions", *Journal of King Saud University- Computer and Information Sciences*, Vol.26,pp. 332-346, Dec. 2013.

[112] R.V.Rao and V.Patel ,” An elitist teaching-learning-based optimization algorithm for solving complex constrained optimization problems” *International Journal of Industrial Engineering Computations* , Vol.3,pp.535-560, March 2012.

[113] R.V.Rao,V.J.Savasani and J.Balic, ” Teaching–learning-based optimization algorithm for unconstrained and constrained real-parameter optimization problems”, *Engineering Optimization*, Vol.44, No.12,pp.1447-1462, Dec. 2012.

[114] R.V.Rao ,” Review of applications of TLBO algorithm and a tutorial for beginners to solve the unconstrained and constrained optimization problems “, *Decision Science Letters*, Vol.5, Issue1,pp.1-30, March 2016.

[115] B.Ram and D.N.Viswakarma ,”Power system protection and switchgear “, *Tata McGraw Hill* , New Delhi , 2010.

[116] L.Liu and L.Fu ,” Minimum breakpoint set determination for directional overcurrent relay coordination in large-scale power networks via matrix computations “, *IEEE Transactions on Power Delivery* , Vol.32, No.4, pp.1784-1789, August 2017

[117] J.Moirangthem, S.S.Dash and R.Ramaswami,” Zero-one integer programming approach to determine the minimum break point set in multi-loop and parallel networks”, *Journal of Electrical Engineering and Technology* , Vol. 7 , No.2 , pp.151-156, March 2012.

[118] J.Moirangthem, S.S.Dash and R.Ramaswami,” Determination of minimum break point set using particle swarm optimization for system-wide protective relay setting and coordination”, *European Transactions on Electrical Power* ,Vol.22, Issue 8, pp.1126-1135, November 2012.

[119] D.Ye, J.Ma and Z.Wang,” A novel method for determining minimum break point set based on network reduction and relays incidence matrix”, *IEEE International Conference on Critical Infrastructure*, Beijing, China, 20-22 September, 2010.

[120] Q.Yue , W.Yu and F.Lu ,” Gene evolution algorithm to determine minimum break point set for optimal coordination of directional protection relays in multiloops networks”, *IEEE Power Systems Conference and Exposition*, New York , USA , 10-13 October ,2004

[121] R.K.Gajbhiye , A.De and S.A.Soman ,” Computation of Optimal Break Point Set of Relays-An Integer Linear Programming Approach”, *IEEE Transactions on Power Delivery*, Vol.22 , No.4,pp. 2087-2098, October 2007.

Publications

Journals Published/ Accepted/ Communicated for Publication:

1. Saptarshi Roy and Dr. P.Suresh Babu , “Distance Relay Performance Evaluation on Series Compensated Transmission Line Under Faulted Conditions,” *Journal of Electrical Engineering , Romania* ,Vol.16 ,edition:3,pp-250-261,Sept.2016 .
2. Saptarshi Roy, Dr. P.Suresh Babu and N.V.Phanendra Babu, “A Synchrophasor Measurement-Based Fault Locator with Novel Fault Detection Technique,” *Journal of Electrical Systems* , Vol.13, Issue:3, pp-457-471, Sept. 2017.
3. Saptarshi Roy and Dr. P.Suresh Babu , “An Advanced Fault Locating Technique with WAMS based Backup Protection Scheme for Power System with Simultaneous Faults,” *Balkan Journal of Electrical & Computer Engineering, Istanbul Technical University* ,DOI: 10.17694/bajece.22170 ,Vol.4,No.1 ,pp.24-36,March 2016 .
4. Saptarshi Roy, Dr. P.Suresh Babu, N.V.Phanendra Babu and Abhishek Kumar, “An Efficient Fault Locating Technique with Backup Protection Scheme using Wide Area Measurement for Power System with Simultaneous Faults,” *International Journal of Electrical Engineering and Informatics*,Vol.9, Issue 1, pp-100-124,March 2017.
5. Saptarshi Roy and Dr. P.Suresh Babu, “Optimal Placement of TCSC and TCPAR using Sensitivity Analysis,” *Journal of Electrical Engineering, Romania*, Vol.18 ,edition:1,pp-301-314, March.2018.
6. Saptarshi Roy, Dr.P.Suresh Babu and N.V.Phanendra Babu, “Intelligent Co-ordination of Overcurrent and Distance Relays using TLBO Algorithm,” Communicated to *Journal of Electrical Systems* (Under Review).
7. Saptarshi Roy, Dr.P.Suresh Babu and N.V.Phanendra Babu,“Intelligent Coordination of Overcurrent and Distance Relays using Meta Heuristic Algorithms,” Communicated to *International Journal on Electrical Engineering and Informatics* (Under Review).
8. Saptarshi Roy, Dr. P.Suresh Babu and N.V.Phanendra Babu, “Meta-heuristic Technique based Combined Overcurrent and Distance Relays Coordination with Novel Relay Minimization Technique,” Communicated to *Swarm and Evolutionary Computation* (Under Review).

Conference Published/ Accepted for Publication:

1. Saptarshi Roy, Dr.P.Suresh Babu, N.V.Phanendra Babu, M.Lohith and K.V.Ramana Reddy, “Distance Relay Performance Evaluation on Series Compensated Transmission Line Protected with Metal Oxide Varistor Under Faulted Condition,” ***National Conference On Power System Protection***, 27-28 Feb 2015,CPRI,Bangalore.
2. Saptarshi Roy and Dr.P.Suresh Babu, “A Backup Protection Scheme Using Wide Area Measurement for Power System with Simultaneous Faults,” ***40th National Systems Conference 2016*** , NIT Warangal , 4-6 November ,2016 .
3. Saptarshi Roy, Dr. P.Suresh Babu and N.V.Phanendra Babu , “Optimal Combined Overcurrent and Distance Relays Coordination using Teaching Learning Based Optimization,” ***INDICON 2017***, IIT Roorkee , 15-17 December ,2017.
4. Saptarshi Roy, Dr. P.Suresh Babu and N.V.Phanendra Babu, “Optimal Combined Overcurrent and Distance Relays Coordination using TLBO Algorithm,” ***SocPros 2017***, IIT Bhubaneswar , 23-24 December ,2017.(Accepted to be included in ***Advances in Intelligent Systems and Computing, Springer (Scopus Indexed, ISSN 2194-5357)***).
5. Saptarshi Roy, Dr.P.Suresh Babu and N.V.Phanendra Babu, “Intelligent Overcurrent and Distance Relays Coordination: A Comparative Analysis using GA, PSO and TLBO,” Accepted for Oral Presentation ***in 4th IEEE International Conference ICEES 2018*** , to be held in SSN College of Engineering, Tamilnadu, 7-9 February, 2018.

Appendix-A

All IEEE Test system data for Chapter 2 are obtained from University of British Columbia Website: http://www.ece.ubc.ca/~hameda/download_files/

IEEE 57 bus data obtained from online link:

http://www.ece.ubc.ca/~hameda/download_files/case57.m

IEEE 118 bus data obtained from online link :

http://www.ece.ubc.ca/~hameda/download_files/case118.m

IEEE 300 bus data obtained from online link :

http://www.ece.ubc.ca/~hameda/download_files/case300.m

Appendix-B

System data for Chapter 3

Series capacitor compensated transmission line system data

Length = 350 KM

Voltage= 500 KV

Positive sequence impedance = $0.0155+j 0.3719 \Omega/Km$

Zero sequence impedance = $0.3546+j 1.0670 \Omega/Km$

Positive sequence admittance = $0 +j 4.4099 \times 10^{-6} \text{ mho/Km}$

Zero sequence admittance = $0 +j 2.7844 \times 10^{-6} \text{ mho/Km}$

Positive and Zero sequence impedances for sending end source are $Z_{S1}=(1+j15) \Omega$,

$Z_{S0}=(2.4 +j25) \Omega$ respectively.

Positive and Zero sequence impedances for receiving end source are $Z_{R1}=(1.2+j18) \Omega$,

$Z_{R0}=(2.6 +j26.5) \Omega$ respectively. Load angle is 30^0 with receiving end source voltage lagging.

Rated current of 2000 A , equivalent of (1750 MVA), is considered for sizing Series Capacitor Protection Unit. MOV rating after considering an overload factor 1.5 is calculated as 273 KV ($= 1.5 \times 2000 \text{ A} \times 91.1 \Omega$).

Appendix-C

System data for Chapter 4

Table-1

Parameters of Network 1 and 2

Parameters	Networks	
	1	2
$U_{LL,RMS}[\text{kV}]$	416	400
\emptyset^0	0	-20
$R [\Omega]$	1.0185892	0.6366183
$L[\text{H}]$	0.0509295	0.0318309
$R_0[\Omega]$	2.0371785	1.2732366
$L_0[\text{H}]$	0.1018589	0.0636618

Table-2

Line Parameters

Parameter	p-and n-sequence	0-sequence
Resistance Ω / Km	0.02021	0.1024
Inductance mH/Km	1.07	3.82727
Capacitance nF/Km	10.938	7.815

400 KV , 100 Km long overhead transmission line

Appendix-D

System data for Chapter 5

System data for WSCC-3-Machine-9-bus system:

Transmission lines:

Positive sequence impedance $= 0.03293 + j0.327 \Omega / \text{Km}$

Zero sequence impedance $= 0.2587 + j1.174 \Omega / \text{Km}$

Positive sequence capacitive reactance $= 280.1 \times 10^3 \Omega / \text{Km}$

Zero sequence capacitive reactance $= 461.2546 \times 10^3 \Omega / \text{Km}$

Any parameter missing is same as ref.[13]

[13]. P.K Nayak, A.K Pradhan, and P. Bajpai, “A Fault Detection Technique for the Series-Compensated Line During Power Swing”, *IEEE Transactions on Power Delivery*, vol. 28, no. 2, April 2013, pp.714-722

IEEE 14 bus test system data is obtained from University of British Columbia website.

Online link : http://www.ece.ubc.ca/~hameda/download_files/case14.m

Appendix-E

System data for Chapter 6

System data for WSCC 3 Machine 9 bus system is same as Appendix-D.

IEEE 57 bus data obtained from University of British Columbia website. online link:

http://www.ece.ubc.ca/~hameda/download_files/case57.m

Appendix-F

System data for Chapter 7

IEEE 5 bus system data

Bus data for IEEE 5 bus system

Bus code (P)	Assumed bus voltage	Generation		Load	
		Megawatts	Megavars	Megawatts	Megavars
1	1.06+j 0.0	0	0	0	0
2	1.0+j 0.0	40	30	20	10
3	1.0+j 0.0	0	0	45	15
4	1.0+j 0.0	0	0	40	5
5	1.0+j 0.0	0	0	60	10

Line data for IEEE 5 bus system

Bus Code p-q	Line impedance Z_{pq}		Line charging $\sqrt{(Y_{pq}/2)}$
	R per unit	X per unit	
1-2	0.02	0.06	X per unit
1-3	0.08	0.24	0.0+j 0.025
2-3	0.06	0.25	0.0+j 0.020
2-4	0.06	0.18	0+j 0.020
2-5	0.04	0.12	0.0+j 0.015
3-4	0.01	0.03	0.0+j 0.010
4-5	0.08	0.24	0.0+j 0.025

MW Limit for Branches in IEEE 5 bus system

Line	MW Limit (p.u)
1-2	0.8
1-3	0.3
2-3	0.2
2-4	0.2
2-5	0.6
3-4	0.1
4-5	0.1

6 bus system data

Lines' information

Line	R(p.u)	X(p.u)	V(kV)
1	0.0018	0.0222	150
2	0.0018	0.0222	150
3	0.0018	0.02	150
4	0.0022	0.02	150
5	0.0022	0.02	150
6	0.0018	0.02	150
7	0.0022	0.0222	150

Generators' information

Generators	X(p.u)	V(kV)
	0.1	10

They are based on 100 MVA and 150 KV.

Any parameter missing is same as ref.[11]

[11] R.M.Chabanloo et. al., "Optimal Combined Over Current and Distance Relays Coordination Incorporating Intelligent Over Current Relay Characteristics Selection", *IEEE Transactions on Power Delivery*, Vol.26, No. 3, pp.1381-1391, July,2011.

WSCC 3 Machine 9 bus data obtained from University of British Columbia website. online link: http://www.ece.ubc.ca/~hameda/download_files/case9.m

IEEE 14 bus data obtained from University of British Columbia website. online link: http://www.ece.ubc.ca/~hameda/download_files/case14.m

IEEE 30 bus data obtained from University of British Columbia website. online link: http://www.ece.ubc.ca/~hameda/download_files/case30.m

IEEE 57 bus data obtained from University of British Columbia website. online link: http://www.ece.ubc.ca/~hameda/download_files/case57.m

